POPULATION DYNAMICS OF FROG SPECIES UNDER SEASONAL FACTORS AND DISEASE TRANSMISSION

BEI SUN

PhD

The Hong Kong Polytechnic University

2025

The Hong Kong Polytechnic University

Department of Applied Mathematics

Population dynamics of frog species under seasonal factors and disease transmission

BEI SUN

A thesis submitted in partial fulfillment of the requirements for
the degree of Doctor of Philosophy
August 2024

CERTIFICATE OF ORIGINALITY

I hereby declare that this thesis is my own work and that, to the best of my knowledge and belief, it reproduces no material previously published or written, nor material that has been accepted for the award of any other degree or diploma, except where due acknowledgment has been made in the text.

Signature: ___________________

Name of Student: BEI SUN

Abstract

Frog populations are essential components of the ecosystem, and their decline or even extinction will significantly harm biodiversity and undermine the stability of the ecosystem. The growth and reproduction of frog population are essentially determined by the presence of seasonal climate conditions and ecological environments suitable for their survival. Comprehending the dynamics of frog populations in response to seasonal weather variations is crucial for forecasting population trends and devising conservation strategies for amphibians in the context of climate change scenarios. The influence of individual behaviors, such as frog mating, on population dynamics is also a worthy subject of exploration. In addition, worldwide amphibian decline and extinction have been observed, highlighting the importance of identifying the underlying factors. This issue has long been recognized as highly significant and continues to receive substantial attention in conservation ecology. Pathogen infection, in particular the chytrid fungus *Batrachochytrium dendrobatidis*, is postulated as a key factor contributing to the decline of certain species within specific regions. These issues will be investigated in this thesis using stage-structured models, which group individuals with similar demographic characteristics together and have proven useful in describing population dynamics.

This thesis begins with a brief introduction in Chapter 1, grounded in both biological perspectives and mathematical motivations. This chapter explains the ecological and mathematical significance of exploring the population dynamics of frog species. In Chapter 2, we present a concise overview of the mathematical foundations, elucidating key mathemat-

ical terminologies and theorems integral to monotone dynamical systems, global attractors, uniform persistence, coexistence states, and the basic reproduction ratio within the context of population models in periodic environments.

Chapter 3 starts from reviewing two widely-used modeling frameworks, in the form of integral equations and age-structured partial differential equations. Both modeling frameworks can be reduced into same differential equation structures with/without time delays under Dirac and gamma distributions for the stage durations. Each framework has its advantages and inherent limitations. The net reproduction number and initial growth rate can be easily defined from the integral equation. However, it becomes challenging to integrate the density-dependent regulations on the stage distribution and survival probabilities in an integral equation, which may be suitably incorporated in partial differential equations.

In Chapter 4, we formulate a stage-structured frog population model in the ecological environment with temperature-dependent effects. Due to the consideration of seasonal developmental duration, the resulting model is a system of piecewise differential equations that incorporate temperature-dependent delays. We propose the quotient space based on the initial natural phase space and prove the strong monotonicity in addition to showing some basic properties of the solutions. We demonstrate that the basic reproduction number, $\mathcal{R}_0$, serves as a critical threshold parameter that dictates whether the frog population will go extinct or persist. According to the theory of monotone dynamical systems, asymptotically periodic semiflows, and the comparison method, we obtain the global dynamics of the frog population system. The final simulations verify the analytic results numerically.

To focus on the pathogen characteristics that can drive host species extinction, both deterministic and stochastic modeling frameworks based on a susceptible-infectious-bacteria epidemic model are proposed in Chapter 5, to assess the influence of pathogen infection on species decline and extinction. Various indices, including the reproduction numbers of the host species, the replication of the pathogen, and the transmission of the pathogen are derived. Theoretical analysis includes the stability of equilibria, the extinction and persistence of host species in the deterministic model, and the evaluation of extinction probability and average extinction time in the stochastic model. Additionally, numerical simulations are conducted to quantify the effects of various factors on host decline and extinction, as well as the probabilities of extinction. We find two crucial conditions for a pathogen to drive host extinction: (i) the pathogen's self-reproduction capacity in the environment, and (ii) the pathogen's impact on the fecundity and survival of the infected host. These findings provide insights that could aid in the design and implementation of effective conservation strategies for amphibians.

Chapter 6 develops a stage-structured model with periodic time-delay for frog populations, comprehensively incorporating factors such as seasonal succession, two-sex division, mating behaviors, and adult competition. This periodic succession model describes the dynamic characteristics of female and male frog populations during both the normal and hibernation periods. Based on this framework, we analyze the basic properties within the natural phase space, including existence and uniqueness, boundedness, monotonicity, and strict subhomogeneity. To further investigate strong monotonicity, we introduce the quotient space, employing a method similar to the analytical approach used in Chapter 4. The global dynamics of the population model are then obtained through the introduction of the basic reproduction number, the use of auxiliary systems, and a series of theories on monotone dynamical systems, periodic semiflows, and the comparison method. Numerical simulations illustrate the influence of time-dependent parameters and validate the related analytic results. Additionally, they assess the impact of two key sensitive parameters—mature mortality rates and mating pairs—on population sizes during the normal growth and hibernation periods across multiple life-cycles and a single life-cycle. The simulations clearly demonstrate that female and male populations ultimately experience significant declines as they approach hibernation. However, a higher number of mating pairs leads to a higher stabilized population size during the normal period before the decline associated with hibernation.

Chapter 7 provides a summary of the results presented in this thesis and discusses potential directions for future research.

Publications Arising from the Thesis

1. Yijun Lou and Bei Sun, "Stage duration distributions and intraspecific competition: a review of continuous stage-structured models", in *Mathematical Biosciences and Engineering*, pp. 7543-7569, 19(8), 2022.
2. Bei Sun, Daozhou Gao, Xueying Wang, and Yijun Lou, "Infection-induced host extinction: deterministic and stochastic models for environmentally transmitted pathogens", manuscript submitted to *Mathematical Biosciences*.
3. Bei Sun and Yijun Lou, "A seasonal succession model for frog population growth under climate change", to be submitted.
4. Bei Sun and Yijun Lou, "Mating behaviors on the frog population and dynamical analysis", to be submitted.

Acknowledgments

First and foremost, I would like to extend my heartfelt gratitude to my esteemed supervisor, Dr. Yijun Lou. His exceptional guidance, insightful discussions, profound ideas, and unwavering support have been the cornerstone of my research journey. Dr. Lou's meticulous attention to the finer details of my research has imparted invaluable lessons that I will carry forward in my academic endeavors. His rigorous scientific approach and fervent enthusiasm for mathematical biology have not only propelled me to strive for excellence in this field but have also instilled in me a lifelong passion for inquiry and discovery. Dr. Lou's influence extends beyond the realm of academia, shaping my personal growth and professional development. For all his contributions and unwavering belief in my potential, I am profoundly grateful.

I gratefully acknowledge the Graduate School for awarding me the PolyU Research Postgraduate Scholarship (PRPgS), which has provided essential financial support for my studies and research endeavors. My sincere thanks also go to the Department of Applied Mathematics, under the leadership of Professor Defeng Sun, for offering me the opportunity to work as a teaching assistant, thereby granting me invaluable work experience. I am profoundly thankful to Professors Zhian Wang and Xingqiu Zhao for their exceptional teaching in applied analysis and mathematical statistics. My gratitude extends to all the staff members in the department for their unwavering support and assistance.

I would like to seize this opportunity to express my heartfelt thanks to Professors Xiaoqiang Zhao for his guidance and encouragement during his visit to PolyU. I am equally indebted to my collaborators, Drs. Daozhou Gao and Xueying Wang, for their enlightening discussions and valuable suggestions that have significantly enriched my research. Special thanks to my master's supervisor, Dr. Xue Zhang, who introduced me to the fascinating field of mathematical biology and has consistently provided encouragement, support and trust, all of which have greatly benefited my academic journey.

I owe a debt of gratitude to Dr. Kaihui Liu for her unwavering encouragement and support, and to Drs. Zhenghong Jin, Dingjie Wang, Shuyang Xue, and Yijie Zha, as well as my friends Cihan Cai, Feng Chen, Weiping Lou, Yizhi Pang, Ke Qi, Weiting Song, and Jian Wang for their camaraderie and support during their time at PolyU. Moreover, my heartfelt thanks go to my dear friends and colleagues at PolyU, especially my best friend Dr. Haorao Zhang. I would also like to offer special thanks to my special friend, Max. Your friendship has made my academic journey a truly wonderful experience. Though I cannot list all your names here, please know that you are always in my thoughts.

Last but certainly not least, I extend my deepest gratitude to my parents and my sister, Ruo Sun. Their understanding, trust, and unwavering support have been the bedrock of my strength and perseverance.

Table of Contents

List of Figures

List of Tables

Chapter 1

Introduction

1.1 Biological perspective

Amphibians are the first tetrapods to invade the land and are an essential part of the planet's biodiversity; they are also critical components of ecosystems. They can be used as key indicators of ecosystem health for biological and population studies, and they are also a rich source of some biopharmaceuticals. Amphibians in nature can be prey and predators, vital elements of aquatic and terrestrial food webs [198]. The decline, and potentially even extinction, of frog populations presents a significant challenge to global ecosystems due to their integral role in maintaining biodiversity [99]. There are many reasons for species declines, such as global warming, habitat loss, pollution, and over-exploitation. Specifically, [149] proposed that epidemic diseases caused by global warming can result in widespread amphibian extinctions and biodiversity erosion. [171] presented the global analysis of amphibians population and quantified the effects of habitat loss, climate change and over-exploitation on declines and extinction risk. The research on the growth and development of frog populations necessitates the accomplishment of three primary objectives: (i) Establishing a series of mechanism models of the frog population and disease transmission and using them for related dynamic analysis. (ii) Exploring the stability of population growth in the system model and pathogen-host system to achieve adequate protection of species in the future. (iii) Integrating models with temperature data to help determine how abiotic factors such as climate, temperature, and ecological environment affect population growth, reproductive outcomes and disease spread.

To fully comprehend frog population dynamics, capturing the environmental variability throughout frogs' remarkable range of life histories is essential. Understanding amphibian dynamics will improve our understanding of how abiotic/biotic factors will promote/inhibit population persistence and assist in developing management strategies to protect the species from extinction, unlike the discrete-time models, in which field and experimental data can easily calibrate and easy to capture the persistence/extinction dynamics of the species. However, it becomes impossible to capture the seasonality of the population in the case of persistence and characterize the effect of environmental variability on the seasonality pattern [153]. A better understanding of the extent to which environmental forces affect population persistence and how this affects the seasonal synchronicity of population responses to environmental fluctuations will quantify the scope of potential losses, predict future population viability, and develop management techniques to preserve biodiversity. Demographic stages subdividing the population into different types of individuals account for differences in vital rate responses between individuals. A within-one-year *R. muscosa* model will be proposed in Chapter 4 with three main stages, tadpoles, juveniles, and adults. Besides, the tadpoles are further classified into year-one and year-two individuals.

Amphibian declines and extinctions have been observed globally at a rapid pace [137, 161, 172]. Reports indicate that out of 5743 described species, 32.5% are threatened. Since 1980, a minimum of 9 species, and potentially up to 122, have become extinct [137]. Compared to either birds or mammals, amphibians are facing a more rapid decline and are under greater threat [172]. Identifying the underlying factors has long been recognized as a highly significant issue and continues to receive substantial attention in ecological research. These studies are crucial for the design and implementation of effective amphibian conservation strategies. Six primary causes of biodiversity loss are postulated to be responsible for modern amphibian declines: commercial use; the introduction of exotic species that compete with, prey on, and parasitize native frogs and salamanders; changes in land use; contaminants; climate change; and infectious diseases [50]. These factors may act alone or together.

Chytridiomycosis arises when the skin of a frog becomes infected with the pathogenic chytrid fungus *Batrachochytrium dendrobatidis* (Bd), resulting in the disruption of crucial skin functions [92]. Following the emergence of the pathogen, numerous amphibian populations have experienced catastrophic collapses, and this persistent expansion of the pathogen's range poses an ongoing threat to amphibian populations worldwide [1, 50, 182]. Consequently, an additional focus of this study is to ascertain whether infectious diseases can single-handedly drive host population extinction. If disease transmission can indeed lead to host extinction, we aim to further explore the underlying mechanisms contributing to such population extinction in Chapter 5. These include the functional responses of pathogen transmission and reproduction within the host or the environment.

In addition, the reproductive cycle of frogs is an intricate phenomenon comprising multiple sequential stages, such as courtship rituals, mating behavior, and oviposition. The breeding season commences with male frogs vocalizing species-specific mating calls to attract potential mates. Upon a female being lured by a male's call, the two individuals engage in amplexus, a characteristic embrace where the male grasps the female tightly with his forelimbs to impede her departure during the act of external fertilization of her ova [67]. The timing and modalities of these events can exhibit substantial variation contingent upon factors like the frog species, their geographical distribution, and the prevailing environmental conditions in their habitats [44]. The characteristics of mating behavior significantly impact the growth and development of amphibian populations [56], prompting us to study this aspect separately in Chapter 6.

1.2 Mathematical motivation

The single-species population dynamics are governed by the growth rate, which is further determined by the survival and reproduction of its individuals. Both the survival and reproduction rates differ from individual to individual, depending on biotic factors such as age and body mass and abiotic factors including the environment. Trivially speaking, individuals in the reproductive stage directly contribute to the birth rate, and the survival rates vary by life stages. In combination, variations in demographic rates among individuals should be appropriately incorporated in a population growth model. Instead of considering too detailed demographic characteristics in laboratory or field experiments, it would be more practical in some cases to lump individuals with similar characteristics together in a specific life stage. On the other hand, ignoring the variations among different stages can lead to misleading predictions on population dynamics [144], and therefore, stage-structured models are proposed as ideal tool to describe population growth, which take a balance between the model complexity and model performance. Usually, individuals in the same stage can be assumed to undergo identical development time (a mean development delay) while omitting variances in stage durations. However in some scenarios, the time an individual takes in a specific life stage is not uniformly distributed. For example, some eggs hatch (e.g., become larvae in some insects) before other eggs laid at the same time [144], and a non-uniform (non-Dirac) distribution for the stage duration should be considered when grouping age-stratified individuals together in a stage. To describe the heterogeneity in development, various distributions for stage durations have been fitted from the stage-frequency data in monitoring cohorts through time, including gamma, Weibull, log-normal, logistic and others [57]. For example, the widely used gamma distribution with a positive integer shape parameter n and rate parameter $n\lambda > 0$ has the following probability density function

$$f(t; n, n\lambda) = \frac{t^{n-1}e^{-n\lambda t}(n\lambda)^n}{\Gamma(n)} = \frac{t^{n-1}e^{-n\lambda t}(n\lambda)^n}{(n-1)!}.$$

This special gamma distribution is also called Erlang distribution as the shape parameter n is a positive integer. The mean value and variance of this distribution are $\frac{1}{\lambda}$ and $\frac{1}{n\lambda^2}$. It has been fitted to the stage-frequency data [57, 197] for different species. When $n = 1$, it becomes the exponential distribution. Taking the limit case when n goes to infinity, it becomes the Dirac distribution (also called Dirac δ-distribution). Different probability density functions are illustrated in Figure 1.1(a) when the mean duration is fixed at $\frac{1}{\lambda} = 10$ days. In this case, the probability of an individual with stage age a reminding in the particular stage is presented in Figure 1.1(b).

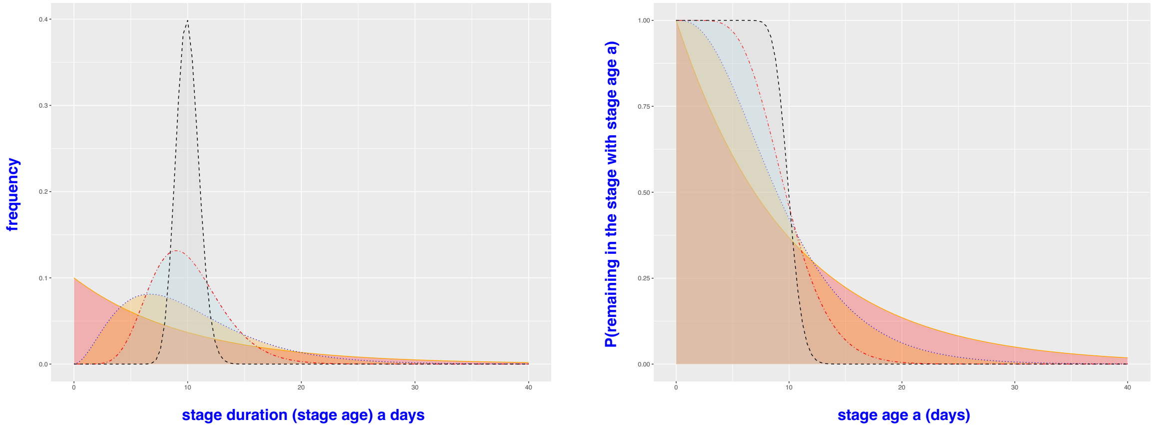

((a)) Probability density function of gamma distributions ((b)) Survival (sojourn) function

Figure 1.1: The probability distributions of an individual with stage age a (days) remaining in the stage under gamma distributions of mean 10 days with different shape parameters $n = 1$, 3, 10 and 100.

Competition occurs when two or more individuals of the same or different populations negatively affect each other striving for limited resources such as food, water, territory, sunlight, mates and so on. There are two different types of competition: intraspecific competition which occurs between individuals of the same species and interspecific competition which occurs between individuals of different species. The logistic growth model incorporates density-dependent population growth rate due to intraspecific competition, and describes the sigmoid growth curve for a single species. Many generalized forms of the logistic equation have been proposed to fit the observed growth phenomena, for example, the Richards model for species growth [154] and epidemic data [194], and a more generalized logistic growth model [103, 183]. When individual movement in a spatial habitat is considered, the Fisher-KPP equation [75] for a continuous spatial domain and multi-patch logistic questions can be formulated [20]. The spatial dynamics can be investigated and the maximal total population problem can be further studied [58, 141, 204]. After almost a century of research, the competition interaction continues to fascinate researchers to understand its role on shaping the population dynamics of a single species and engaging species in a community.

Therefore, on the one hand, we focus on reviewing stage-structured models of single-species populations using two approaches: integral forms and partial differential equations, under both gamma and Dirac distributions. We then consider various types of models with Dirac distributions under different assumptions regarding the influence of intraspecific competition in Chapter 3. On the other hand, motivated by biological considerations, we develop a series of models addressing seasonal succession, population competition, environmental pathogen transmission, and mating behaviors in the subsequent chapters (i.e., Chapter 4, Chapter 5, and Chapter 6). We explore some basic properties and global dynamics using the theories of monotone dynamical systems, global attractors, uniform persistence, coexistence states, and the basic reproduction number as introduced in the preliminaries in Chapter 2. Finally, numerical simulations are employed to verify theoretical results, to quantify the sensitivity of certain parameters and to evaluate the influencing factors on the population systems.

Chapter 2

Preliminaries

In this chapter, we introduce the terminologies and established results that will be utilized throughout this thesis. These include monotone dynamical systems, the theories of global attractors, uniform persistence and coexistence states, and basic reproduction radio for seasonal succession population models in periodic environments.

2.1 Monotone dynamics

Consider an ordered Banach space E with an order cone P that has a non-empty interior $int(P)$. For $x, y \in E$, we denote:

(i) $x > y$, if $x - y \in P \backslash \{0\}$;

(ii) $x \geq y$, if $x - y \in P$;

(iii) $x \gg y$, if $x - y \in int(P)$.

We define the order interval $[a, b] := \{x \in E : a \leq x \leq b\}$ provided that $a < b$.

Definition 2.1.1. *Let U be a subset of E, and let $f : U \to U$ be a continuous map. The map f is defined as:*

(i) ***monotone*** *if $x \geq y$ implies $f(x) \geq f(y)$;*

(ii) ***strictly monotone*** *if $x > y$ implies $f(x) > f(y)$;*

(iii) ***strongly monotone*** *if $x > y$ implies $f(x) \gg f(y)$.*

Theorem 2.1.1. *(Dancer-Hess connecting orbit theorem) [94, Proposition 1] Suppose $u_1 < u_2$ are fixed points of the strictly monotone continuous mapping $f : U \to U$, let $I := [u_1, u_2] \subset U$, and assume $f(I)$ is relatively compact and that f has no fixed points other than u_1 and u_2 in I. Then, one of the following holds:*

(i) there exists an entire orbit $\{x_n\}_{n=-\infty}^{\infty}$ of f in I such that $x_{n+1} > x_n$ for all $n \in \mathbb{Z}$, and $\lim_{n\to-\infty} x_n = u_1$ and $\lim_{n\to\infty} x_n = u_2$; or

(ii) there exists an entire orbit $\{y_n\}_{n=-\infty}^{\infty}$ of f in I such that $y_{n+1} < y_n$ for all $n \in \mathbb{Z}$, and $\lim_{n\to-\infty} y_n = u_2$ and $\lim_{n\to\infty} y_n = u_1$.

Recall that a subset K of E is termed order convex if $[u, v] \in K$ whenever $u, v \in K$ and $u < v$ are satisfied.

Definition 2.1.2. *Suppose $U \subset P$ is a nonempty, closed, and order-convex subset. A continuous map $f : U \to U$ is defined as:*

(i) ***subhomogeneous*** *if $f(\lambda x) \geq \lambda f(x)$ for all $x \in U$ and $\lambda \in [0, 1]$;*

(ii) ***strictly subhomogeneous*** *if $f(\lambda x) > \lambda f(x)$ for all $x \in U$ with $x \gg 0$ and $\lambda \in (0, 1)$;*

(iii) ***strongly subhomogeneous*** *if $f(\lambda x) \gg \lambda f(x)$ for all $x \in U$ with $x \gg 0$ and $\lambda \in (0, 1)$.*

Theorem 2.1.2. *[207, Theorem 2.3.2] Assume $f : U \to U$ satisfies one of the following conditions:*

(i) f is monotone and strongly subhomogeneous; or

(ii) f *is strongly monotone and strictly subhomogeneous.*

If there exists a nonempty compact invariant set $K \subset int(P)$ *for* $f : U \to U$*, then* f *has a fixed point* $e \gg 0$ *such that every nonempty compact invariant set of* f *within* $int(P)$ *consists solely of* e*.*

Recall that a continuous mapping $f : X \to X$ is described as asymptotically smooth if, for any nonempty closed bounded subset $B \subset X$ with $f(B) \subset B$, there exists a compact subset $J \subset B$ that attracts B. If the Fréchet derivative of f at $u = a$ exists, denote it by $Df(a)$, and let $r(Df(a))$ represent the spectral radius of the linear operator $Df(a) : E \to E$.

Theorem 2.1.3. *(Threshold dynamics) [207, Theorem 2.3.4] Consider* $V = [0, b]$ *with* $b \gg 0$*, and let* $f : V \to V$ *be a continuous map. Suppose that:*

- *(i)* $f : V \to V$ *satisfies one of the following criteria:*
  - *(a)* f *is monotone and strongly subhomogeneous; or*
  - *(b)* f *is strongly monotone and strictly subhomogeneous;*
- *(ii)* $f : V \to V$ *is asymptotically smooth, and every positive orbit of* f *in* V *is bounded;*
- *(iii)* $f(0) = 0$*, and* $Df(0)$ *is compact and strongly positive.*

Then the system exhibits threshold dynamics:

- *(i) If* $r(Df(0)) \leq 1$*, then every positive orbit in* V *converges to* 0*;*
- *(ii) If* $r(Df(0)) > 1$*, then there exists a unique fixed point* $u^* \gg 0$ *in* V *such that every positive orbit in* $V \backslash \{0\}$ *converges to* u^**.*

2.2 Uniform persistence and coexistence states

Assume X is a metric space equipped with the metric d. Consider a continuous map $f : X \to X$ and an open subset $X_0 \subset X$. Define $\partial X_0 := X \backslash X_0$, and let $M_\partial := x \in \partial X_0 : f^n(x) \in \partial X_0, \forall n \geq 0$, which may be empty.

Definition 2.2.1. *A bounded set A is defined to attract a bounded set B in X if*

$$\lim_{n\to\infty, x\in B} \sup \{d(f^n(x), A)\} = 0.$$

A subset $A \subset X$ is called an attractor for f if A is nonempty, compact, and invariant (i.e., $f(A) = A$), and A attracts some open neighborhood of itself. A global attractor for $f : X \to X$ is an attractor that attracts every point in X. For a nonempty invariant set M, the set $W^s(M) := x \in X : \lim_{n\to\infty} d(f^n(x), M) = 0$ is referred to as the stable set of M.

Recall that a continuous mapping $f : X \to X$ is described as point dissipative if there exists a bounded set B_0 in X that attracts every point in X.

Theorem 2.2.1. *[207, Theorem 1.1.3] If $f : X \to X$ is compact and point dissipative, then there exists a connected global attractor A that attracts every bounded subset within X.*

Definition 2.2.2. *The mapping f is considered uniformly persistent with respect to $(X_0, \partial X_0)$ if there is an $\eta > 0$ such that $\liminf_{n\to\infty} d(f^n(x), \partial X_0) \geq \eta$ for all $x \in X_0$.*

Definition 2.2.3. *Let $A \subset X$ be a nonempty invariant set for the function f. The set A is said to be internally chain-transitive if for any $a, b \in A$ and any $\epsilon > 0$, there exists a finite sequence $x_1, \ldots, x_m$ in A with $x_1 = a$ and $x_m = b$ such that $d(f(x_i), x_{i+1}) < \epsilon$ for $1 \leq i \leq m - 1$. This sequence $x_1, \ldots, x_m$ is referred to as an ϵ-chain in A connecting a and b.*

Definition 2.2.4. *A lower semicontinuous function $p : X \to \mathbb{R}_+$ is termed a generalized distance function for $f : X \to X$ if for every $x \in (X_0 \cap p^{-1}(0)) \cup p^{-1}(0, \infty)$, it holds that $p(f^n(x)) > 0$ for all $n \geq 1$.*

Theorem 2.2.2. *[207, Theorem 1.3.2] (or [169, Theorem 3]) Let p be a generalized distance function for the continuous map $f : X \to X$. Suppose that:*

(i) f possesses a global attractor;

(ii) There is a finite sequence $M = \{M_1, \ldots, M_k\}$ of disjoint, compact, and isolated invariant sets within ∂X_0 that satisfy the following conditions:

  (a) $\cup_{x \in M_\partial} w(x) \subset \cup_{i=1}^{k} M_i$, where $w(x)$ denotes the omega limit set of x;

  (b) no subset of M forms a cycle in ∂X_0;

  (c) M_i is isolated within X;

  (d) $W^s(M_i) \cap p^{-1}(0, \infty) = \emptyset$ for each $1 \leq i \leq k$, where $W^s(M_i)$ is the stable set of M_i.

Then there is a $\delta > 0$ such that for any compact chain transitive set L with $L \not\subset M_i$, for all $1 \leq i \leq k$, it holds that $\min_{x \in L} p(x) > \delta$. In particular, f is uniformly persisitent in the sense that there is an $\eta > 0$ such that $\liminf_{n \to \infty} d(f^n(x), \partial X_0) \geq \eta$ for all $x \in X_0$.

Suppose $T > 0$. A family of mapping $\Phi(t) : X \to X$, $t \geq 0$, is defined as a T-periodic semiflow on X if it satisfies the following conditions:

(a) $\Phi(0) = I$, where I denotes the identity mapping on X;

(b) $\Phi(t + T) = \Phi(t) \circ \Phi(T)$ for all $t \geq 0$;

(c) $\Phi(t)x$ is continuous with respect to $(t, x) \in [0, \infty) \times X$.

The mapping $\Phi(T)$ is referred to as the Poincaré map (or period map) associated with this periodic semiflow. Specifically, if condition (b) holds for any $T > 0$, then $\Phi(t)$ is termed an autonomous semiflow.

Theorem 2.2.3. *[207, Theorem 3.1.1] Let $\Phi(t)$ be a T-periodic semiflow on X such that $\Phi(t)X_0 \subset X_0$ for all $t \geq 0$. Suppose $S := \Phi(T)$ is point dissipative and compact in X. Then the uniform persistence of S with respect to $(X_0, \partial X_0)$ implies the uniform persistence of $\Phi(t) : X \to X$.*

2.3 Basic reproduction ratio in periodic environments

A fundamental concept in epidemiology is the basic reproduction number, denoted as $\mathcal{R}_0$, which represents the expected number of secondary cases produced by a typical infective individual in a completely susceptible population (see, e.g., [18, 61]). If $\mathcal{R}_0 > 1$, the disease is expected to spread within the population, suggesting the necessity of reducing $\mathcal{R}_0$ to below 1 to achieve eradication. An explicit formula for $\mathcal{R}_0$ in a wide range of autonomous compartmental epidemic models was provided in [184], and this work has been extended to periodic models in [193].

In population dynamics, the basic reproduction number, $\mathcal{R}_0$, is similarly crucial. It is defined as the expected number of new offspring produced by a typical individual over its lifetime. This threshold value determines the fate of the population: if $\mathcal{R}_0 \leq 1$, the population is likely to go extinct, whereas if $\mathcal{R}_0 > 1$, the population is expected to persist uniformly.

In this section, we introduce the theory of the basic reproduction number for abstract delay differential equations, including both periodic and time-delayed models, as formulated in [206]. Let $\tau \geq 0$ be a given parameter, and define $X = C([-\tau, 0], \mathbb{R}^m)$ and $X^+ = C([-\tau, 0], \mathbb{R}^m_+)$. Then (X, X^+) forms an ordered Banach space equipped with the maximum norm and the positive cone X^+. Consider a map $F : \mathbb{R} \to \mathcal{L}(X, \mathbb{R}^m)$ and let $V(t)$ be a continuous $m \times m$ matrix function on $\mathbb{R}$. Suppose that $F(t)$ and $V(t)$ are T-periodic in t for some real number $T > 0$. For a continuous function $u : [-\tau, \sigma) \to \mathbb{R}^m$

with $\sigma > 0$, define $u_t \in X$ by

$$u_t := u(t+\theta), \ \ \forall \theta \in [-\tau, 0]$$

for any $t \in [0, \sigma)$.

By linearizing a population growth model at its extinction equilibrium, we obtain the following linear and periodic functional differential system:

$$\frac{\mathrm{d}u(t)}{\mathrm{d}t} = F(t)u_t - V(t)u(t), \ \ t \geq 0, \tag{2.1}$$

where $F(t)u_t$ represents the newly born individuals at time t, which are linearly dependent on the reproductive individuals within the interval $[t-\tau, t]$. Moreover, the internal dynamics of individuals within the reproductive compartments, such as natural deaths and transitions among compartments, are governed by the following linear ordinary differential system:

$$\frac{\mathrm{d}u(t)}{\mathrm{d}t} = -V(t)u(t), \ \ t \geq 0. \tag{2.2}$$

We consider that $F(t) : X \to \mathbb{R}^m$ is defined as

$$F(t)\phi = \int_{-\tau}^{0} d[\eta(t,\theta)]\phi(\theta), \ \ \forall t \in \mathbb{R}, \ \ \phi \in X,$$

where $\eta(t,\theta)$ is an $m \times m$ matrix function that is measurable in $(t,\theta) \in \mathbb{R} \times \mathbb{R}$ and normalized such that $\eta(t,\theta) = 0$ for all $\theta \geq 0$ and $\eta(t,\theta) = \eta(t,-\tau)$ for all $\theta \leq -\tau$. Additionally, $\eta(t,\theta)$ is left-continuous in θ on $(-\tau, 0)$ for each t, and the variation of $\eta(t,\cdot)$ on $[-\tau, 0]$ satisfies $\mathrm{Var}_{[-\tau,0]}\eta(t,\cdot) \leq m(t)$ for some $m \in \mathbb{L}_1^{\mathrm{loc}}((-\infty,\infty),\mathbb{R})$, the space of functions from $(-\infty,\infty)$ to $\mathbb{R}$ that are Lebesgue integrable on each compact set of $(-\infty,\infty)$. Given that $F(t)$ is T-periodic in t, there exists

$$\sup_{t\in\mathbb{R}} \parallel F(t) \parallel = \sup_{0\leq t\leq T} \parallel F(t) \parallel \leq \sup_{0\leq t\leq T} m(t).$$

We introduce the evolution operators $U(t,s)$ on X associated with system (2.1) as follows:

$$U(t,x)\phi = u_t(s,\phi), \forall \phi \in X, \ \ t \geq s, \ \ s \in \mathbb{R},$$

where $u(t,s,\phi)$ represents the unique solution of (2.1) on $[s,\infty)$ with the initial condition $u_s = \phi$, i.e., $u_t(s,\phi)(\theta) = u(t+\theta,s,\phi)$ for all $\theta \in [-\tau,0]$. Consequently, each operator $U(t,s)$ is continuous and satisfies

$$U(s,s) = I, \ \ U(t,s)U(s,r) = U(t,r), \ \ U(t+T,s+T) = U(t,s), \ \ \forall t \geq s \geq r.$$

Suppose $\Phi(t,s)$, $t \geq s$, be the evolution matrices associated with system (2.2). These matrices satisfy the following conditions:

$$\frac{\partial}{\partial t}\Phi(t,s) = -V(t)\Phi(t,s), \ \ \forall t \geq s, \ \ \text{and} \ \ \Phi(s,s) = I, \ \ \forall s \in \mathbb{R},$$

where $w(\Phi)$ denotes the exponential growth bound of $\Phi(t,s)$, defined as

$$w(\Phi) = \inf\{\widetilde{w} : \exists M \geq 1 \ \ \text{such that} \ \ \| \ \Phi(t+s,s) \ \| \leq Me^{\widetilde{w}t}, \ \ \forall s \in \mathbb{R}, \ t \geq 0\}.$$

We assume the following conditions:

(i) Each operator $F(t) : X \to \mathbb{R}^m$ is positive in the sense that $F(t)X^+ \subset \mathbb{R}^m_+$.

(ii) Each matrix $-V(t)$ is cooperative, and $w(\Phi) < 0$.

Assume that the initial distribution of newly born individuals, $v(t)$, is T-periodic in t to reflect the periodic environment. For any given $s \geq 0$, $F(t-s)v_{t-s}$ represents the distribution of newly born individuals at time $t-s$, originating from the reproductive individuals who matured during the interval $[t-s-\tau, t-s]$. Subsequently, $\Phi(t,t-s)F(t-s)v_{t-s}$ denotes the distribution of those newborns who were born at time $t-s$ and remain in the immature compartments at time t. Hence, it follows that

$$\int_0^\infty \Phi(t,t-s)F(t-s)v_{t-s}ds = \int_0^\infty \Phi(t,t-s)F(t-s)v(t-s+\cdot)ds$$

represents the cumulative distribution of newborns at time t generated by all reproductive individuals introduced at all preceding times up to t.

Let C_T denote the ordered Banach space consisting of all continuous and T-periodic functions from $\mathbb{R}$ to $\mathbb{R}^m$, equipped with the maximum norm and the positive cone $C_T^+ := \{v \in C_T : v(t) \geq 0,\ \forall t \in \mathbb{R}\}$. We can subsequently define the following linear operator on C_T as follows:

$$[Lv](t) = \int_0^\infty \Phi(t,t-s)F(t-s)v(t-s+\cdot)ds,\ \ \forall t \in \mathbb{R},\ \ v \in C_T,$$

and

$$[\hat{L}v](t) = F(t)\int_0^\infty \Phi(t+\cdot,t-s+\cdot)v(t-s+\cdot)ds,\ \ \forall t \in \mathbb{R},\ \ v \in C_T.$$

Let A and B be two bounded linear operator on $\mathbb{X}$ defined by

$$[Av](t) = \int_0^\infty \Phi(t,t-s)v(t-s)ds,\ \ [Bv](t) = F(t)v_t,\ \ \forall t \in \mathbb{R},\ \ v \in \mathbb{X}.$$

It then follows that $L = A \circ B$ and $\hat{L} = B \circ A$, thereby implying that L and $\hat{L}$ share the same spectral radius. Consequently, the basic reproduction number for the periodic system (2.1) is defined as the spectral radius of L and $\hat{L}$, in accordance with the concept of next generation operators [25, 62, 71, 72, 179, 184], i.e.,

$$\mathcal{R}_0 := r(L) = r(\hat{L}).$$

Let $U(T,0)$ be the Poincaré (period) map of system (2.1) on X. The following theorem shows that $\mathcal{R}_0$ can also be used to measure the stability of the zero solution for periodic system (2.1), that is, if $\mathcal{R}_0 < 1$, the zero solution is stable, while it is unstable if $\mathcal{R}_0 > 1$.

Theorem 2.3.1. *[206, Theorem 2.1] The following statements are valid:*

(i) $\mathcal{R}_0 = 1$ *if and only if* $r(U(T,0)) = 1$*;*

(ii) $\mathcal{R}_0 > 1$ *if and only if* $r(U(T,0)) > 1$*;*

(iii) $\mathcal{R}_0 < 1$ *if and only if* $r(U(T,0)) < 1$.

Thus, $\mathcal{R}_0 - 1$ *has the same sign as* $r(U(T,0)) - 1$.

Let $\{U(t,s,\lambda) : t \geq s\}$ be the evolution operators on X of the following linear periodic system with $\lambda \in (0,+\infty)$:

$$\frac{\mathrm{d}u(t)}{\mathrm{d}t} = \frac{1}{\lambda}F(t)u_t - V(t)u(t), \;\; t \geq 0.$$

The following result was presented in [206], which provides a fantastic idea of numerically computing $\mathcal{R}_0$.

Theorem 2.3.2. *[206, Theorem 2.2] If* $\mathcal{R}_0 > 0$*, then* $\lambda = \mathcal{R}_0$ *is the unique solution of* $r(U(T,0,\lambda)) = 1$.

Chapter 3

Stage duration distributions and intraspecific competition of continuous stage-structured models

3.1 Introduction

The main focus in this chapter is on stage-structured models when individuals of same species compete for the same resources in an ecosystem (e.g. food or living space). This modeling idea will be employed in later chapters. However, it should be noted that the stage-structured modeling idea for a single population growth has been widely employed in other research areas, such as for disease transmission with various infectious period distributions [36, 45, 79, 80] and stage-dependent exposure [155], spatial population dynamics in continuous [43] and discrete [132] habitats, within-host virus dynamics to account the stages of the viral life cycle before viral production [34], the immune responses of T cell life stages [46], waning of immunity of a vaccinated individual [78] and so on.

In this chapter, two basic modeling approaches, in terms of integral equations and partial differential equations, will be presented in consequent Section 3.2. Both frameworks are further reduced into ordinary differential equations with or without time delay under further Dirac and gamma distribution assumptions on the development time, respectively. Further remarks on advantages and inherent limitations are briefly discussed in the same section. Section 3.3 is devoted to presenting recent modeling studies, when the mean stage duration and survival probability are regulated by population density due to intraspecific competition. Section 3.4 concludes the chapter by discussing some related problems on the topic.

3.2 Two physiologically-structured modeling approaches

In this section, we will review two basic structured modeling frameworks [112] in the form of integral equations and partial differential equation models. The main focus will be reducing the models under gamma and Dirac distributions for stage progression. Without loss of generality, we consider the simplest case when there are two stages, denoted as immature (pre-reproductive) and mature (reproductive) stages with population sizes $I(t)$ and $M(t)$, respectively. The sojourn functions $P_I(a)$ and $P_M(a)$ describe the probabilities that a living individual remains in immature and mature stages for a units of time (stage age a), respectively, and satisfy the following properties: (i) $0 \leq P_X(a) \leq 1$; (ii) $P_X(a)$ in nonincreasing on a; (iii) $\int_0^\infty P_X(a)da < \infty$, where $X = I, M$. Please note that we assume the function $P_X(a)$ is differentiable with derivative $P'_X(a)$ for the ease of notational simplicity. When it is not differentiable, the Riemann integrals should be represented in Riemann-Stieltjes integrals and rigorous treatments can be found in [180]. Further interesting biological indices can be derived from this sojourn function [180], such as: (i) the mean sojourn time in the stage X (mean duration of the stage) can be directly computed as $D = \int_0^\infty P_X(a)da$; (ii) the expected remaining sojourn times at stage age s would be $D(s) = \frac{1}{P_X(s)} \int_s^\infty P_X(\eta)d\eta$ and $D = D(0)$; (iii) the average expectation of

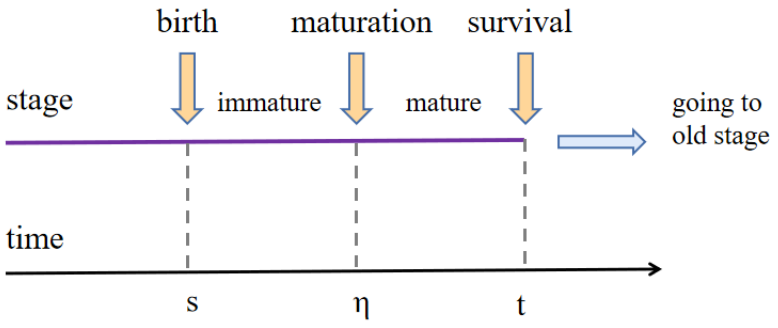

Figure 3.1: Stage progression of individuals from immature to mature stages. Since individuals in non-reproductive old stage do not contribute to the birth rate, the old stage is not considered in the model. However, the duration distribution for the M stage may be incorporated to describe the progression from M-stage to the old stage.

remaining sojourn (duration) $E = \dfrac{\int_0^\infty aP_X(a)da}{\int_0^\infty P_X(a)da}$; (iv) the variance of the stage duration is $V = D(2E - D)$.

Population dynamics are intuitively dependent on the stage duration distributions $P_X(a)$, and Dirac and gamma distributions will be further discussed in more details. By default, the term "age" represents the chronological age of an individual. In this section, the *stage-specific age* will be used in some arguments, instead of the chronological age, to measure the time since entering the stage (also called age within stage). Taking a mature individual with chronological age η who matures at chronological age s for example, this individual develops to the mature stage at I*-stage age* s and has M*-stage age* $\eta - s$.

3.2.1 Structured population model in integral form

Individuals in the immature stage I at time t include those born at a previous time s, surviving to time t with survival probability $\Pi_I(t-s)$ and staying in the stage with probability $P_I(t-s)$, as well as those introduced at initial time but still be alive and staying in the stage.

These arguments lead to the following integral form for the population size of immatures:

$$I(t) = \int_0^t \underbrace{B(M(s))}_{\text{born at time s}} \overbrace{P_I(t-s)}^{\text{stay in the stage}} \underbrace{\Pi_I(t-s)}_{\text{survival}} ds + \underbrace{I_0(t)}_{\text{remaining immatures}} . \tag{3.1}$$

Here the birth rate $B(M(t))$ at time t is a function of the population size of reproductive stage $M(t)$. The size of immatures that were introduced at the initial time and still stay in the stage is

$$I_0(t) = I(0)P_I(t)\Pi_I(t).$$

The dynamic evolution of the matured population size $M(t)$ can be depicted in Figure 3.1 with consideration of birth, survival and stage progression from the previous I stage, as well as development to a consequent old stage. Individuals in the mature stage M at time t include (i) those entering the stage at time η, surviving in the stage with survival probability $\Pi_M(t-\eta)$ and staying in the stage with stage distribution function $P_M(t-\eta)$, and (ii) those mature individuals stay in the stage from the initial time or those developed from initially introduced immatures ($M_0(t)$ in equation (3.2)). Please note that individuals entering the M-stage at time η have M-stage age $t-\eta$. Furthermore, individuals entering to the mature stage at time η is exactly those born at time $s \leq \eta$, surviving through the immature stage with probability $\Pi_I(\eta - s)$ and maturing at time η at rate $-P_I'(\eta - s)$ (these individuals entering the mature stage have the I-stage age $\eta - s$). Here, we should mention that the development rate of immature individuals with I-stage age a is given by the derivative $-P_I'(a)$. This term in the form of the probability density function can be derived from the following observations: An individual leaves I-stage and enters to the M-stage during the age interval $(a, a + \Delta a)$ with probability $P_I(a) - P_I(a + \Delta a)$. Taking the limit when Δa goes to zero, the individuals with I-stage age a develop to M-stage at rate $-P_I'(a)$. These arguments give rise to the following equation

$$\begin{aligned} M(t) & \\ =& \int_0^t \int_0^\eta \underbrace{B(M(s))}_{\text{birth at } s} \overbrace{(-P_I'(\eta - s))}^{\text{enter } M\text{-stage at } \eta} \underbrace{\Pi_I(\eta - s)}_{\text{survive to } \eta \text{ in } I\text{-stage}} ds \underbrace{P_M(t-\eta)}_{\text{stay in } M\text{-stage}} \overbrace{\Pi_M(t-\eta)}^{\text{survive in } M\text{-stage}} d\eta \\ +& \underbrace{M_0(t)}_{\substack{\text{remained or developed from} \\ \text{initially introduced } I}} \end{aligned} \tag{3.2}$$

The term $M_0(t)$ can be expressed as

$$M_0(t) = M(0)P_M(t)\Pi_M(t) + I(0) \int_0^t \Pi_I(\eta)(-P_I'(\eta))\Pi_M(t-\eta)P_M(t-\eta)d\eta, \tag{3.3}$$

with $M(0)P_M(t)\Pi_M(t)$ capturing the size of remaining mature individuals introduced at time 0 and $I(0)\int_0^t \Pi_I(u)(-P_I'(u))\Pi_M(t-u)P_M(t-u)du$ measuring the size of mature individuals developed from immatures introduced at time 0. On the other hand, if we introduce the following term to represent the maturation rate at time η

$$F(\eta) = \int_0^\eta B(M(s))(-P_I'(\eta - s))\Pi_I(\eta - s)ds + I(0)\Pi_I(\eta)(-P_I'(\eta)), \tag{3.4}$$

then we can rewrite the equations (3.2) and (3.3) into

$$M(t) = \int_0^t \underbrace{F(\eta)}_{\text{maturation rate at time } \eta} \overbrace{\Pi_M(t-\eta)}^{\text{survive in } M\text{-stage}} \underbrace{P_M(t-\eta)}_{\text{stay in } M\text{-stage}} d\eta + \underbrace{M(0)P_M(t)\Pi_M(t)}_{\text{remaining mature individuals}}. \tag{3.5}$$

If one regards the maturation rate as the "birth rate" to the mature stage, then $M(t)$ equation (3.5) takes a similar form as $I(t)$ equation (3.1). We wold like to remark that the stage structured models in integral form go back to Lotka [119]. The model derivation was rigorously presented in [180, Chapter 13] by careful consideration of the movement through a stage, of stage contents, stage input and stage outputs, which also relaxes the differentiability assumption on $P_I(a)$ by using Stieltjes integrals.

Since the stage duration distribution is our main focus of the current study, we take simple exponential distributions for the survival functions $\Pi_I(a)$ and $\Pi_M(a)$, that is

$$\Pi_I(a) = e^{-\mu_I a} \text{ and } \Pi_M(a) = e^{-\mu_M a} \tag{3.6}$$

for individual staying with stage age a in the I-stage and M-stage, respectively. Parameters μ_I and μ_M denote the death rates in immature and mature stages. When the stage duration distributions take some ecologically justified functions, the integral stage-structured model (3.1) and (3.2) can be rewritten into ordinary differential equations with/without time delays. In the following, gamma and Dirac distributions will be discussed. However, we should mention that other stage length distributions would be more appropriate in some scenarios, for example, the distribution of the time duration from infection to disease death is better fitted by a lognormal distribution than by a Gamma distribution [76] and Weibull distributions. More interesting investigations on log-normally distributed stage durations can be found in [76] and [180, Section 12.8].

(I) Gamma stage duration distribution

Assume the stage duration follows gamma distribution, then the probabilities of an individual with stage age a remaining in each stage are given by

$$P_I(a) = G^n_{n\lambda}(a) = \sum_{j=1}^{n} \frac{(n\lambda a)^{j-1} e^{-n\lambda a}}{(j-1)!} \tag{3.7}$$

and

$$P_M(a) = G^m_{m\gamma}(a) = \sum_{i=1}^{m} \frac{(m\gamma a)^{i-1} e^{-m\gamma a}}{(i-1)!} \tag{3.8}$$

with shape and rate parameter sets $(n, n\lambda)$ and $(m, m\gamma)$ respectively. It should be highlighted that age a is not chronological age, but the stage-specific age for the actual amount of time an individual has been alive in the I and M-stages respectively.

With the exponential survival probability for immatures, we have

$$I_0(t) = I(0)P_I(t)\Pi_I(t) = I(0)e^{-\mu_I t}\sum_{j=1}^{n}\frac{(n\lambda t)^{j-1}e^{-n\lambda t}}{(j-1)!}.$$

Substituting (3.7) into the $I(t)$ equation (3.1) gives

$$\begin{aligned}
&I(t)\\
=&\int_0^t B(M(s))e^{-\mu_I(t-s)}\sum_{j=1}^{n}\frac{(n\lambda(t-s))^{j-1}e^{-n\lambda(t-s)}}{(j-1)!}ds + I(0)e^{-\mu_I t}\sum_{j=1}^{n}\frac{(n\lambda t)^{j-1}e^{-n\lambda t}}{(j-1)!}\\
=&\sum_{j=1}^{n}\left(\int_0^t B(M(s))e^{-\mu_I(t-s)}\frac{(n\lambda(t-s))^{j-1}e^{-n\lambda(t-s)}}{(j-1)!}ds + I(0)e^{-\mu_I t}\frac{(n\lambda t)^{j-1}e^{-n\lambda t}}{(j-1)!}\right)\\
=&\sum_{j=1}^{n} I_j(t),
\end{aligned}$$

where

$$I_j(t) = \int_0^t B(M(s))e^{-(\mu_I+n\lambda)(t-s)}\frac{(n\lambda(t-s))^{j-1}}{(j-1)!}ds + I_{j0}(t), \quad 1 \le j \le n \tag{3.9}$$

with $I_{j0}(t) = I(0)e^{-(\mu_I+n\lambda)t}\frac{(n\lambda t)^{j-1}}{(j-1)!}$. Using these sub-stage variables $I_j(t)$, a differential equation system can be derived as follows by taking derivative of each $I_j(t)$ with respect to t:

$$\begin{aligned}
I_1'(t) &= B(M(t)) - (n\lambda + \mu_I)\left(\int_0^t B(M(s))e^{-(\mu_I+n\lambda)(t-s)}ds + I(0)e^{-(\mu_I+n\lambda)t}\right)\\
&= B(M(t)) - (n\lambda + \mu_I)I_1(t),
\end{aligned}$$

and for $2 \le j \le n$,

$$
\begin{aligned}
&I_j'(t)\\
=&B(M(t))e^{-\mu_I\cdot 0}\frac{(n\lambda\cdot 0)^{j-1}e^{-n\lambda\cdot 0}}{(j-1)!}+\int_0^t B(M(s))\frac{d}{dt}\left(e^{-(\mu_I+n\lambda)(t-s)}\frac{(n\lambda(t-s))^{j-1}}{(j-1)!}\right)ds\\
&+I(0)\frac{d}{dt}\left(e^{-(\mu_I+n\lambda)(t-s)}\frac{(n\lambda t)^{j-1}}{(j-1)!}\right)\\
=&-(\mu_I+n\lambda)\left[\int_0^t B(M(s))\frac{(n\lambda(t-s))^{j-1}}{(j-1)!}ds+I(0)(e^{-(\mu_I+n\lambda)t}\frac{(n\lambda t)^{j-1}}{(j-1)!})\right]\\
&+n\lambda\left[\int_0^t B(M(s))e^{-(\mu_I+n\lambda)(t-s)}\frac{(n\lambda(t-s))^{j-2}}{(j-2)!}ds+I(0)e^{-(\mu_I+n\lambda)t}\frac{(n\lambda(t-s))^{j-2}}{(j-2)!}\right]\\
=&n\lambda I_{j-1}(t)-(n\lambda+\mu_I)I_j(t).
\end{aligned}
$$

Note that the probability density function for gamma distribution $P_I(t)$ satisfies

$$
-P_I'(a)=n\lambda\frac{(n\lambda a)^{n-1}e^{-n\lambda a}}{(n-1)!}
$$

The maturation rate in (3.4) becomes

$$
\begin{aligned}
&F(t)\\
=&\int_0^t n\lambda\left[\frac{(n\lambda a)^{n-1}e^{-n\lambda a}}{(n-1)!}\right]B(M(t-a))e^{-\mu_I a}da-n\lambda\frac{(n\lambda t)^{n-1}e^{-n\lambda t}}{(n-1)!}e^{-\mu_I t}I(0)\\
=&n\lambda I_n(t).
\end{aligned}
$$

The equation for mature stage (3.5) can be rewritten into

$$
\begin{aligned}
&M(t)\\
=&\int_0^t F(\eta)P_M(t-\eta)\Pi_M(t-\eta)d\eta+M(0)P_M(t)\Pi_M(t)\\
=&\int_0^t F(\eta)e^{-(\mu_M+m\gamma)(t-\eta)}\sum_{i=1}^{m}\frac{(m\gamma(t-\eta))^{i-1}}{(i-1)!}d\eta+M(0)e^{-(\mu_M+m\gamma)t}\sum_{i=1}^{m}\frac{(m\gamma t)^{i-1}}{(i-1)!}\\
=&\sum_{i=1}^{m}M_i(t).
\end{aligned}
$$

Similar arguments as those for $I_j(t)$ lead to a series of equations for variables of mature individuals in each sub-stage:

$$
\begin{aligned}
M_1^{'}(t) =& F(t) - (\mu_M + m\gamma)M_1(t) = n\lambda I_n(t) - (\mu_M + m\gamma)M_1(t), \\
M_i^{'}(t) =& m\gamma M_{i-1}(t) - (m\gamma + \mu_M)M_i(t), \ \ 1 < i \leq m.
\end{aligned}
$$

Therefore, by introducing sub-stage variables $I_j(t)$ and $M_i(t)$, a closed ordinary differential equation model can be derived from the integral form (3.1) and (3.2) when the stage duration distributions follow gamma distributions in (3.7) and (3.8):

$$
\begin{aligned}
\frac{dI_1(t)}{dt} =& B(M(t)) - (n\lambda + \mu_I)I_1(t), \\
\frac{dI_j(t)}{dt} =& n\lambda I_{j-1}(t) - (n\lambda + \mu_I)I_j(t), \ 1 < j \leq n, \\
\frac{dM_1(t)}{dt} =& n\lambda I_n(t) - (\mu_M + m\gamma)M_1(t), \\
\frac{dM_i(t)}{dt} =& m\gamma M_{i-1}(t) - m\gamma M_i(t) - \mu_M M_i(t), \ 1 < i \leq m.
\end{aligned}
\tag{3.10}
$$

(II) Dirac stage duration distribution

The Dirac stage distribution is suitable to describe the case when individuals entering a specific stage together are assumed to undergo identical development time which equal to the mean development delay while omitting variances in the stage duration [57]. For the convenience of illustration, we simply assume that $P_M(\xi) \equiv 1$ for all M-stage age ξ, that is, the mature individuals, if alive, will always stay in the stage. The probability function for immature stage duration with mean value τ can be expressed as

$$
P_I(a) = \begin{cases} 1, & 0 \leq a \leq \tau \\ 0, & a > \tau. \end{cases}
$$

This means alive individuals with I-stage age smaller than τ always stay in I-stage, while those with age larger than τ develop to M-stage. Please note that $P_I(a)$ is not differentiable. However, for notational simplicity, we use the concept of Dirac delta function $\delta(x)$

to represent its probability density function. Arguments to deal with non-differentiable sojourn functions can be found in [180, Chapter 13]. We consider the case when $t > \tau$ (by resetting the initial timing) and therefore, all immature individuals introduced at time 0 will either die or develop to the M-stage after time t, that is $I_0(t) = 0$ for all $t > \tau$. The assumption $t > \tau$ also implies $M_0(t) = e^{-\mu_M t}M(0) + I(0)e^{-(\mu_I\tau+\mu_M(t-\tau))}$. Then we have,

$$I(t) = \int_0^t B(M(s))e^{-\mu_I(t-s)}P_I(t-s)ds + I_0(t) = \int_{t-\tau}^t B(M(s))e^{-\mu_I(t-s)}ds,$$

which can be written into a differential equation

$$\begin{aligned} I'(t) =& B(M(t)) - \mu_I \int_{t-\tau}^t B(M(s))e^{-\mu_I(t-s)}ds - B(M(t-\tau))e^{-\mu_I\tau} \\ =& B(M(t)) - \mu_I I(t) - B(M(t-\tau))e^{-\mu_I\tau}. \end{aligned}$$

The equation (3.2) for $M(t)$ now becomes

$$\begin{aligned} & M(t) \\ =& \int_0^t \int_0^\eta B(M(s))(-P_I'(\eta-s))e^{-\mu_I(\eta-s)}ds e^{-\mu_M(t-\eta)}d\eta + e^{-\mu_M t}M(0) \\ & + I(0)e^{-(\mu_I\tau+\mu_M(t-\tau))} \\ =& \int_0^t \int_0^\eta B(M(s))\delta(\eta-s-\tau)e^{-\mu_I(\eta-s)}ds e^{-\mu_M(t-\eta)}d\eta + e^{-\mu_M t}M(0) \\ & + I(0)e^{-(\mu_I\tau+\mu_M(t-\tau))} \\ =& \int_\tau^t B(M(\eta-\tau))e^{-\mu_I\tau}e^{-\mu_M(t-\eta)}d\eta + e^{-\mu_M t}M(0) + I(0)e^{-(\mu_I\tau+\mu_M(t-\tau))}. \end{aligned}$$

Please note $\delta(\cdot)$ is the corresponding Dirac delta function. Taking derivative of $M(t)$, we obtain

$$M'(t) = B(M(t-\tau))e^{-\mu_I\tau} - \mu_M M(t).$$

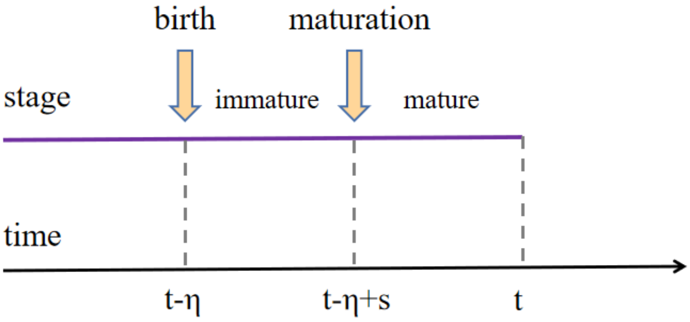

Figure 3.2: Dynamic process involving birth, survival and stage progression for a typical mature individual with chronological age η at time t. This individual matures at I-stage age s and has M-stage age $\eta - s$.

(III) Basic reproduction number and initial growth rate

The integral form can be written into other equivalent forms through different biological arguments on stage progression, birth and survival. If we consider the stage progression of individuals as illustrated in Figure 3.2, then the integral form (3.2) can be written into

$$M(t)$$

$$= \int_0^t \underbrace{B(M(t-\eta))}_{\text{birth}} \overbrace{\int_0^\eta \underbrace{\Pi_I(s)}_{\text{survive through } I\text{-stage}} \underbrace{(-P_I'(s))}_{\text{enter } M\text{-stage}} \underbrace{P_M(\eta-s)\Pi_I(\eta-s)}_{\text{alive and stay in } M\text{-stage}} \, ds}^{\text{probability of entering and staying alive in } M\text{-stage with chronological age } \eta} \, d\eta + M_0(t)$$

with $M_0(t)$ given in (3.3). In this expression, the integral term accounts individuals having chronological age η at time t (those born at a previous time $t - \eta$ with $\eta \in [0, t]$) and successfully entering and staying in the M-stage alive.

It is easy to obtain the net reproduction number $\mathcal{R}_0$ with the following renew argument for the Volterra integral form (see for example [101]). In fact, if we assume the population size is very small and the density-dependent regulations on the birth rate function $B(M(t))$ can be ignored, then the birth rate at time t can be approximated by

$$B(M(t)) \approx b \cdot M(t)$$

with a constant per-capita birth rate b. Let

$$\Phi(\eta) = b \times \underbrace{\int_0^\eta -P_I^{'}(s)\Pi_I(s)P_M(\eta - s)\Pi_M(\eta - s)ds}_{\substack{\text{the probability that an individual with chronological age } \eta \\ \text{developing to and staying in the } M\text{-stage}}},$$

then we have the following Volterra integral form for the population size of the M-stage

$$M(t) = \int_0^t M(t-\eta)\Phi(\eta)d\eta + M_0(t).$$

The net reproduction number in demography can be defined as

$$\mathcal{R}_0 = \int_0^\infty \Phi(\eta)d\eta.$$

Suppose $P_I(x)$ takes gamma distribution function (3.7) and $P_M(x) = 1$. By taking the exponential survival probability (3.6), we have

$$\begin{aligned}
\Phi(\eta) =& b\int_0^\eta -\sum_{j=1}^{n}\left(\frac{n\lambda(n\lambda s)^{j-2}e^{-n\lambda s}}{(j-2)!} - \frac{n\lambda(n\lambda s)^{j-1}e^{-n\lambda s}}{(j-1)!}\right) e^{-\mu_I s}e^{-\mu_M(\eta - s)}ds \\
=& b\int_0^\eta \frac{n\lambda(n\lambda)^{n-1}s^{n-1}}{(n-1)!}e^{-(n\lambda+\mu_I-\mu_M)s}e^{-\mu_M\eta}ds \\
=& b \cdot e^{-\mu_M\eta} \cdot \frac{(n\lambda)^n}{n!}\int_0^\eta e^{-(n\lambda+\mu_I-\mu_M)s}ds^n \\
=& \frac{bn(n\lambda)^n e^{-\mu_M\eta}}{n!}\left[e^{-(n\lambda+\mu_I-\mu_M)\eta}\sum_{i=0}^{n-1}(-1)^{n-1-i}\frac{(n-1)!\cdot\eta^i}{i!\cdot(-(n\lambda+\mu_I-\mu_M))^{n-i}}\right. \\
& - (-1)^{n-1}\cdot\frac{(n-1)!}{(-(n\lambda+\mu_I-\mu_M))^n},
\end{aligned}$$

which implies that

$$\begin{aligned}
\mathcal{R}_0 =& \frac{bn(n\lambda)^n}{n!}\int_0^\infty e^{-(n\lambda+\mu_I)\eta}\sum_{i=0}^{n-1}(-1)^{n-1-i}\frac{(n-1)!\cdot\eta^i}{i!\cdot(-(n\lambda+\mu_I-\mu_M))^{n-i}}d\eta \\
&+\frac{b(-n\lambda)^n}{(-(n\lambda+\mu_I-\mu_M))^n}\int_0^\infty e^{-\mu_M\eta}d\eta \\
=& b\cdot(n\lambda)^n\cdot\sum_{i=0}^{n-1}\frac{-1}{(n\lambda+\mu_I)^{i+1}(n\lambda+\mu_I-\mu_M)^{n-i}}+\frac{b}{\mu_M}\cdot\frac{(n\lambda)^n}{(n\lambda+\mu_I-\mu_M)^n} \\
=& \frac{b\cdot(n\lambda)^n}{(n\lambda+\mu_I)^{n+1}}\left[\sum_{i=0}^{n-1}\frac{-1}{(\frac{n\lambda+\mu_I-\mu_M}{n\lambda+\mu_I})^{n-i}}+\frac{(n\lambda+\mu_I)^{n+1}}{\mu_M(n\lambda+\mu_I-\mu_M)^n}\right] \\
=& \frac{b}{\mu_M}\left(\frac{n\lambda}{n\lambda+\mu_I}\right)^n.
\end{aligned}$$

For the simple case that the immature stage duration follows an exponential distribution with mean duration $1/\lambda$, namely $P_I(a)=e^{-\lambda a}$, then

$$\mathcal{R}_0=\frac{b\lambda}{\mu_M(\lambda+\mu_I)}.$$

When $P_I(a)$ takes the Dirac distribution with mean duration τ and $P_M(a)\equiv 1$ as those in Subsection 3.2.1 (II), we have

$$\Phi(\eta)=b\times\int_0^\eta -P_I'(s)e^{-\mu_I s}e^{-\mu_M(\eta-s)}ds=b\times\int_0^\eta \delta(s-\tau)e^{-\mu_I s}e^{-\mu_M(\eta-s)}ds,$$

and therefore,

$$\mathcal{R}_0=\int_0^\infty\Phi(\eta)d\eta=\int_\tau^\infty be^{-\mu_I\tau}e^{-\mu_M(\eta-\tau)}d\eta=\frac{be^{-\mu_I\tau}}{\mu_M}.$$

By seeking the solution to the following characteristic equation (Euler-Lotka equation)

$$\int_0^\infty e^{-r\eta}\Phi(\eta)d\eta=1,$$

one can determine the initial growth rate (also called intrinsic growth rate or Malthusian parameter [93]). Let $f(r) = \int_0^\infty e^{-r\eta}\Phi(\eta)d\eta$, and assume there exists a real number $\hat{r}$ such that $1 \leq f(\hat{r}) < \infty$ (for most biological models, we may always find such a negative $\hat{r}$). Then it is interesting to observe the following facts: (i) $f(r)$ is a nonincreasing and continuous function of r, (ii) $f(\hat{r}) \geq 1$ and (iii) $\lim\limits_{r\to\infty} f(r) = 0$. Therefore, the above equation $f(r) = 1$ admits a unique real root $r = r_0 \in [\hat{r}, \infty)$, which is the intrinsic growth rate. Using the identity that $\mathcal{R}_0 = f(0)$ and the monotonicity of $f(r)$, it is evident that the sign of r_0 is same as that of $\mathcal{R}_0 - 1$. Furthermore, the monotonicity $f(r)$ and uniqueness of the real root to the equation $f(r) = 1$ facilitate designing efficient numerical algorithms, such as the bisection method algorithm, to compute the initial growth rate.

3.2.2 Structured model with partial differential equations

Assume $u(a,t)$ and $v(\xi,t)$ are the population densities of immature and mature individuals at time t with stage-specific age a and ξ, respectively. Then sizes of the populations in the immature and mature stages can be expressed as

$$I(t) = \int_0^\infty P_I(a)u(a,t)da \quad \text{and} \quad M(t) = \int_0^\infty P_M(\xi)v(\xi,t)d\xi,$$

where $P_I(a)$ and $P_M(\xi)$ represent the probability functions of individuals with stage-age a staying in the immature and mature stages, respectively. On the other hand, the following partial differential equation, originally proposed by McKendrick [136] and widely used in recent studies such as [54, 100, 112, 125], can be employed to describe the dynamics of age-dependent variables

$$\begin{aligned} &\frac{\partial u(a,t)}{\partial a} + \frac{\partial u(a,t)}{\partial t} = -\mu_I u(a,t), \\ &u(a,0) = u_0(a), \end{aligned} \tag{3.11}$$

and

$$\begin{aligned} &\frac{\partial v(\xi,t)}{\partial \xi} + \frac{\partial v(\xi,t)}{\partial t} = -\mu_M v(\xi,t), \\ &v(\xi,0) = v_0(\xi) \end{aligned} \tag{3.12}$$

with natural death rates μ_I and μ_M in each stage.

It is reasonable to assume that the density of the immatures $u(0,t)$ with age 0 at time t is exactly the birth rate, that is

$$u(0,t) = B(M(t)).$$

The density of mature individuals with M-stage age 0 at time t is that of immature individuals developing to the M-stage at time t, that is

$$v(0,t) = \int_0^\infty [-P_I'(a)]u(a,t)da,$$

where $-P_I'(a)$ represents the development rate of immature individuals with I-stage age a, as discussed in Section 3.2.1.

(I) Gamma stage duration distribution

When the stage duration follows gamma distributions as in (3.7) and (3.8), we have

$$v(0,t) = \int_0^\infty [-P_I'(a)]u(a,t)da = \int_0^\infty n\lambda \left[\frac{(n\lambda a)^{n-1}e^{-n\lambda a}}{(n-1)!}\right] u(a,t)da = n\lambda I_n(t).$$

By introducing sub-stage population densities as those in subsection 3.2.1:

$$I_j(t) = \int_0^\infty \frac{(n\lambda a)^{j-1}e^{-n\lambda a}}{(j-1)!} u(a,t)da,\ 1 \le j \le n,$$

and

$$M_i(t) = \int_0^\infty \frac{(m\gamma\xi)^{i-1}e^{-m\gamma\xi}}{(i-1)!} v(\xi,t)d\xi,\ 1 \le i \le m,$$

the immature population size and the matured population size can be represented as

$$I(t) = \sum_{j=1}^{n} I_j(t) \quad \text{and} \quad M(t) = \sum_{i=1}^{m} M_i(t), \text{ respectively.}$$

Differentiating each $I_j(t)$, $M_i(t)$, and using (3.11) and (3.12), we can obtain a stage-structured model in ordinary differential equation form, which is same as system (3.10).

(II) Dirac stage duration distribution

In this subsection, we assume the stage distribution follows a Dirac distribution. Similar to those in Subsection 3.2.1 (II), we assume $P_M(\xi) \equiv 1$ for all M-stage age ξ and the distribution function for the immature stage has a mean duration τ. In this case,

$$v(0,t) = \int_0^\infty [-P_I'(a)]u(a,t)da = \int_0^\infty \delta(a-\tau)u(a,t)da = u(\tau,t)$$

and the sizes of immature $I(t)$ and mature $M(t)$ individuals can be expressed as

$$I(t) = \int_0^\tau u(a,t)da \quad \text{and} \quad M(t) = \int_0^\infty v(\xi,t)d\xi,$$

respectively. Therefore, (3.11) gives

$$\begin{aligned}\frac{dI(t)}{dt} &= \frac{d}{dt}\left(\int_0^\tau u(a,t)da\right) = \int_0^\tau \left(-\frac{\partial u(a,t)}{\partial a} - \mu_I u(a,t)\right) da \\ &= -u(\tau,t) + u(0,t) - \mu_I I(t).\end{aligned}$$

Similarly, we have the following equation for the matured population size $M(t)$:

$$\frac{dM(t)}{dt} = \int_0^\infty \left(-\frac{\partial v(\xi,t)}{\partial \xi} - \mu_M v(\xi,t)\right) d\xi = u(\tau,t) - \mu_M M(t).$$

It remains to find the maturation rate $u(\tau,t)$, which can be achieved by integration along characteristics. Let $V^s(t) = u(t-s,t)$, then we have

$$\frac{d}{dt}V^s(t) = -\mu_I V^s(t)$$

and $V^s(t) = e^{-\mu_I(t-t_0)}V^s(t_0)$. If $t \geq \tau$, setting $s = t-\tau$ and $t_0 = t-\tau$ gives

$$u(\tau,t) = V^{t-\tau}(t) = e^{-\mu_I \tau}V^{t-\tau}(t-\tau) = e^{-\mu_I \tau}u(0,t-\tau) = B(M(t-\tau))e^{-\mu_I \tau}.$$

If $t < \tau$, let $s = t-\tau$ and $t_0 = 0$, then

$$u(\tau,t) = V^{t-\tau}(t) = e^{-\mu_I t}V^{t-\tau}(0) = e^{-\mu_I t}u(\tau-t,0).$$

Therefore, the stage-structured population dynamics with Dirac distribution for immature stage duration can be described by two sets of systems on different time intervals respectively:

$$\left.\begin{aligned}\frac{dI(t)}{dt} =& B(M(t)) - u(\tau-t,0)e^{-\mu_I \tau} - \mu_I I(t)\\ \frac{dM(t)}{dt} =& u(\tau-t,0)e^{-\mu_I \tau} - \mu_M M(t)\end{aligned}\right\} \text{for } t \in [0,\tau]$$

and

$$\left.\begin{aligned}\frac{dI(t)}{dt} =& B(M(t)) - B(M(t-\tau))e^{-\mu_I \tau} - \mu_I I(t)\\ \frac{dM(t)}{dt} =& B(M(t-\tau))e^{-\mu_I \tau} - \mu_M M(t)\end{aligned}\right\} \text{for } t \in [\tau,\infty) \tag{3.13}$$

It should be noted that the variable $M(t)$ can be decoupled from the whole model system. Moreover, a scalar delay differential equation (the second equation of (3.13)) would be sufficient to reflect the long term dynamics of mature stage [158] with suitable initial value specified for $M(\theta)$ with $\theta \in [-\tau,0]$.

3.2.3 Remarks on two modeling approaches

In Subsections 3.2.1 and 3.2.2, two modeling approaches for physically structured population growth are presented in the form of integral system (equations (3.1) and (3.2)) and partial differential system (equations (3.11) and (3.12)). The relationship between the integral equation approach and the PDE approach was established in [180, Chapter 13]. When the stage duration follows a gamma distribution, both modeling frameworks can be reduced into a system of ordinary differential equations, while a system of delay differential equations can be derived when the stage distribution follows a Dirac distribution. The reduction, without losing relevant growth information, makes it easier to investigate the population dynamics. The possibility of reducing a physiologically structured population model, such as those in Subsection 3.2.1, to an ordinary differential equation model has been investigated [60].

The integral system can be naturally formulated through ecological arguments in terms of birth, stage progression and survival. Furthermore, the net reproduction of the population growth can be intuitively derived by using the integral equation nature of the system, with each term having clear biological interpretations. Moreover, the initial growth rate can be easily defined with the help of the linearized system, and its existence and uniqueness can be established through simple mathematical arguments. As a byproduct, the important relationship between the net reproduction number $\mathcal{R}_0$ and the initial growth rate r_0 can be easily established: the sign of $\mathcal{R}_0 - 1$ is same as that of r_0.

It should be noted that a general birth function $B(M(t))$ is assumed in the last two subsections, which can easily accommodate the density-dependent self-regulation on the birth rate. However, the density-independence assumptions are imposed for the survivorship and stage-to-stage progression. When it comes to relax the density-independence assumptions on the stage-progression function $P_X(t)$ and survivorship $\Pi_X(t)$ for the immature $(X = I)$ and mature $(X = M)$ stages, it may become challenging to propose appropriate probability functions. In this sense, the integral framework may not be a convenient way to describe the structured population size when more complicated density-dependent self-regulation are considered, as the model (3.14) presented later and those reviewed in the coming Section 3.3. Furthermore, an integral system can also be derived from a state-structured partial differential equation when the related survival and stage-progression functions can be formulated from the corresponding evolution system [60].

To conclude this section, we show that the age-structured partial differential system can be extended to accommodate the density-dependent survivorship due to intra-specific competition when the gamma distribution is assumed. In this scenario, equations (3.11) and (3.12) can be revised to account excess density-dependent mortality rate due to competition:

$$\begin{aligned}\frac{\partial u(a,t)}{\partial a}+\frac{\partial u(a,t)}{\partial t}=&-\mu_I u(a,t)-f(I(t))u(a,t),\\ \frac{\partial v(\xi,t)}{\partial \xi}+\frac{\partial v(\xi,t)}{\partial t}=&-\mu_M v(\xi,t)-g(M(t))v(\xi,t),\\ u(0,t)=B(M(t)),\ u(a,0)=u_0(a),\ v(0,t)=&\,n\lambda I_n(t)\text{ and }v(\xi,0)=u_0(\xi),\end{aligned}\tag{3.14}$$

where functions $f(\cdot)$ and $g(\cdot)$ represent the excess death rates due to intraspecific competition, dependent on total population sizes of the respective stage. Differentiating each sub-stage variable in Subsection 3.2.2 for immatures $I_j(t)$, we have

$$\frac{dI_1(t)}{dt}=B(M(t))-(n\lambda+\mu_I+f(I(t)))I_1(t),$$

and

$$\frac{dI_j(t)}{dt}=n\lambda I_{j-1}(t)-(n\lambda+\mu_I+f(I(t)))I_j(t),\ 1<j\le n.$$

Similarly, for the sub-stages of mature individuals, we have

$$\begin{aligned}\frac{dM_1(t)}{dt}=&-e^{-m\gamma\xi}v(\xi,t)\big|_0^\infty-(m\gamma+\mu_M+g(M(t)))\int_0^\infty e^{-m\gamma\xi}v(\xi,t)d\xi\\ =&n\lambda I_n(t)-(m\gamma+\mu_M+g(M(t)))M_1(t),\end{aligned}$$

and

$$\frac{dM_i(t)}{dt} = m\gamma M_{i-1}(t) - (m\gamma + \mu_M + g(M(t)))M_i(t),\ 1 < i \leq m.$$

In summary, when intraspecific competition induces excess mortality on immatures and the immature stage duration follows a gamma distribution, an ordinary differential system can be reformulated from the age-structured partial differential equation modeling approach:

$$\begin{aligned}
\frac{dI_1(t)}{dt} &= B(M(t)) - (n\lambda + \mu_I + f(I(t)))I_1(t),\\
\frac{dI_j(t)}{dt} &= n\lambda I_{j-1}(t) - (n\lambda + \mu_I + f(I(t)))I_j(t),\ 1 < j \leq n,\\
\frac{dM_1(t)}{dt} &= n\lambda I_n(t) - (m\gamma + \mu_M + g(M(t)))M_1(t),\\
\frac{dM_i(t)}{dt} &= m\gamma M_{i-1}(t) - (m\gamma + \mu_M + g(M(t)))M_i(t),\ 1 < i \leq m.
\end{aligned} \tag{3.15}$$

3.3 Stage structured model with Dirac distribution and intraspecific competition

This section is devoted to review some population models under Dirac distribution for immature stage duration and intraspecific competition. In particular, we are interested in presenting different types of models that can be formulated under various assumptions on the effect of immature competition.

3.3.1 Excess mortality due to competition among the same age cohort

Considering the immature competition of the same age, Gourley and Liu [87] explored the following evolution equation for the population density $u(a,t)$ of age a at time t

$$\begin{aligned}
\frac{\partial u(a,t)}{\partial a} + \frac{\partial u(a,t)}{\partial t} &= -\mu_I u(a,t) - T(u(a,t)),\ \ 0 < a \leq \tau\\
\frac{\partial u(a,t)}{\partial a} + \frac{\partial u(a,t)}{\partial t} &= -\mu_M u(a,t),\ \ a > \tau.
\end{aligned} \tag{3.16}$$

In this model, the competitive effects between immatures are given by a nonlinear function $T(u(a,t))$, describing the influence of intraspecific competition among the immature individuals due to limited living space and resources. The competition among mature individuals is not taken into account.

By taking a similar arguments as those in Subsection 3.2.2 (II), $M(t)$-equation can be written as

$$\frac{dM(t)}{dt} = u(\tau, t) - \mu_M M(t).$$

To close this equation, it is essential to obtain the explicit form of the maturation rate $u(\tau, t)$, which can be found through the integration along characteristics. By introducing the function $u^\xi(a) = u(a, a+\xi)$, the authors obtained

$$\frac{du^\xi(a)}{da} = \left[\frac{\partial u(a,t)}{\partial a} + \frac{\partial u(a,t)}{\partial t}\right]_{t=a+\xi} = \left[-\mu_I u(a,t) - T(u(a,t))\right]_{t=a+\xi},$$

which implies that

$$\frac{du^\xi(a)}{da} = -\mu_I u^\xi(a) - T(u^\xi(a)),$$

and hence

$$\int_{u^\xi(0)}^{u^\xi(a)} \frac{d\eta}{\mu_I \eta + T(\eta)} = -a.$$

Here, $u^\xi(0) = u(0,\xi) = B(M(\xi))$. Choosing $a = \tau$ and $\xi = t - \tau$, the maturation rate $u(\tau, t)$ at time $t > \tau$ can be solved explicitly from

$$\int_{u(\tau,t)}^{B(M(t-\tau))} \frac{d\eta}{\mu_I \eta + T(\eta)} = \tau.$$

Since the function T: $(0, \infty) \to \mathbb{R}_+$ may possibly be nonlinear, it is impossible to obtain an explicit expression $u(\tau, t) = Q(B(M(t-\tau)))$ to illustrate the relationship between the maturation rate $u(\tau, t)$ at time t and birth rate $B(M(t-\tau))$ at time $t-\tau$. However, this relationship $y = Q(x)$ can be implicitly defined by

$$\int_{Q(x)}^{x} \frac{d\eta}{\mu_I \eta + T(\eta)} = \tau, \quad y > 0. \tag{3.17}$$

Moreover, the function $y = Q(x)$ is well-defined as $T(\cdot)$ is nonnegative and nondecreasing. Then

$$\frac{dM(t)}{dt} = Q(B(M(t-\tau))) - \mu_M M(t).$$

With this kind of competition in consideration, [87] shows that all solutions are bounded for any birth function $B(\cdot)$. Linearizing the model at a boundary equilibrium gives verifiable and biologically interpretable conditions for its stability. In what follows, we will present several models of this type.

(I) The case when $T(u(a,t)) = \beta_I (u(a,t))^2$

By specifying the nonlinear function as $T(u(a,t)) = \beta_I (u(a,t))^2$ in (3.16), Liu, Röst and Gourley [118] investigated the following model

$$\frac{\partial u(a,t)}{\partial a} + \frac{\partial u(a,t)}{\partial t} = -\mu_I u(a,t) - \beta_I (u(a,t))^2, \quad 0 < a < \tau \tag{3.18}$$

where β_I denotes the effect of intraspecific competition among immature individuals. In this case, it is possible to write down the function (3.17) explicitly. In fact, the new variable $u^\xi(a) = u(a, a+\xi)$ satisfies

$$\frac{d}{dt} u^\xi(a) = -\mu_I u^\xi(a) - \beta_I (u^\xi(a))^2,$$

which takes the form of a Bernoulli differential equation, with solution explicitly given by

$$u^\xi(a) = \frac{\mu_I u^\xi(0) e^{-\mu_I a}}{\mu_I + \beta_I u^\xi(0)(1 - e^{-\mu_I a})}.$$

Therefore, when $t > \tau$, setting $a = \tau$ and $\xi = t - \tau$ gives $u^{t-\tau}(0) = u(0, t - \tau) = B(M(t - \tau))$ and

$$u(\tau, t) = Q(B(M(t-\tau))) = \frac{\mu_I B(M(t-\tau))e^{-\mu_I \tau}}{\mu_I + \beta_I B(M(t-\tau))(1 - e^{-\mu_I \tau})}.$$

With this special nonlinear function $T(u(a,t)) = \beta_I (u(a,t))^2$, long term dynamics of $M(t)$ can be described by the following delay differential equation:

$$\frac{dM(t)}{dt} = \frac{\mu_I B(M(t-\tau))e^{-\mu_I \tau}}{\mu_I + \beta_I B(M(t-\tau))(1 - e^{-\mu_I \tau})} - \mu_M M(t).$$

(II) An alternative formulation for a delayed logistic equation

Arino, Wang and Wolkowicz [21] derived a model through a different approach with the aid of survival arguments for those being alive at time $t - \tau$ that are still alive at time t for the following evolution equation

$$\widetilde{N}'(t) = -\mu \widetilde{N}(t) - \kappa \widetilde{N}^2(t).$$

By the technique of separation of variables and integration from $t - \tau$ to t, they obtained

$$\widetilde{N}(t) = \frac{\mu \widetilde{N}(t-\tau)}{\mu e^{\mu\tau} + \kappa(e^{\mu\tau} - 1)\widetilde{N}(t-\tau)}.$$

Putting this density-dependent term into a logistic equation with a birth rate γ, the authors formulated an alternative logistic delay differential equation with time delay τ:

$$N'(t) = \frac{\gamma \mu N(t-\tau)}{\mu e^{\mu\tau} + \kappa(e^{\mu\tau} - 1)N(t-\tau)} - \mu N(t) - \kappa N^2(t). \tag{3.19}$$

It is shown that the population dies out when the delay is too large. The existence of a positive equilibrium, and its relationship with parameter values are further illustrated in [21].

(III) An alternative formulation for a distributed delayed logistic equation

Using a similar argument as that in [21], Lin, Wang and Wolkowicz [116] formulated a logistic equation with distributed delays. The time delay is distributed in line with a kernel function $k(s)$ with a mean delay τ, that is:

$$k(s) \geq 0, \quad \int_0^\infty k(s)ds = 1, \quad \int_0^\infty sk(s)ds = \tau.$$

Then the discrete delay logistic-type equation (3.19) can be extended to the following one:

$$N'(t) = \gamma \int_0^\infty \frac{\mu e^{-\mu s} N(t-s)k(s)}{\mu + \kappa(1-e^{-\mu s})N(t-s)} ds - \mu N(t) - \kappa N^2(t). \tag{3.20}$$

The delay kernel can take a variety of functions, such as Dirac delta function, uniform distribution, gamma distribution and tent distribution. When the kernel function is Dirac delta function, equation (3.20) is exactly the discrete delay case for equation (3.19). A threshold result for survival and extinction is established in [116]: the global attractivity of the unique positive equilibrium and the zero equilibrium are shown under different parameter regimes.

3.3.2 Excess mortality due to competition among the same stage

Considering the excess mortality due to intraspecific competition between individuals of the same life stage, Fang, Gourley and Lou [74] assumed the Dirac distribution for immatures for the model (3.14), copied as follows for easy reference:

$$\begin{aligned}
\frac{\partial u(a,t)}{\partial a} + \frac{\partial u(a,t)}{\partial t} &= -\mu_I u(a,t) - f(I(t))u(a,t), \qquad a \leq \tau \\
\frac{\partial u(a,t)}{\partial a} + \frac{\partial u(a,t)}{\partial t} &= -\mu_M u(a,t) - g(M(t))u(a,t), \quad a > \tau
\end{aligned}$$

with

$$u(0,t) = B(M(t)) \quad \text{and} \quad u(a,0) = u_0(a).$$

In this case, the sizes of individuals in each stage are

$$I(t) = \int_0^\tau u(a,t)da \quad \text{and} \quad M(t) = \int_\tau^\infty u(a,t)da.$$

Differential equations for two variables $I(t)$ and $M(t)$ when $t > \tau$ can be derived as

$$\begin{aligned}\frac{dI(t)}{dt} &= -u(\tau,t) + u(0,t) - \mu_I I(t) - f(I(t))I(t),\\ \frac{dM(t)}{dt} &= -u(\infty,t) + u(\tau,t) - \mu_M M(t) - g(M(t))M(t),\end{aligned} \tag{3.21}$$

where $u(0,t) = B(M(t))$ and $u(\infty,t) = 0$. The maturation rate $u(\tau,t)$ can be explicitly solved by integration along characteristics, which is

$$u(\tau,t) = V^{t-\tau}(t) = B(M(t-\tau))e^{-\mu_I\tau - \int_0^\tau f(I(t-\tau+\xi))d\xi} \text{ for } t > \tau.$$

It should be highlighted that (3.21) explicitly couples both variables $I(t)$ and $M(t)$ together, which is different from previous scalar delay differential equation for the population size of mature stage (such as those in Subsections 3.2.1 (II) and 3.2.2 (II), and Subsection 3.3.1). Furthermore, since the maturation rate $u(\tau,t)$ is a decreasing function of I as the function $f(\cdot)$ is assumed to be increasing, which brings novel challenges on theoretical analysis. In particular, stability analysis of equilibria becomes difficult due to the strong coupling of two state variables. A generic convergence result is established for small delays by using monotone dynamical systems theory and exponential ordering [74].

(I) Age-dependent larval competition model

Another larval competition model was proposed and studied in Liu, Röst and Gourley [118] as follows

$$\frac{\partial u(a,t)}{\partial a} + \frac{\partial u(a,t)}{\partial t} = -\mu_I u(a,t) - \epsilon u(a,t)\int_0^\tau p(\bar{a},a)u(\bar{a},t)d\bar{a}, \quad 0 < a < \tau. \tag{3.22}$$

In this model, ϵ characterizes the intensity of population competition among the immature individuals, and $p(\overline{a}, a)$ is an adjustable parameter to describe various competition types: (i) $p(\overline{a}, a)$ being a constant if an immature individual is likely to compete with all other immature individuals with the same competitive pressure, regardless of age; (ii) $p(\overline{a}, a) = 0$ as $\overline{a} < a$, implying that an immature individual only compete with older individuals; (iii) $p(\overline{a}, a) = \delta(\overline{a} - a)$ with a Dirac delta function $\delta(\cdot)$ if competition occurs among individuals in the same age, which was considered in (3.18).

To rewrite the model into an ordinary differential equation form with time delay, it is essential to find the maturation rate rate $u(\tau, t)$ by using the evolution of immature population density (3.22). It seems impossible to obtain explicit solutions for general cases, and the authors in [118] applied perturbation theory to seek the solution of the following two specific forms:

$$u(a,t) = u_0(a,t) + \epsilon u_1(a,t) + O(\epsilon^2) \text{ and } u(a,t) = u_0(a,t)\exp(-\epsilon u_1(a,t) + O(\epsilon^2)),$$

with $u_0(0, t) = B(M(t))$ and $u_1(0, t) = 0$. Integrating (3.22) along characteristics gives the maturation rate $u(\tau, t)$ when $t > \tau$, and two alternative models for the mature population $M(t)$ are given by

$$\begin{aligned}&\frac{dM(t)}{dt}\\ =&B(M(t-\tau))e^{-\mu_I\tau}\left[1-\epsilon\int_0^\tau\int_0^\tau p(\overline{a},s)B(M(s+t-\tau-\overline{a}))e^{-\mu_I\overline{a}}d\overline{a}ds\right]-\mu_M M(t)\end{aligned}$$

and

$$\begin{aligned}&\frac{dM(t)}{dt}\\ =&B(M(t-\tau))e^{-\mu_I\tau}\exp(-\epsilon\int_0^\tau\int_0^\tau p(\overline{a},s)B(M(s+t-\tau-\overline{a}))e^{-\mu_I\overline{a}}d\overline{a}ds)-\mu_M M(t).\end{aligned}$$

This model, proposed under the simple assumption that an individual larva experiences competition from other larvae during development, poses rich dynamics. In particular, the existence of multiple co-existing equilibria is shown in some parameter regimes.

3.3.3 Stage distribution regulated by population density

When the duration staying in the immature stage is regulated by the population density, it would be more convenient to use another variable x called “state” [93], which generalizes the concept of the age, to describe the population density evolution. Based on the fact that maturation can be measured to some extent by state, the maturity of an individual occurs when its state x achieves a fixed threshold l. Let $u(x,t)$ represent the population density of immature individuals of state x at time t, then immature population size $I(t)$ at time t counts all individuals with state variable x smaller than l, that is

$$I(t) = \int_0^l u(x,t)dx.$$

This new variable makes it possible to describe the case that the rate of change of the state x with respect to time is not a constant, but dependent on the population density (see equation (3.23)).

(I) A size-structured model with decreased development rate due to competition

Assuming all individuals at the immature stage compete for limited resources, which slows their development, Gourley, Liu and Lou [88] used the following equation to describe the rate of change for the length variable x at time t:

$$\frac{dx}{dt} = P(t, I(t)), \tag{3.23}$$

which relies both on time t and on the total number of immature population $I(t)$. Here, function $P(t,I)$ is decreasing on variable I and is dependent on time t to reflect the time-changing environmental impacts on development.

To derive the partial differential equation for $u(x,t)$ as that in (3.16), the authors used the following argument: After a period of δt, an immature individual will have developed a length of δx, namely

$$u(x+\delta t, t+\delta t) = u(x,t) - \mu_I u(x,t)\delta t,$$

which implies that

$$\frac{\partial u(x,t)}{\partial t} + P(t, I(t))\frac{\partial u(x,t)}{\partial x} = -\mu_I u(x,t),\ x \leq l \tag{3.24}$$

by a Taylor expansion. Taking derivative of $I(t)$ and using equation (3.24), one obtains

$$\frac{dI(t)}{dt} = -\mu_I I(t) + P(t, I(t))(i(0,t) - i(l,t)),$$

where $P(t, I(t))i(0,t)$ denotes the birth rate, that is $P(t, I(t))i(0,t) = B(M(t))$, and $P(t, I(t))i(l,t)$ denotes the maturation rate, which will be calculated in line with the birth rate at time $t - \tau(t)$. The term $u(x,t)$ relies on whether (x,t) is above or below the characteristic $x = X(t)$, where

$$X(t) = \int_0^t P(\xi, I(\xi))d\xi.$$

Introducing a parameter s such that $\frac{dt}{ds} = 1$, then $\frac{dx}{ds} = P(t, I(t))$. The parameter s is used to describe position along a particular characteristic and $s = 0$ corresponds to a boundary.

When $x \geq X(t)$, a characteristic $(x(s), t(s))$ meets the x-axis, which implies that $t = 0$ when $s = 0$. Setting $t(0) = 0$ obtains $x - x(0) = X(t)$. It follows from (3.24) that

$$\frac{d}{ds}u(x(s), t(s)) = -\mu_i u(x(s), t(s)),$$

which implies that

$$u(x(s), t(s)) = u(x(0), t(0))e^{-\mu_i s},$$

and thus

$$u(x,t) = u(x - X(t), 0)e^{-\mu_i t}, \;\; x \geq X(t).$$

When $x \leq X(t)$, a characteristic $(x(s), t(s))$ meets the x-axis, which implies that $x(0) = 0$ and $t = s + t(0)$. The corresponding s-value for a particular point (x, t) can be defined by

$$x = \int_{t(0)}^{t} P(\xi, I(\xi))d\xi = \int_{t-s}^{t} P(\xi, I(\xi))d\xi.$$

Define $L(x, t)$ to be the root s, which implies that

$$\int_{t-L(x,t)}^{t} P(\xi, I(\xi))d\xi = x.$$

Therefore,

$$u(x,t) = i(0, t - L(x,t))e^{-\mu_i L(x,t)} = \frac{B(M(t - L(x,t)))}{P(t - L(x,t), I(t - L(x,t)))} e^{-\mu_i L(x,t)}, \;\; x \leq X(t).$$

Hence,

$$i(l,t) = i(0, t - L(l,t))e^{-\mu_i L(l,t)} = \frac{B(M(t - L(l,t)))}{P(t - L(l,t), I(t - L(l,t)))} e^{-\mu_i L(l,t)},$$

and the corresponding maturation delay $\tau(t) = L(l, t)$ for individuals developing to the mature stage at time t depends on the immature population size $I(t)$ as specified by

$$\int_{t-\tau(t)}^{t} P(\xi, I(\xi))d\xi = l.$$

The last integral-algebraic equation has a clear biological interpretation: an individual develops to the mature stage at time t should be born at $t - \tau(t)$ such that the accumulative length increase during the time interval $[t - \tau(t), t]$ attains the critical value l. We should mention that similar integral forms to characterize the density-dependent time delay can also be found in other earlier studies, such as [51, 97].

Based on the fact that the variable x remains valid for the immature population, the equation describing the number of the mature stage can be expressed as

$$\begin{aligned}\frac{dM(t)}{dt} &= -\mu_M M(t) + \text{maturation rate}\\ &= -\mu_M M(t) + P(t, I(t))\frac{B(M(t-\tau(t)))}{P(t-\tau(t), I(t-\tau(t)))}e^{-\mu_i \tau(t)}.\end{aligned}$$

In addition, the number of the immature population $I(t)$ satisfies

$$\frac{dI(t)}{dt} = -\mu_I I(t) + B(M(t)) - P(t, I(t))\frac{B(M(t-\tau(t)))}{P(t-\tau(t), I(t-\tau(t)))}e^{-\mu_i \tau(t)}.$$

Results on the boundedness of solutions and the linear stability of equilibria are established in [88]. The boundedness of solutions hold even for unbounded birth functions within certain conditions. It is also shown that if an equilibrium is locally stable in the absence of competition among larvae, then the equilibrium is stable in the presence of weak competition.

3.3.4 Paused development due to immature competition

Considering extreme cases that the development may be paused due to immature competition, termed as diapause, Brunner, Gourley, Liu and Xiao [41] studied the following size growth rate function

$$P(I) = \begin{cases} P_0, & I \le I_c, \\ 0, & I > I_c, \end{cases}$$

with constant P_0. This form implies that the immature individuals develop at a constant rate P_0 when their total number is less than I_c, while the growth of the immature population is paused due to high competition pressure when its size exceeds I_c. Therefore, the change of an immature individual's size can be described as $\frac{dx}{dt} = P(I(t))$, and the growth rate function is dependent on the immature population size $I(t)$.

Since the occurrence of diapause may increase the maturation time $\tau(t)$ needed, $\tau(t) \geq l/P_0$ with l being the critical size at maturity. As a matter of fact, when $P(\cdot)$ is nonnegative, but not strictly positive everywhere, $\tau(t)$ can be defined as

$$\tau(t) = \inf\{s > 0 : \int_{t-s}^{s} P(I(\xi))d\xi = l\},$$

which reduces to

$$\int_{t-\tau(t)}^{t} P(I(\xi))d\xi = l$$

if $P(\cdot)$ is strictly positive. Based on the integration along characteristics, the delay differential system can be formulated as follows:

$$\begin{aligned}\frac{dI(t)}{dt} =& -\mu_I I(t) + B(M(t)) - B(M(t-\tau(t)))\frac{P(I(t))}{P(I(t-\tau(t)))}e^{-\mu_i\tau(t)},\\ \frac{dM(t)}{dt} =& -\mu_M M(t) + B(M(t-\tau(t)))\frac{P(I(t))}{P(I(t-\tau(t)))}e^{-\mu_i\tau(t)}.\end{aligned}$$

When an Allee effect is assumed in the birth rate function $B(\cdot)$, diapause may induce population extinction even for large initial population size. Diapause may also introduce periodic solutions that can arise even for a strictly increasing birth function.

3.4 Discussion

Development from one life stage to the next takes time while the time spent in each stage may be synchronized or varies between individuals, giving rise to various distributions of development time in each stage for different species. These distributions intuitively can play important roles in the transition rates among different life stages. In this chapter, two basic modeling frameworks for demographic changes of population dynamics, based on integral and partial differential systems, are presented. These models can be reduced into ordinary and delay differential stage-structured models under gamma and Dirac distributions. It is evident that each framework has its advantages and inherent limitations. In particular, the integral equation can be naturally formulated through checking the stage progression of individuals. Furthermore, the net reproduction number and initial growth rate can be explicitly derived from the integral system. However, it becomes challenging to integrate the density-dependent regulations on the stage distribution and survival probabilities in an integral equation due to difficulties in formulating appropriate survival probability functions and stage duration distributions. This may be suitably conquered through structured partial differential equation models. By further assumptions on these density-dependent regulations, the partial differential system can be reduced into different forms, and in particular, various delay differential equation models were reviewed in this study.

When the impact of density regulation on immature individual survival and development is negligible, it is evident from Section 3.2 that the equation for the matured population size is decoupled from the integral system ((3.1) and (3.2)) as the variable accounting the immature population size does not appear in (3.2). Similar observation can be gained for the delay differential equation model in Subsections 3.2.1 (II) and 3.2.2 (II) when the Dirac distribution is assumed for stage duration of immatures. From an analytical point of view, this observation makes it possible to analyze the dynamics of the mature stage $M(t)$ first, and then to feed the equation of the immature stage with the dynamic profile $M(t)$. Since the extinction and persistence of the species can be predicted from those of each stage, it would be sufficient to show the extinction/persistence of mature individuals from the decoupled equation for $M(t)$, as analyzed in [74] for the case when the immature competition force $f(\cdot) = 0$. When gamma distribution is assumed for stage duration of immatures, the maturation rate becomes $n\lambda I_n(t)$ in the system of ordinary differential equations in Subsections 3.2.1 (II) and 3.2.2 (II), which makes it impossible to decouple the variables for mature stages from the whole system at first glance. However, if one revisits the definition of $I_n(t)$ in (3.9), it can be expressed in terms of $M(t)$ with a distributed delay kernel.

Furthermore, Dirac distribution with an average duration τ can be approximated by a gamma distribution in (3.7) with $\gamma = 1/\tau$ and large n (such that the variance of the gamma distribution τ^2/n is very small), as shown in Figure 1.1. Intuitively, the delay differential equation model under Dirac distribution assumption would also be approximated by n ordinary differential equations under gamma distribution assumption for large n. As a matter of fact, this can be rigorously shown by the linear chain trick [168], as illustrated in Subsection 3.2.2 (II) by observing the maturation rate when $t > \tau$ is

$$\begin{aligned} v(0,t) = u(\tau,t) = B(M(t-\tau))e^{-\mu_I \tau} &= \int_0^\infty \delta(a-\tau)e^{-\mu_I a}B(M(t-a))da \\ &\approx \int_0^\infty [-P_I'(a)]e^{-\mu_I a}B(M(t-a))da. \end{aligned}$$

In the above expression, $\delta(\cdot)$ is the Dirac-delta function and $P_I(a)$ takes the gamma distribution as in (3.7).

The stage-structured modeling idea can be easily adopted to incorporate spatial movements of individuals. In particular, when individuals are performing random movements, a reaction-diffusion model with/without time delay can be formulated when the exponential and Dirac distributions are assumed for the stage duration [39, 43, 90]. In particular, a nonlocal delay term can be formulated when the Dirac distribution is assumed and immature individuals move during development. Interested readers may refer pioneering model formulations by Stephen Gourley and his collaborators, such as [12, 13, 90, 108].

Other modeling frameworks, such as matrix population models and individual-based models are also important tools to incorporate the variation of individual-level demographic characteristics, which are beyond the scope of this chapter. We refer the interested readers to [57, 144] for incorporating stage duration distributions in other model forms, such as matrix models and statistical stage-duration distribution models. Further biotic and abiotic factors may also impact the stage duration distributions, for example, the seasonal environmental oscillations can induce seasonal developmental delays and seasonal diapauses, which have been modeled in [120, 122]. We leave these topics for further investigation.

Chapter 4

A seasonal succession model for frog population growth

4.1 Introduction

This chapter is going to investigate the frog population growth through mathematical modeling. There have been some related models in amphibian populations. Gener- and stage-structured models for the boreal toad and transmission of the fungal pathogen *Batrachochytrium dendrobatidis* (*Bd*) were proposed in [130]. The models take the form of systems of difference equations. Stability and permanence were further analyzed regarding two threshold indices, the basic reproduction numbers for the population and fungal disease. A discrete-time model was proposed in [38] to simulate the *Rana muscos* (yellow-legged frog) dynamics and then combined with a continuous-time model for the *B. dendrobatidi* pathogen invasion to a new lake. An amphibian juvenile-adult population model with individuals dispersing between ponds [5], in the form of a system of first-order nonlocal hyperbolic equations, is considered, and finite difference numerical approximation is developed. By considering an amphibian juvenile-adult population model with individuals dispersing between ponds, [5] formulated a system of first-order nonlocal hyperbolic equations and developed a finite difference approximation. The model extends that in [4] as it considers the adult dispersal among different ponds. Stochastic juvenile-adult stage-structured models were proposed in [6] to understand the demographic stochasticity of the dynamics of an urban green tree frog. The juvenile stage's density-dependence mortality rate is assumed in [4, 6, 5]. A juvenile-adult stage-structured model was proposed in [3] to describe the population growth of green tree frogs; the wellposedness of the system, extinction, and persistence of the species were also investigated. Sensitivity partial differential equations, extended from the model in [3], for the sensitivities of the solution concerning the reproduction and mortality rates for adults were proposed in [7]. The models in [3, 4] were further fitted for green tree frog field data in [2], which presented an infinite-dimensional least-squares approach to compare a mathematical population model with the statistical population estimates, involving parameter estimates and model sensitivity. Motivated by the green tree frog (*Hyla cinerea*) growth, a discrete two-stage population model was analyzed where tadpoles and adult frogs compete for different resources [9]. It is extended to a three-stage discrete-time population model in [8]. More general persistence and extinction results for discrete-time dynamical systems can be found in [104]. A system of impulsive differential equations for five stages is presented and simulated for the wood frog population [11].

Some existing studies also integrated the amphibian population growth with fungal transmission. Most models form a matrix model, with the survival and transition parameters in the matrix estimated implicitly by considering the environmental variations during one year. A discrete-time SIR epidemic model was proposed to spread the pathogen in a structured host population [68]. The host population was subdivided into three developmental stages, namely larva, juvenile, and adult, and the pathogen can infect each stage. A discrete-time stage-structured fungal disease model was studied [159] for the population's persistence and disease transmission. A discrete-time model with periodic coefficients and a stochastic epidemic model were proposed with applications to a fungal pathogen affecting amphibian populations [69]. The species decline, and extinction are investigated in a host-parasite model with density-dependent (mass action) incidence term and a critical Allee effect in host growth [181]. Population and disease persistence criteria were given for a discrete-time epidemic model [160]. The mathematical model [138] that persistence of *B. dendrobatidis* outside the amphibian host can significantly increase the probability of host extinction. A mathematical model was proposed in [37] to test the hypothesis that fungal load dynamics can explain the different population-level outcomes of *Bd* observed in different areas. The transmission rate of the fungal pathogen *Batrachochytrium dendroba* was quantified in the mountain yellow-legged frog *Rana muscosa* through laboratory and field experiments [151]. A model is proposed to investigate the relative importance of transmission compared to load-dependent host resistance and tolerance in [199]. The model in [138] was further extended in [63] by including stochastic effects and to fit with the field data. A between-season *R. muscosa* model was proposed in [199] with two main stages, tadpoles, and adults, while the tadpoles are further classified into three classes: year-one, year-two, and year-three tadpoles. A discrete-time, female-based stage-structured model is proposed for *R. luteiventris* frog population dynamics, which counts the densities of juvenile, subadult female, adult male, and adult female. Hence, we hope to find the model in this project as a continuous-time version, which may facilitate the description of the processes involved in population growth.

Regarding the impact of the ecological environment on the population, a mathematical model of a frog population infected with chytridiomycosis was formulated to explore the impacts of the inoculation of *Janthinobacterium lividum* and temperature on the disease dynamics in [1]. Structure equation models and multi-state models were employed to analyze the effects of climate changes on *Batrachochytrium dendrobatidis* prevalence and the interplay of grazing, weather, and *Bd* infection on adult survival, respectively [29]. Data from future climate and vegetation cover models were used to study the effects of climate variation on the amphibian population in [30, 162]. The contribution of egg mortality to amphibian declines was assessed through a demographic mode in [187]. A simple model of disease dynamics was presented to investigate the extinction and persistence of diseases in the frog population [38]. A population viability analysis framework for the gopher frog was applied to discuss population sensitivity to the frequency of droughts and forecast future population viability in [53]. An occupancy model and some estimated parameters in a Bayesian framework were developed to investigate the breeding occurrence and metamorph occupancy of amphibian populations in [91]. A discrete stage-structured model of California newt species was introduced to explore the population dynamics under drought in [105]. Some statistical study was used to evaluate the relationship among climate changes, annual survival, fecundity and breeding site heterogeneity, and growth rate of Columbia spotted frog and Boreal Toads populations in [134], [133] and [140], respectively.

Few modeling studies have evaluated the effects of environmental variability on the seasonality of amphibian population dynamics. There exist some environmental factors that can regulate growth. Climate change, rainfall, and habitat availability affect egg production, mortality, and survival probability at each stage [105, 187], which explains why we set and analyze the periodic parameters in the following study. For example, juveniles and adults in high-elevation temperate environments have much shorter growing seasons than low-elevation individuals; amphibians may winter kill due to freezing or hypoxia; reduced precipitation and a warm environment could result in less water amphibian species which rely on ephemeral pools for reproduction and foraging [134]. Decreased winter severity increases the viability of a montane frog population.

Considering the life cycle stages of the boreal toad during one or two years, such as hibernation and metamorphosis, we plan to focus on these seasonal factors and formulate a seasonal succession model describing the growth development of the frog population. The rest of this chapter is organized as follows. We derive the population model with piecewise differential equations in the next section. Later in Section 4.3, we establish some properties of solutions based on the natural phase and quotient spaces, thereby analyzing the threshold dynamics of the model in terms of the basic reproduction number. The brief discussion and conclusion finish the chapter.

4.2 Model formulation

In order to formulate a model to describe the maturation, fecundity, and survival of individuals during different seasons of 1 or 2 years and consider different types of individuals that will metamorphose and reproduce in different patterns, we may start with a seasonal succession model to describe frogs' different seasons of breeding, development, and hibernation. Here we may specifically study the boreal toad *Bufo boreas boreas* [130, 162], whose population size is associated with the spread of chytridiomycosis. Besides, we may also use the *R. muscosa* and *R. sierrae* as the motivating species for amphibian populations. Each frog individual may breed every 1 or 2 years, depending on its body size and living conditions. Eggs hatch into tadpoles and then enter the subadult stage through metamorphosis, which lasts two years, and develops into a reproductive adult [37, 38]. To make things simple, we only assume the following:

(i) There are two seasons, breeding season (from the beginning of year 0 to time T) and hibernation season (from timing T to the end of the year); during the breeding season, the individual may develop, give birth and die, with the rates dependent on varying environmental conditions, that is, these rates can be regarded as a function of time t within the year. However, during the hibernation season, there is no development and reproduction.

(ii) There are two tadpole year classes (spend 1 or 2 years in tadpole stage) L_i, one juvenile stage J and one adult stage A [38, 209]. Most models consider the case that tadpoles can develop within a year. However, [38] and [209] presented *R. muscosa*'s multiyear tadpole stage up to three years due to the relatively unsuitable habitat environment. Hence, we assume that the tadpoles that spend one year growing and developing can complete their development before entering hibernation.

(iii) Instead of using female-only models [53], we characterize the birth rate in terms of per pair birth rate as in [138]. When there is only one adult stage, it can be justified that only a proportion of adults reproduce in a particular year by assuming a linear birth function $B(t, A(t))$.

(iv) It is assumed that juveniles live in an environment with abundant resources and thus do not compete. In contrast, adults live in an environment with limited resources, and thus competition occurs. This competition assumption is accounted for in recruiting juveniles to adulthood by incorporating a decreasing function of the current adult density. The density-dependent function regulates the recruitment rate from the juvenile stage to the adult stage in the form of $(1 - (A(t)/K))r_J(t)j(1,t)$ with K describing the strength of population regulation. This density-dependence regulation defines the assumption that excess juveniles leave the population to search new breeding sites, which is the dominant form of amphibian dispersal [138].

Introduce the notation $\lfloor t \rfloor$ represents the floor function giving the nearest integer less than or equal to t and therefore, $t - \lfloor t \rfloor \in [0, T]$ and $t - \lfloor t \rfloor \in (T, 1)$ represent the breeding and hibernation seasons respectively. To characterize the development of different stages, we are using the idea in [195] by introducing a measurement q to characterize the development proportion to the next stage, that is, $q = 0$ represents the individuals just moving to the stage. Then the total numbers of tadpole in each class are $L_i = \int_0^1 l_i(q,t)\mathrm{d}q$ while the total number of juveniles at time t is $J(t) = \int_0^1 j(q,t)\mathrm{d}q$. During the normal growing season, when $t - \lfloor t \rfloor \in [0, T]$, the dynamics of the population sizes can be described by the following system. During the normal growing season, that is, when $t - \lfloor t \rfloor \in [0, T]$, the dynamics of the population sizes can be described by the following system

$$\begin{cases} \dfrac{\partial l_i(q,t)}{\partial t} + \dfrac{\partial}{\partial q}[r_i(t)l_i(q,t)] = -\mu_i(t)l_i(q,t), & t - \lfloor t \rfloor \in [0,T],\ i = 1,\ 2 \\ \dfrac{\partial j(q,t)}{\partial t} + \dfrac{\partial}{\partial q}[r_J(t)j(q,t)] = -\mu_J(t)j(q,t), & t - \lfloor t \rfloor \in [0,T], \\ \dfrac{\mathrm{d}A(t)}{\mathrm{d}t} = M(t) - \mu_A(t)A(t), & t - \lfloor t \rfloor \in [0,T]. \end{cases} \tag{4.1}$$

with the boundary conditions for variables $l_i(q,t)$ and $j(q,t)$ given by

$$r_1(t)l_1(0,t) = p_1 B(t, A(t)), \qquad r_2(t)l_2(0,t) = (1-p_1)B(t, A(t)),$$
$$r_J(t)j(0,t) = r_1(t)l_1(1,t) + r_2(t)l_2(1,t), \qquad \text{and } M(t) = \left(1 - \frac{A(t)}{K}\right) r_J(t)j(1,t).$$

where the birth function $B(t,x)$ can take the linear growth function as $B(t,x) = b(t)x$. The development of adult frogs $M(t)$ is constrained by a density-dependent function $\left(1 - \frac{A(t)}{K}\right)$, where K regulates the strength of the population capacity. We assume that excess juvenile frogs will move out from the population, entering other breeding sites. The parameters $\mu_1(t)$, $\mu_2(t)$, $\mu_J(t)$ and $\mu_A(t)$ are the mortality rates of tadpoles, juveniles, and adult frogs during the normal growing season, respectively.

During the hibernation season when $t - \lfloor t \rfloor \in (T, 1)$, there is no individual development, maturation, and fecundity, that is $r_i(t)$, $r_J(t)$ and $M(t)$ are equal to zero in (4.1) in the hibernation season. Suppose $d_1(t)$, $d_2(t)$, $d_J(t)$ and $d_A(t)$ be the mortality rates of hibernated tadpoles, juvenile, and adult frogs, respectively. Thus the dynamics of the population sizes can be described by the following system

$$\begin{cases} \dfrac{\partial l_1(q,t)}{\partial t} = -d_1(t)l_1(q,t), & t - \lfloor t \rfloor \in (T,1), \\ \dfrac{\partial l_2(q,t)}{\partial t} = -d_2(t)l_2(q,t), & t - \lfloor t \rfloor \in (T,1), \\ \dfrac{\partial j(q,t)}{\partial t} = -d_J(t)j(q,t), & t - \lfloor t \rfloor \in (T,1), \\ \dfrac{\mathrm{d}A(t)}{\mathrm{d}t} = -d_A(t)A(t), & t - \lfloor t \rfloor \in (T,1). \end{cases} \tag{4.2}$$

This implies that when $t - \lfloor t \rfloor \in (T, 1)$, there exist

$$\begin{aligned} \frac{\mathrm{d}L_1(t)}{dt} &= -d_1(t)L_1(t), \\ \frac{\mathrm{d}L_2(t)}{dt} &= -d_2(t)L_2(t), \\ \frac{\mathrm{d}J(t)}{dt} &= -d_J(t)J(t), \\ \frac{\mathrm{d}A(t)}{dt} &= -d_A(t)A(t). \end{aligned} \tag{4.3}$$

Suppose $r_i(t)$ be the temperature-dependent parameters with $i = 1, 2, J$. Also, $q = q_1 = 0$ denotes the start of stage L_1, $q = q_2 = 0$ denotes the start of stage L_2, $q = q_J$ denotes the transition from L to J. Let l_i be the density of tadpoles with development level q at time t. Since

$$\frac{\partial l_1(q,t)}{\partial t} = -\frac{\partial}{\partial q}[r_1(t)l_1(q,t)] - \mu_1(t)l_1(q,t). \tag{4.4}$$

Equation (4.4) has the boundary condition

$$l_1(q_1,t) = \frac{p_1 B(t, A(t))}{r_1(t)}$$

To solve equation (4.4) with this boundary condition, we introduce a new variable

$$\xi = h(t) := q_1 + \int_0^t r_1(s)ds.$$

Suppose $h^{-1}(\xi)$ be the inverse function of $h(t)$, and define

$$\hat{l_1}(q,\xi) = l_1(q, h^{-1}(\xi)),\ \hat{\mu_1}(\xi) = \mu_1(h^{-1}(\xi)),\ \hat{r_1}(\xi) = r_1(h^{-1}(\xi)).$$

It follows from (4.4) that

$$\frac{\partial \hat{l_1}(q,\xi)}{\partial \xi} = -\frac{\partial \hat{l_1}(q,\xi)}{\partial q} - \frac{\hat{\mu_1}(\xi)}{\hat{r_1}(\xi)}\hat{l_1}(q,\xi). \tag{4.5}$$

Let $V(s) = \hat{l_1}(s + q - \xi, s)$. For (4.5), we have

$$\frac{dV(s)}{ds} = -\frac{\hat{\mu_1}(s)}{\hat{r_1}(s)}V(s).$$

Since $\xi - (q - q_1) \leq \xi$, there exists

$$V(\xi) = V(\xi - (q - q_1))e^{-\int_{\xi-(q-q_1)}^{\xi} \frac{\hat{\mu_1}(s)}{\hat{r_1}(s)}ds},$$

which implies that

$$\hat{l_1}(q,\xi) = \hat{l_1}(q_1, \xi - q + q_1)e^{-\int_{\xi-(q-q_1)}^{\xi} \frac{\hat{\mu_1}(s)}{\hat{r_1}(s)} ds}.$$

Define $\theta_1(q,t)$ to be the time taken to grow from development level q_1 to level q by tadpoles who arrive at development level q at time t. Since $\frac{dq}{dt} = r_1(t)$, we obtain

$$q - q_1 = \int_{t-\theta_1(q,t)}^{t} r_1(s)ds, \tag{4.6}$$

which implies that

$$h(t - \theta_1(q,t)) = h(t) - \int_{t-\theta_1(q,t)}^{t} r_1(s)ds = h(t) - (q - q_1).$$

By a change of variable $s = h(\alpha)$, we have

$$\int_{\xi-(q-q_1)}^{\xi} \frac{\hat{\mu_1}(s)}{\hat{r_1}(s)} ds = \int_{t-\theta_1(q,t)}^{t} \mu_1(\alpha)d\alpha.$$

It follows that

$$\begin{aligned} l_1(q,t) &= \hat{l_1}(q, h(t)) \\ &= l_1(q_1, t - \theta_1(q,t))e^{-\int_{t-\theta_1(q,t)}^{t} \mu_1(\alpha)d\alpha} \\ &= \frac{B(t-\theta_1(q,t), A(t-\theta_1(q,t)))}{r_1(t-\theta_1(q,t))} e^{-\int_{t-\theta_1(q,t)}^{t} \mu_1(\alpha)d\alpha}. \end{aligned}$$

Define $\theta_1(t) := \theta_1(q_J, t)$, and obtain

$$r_1(t)l_1(q_J,t) = B(t-\theta_1(t), A(t-\theta_1(t)))\frac{r_1(t)}{r_1(t-\theta_1(t))} e^{-\int_{t-\theta_1(t)}^{t} \mu_1(\alpha)d\alpha}.$$

Letting $q = q_J$ in (4.6), we have

$$q_J - q_1 = \int_{t-\theta_1(t)}^{t} r_1(s)ds. \tag{4.7}$$

Taking the derivative with respect to t on both sides of (4.7), we get

$$1-\theta_1'(t)=\frac{r_1(t)}{r_1(t-\theta_1(t))}$$

Thus $1-\theta_1'(t)>0$.

Define $\theta_2(q,t)$ to be the time taken to grow from development level q_2 to level q by tadpoles that arrive at development level q at time t. Then there exists

$$q-q_2=\int_{t-\theta_2(q,t)}^{\lfloor t\rfloor-1+T} r_2(s)ds+\int_{\lfloor t\rfloor}^{t} r_2(s)ds. \tag{4.8}$$

Supposing $\theta_2(t)=\theta_2(q_J,t)$ and letting $q=q_J$ in (4.8), we obtain

$$q_J-q_2=\int_{t-\theta_2(t)}^{\lfloor t\rfloor-1+T} r_2(s)ds+\int_{\lfloor t\rfloor}^{t} r_2(s)ds. \tag{4.9}$$

Taking the derivatives with respect to t on both sides of (4.9), we have

$$1-\theta_2'(t)=\frac{r_2(\lfloor t\rfloor-1+T)}{r_2(t-\theta_2(t))}+\frac{r_2(t)}{r_2(\lfloor t\rfloor)}>0.$$

Define $\theta_J(q,t)$ to be the time taken to grow from development level q_J to level q by juvenile frogs that arrive at development level q at time t. Then there exists

$$q-q_J=\int_{t-\theta_J(q,t)}^{t} r_J(s)ds. \tag{4.10}$$

Supposing $\theta_J(t)=\theta_J(q_A,t)$ and letting $q=q_A$ in (4.10), we obtain

$$q_A-q_J=\int_{t-\theta_J(t)}^{t} r_J(s)ds. \tag{4.11}$$

Taking the derivatives with respect to t on both sides of (4.11), we have

$$1-\theta_J'(t)=\frac{r_J(t)}{r_J(t-\theta_J(t))}>0.$$

Hence, when $t - \lfloor t \rfloor \in [0, T]$, we arrive at the following model system:

$$
\begin{aligned}
\frac{\mathrm{d}L_1(t)}{dt} =& p_1 B(t, A(t)) - p_1(1 - \theta_1'(t)) B(t - \theta_1(t), A(t - \theta_1(t))) e^{-\int_{t-\theta_1(t)}^{t} \mu_1(\alpha) d\alpha} \\
& - \mu_1(t) L_1(t), \\
\frac{\mathrm{d}L_2(t)}{dt} =& (1 - p_1) B(t, A(t)) - (1 - p_1)(1 - \theta_2'(t)) B(t - \theta_2(t), A(t - \theta_2(t))) \\
& \cdot e^{-\int_{t-\theta_2(t)}^{\lfloor t \rfloor - 1 + T} \mu_2(\alpha) d\alpha - \int_{\lfloor t \rfloor - 1 + T}^{\lfloor t \rfloor} d_2(\alpha) d\alpha - \int_{\lfloor t \rfloor}^{t} \mu_2(\alpha) d\alpha} - \mu_2(t) L_2(t), \\
\frac{\mathrm{d}J(t)}{dt} =& p_1(1 - \theta_1'(t)) B(t - \theta_1(t), A(t - \theta_1(t))) e^{-\int_{t-\theta_1(t)}^{t} \mu_1(\alpha) d\alpha} + (1 - p_1)(1 - \theta_2'(t)) \\
& \cdot B(t - \theta_2(t), A(t - \theta_2(t))) e^{-\int_{t-\theta_2(t)}^{\lfloor t \rfloor - 1 + T} \mu_2(\alpha) d\alpha - \int_{\lfloor t \rfloor - 1 + T}^{\lfloor t \rfloor} d_2(\alpha) d\alpha - \int_{\lfloor t \rfloor}^{t} \mu_2(\alpha) d\alpha} \\
& - p_1 B(t - \theta_J(t) - \theta_1(t - \theta_J(t)), A(t - \theta_J(t) - \theta_1(t - \theta_J(t)))) \\
& \cdot (1 - \theta_1'(t - \theta_J(t))) e^{-\int_{t-\theta_J(t)-\theta_1(t-\theta_J(t))}^{t-\theta_J(t)} \mu_1(\alpha) d\alpha} (1 - \theta_J'(t)) e^{-\int_{t-\theta_J(t)}^{t} \mu_J(\alpha) d\alpha} \\
& - (1 - p_1) B(t - \theta_J(t) - \theta_2(t - \theta_J(t)), A(t - \theta_J(t) - \theta_2(t - \theta_J(t)))) \\
& \cdot (1 - \theta_2'(t - \theta_J(t))) \cdot e^{-\int_{t-\theta_J(t)-\theta_2(t-\theta_J(t))}^{\lfloor t \rfloor - 2 + T} \mu_2(\alpha) d\alpha} e^{-\int_{\lfloor t \rfloor - 2 + T}^{\lfloor t \rfloor - 1} d_2(\alpha) d\alpha - \int_{\lfloor t \rfloor - 1}^{t - \theta_J(t)} \mu_2(\alpha) d\alpha} \\
& \cdot (1 - \theta_J'(t)) \cdot e^{-\int_{t-\theta_J(t)}^{t} \mu_J(\alpha) d\alpha} - \mu_J(t) J(t), \\
\frac{\mathrm{d}A(t)}{dt} =& p_1 \left(1 - \frac{A(t)}{K}\right) B(t - \theta_J(t) - \theta_1(t - \theta_J(t)), A(t - \theta_J(t) - \theta_1(t - \theta_J(t)))) \\
& \cdot (1 - \theta_1'(t - \theta_J(t))) e^{-\int_{t-\theta_J(t)-\theta_1(t-\theta_J(t))}^{t-\theta_J(t)} \mu_1(\alpha) d\alpha} (1 - \theta_J'(t)) e^{-\int_{t-\theta_J(t)}^{t} \mu_J(\alpha) d\alpha} \\
& + (1 - p_1) \left(1 - \frac{A(t)}{K}\right) B(t - \theta_J(t) - \theta_2(t - \theta_J(t)), A(t - \theta_J(t) - \theta_2(t - \theta_J(t)))) \\
& \cdot (1 - \theta_2'(t - \theta_J(t))) \cdot e^{-\int_{t-\theta_J(t)-\theta_2(t-\theta_J(t))}^{\lfloor t \rfloor - 2 + T} \mu_2(\alpha) d\alpha - \int_{\lfloor t \rfloor - 2 + T}^{\lfloor t \rfloor - 1} d_2(\alpha) d\alpha - \int_{\lfloor t \rfloor - 1}^{t - \theta_J(t)} \mu_2(\alpha) d\alpha} \\
& \cdot (1 - \theta_J'(t)) \cdot e^{-\int_{t-\theta_J(t)}^{t} \mu_J(\alpha) d\alpha} - \mu_A(t) A(t).
\end{aligned}
\tag{4.12}
$$

Since the last equations in system (4.12) and system (4.3) are decoupled from the other equations, respectively, we focus on the following delay differential equation

$$
\begin{aligned}
\frac{\mathrm{d}A(t)}{dt} =& p_1 \left(1 - \frac{A(t)}{K}\right) B(t - \theta_J(t) - \theta_1(t - \theta_J(t)), A(t - \theta_J(t) - \theta_1(t - \theta_J(t))))\\
& \cdot (1 - \theta_1^{'}(t - \theta_J(t)))e^{-\int_{t-\theta_J(t)-\theta_1(t-\theta_J(t))}^{t-\theta_J(t)} \mu_1(\alpha)d\alpha}(1 - \theta_J^{'}(t))e^{-\int_{t-\theta_J(t)}^{t} \mu_J(\alpha)d\alpha}\\
& + (1 - p_1) \left(1 - \frac{A(t)}{K}\right) B(t - \theta_J(t) - \theta_2(t - \theta_J(t)), A(t - \theta_J(t) - \theta_2(t - \theta_J(t))))\\
& \cdot (1 - \theta_2^{'}(t - \theta_J(t))) \cdot e^{-\int_{t-\theta_J(t)-\theta_2(t-\theta_J(t))}^{\lfloor t \rfloor -2+T} \mu_2(\alpha)d\alpha - \int_{\lfloor t \rfloor -2+T}^{\lfloor t \rfloor -1} d_2(\alpha)d\alpha - \int_{\lfloor t \rfloor -1}^{t-\theta_J(t)} \mu_2(\alpha)d\alpha}\\
& \cdot (1 - \theta_J^{'}(t)) \cdot e^{-\int_{t-\theta_J(t)}^{t} \mu_J(\alpha)d\alpha} - \mu_A(t)A(t), \quad t - \lfloor t \rfloor \in [0, T],\\
\frac{\mathrm{d}A(t)}{\mathrm{d}t} =& - d_A(t)A(t), \quad t - \lfloor t \rfloor \in (T, 1).
\end{aligned}
\tag{4.13}
$$

Taking the birth function $B(t, A(t))$ as the linear form $B(t, A(t)) = b(t)A(t)$ and denoting

$$
\begin{aligned}
\delta_1(t) =& p_1 b(t - \theta_J(t) - \theta_1(t - \theta_J(t)))(1 - \theta_1^{'}(t - \theta_J(t)))\\
& \cdot e^{-\int_{t-\theta_J(t)-\theta_1(t-\theta_J(t))}^{t-\theta_J(t)} \mu_1(\alpha)d\alpha}(1 - \theta_J^{'}(t))e^{-\int_{t-\theta_J(t)}^{t} \mu_J(\alpha)d\alpha}
\end{aligned}
$$

and

$$
\begin{aligned}
\delta_2(t) =& (1 - p_1)b(t - \theta_J(t) - \theta_2(t - \theta_J(t)))(1 - \theta_2^{'}(t - \theta_J(t)))\\
& \cdot e^{-\int_{t-\theta_J(t)-\theta_2(t-\theta_J(t))}^{\lfloor t \rfloor -2+T} \mu_2(\alpha)d\alpha - \int_{\lfloor t \rfloor -2+T}^{\lfloor t \rfloor -1} d_2(\alpha)d\alpha - \int_{\lfloor t \rfloor -1}^{t-\theta_J(t)} \mu_2(\alpha)d\alpha}\\
& \cdot (1 - \theta_J^{'}(t))e^{-\int_{t-\theta_J(t)}^{t} \mu_J(\alpha)d\alpha},
\end{aligned}
$$

we can rewrite (4.13) as

$$
\begin{aligned}
\frac{\mathrm{d}A(t)}{dt} =& \delta_1(t) \left(1 - \frac{A(t)}{K}\right) A(t - \tau_1(t)) + \delta_2(t) \left(1 - \frac{A(t)}{K}\right) A(t - \tau_2(t))\\
& - \mu_A(t)A(t), \quad t - \lfloor t \rfloor \in [0, T],\\
\frac{\mathrm{d}A(t)}{\mathrm{d}t} =& - d_A(t)A(t), \quad t - \lfloor t \rfloor \in (T, 1).
\end{aligned}
\tag{4.14}
$$

where $\tau_1(t) = \theta_J(t) + \theta_1(t - \theta_J(t))$ and $\tau_2(t) = \theta_J(t) + \theta_2(t - \theta_J(t))$.

4.3 Threshold dynamics

4.3.1 Natural phase space and basic properties of solutions

Based on the frog ecology, we assume $0 < \tau_1(t) < 1 < \tau_2(t) < 2$. Let $\hat{\tau} = \max_{t\in[0,T]} \tau_2(t)$, $\mathcal{X} = C([-\hat{\tau}, 0], \mathbb{R})$, $\mathcal{X}^+ = C([-\hat{\tau}, 0], \mathbb{R}_+)$. When we choose the natural phase space $\mathcal{X}$, it is a Banach space when equipped with the supremum norm

$$\|\varphi\|_{\mathcal{X}} = \max_{\theta\in[-\hat{\tau},0]} \{|\varphi(\theta)|\}.$$

A closed convex subset $\mathcal{X}^+ \in \mathcal{X}$ can be introduced as $\mathcal{X}^+ = \{\varphi \in \mathcal{X} : \varphi(\theta) \geq 0 \text{ for all } \theta \in [-\hat{\tau}, 0]\}$, which induces a partial ordering on the Banach space $(\mathcal{X}, \|\cdot\|_{\mathcal{X}})$. Furthermore, $\mathcal{X}^+$ has a nonempty interior $\mathrm{int}(\mathcal{X}^+) = \{\varphi \in \mathcal{X} : \varphi(\theta) > 0 \text{ for all } \theta \in [-\hat{\tau}, 0]\}$. The partial ordering induced by the cone serves to compare any two elemennts φ and ψ of $\mathcal{X}$. Considering the cone $\mathcal{X}^+$, we define three relationships: (i) $\varphi \geq \psi$ if and only if $\varphi - \psi \in \mathcal{X}^+$; (ii) $\varphi > \psi$ if and only if $\varphi \geq \psi$ and $\varphi \neq \psi$; (iii) $\varphi \gg \psi$ if and only if $\varphi - \psi \in \mathrm{int}(\mathcal{X}^+)$. Then $(\mathcal{X}, \mathcal{X}^+)$ is an ordered Banach space equipped with the maximum norm and the partial order induced by the positive cone $\mathcal{X}^+$. For any given continuous function $v : [-\hat{\tau}, \sigma) \to \mathbb{R}$ with $\sigma > 0$, we define $v_t \in \mathcal{X}$ by

$$v_t(\theta) = v(t + \theta), \forall\theta \in [-\hat{\tau}, 0]$$

for any $t \in [0, \sigma)$. Then we have the following results.

Lemma 4.3.1. *For any $\varphi \in \mathcal{X}^+$, system (4.14) has a unique solution $v(t; \varphi)$ with $v_0 = \varphi$, and $v_t(\varphi) \in \mathcal{X}^+$ for all $t \geq 0$. Moreover, there exists $m > 1$ such that $0 \leq \varphi(\theta) \leq mK$ for all $\theta \in [-\hat{\tau}, 0]$, then $0 \leq v(t; \varphi) \leq mK$.*

Proof. Let $\overline{\tau} = \min\{\min_{t\in[0,T]} \tau_1(t), T\}$. Since $1 - \tau_1^{'}(t) > 0$ and $1 - \tau_2^{'}(t) > 0$, $t - \tau_1(t)$

and $t - \tau_2(t)$ are strictly increasing in t. For any $t \in [0, \overline{\tau}]$, we have

$$\begin{aligned} &-\tau_1(0) = 0 - \tau_1(0) \leq t - \tau_1(t) \leq \overline{\tau} - \tau_1(\overline{\tau}) \leq \overline{\tau} - \overline{\tau} = 0, \\ \text{and } &-\tau_2(0) = 0 - \tau_2(0) \leq t - \tau_2(t) \leq \overline{\tau} - \tau_2(\overline{\tau}) \leq \overline{\tau} - \overline{\tau} = 0. \end{aligned}$$

It follows that

$$v(t - \tau_1(t)) = \varphi(t - \tau_1(t)) \ \text{ and } \ v(t - \tau_2(t)) = \varphi(t - \tau_2(t)),$$

which are specified by the initial value function φ. Thus for $t \in [0, \overline{\tau}]$, we have the following non-autonomous ordinary differential equation

$$\frac{dv(t)}{dt} = \left(1 - \frac{v(t)}{K}\right) [\delta_1(t)\varphi(t - \tau_1(t)) + \delta_2(t)\varphi(t - \tau_2(t))] - \mu_A(t)v(t). \tag{4.15}$$

According to the existence and uniqueness of solutions, there exists $t_\varphi > 0$ such that the solution $v(t)$ exists on $[0, t_\varphi]$. Actually, the solution to (4.15) can be expressed as

$$v(t) = \varphi(0)e^{\int_0^t \left(-\mu_A(s) - \frac{q(s)}{K}\right)ds} + e^{\int_0^t \left(-\mu_A(s) - \frac{q(s)}{K}\right)ds} \cdot \int_0^t q(s)e^{\int_0^s \left(\mu_A(\xi) + \frac{q(\xi)}{K}\right)d\xi} ds,$$

where $q(s) = \delta_1(s)\varphi(s - \tau_1(s)) + \delta_2(s)\varphi(s - \tau_2(s)) \geq 0$. Therefore, $v(t) \geq 0$. For any $\varphi \in \mathcal{X}^+$, there exists $m > 1$ such that $0 \leq \varphi(\theta) \leq m \cdot K$ with $\theta \in [-\hat{\tau}, 0]$. Then we have

$$\begin{aligned} v(t) =& \varphi(0)e^{-\int_0^t \left(\frac{q(\xi)}{K} + \mu_A(\xi)\right)d\xi} + K \left[\int_0^t \frac{q(s)}{K} e^{-\int_s^t \left(\frac{q(\xi)}{K} + \mu_A(\xi)\right)d\xi} ds\right] \\ =& \varphi(0)e^{-\int_0^t \left(\frac{q(\xi)}{K} + \mu_A(\xi)\right)d\xi} + K \left[\int_0^t \left(\frac{q(s)}{K} + \mu_A(s)\right) e^{-\int_s^t \left(\frac{q(\xi)}{K} + \mu_A(\xi)\right)d\xi} ds\right] \\ & - K \int_0^t \mu_A(s)e^{-\int_s^t \left(\frac{q(\xi)}{K} + \mu_A(\xi)\right)d\xi} ds \\ =& \varphi(0)e^{-\int_0^t \left(\frac{q(\xi)}{K} + \mu_A(\xi)\right)d\xi} + K \left[1 - e^{-\int_0^t \left(\frac{q(\xi)}{K} + \mu_A(\xi)\right)d\xi} - \int_0^t \mu_A(s)e^{-\int_s^t \left(\frac{q(\xi)}{K} + \mu_A(\xi)\right)d\xi} ds\right] \\ \leq& (m-1)Ke^{-\int_0^t \left(\frac{q(\xi)}{K} + \mu_A(\xi)\right)d\xi} + K \left[1 - \int_0^s \mu_A(\eta)e^{-\int_\eta^s \left(\frac{q(\xi)}{K} + \mu_A(\xi)\right)d\xi} d\eta\right] \\ \leq& (m-1)K + K \leq mK. \end{aligned}$$

Hence $0 \leq v(t) \leq mK$ and the solution exists for $t \in [0, \overline{\tau}]$.

Similar arguments remain valid for $t \in [\overline{\tau}, 2\overline{\tau}], [2\overline{\tau}, 3\overline{\tau}], \ldots, [\lfloor n \rfloor \overline{\tau}, n\overline{\tau}]$, with $n = \frac{T}{\overline{\tau}}$. Therefore, the solution $v(t)$ exists for $0 \leq t \leq T$ and $0 \leq v(t) \leq mK$. For $t \in (T, 1)$, we have

$$\frac{dv(t)}{dt} = -d_A(t)v(t),$$

where $v(T)$ is known. Then it is obvious that the unique solution $v(t) = v(T)e^{-\int_T^t d_A(s)ds}$ exists and $0 \leq v(t) \leq mK$ for $t \in [T, 1]$. By repeating the similar arguments to time intervals $[1, 2], [2, 3], \ldots$, the statement holds. ☐

Based on the expression of $v(t)$ in the proof, we can further observe that $\limsup_{t \to \infty} v(t) \leq K$ for any $\varphi \in \mathcal{X}^+$. Therefore, it is sufficient to study the long-term behaviors of solutions through initial values φ with $\varphi \in \mathcal{X}_K := \{\varphi : 0 \leq \varphi(\theta) \leq K \text{ for all } \theta \in [-\hat{\tau}, 0]\}$. Suppose $\Phi(t)$ be the solution maps of system (4.14) on $\mathcal{X}$, such that $\Phi(t)\varphi = v_t(\varphi)$, $t \geq 0$, where $v(t; \varphi)$ is the unique solution of system (4.14) with $v_0 = \varphi \in \mathcal{X}$. Without loss of generality, we assume initial value φ satisfies $0 \leq \varphi(0) \leq K$. Based on Lemma 3.5 in [122], we obtain the following statements.

Lemma 4.3.2. *$\Phi(t) : \mathcal{X} \to \mathcal{X}$ is an 1-periodic semiflow in the sense that (i) $\Phi(0) = I$; (ii) $\Phi(t+1) = \Phi(t) \circ \Phi(1), \forall t \geq 0$; (iii) $\Phi(t)\varphi$ is continuous in $(t, \varphi) \in [0, \infty) \times \mathcal{X}$.*

The following lemma presents that the periodic semiflow $\Phi(t)$ is monotone and strictly subhomogeneous.

Lemma 4.3.3. *(i) For any φ and ψ in $\mathcal{X}_K$ with $\varphi \geq \psi$, the solutions $u(t; \varphi)$ and $u(t; \psi)$ of equation (4.14) with $u_0(\cdot; \varphi) = \varphi$ and $u_0(\cdot; \psi) = \psi$, respectively, satisfy $u(t; \varphi) \geq u(t; \psi)$ for all $t \geq 0$;*

(ii) If there is some $t_0 \geq 0$ such that $u(t_0; \varphi) > u(t_0; \psi)$, then we have $u(t; \varphi) > u(t; \psi)$ for all $t \geq t_0$;

(iii) For any $\varphi \gg 0$ in $\mathcal{X}_K$ and any $\gamma \in (0, 1)$, we have $u(t; \gamma\varphi) > \gamma u(t; \varphi)$ for all $t > 0$.

Proof. (i) Denote $v(t) = u(t;\varphi)$ and $w(t) = u(t;\psi)$, then we have $v_t(\cdot) \in \mathcal{X}_K$ with $v_0(\cdot) = \varphi$ and $w_t(\cdot) \in \mathcal{X}_K$ with $w_0(\cdot) = \psi$. For $t \in [0, \overline{\tau}]$, we have

$$\begin{aligned} v^{'}(t) &= \left(1 - \frac{v(t)}{K}\right) q(t) - \mu_A(t)v(t),\ v(0) = \varphi(0); \\ w^{'}(t) &= \left(1 - \frac{w(t)}{K}\right) p(t) - \mu_A(t)w(t),\ w(0) = \psi(0), \end{aligned}$$

where $q(t) = \delta_1(t)\varphi(t-\tau_1(t)) + \delta_2(t)\varphi(t-\tau_2(t))$ and $p(t) = \delta_1(t)\psi(t-\tau_1(t)) + \delta_2(t)\psi(t-\tau_2(t))$.

Assume that a function $z(t)$ satisfies the following equation

$$z^{'}(t) = \left(1 - \frac{z(t)}{K}\right) q(t) - \mu_A(t)z(t),\ z(0) = \psi(0).$$

It follows that $z(t) = e^{-\int_0^t \left(\frac{q(s)}{K} + \mu_A(s)\right)ds} \left(\psi(0) + \int_0^t e^{\int_0^s \left(\frac{q(\xi)}{K} + \mu_A(\xi)\right)d\xi} \cdot q(s)ds\right)$, and

$$\begin{aligned} z(t) =& \psi(0)e^{-\int_0^t \left(\frac{q(\xi)}{K} + \mu_A(\xi)\right)d\xi} + K\left[\int_0^t \frac{q(s)}{K} e^{-\int_s^t \left(\frac{q(\xi)}{K} + \mu_A(\xi)\right)d\xi} ds\right] \\ =& \psi(0)e^{-\int_0^t \left(\frac{q(\xi)}{K} + \mu_A(\xi)\right)d\xi} + K\left[\int_0^t \left(\frac{q(s)}{K} + \mu_A(s)\right) e^{-\int_s^t \left(\frac{q(\xi)}{K} + \mu_A(\xi)\right)d\xi} ds\right] \\ &- K\int_0^t \mu_A(s) e^{-\int_s^t \left(\frac{q(\xi)}{K} + \mu_A(\xi)\right)d\xi} ds \\ =& \psi(0)e^{-\int_0^t \left(\frac{q(\xi)}{K} + \mu_A(\xi)\right)d\xi} + K\left[1 - e^{-\int_0^t \left(\frac{q(\xi)}{K} + \mu_A(\xi)\right)d\xi} - \int_0^t \mu_A(s) e^{-\int_s^t \left(\frac{q(\xi)}{K} + \mu_A(\xi)\right)d\xi} ds\right] \\ \leq& K - K\int_0^s \mu_A(\eta) e^{-\int_\eta^s \left(\frac{q(\xi)}{K} + \mu_A(\xi)\right)d\xi} d\eta \leq K, \end{aligned}$$

which implies that $0 \leq z(t) \leq K$. Then we have

$$(v(t) - z(t))^{'} = v^{'}(t) - z^{'}(t) = -\left(\frac{q(t)}{K} + \mu_A(t)\right)(v(t) - z(t)),$$

and $v(0) - z(0) = \varphi(0) - \psi(0)$, which implies that

$$v(t) - z(t) = (\varphi(0) - \psi(0))e^{-\int_0^t \left(\frac{q(s)}{K} + \mu_A(s)\right)ds}.$$

Similarly, we have

$$
\begin{aligned}
(z(t)-w(t))^{'} =& z^{'}(t)-w^{'}(t) \\
=& -\left(\frac{p(t)}{K}+\mu_A(t)\right)(z(t)-w(t))+\left(1-\frac{z(t)}{K}\right)(q(t)-p(t)),
\end{aligned}
$$

and $z(0)-w(0)=0$, which means that

$$
z(t)-w(t)=e^{-\int_0^t\left(\frac{p(\xi)}{K}+\mu_A(\xi)\right)d\xi}\int_0^t(q(s)-p(s))\left(1-\frac{z(s)}{K}\right)e^{\int_0^s\left(\frac{p(\xi)}{K}+\mu_A(\xi)\right)}ds.
$$

Hence, there exists

$$
\begin{aligned}
v(t)-w(t) &= (v(t)-z(t))+(z(t)-w(t)) \\
&= (\varphi(0)-\psi(0))e^{-\int_0^t\left(\frac{q(s)}{K}+\mu_A(s)\right)ds}+e^{-\int_0^t\left(\frac{q(s)+\mu_A(s)}{K}\right)ds}\int_0^t(q(s) \\
&\quad -p(s))\left(1-\frac{z(s)}{K}\right)e^{\int_0^s\left(\frac{p(\xi)}{K}+\mu_A(\xi)\right)d\xi}ds \\
&\geq 0.
\end{aligned}
$$

Repeating the similar arguments for $t\in[\overline{\tau},2\overline{\tau}],[2\overline{\tau},3\overline{\tau}],\dots,[\lfloor n\rfloor\overline{\tau},n\overline{\tau}]$, with $n=\frac{T}{\overline{\tau}}$, we have $v(t)\geq w(t)$ for all $t\in[0,T]$.

For $t\in(T,1)$, it follows that $v(t)=v(T)e^{-\int_t^T d_A(s)ds}$ and $w(t)=w(T)e^{-\int_t^T d_A(s)ds}$. Since $\varphi(T)\geq\psi(T)$, we have

$$
v(t)-w(t)=(\varphi(T)-\psi(T))e^{-\int_t^T d_A(s)ds}\geq 0.
$$

Thus $\Phi(t):\mathcal{X}\to\mathcal{X}$ is monotone for $t\in[0,1]$. Repeating the process to the next intervals $[1,2],[2,3],\dots$, we prove that $\Phi(t):\mathcal{X}\to\mathcal{X}$ is monotone for all $t\geq 0$.

(ii) If there exists a $0\leq t_0\leq T$ such that $u(t_0;\varphi)>u(t_0;\psi)$, we may choose $\hat{\varphi}=u_{t_0}(\cdot;\varphi)\in\mathcal{X}_K$ and $\hat{\psi}=u_{t_0}(\cdot;\psi)\in\mathcal{X}_K$. Then $\hat{\varphi}\geq\hat{\psi}$ and $\hat{\varphi}(0)=u(t_0;\varphi)>u(t_0;\psi)=$

$\hat{\psi}(0)$. For any $t_0 \leq t \leq T$, we have

$$\begin{aligned} v(t) - w(t) =& (\hat{\varphi}(t_0) - \hat{\psi}(t_0)) e^{-\int_{t_0}^{t} \left(\frac{q(s)}{K} + \mu_A(s)\right) ds} + e^{-\int_{t_0}^{t} \left(\frac{q(s)+\mu_A(s)}{K}\right) ds} \int_{t_0}^{t} (q(s) \\ & - p(s)) \left(1 - \frac{z(s)}{K}\right) e^{\int_{t_0}^{s} \left(\frac{p(\xi)}{K} + \mu_A(\xi)\right) d\xi} ds > 0. \end{aligned}$$

If $T \leq t_0 \leq 1$, for $t_0 \leq t \leq 1$, we have

$$v(t) - w(t) = (v(t_0) - w(t_0)) e^{-\int_{t_0}^{t} d_A(s) ds} > 0.$$

Similar arguments hold if t_0 is in other intervals $[1, 2], [2, 3], \ldots$. The arguments show that if for show $t_0 \geq 0$, we have $v(t_0) > w(t_0)$, then $v(t) > w(t)$ for all $t \geq t_0$.

(iii) Denote $z(t) = u(t; \gamma\varphi)$ and $v(t) = u(t; \varphi)$ with $z_0(\cdot) = \gamma\varphi$ and $v_0(\cdot) = \varphi \gg 0$ in $\mathcal{X}_K$. It follows from item (ii) that $z(t) > 0$ and $v(t) > 0$ for all $t > 0$. For any $t \in [0, \overline{\tau}]$ and $0 < \gamma < 1$, we have

$$\begin{aligned} z(t) &= \gamma\varphi(0) e^{\int_0^t \left(-\mu_A(s) - \frac{\gamma q(s)}{K}\right) ds} + \int_0^t \gamma q(s) e^{-\int_s^t \left(\mu_A(\xi) + \frac{\gamma q(\xi)}{K}\right) d\xi} ds \\ &> \gamma\varphi(0) e^{\int_0^t \left(-\mu_A(s) - \frac{q(s)}{K}\right) ds} + \int_0^t \gamma q(s) e^{-\int_s^t \left(\mu_A(\xi) + \frac{q(\xi)}{K}\right) d\xi} ds \\ &= \gamma v(t), \end{aligned}$$

where $q(s) = \delta_1(s)\varphi(s - \tau_1(s)) + \delta_2(s)\varphi(s - \tau_2(s))$. Similar arguments implies that $z(t) > \gamma v(t)$ for all $t \in [\overline{\tau}, T]$. Then it is obviously shown that $z(T) > \gamma v(T)$. For any $t \in [T, 1]$, we have

$$\begin{aligned} z(t) &= z(T) e^{-\int_T^t d_A(s) ds} \\ &> \gamma v(T) e^{-\int_T^t d_A(s) ds} \\ &= \gamma v(t), \end{aligned}$$

which implies that $z(t) > \gamma v(t)$ for $t \in [0, 1]$. Repeating the process for $t \in [1, 2], [2, 3], \ldots$, we obtain $z(t) > \gamma v(t)$ for all $t > 0$. □

4.3.2 Quotient space and strong monotonicity

It follows from Lemma 4.3.3(i) that the periodic semiflow defined on the natural phase space $\mathcal{X}$ is monotone in the sense that $\Phi(t)\varphi \geq \Phi(t)\psi$ if $\varphi \geq \psi$. However, as we may show later than it is not eventually strongly monotone in the sense that for any two initial data $\varphi > \psi$, there is t_0 such that when $t \geq t_0$,

$$\Phi(t)\varphi \gg \Phi(t)\psi.$$

However, sometimes strong monotonicity property of the solution semiflow is essential to establish global attractivity results (see, for example, [95, 167, 207]).

Regarding the equation as an ordinary differential equation, we have the following observations:

(i) When $t \in [0, T]$, we need the values of $u(0)$, $u(t - \tau_1(t))$ and $u(t - \tau_2(t))$. It is easy to see that $t - \tau_1(t) \in I_1$ and $t - \tau_2(t) \in I_2$ by the monotonicity of functions $f_1(t) = t - \tau_1(t)$ and $f_2(t) = t - \tau_2(t)$. Since $t - \tau_1(t)$ is strictly increasing, then we have a more reasonable choice of $t - \tau_1(t) \in I_1 := [-\tau_1(0), \min\{T - \tau_1(T), 0\}]$. Similarly, we have $t - \tau_2(t) \in I_2 := [-\tau_2(0), T - \tau_2(T)]$. That is, the information of initial value is on the set $\{0\} \bigcup I_1 \bigcup I_2$.

(ii) When $t \in [1, 1 + T]$, we have $t - \tau_1(t) > 0$, but it is still possible that $t - \tau_2(t) < 0$. Therefore, the specific historical value at $t - \tau_2(t)$ should be given. In this sense, the initial value on the interval $I_3 := [1 - \tau_2(1), \min\{0, 1 + T - \tau_2(1 + T)\}]$ should be given.

By checking the structure of the model, we define a closed set $A \subset \mathcal{X}$ as

$$A = \{\varphi \in \mathcal{X} : \varphi(\theta) = 0 \text{ for all } \theta \in \{0\} \cup I_1 \cup I_2 \cup I_3\}. \tag{4.16}$$

Based on the set A, we have the following interesting observations:

Lemma 4.3.4. *For any two initial data* $\varphi,\ \psi \in \mathcal{X}$ *and the respective solutions through them* $u(t;\varphi)$ *and* $u(t;\psi)$*,*

(i) if $\varphi - \psi \in A$*, then* $u(t;\varphi) - u(t;\psi) \equiv 0$ *for all* $t \geq 0$*;*

(ii) if furthermore, $\varphi \in A$*, then* $u(t;\varphi) \equiv 0$ *for all* $t \geq 0$*.*

Proof. When $\varphi - \psi \in A$, two solutions $u(t;\varphi)$ and $u(t;\psi)$ satisfy $u(0;\varphi) - u(0;\psi) = \varphi(0) - \psi(0) = 0$. For $t \in [0, \overline{\tau}]$, we have

$$\begin{aligned}\frac{du(t;\varphi)}{dt} &= q(t)\left(1 - \frac{u(t;\varphi)}{K}\right) - \mu_A(t)u(t;\varphi);\\ \frac{du(t;\psi)}{dt} &= p(t)\left(1 - \frac{u(t;\psi)}{K}\right) - \mu_A(t)u(t;\psi),\end{aligned}$$

where $q(t) = \delta_1(t)\varphi(t-\tau_1(t)) + \delta_2(t)\varphi(t-\tau_2(t))$ and $p(t) = \delta_1(t)\psi(t-\tau_1(t)) + \delta_2(t)\psi(t-\tau_2(t))$. Since $t - \tau_1(t) \in [-\tau_1(0), \overline{\tau} - \tau_1(\overline{\tau})] \subseteq I_1$, then $\varphi(t - \tau_1(t)) = \psi(t - \tau_1(t))$. Similarly, $t - \tau_2(t) \in [-\tau_2(0), \overline{\tau} - \tau_2(\overline{\tau})] \subseteq I_2$ implies that $\varphi(t - \tau_2(t)) = \psi(t - \tau_2(t))$. Thus $q(t) = p(t)$ and then

$$\begin{aligned}\frac{du(t;\varphi)}{dt} - \frac{du(t;\psi)}{dt} &= q(t)\left[\left(1 - \frac{u(t;\varphi)}{K}\right) - \left(1 - \frac{u(t;\psi)}{K}\right)\right] - \mu_A(t)[u(t;\varphi) - u(t;\psi)]\\ &= \left[-\frac{q(t)}{K} - \mu_A(t)\right][u(t;\varphi) - u(t;\psi)].\end{aligned} \tag{4.17}$$

Since equation (4.17) is linear and the initial value $u(0;\phi) - u(0;\psi) = 0$, then $u(t;\varphi) - u(t;\psi) \equiv 0$ for all $0 \leq t \leq \overline{\tau}$ if $\varphi - \psi \in A$. Similar arguments hold for $t \in [\overline{\tau}, 2\overline{\tau}], [2\overline{\tau}, 3\overline{\tau}], \ldots, [\lfloor n \rfloor \overline{\tau}, n\overline{\tau}]$, with $n = \frac{T}{\overline{\tau}}$, we have $u(t;\varphi) - u(t;\psi) \equiv 0$ for all $t \in [0, T]$.

For $t \in (T, 1)$, we have

$$\frac{d(u(t;\varphi) - u(t;\psi))}{dt} = -d_A(t)(u(t;\varphi) - u(t;\psi)).$$

Therefore, $u(t;\varphi) - u(t;\psi) \equiv 0$ for all $t \in [T, 1]$ if $\varphi - \psi \in A$. Repeating these arguments to all time intervals $[1, 2], [2, 3], \ldots$, we have $u(t;\varphi) - u(t;\psi) \equiv 0$ for all $t \geq 0$. Therefore, statement (i) holds.

If $\varphi \in A$, choosing $\psi = 0$ as the zero function in $\mathcal{X}$, then $\varphi - \psi \in A$ and the solution through ψ is identically zero for all $t \geq 0$. Hence

$$u(t;\varphi) \equiv u(t;\psi) \equiv 0,$$

which implies that statement (ii) holds. $\square$

Therefore, if we choose two initial data $\varphi > \psi$ in the ordering $\mathcal{X}^+$, but $\varphi - \psi \in A$, then $u(t;\varphi) - u(t;\psi) \equiv 0$. Hence, the periodic semiflow $\Phi(t)$ is not strongly monotone. The above observation on the identical solutions through two initial values φ and ψ with $\varphi - \psi \in A$ motivates us to classify these initial data into the same class and partition the phase space $\mathcal{X}$ into different classes [59, 89]. This can be done by using the quotient space $\mathcal{Q} = \mathcal{X}/A$, consisting of equivalence classes

$$[\varphi] = \{\varphi + a : a \in A\}. \tag{4.18}$$

As solutions from two initial values φ_1 and φ_2 taken from an equivalence class has the property that $\varphi_1 - \varphi_2 \in A$, Lemma 4.3.4 illustrates that the solutions $u(t;\varphi_1) - u(t;\varphi_2) \equiv 0$ for all $t \geq 0$. Then we may study the solution through a given equivalence class from the quotient space $\mathcal{Q}$. For $[\varphi] \in \mathcal{Q}$, the solution through this equivalence is exactly the solution $u(t;\varphi)$, based on which, the solution map $\tilde{\Phi}(t) : \mathcal{Q} \to \mathcal{Q}$ can be defined as

$$\tilde{\Phi}(t)([\varphi]) = [\Phi_t(\varphi)] = [u_t(\cdot;\varphi)]$$

with $u_t(\theta;\varphi) = u(t+\theta;\varphi)$ for all $\theta \in [-\hat{\tau}_2, 0]$.

Then the positive cone $\mathcal{Q}^+ \subset \mathcal{Q}$ can be introduced, consisting of equivalence classes $[\varphi]$ with

$$\mathcal{Q}^+ := \{[\varphi] \in \mathcal{Q} : \varphi(\theta) \geq 0 \text{ for all } \theta \in \{0\} \cup I_1 \cup I_2 \cup I_3\}.$$

For the coned space $(\mathcal{Q}, \mathcal{Q}^+)$, we can show that the solution map $\tilde{\Phi}(t)$ is strongly monotone when $t \geq 4$.

Lemma 4.3.5. *For any two initial data equivalence classes* $[\varphi]$ *and* $[\psi]$*, if* $[\varphi] > [\psi]$ *under the cone* $\mathcal{Q}^+$*, then* $\tilde{\Phi}(t)([\varphi]) \gg \tilde{\Phi}(t)([\psi])$ *when* $t \geq 4$.

Proof. Suppose two typical elements φ and ψ are from two different equivalence classes, and $[\varphi] > [\psi]$ with partial ordering defined by $\mathcal{Q}^+$, then $\varphi(\theta) \geq \psi(\theta)$ for all $\theta \in \{0\} \cup I_1 \cup I_2 \cup I_3$, and there is $\theta_0 \in \{0\} \cup I_1 \cup I_2 \cup I_3$ such that $\varphi(\theta_0) > \psi(\theta_0)$.

Denote $v(t) = u(t; \varphi)$ and $w(t) = u(t; \psi)$, then we have $v_t(\cdot) \in \mathcal{Q}^+$ with $v_0(\cdot) = \varphi$ and $w_t(\cdot) \in \mathcal{Q}^+$ with $w_0(\cdot) = \psi$. It follows that

$$\begin{aligned} v(t) - w(t) = (\varphi(0) - \psi(0))e^{-\int_0^t \left(\frac{q(s)}{K} + \mu_A(s)\right) ds} + e^{-\int_0^t \left(\frac{q(s)+\mu_A(s)}{K}\right) ds} \int_0^t (q(s) \\ - p(s)) \left(1 - \frac{z(s)}{K}\right) e^{\int_0^s \left(\frac{p(\xi)}{K} + \mu_A(\xi)\right) d\xi} ds, \end{aligned} \tag{4.19}$$

where $q(s) = \delta_1(s)\varphi(s - \tau_1(s)) + \delta_2(s)\varphi(s - \tau_2(s))$ and $p(s) = \delta_1(s)\psi(s - \tau_1(s)) + \delta_2(s)\psi(s - \tau_2(s))$. This implies that

(i) If $\theta_0 \in \{0\}$, we have $\varphi(0) > \psi(0)$. Then $v(t) - w(t) > 0$ for all $t > 0$.

(ii) If $\theta_0 \in I_1$, we choose a unique $t_1 \in [0, T]$ such that $t_1 - \tau_1(t_1) = \theta_0$. These uniqueness and existence of t_1 is guaranteed by the fact that the inverse function of the bijection function $f_1(t) = t - \tau_1(t)$ with domain $[0, 1]$ and range I_1 exists. Next we will prove $v(t_1) > w(t_1)$. If $t_1 \in [0, \overline{\tau}]$ and suppose, for a contradiction, that $v(t_1) = w(t_1)$. Then from (4.19), we have $\varphi(0) = \psi(0)$ and $q(s) = p(s)$ for all $s \in [0, t_1]$. Since $\delta_1(s) > 0$ and $\delta_2(s) > 0$ for all $s \in [0, t_1]$, then there exists

$$\delta_1(s)\varphi(s - \tau_1(s)) + \delta_2(s)\varphi(s - \tau_2(s)) = \delta_1(s)\psi(s - \tau_1(s)) + \delta_2(s)\psi(s - \tau_2(s))$$

for all $s \in [0, t_1]$. On the other hand, when $s = t_1$, we have $\varphi(\theta_0) = \varphi(t_1 - \tau_1(t_1)) =$

$\psi(t_1 - \tau_1(t_1)) = \psi(\theta_0)$, which contradicts with $\varphi(\theta_0) > \psi(\theta_0)$. If $t_1 \in [\overline{\tau}, T]$, similar arguments are valid.

(iii) If $\theta_0 \in I_2$, then we choose a unique $t_2 \in [0, T]$ such that $t_2 - \tau_2(t_2) = \theta_0$. These uniqueness and existence of t_2 is guaranteed by the fact that the inverse function of the bijection function $f_2(t) = t - \tau_2(t)$ with domain $[0, 1]$ and range I_2 exists. If $t_2 \in [0, \overline{\tau}]$, we suppose $v(t_2) = w(t_2)$. Then we have $\varphi(0) = \psi(0)$ and $q(s) = p(s)$ for all $s \in [0, t_2]$. Since $\delta_1(s) > 0$ and $\delta_2(s) > 0$ for all $s \in [0, t_2]$, there exists

$$\delta_1(s)\varphi(s - \tau_1(s)) + \delta_2(s)\varphi(s - \tau_2(s)) = \delta_1(s)\psi(s - \tau_1(s)) + \delta_2(s)\psi(s - \tau_2(s))$$

for all $s \in [0, t_2]$. However, at $s = t_2$, we have $\varphi(\theta_0) = \varphi(t_2 - \tau_2(t_2)) = \psi(t_2 - \tau_2(t_2)) = \psi(\theta_0)$, which contradicts with $\varphi(\theta_0) > \psi(\theta_0)$.

(iv) If $\theta_0 \in I_3$, choose $t_3 - \tau_2(t_3) = \theta_0$ for $t_3 \in [1, 1 + T]$. It follows from the bijection function $f_3(t) = t - \tau_2(t)$ for $t \in [1, 1 + T]$ that t_3 exists and is unique, then

$$\begin{aligned} v(t) - w(t) =&(v(1) - w(1))e^{-\int_1^t \left(\frac{q(s)}{K} + \mu_A(s)\right)ds} + e^{-\int_1^t \left(\frac{q(s)+\mu_A(s)}{K}\right)ds} \int_1^t (q(s) \\ &- p(s))\left(1 - \frac{z(s)}{K}\right) e^{\int_1^s \left(\frac{p(\xi)}{K} + \mu_A(\xi)\right)d\xi} ds. \end{aligned}$$

where $q(s) = \delta_1(s)\varphi(s - \tau_1(s)) + \delta_2(s)\varphi(s - \tau_2(s))$ and $p(s) = \delta_1(s)\psi(s - \tau_1(s)) + \delta_2(s)\psi(s - \tau_2(s))$. Suppose $v(t_3) = w(t_3)$. Then we have $v(1) = w(1)$ and for all $s \in [1, t_3]$, there exists

$$\delta_1(s)v_s(-\tau_1(s)) + \delta_2(s)v_s(-\tau_2(s)) = \delta_1(s)w_s(-\tau_1(s)) + \delta_2(s)w_s(-\tau_2(s)).$$

Since $\delta_1(s) > 0$ and $\delta_2(s) > 0$, we must have $\varphi(\theta_0) = v_{t_3}(-\tau_2(t_3)) = w_{t_3}(-\tau_2(t_3)) = \psi(\theta_0)$ when $s = t_3$. This contradicts with $\varphi(\theta_0) > \psi(\theta_0)$.

Hence, we can always find an $t_0 \in [0, 1 + T]$ (which may be t_1, t_2 or t_3) such that $v(t_0) > w(t_0)$. It follows from Lemma 4.3.3(ii) that $u(t; \varphi) > u(t; \psi)$ for all $t \geq 2 > t_0$. Hence, the solution map $\tilde{\Phi}(t)$ is strongly monotone whenever $t \geq 4$. $\square$

4.3.3 Basic reproduction number and global dynamics

The basic reproduction number $\mathcal{R}_0$ is the threshold quantity which measures the average expected number of new adult offsprings produced by a single adult frog during its life cycle [196]. Then we study the dynamics of the basic reproduction number $\mathcal{R}_0$ by the theories in [207] and [206] (see also Section 2.3 in Chapter 2).

Linearizing Equation (4.14), we have

$$\begin{aligned} \frac{\mathrm{d}A(t)}{dt} &= \delta_1(t)A(t-\tau_1(t)) + \delta_2(t)A(t-\tau_2(t)) - \mu_A(t)A(t), \;\; t-\lfloor t \rfloor \in [0,T], \\ \frac{\mathrm{d}A(t)}{\mathrm{d}t} &= -d_A(t)A(t), \;\; t-\lfloor t \rfloor \in (T,1). \end{aligned} \tag{4.20}$$

The recruitment is denoted by $F : \mathbb{R} \to \mathcal{L}(\mathcal{X}, \mathbb{R})$ defined by

$$F(t)\varphi = \begin{cases} \delta_1(t)\varphi(-\tau_1(t)) + \delta_2(t)\varphi(-\tau_2(t)), & t-\lfloor t \rfloor \in [0,T], \\ 0, & t-\lfloor t \rfloor \in (T,1), \end{cases}$$

and the evolution is denoted by V :

$$V(t) = \begin{cases} \mu_A(t), & t-\lfloor t \rfloor \in [0,T], \\ d_A(t), & t-\lfloor t \rfloor \in (T,1). \end{cases}$$

The evolution process of the adult frogs is governed by

$$\frac{du(t)}{dt} = -V(t)u(t).$$

Let $\Phi(t,s)$, $t \geq s$, be the evolution operator of the above system, satisfying

$$\frac{\partial}{\partial t}\Phi(t,s) = -V(t)\Phi(t,s), \forall t \geq s, \text{and } \Phi(s,s) = 1, \forall s \in \mathbb{R},$$

which implies that

$$\Phi(t,s) = e^{-\int_s^t V(r)dr}.$$

Let C_1 be the ordered Banach space of all continuous and 1-periodic functions from $\mathbb{R}$ to $\mathbb{R}$, equipped with the maximum norm and the positive cone $C_1^+ := \{v \in C_1 : v(t) \geq 0, \forall t \in \mathbb{R}\}$. Suppose $v \in C_1$ be the initial number of adult frogs. Then for any given $s \geq 0$, $F(t-s)v_{t-s}$ is the number of frogs that are newly recruited into adult stage per unit time at time $t-s$, which are produced by the adult frogs who were introduced over the time interval $[t-s-2\hat{\tau}, t-s]$. Then $\Phi(t,t-s)F(t-s)v_{t-s}$ is the number of those adult frogs who newly entered into adult stage at time $t-s$ and remain alive at time t. It follows that

$$\int_0^\infty \Phi(t,t-s)F(t-s)v_{t-s}ds = \int_0^\infty \Phi(t,t-s)F(t-s)v(t-s+\cdot)ds$$

is the number of accumulative new adult individuals at time t produced by all those adult frogs introduced at all previous time to t.

Define a linear operator L on C_1 by

$$\begin{aligned} [Lv](t) &= \textstyle\int_0^\infty \Phi(t,t-s)F(t-s)v(t-s+\cdot)ds \\ &= \textstyle\int_{-\infty}^t \Phi(t,\xi)F(\xi)v(\xi+\cdot)d\xi \\ &= \textstyle\int_{-\infty}^t \Phi(t,s)F(s)v(s+\cdot)ds, \forall t \in \mathbb{R}, v \in C_1. \end{aligned}$$

Next, we show that the operator L maps a continuous function $v \in C_1$ to a periodic and continuous function $Lv \in C_1$, that is $L : C_1 \to C_1$. For any given $v \in C_1$, it is obviously known that v is bounded, then $F(s)v(s+\cdot)$ is also bounded, namely to assume that there exists an upper bounded B such that $|F(s)v(s+\cdot)| \leq B$. Then for any t, we have

$$\begin{aligned} |\textstyle\int_{-\infty}^t \Phi(t,s)F(s)v(s+\cdot)ds| &\leq \textstyle\int_{-\infty}^t \Phi(t,s)\cdot B\, ds \\ &\leq B\textstyle\int_{-\infty}^t e^{-\mu(t-s)}ds \\ &\leq \tfrac{B}{\mu}, \end{aligned}$$

where $\mu = \min\{\mu_A(s), d_A(s)\}$. For any $t \geq s$, we have $\Phi(t,s) \leq 1$. For any $\epsilon > 0$, choose $\delta = \min\{\frac{\epsilon}{2B}, -\frac{\ln(1-\frac{\epsilon\mu}{2B})}{\hat{\mu}}\}$ with $\hat{\mu} = \max_{t\in[0,1]}\{\mu_A(s), d_A(s)\}$. For any $t_1 \geq t_2 \geq s$, we have $\Phi(t_1,s) = \Phi(t_1,t_2)\Phi(t_2,s)$ and $\Phi(t_1,t_2) \geq e^{-\hat{\mu}(t_1-t_2)}$. Furthermore, when $|t_1 - t_2| < \delta$, we have

$$\begin{array}{rl} & |[Lv](t_1) - [Lv](t_2)| \\ = & |\int_{-\infty}^{t_1} \Phi(t_1,s)F(s)v(s+\cdot)ds - \int_{-\infty}^{t_2} \Phi(t_2,s)F(s)v(s+\cdot)ds| \\ = & |\int_{-\infty}^{t_1} \Phi(t_1,s)F(s)v(s+\cdot)ds - \int_{-\infty}^{t_2} \Phi(t_1,s)F(s)v(s+\cdot)ds \\ & +\int_{-\infty}^{t_2} \Phi(t_1,s)F(s)v(s+\cdot)ds - \int_{-\infty}^{t_2} \Phi(t_2,s)F(s)v(s+\cdot)ds| \\ \leq & |\int_{t_2}^{t_1} \Phi(t_1,s)F(s)v(s+\cdot)ds| + |\int_{-\infty}^{t_2}[\Phi(t_2,s) - \Phi(t_1,s)]F(s)v(s+\cdot)ds| \\ \leq & (t_1 - t_2)\cdot 1 \cdot B + (1 - \Phi(t_1,t_2))\int_{-\infty}^{t_2} \Phi(t_2,s)F(s)v(s+\cdot)ds \\ \leq & B(t_1 - t_2) + (1 - e^{-\hat{\mu}(t_1-t_2)})\cdot \frac{B}{\mu} \\ \leq & \epsilon. \end{array}$$

This proves the continuity of $[Lv](t)$.

Suppose $v(t+1) = v(t), \forall t \in \mathbb{R}$. Since

$$\begin{aligned} [Lv](t+1) &= \int_0^\infty \Phi(t+1, t+1-s)F(t+1-s)v(t+1-s+\cdot)ds \\ &= \int_0^\infty \Phi(t, t-s)F(t-s)v(t-s+\cdot)ds \\ &= [Lv](t), \end{aligned}$$

it follows that $[Lv](t)$ is also periodic with respect to t. Therefore, we have $L : C_1 \to C_1$. According to some properties in [206] (or Section 2.3), we define $\mathcal{R}_0 = r(L)$, the spectral radius of L.

For any given $t \geq 0$, let $W(t)$ be the solution map of system (4.20) on $\mathcal{X}$, such that $W(t)\varphi = w_t(\varphi)$, $t \geq 0$, where $w(t;\varphi)$ is the unique solution of (4.20) with $w_0 = \varphi \in \mathcal{X}$. Then $W := W(1)$ is the Poincaré map associated with linear system (4.20). Let $r(W)$ be the spectral radius of W. By Theorem 2.3.1, we obtain

Lemma 4.3.6. *$\mathcal{R}_0 - 1$ has the same sign as $r(W(1)) - 1$.*

In addition, for any given $t \geq 0$, let $\tilde{W}(t)$ be the solution map of system (4.20) on $\mathcal{Q}^+$, such that $\tilde{W}(t)\varphi = \tilde{w}_t(\varphi)$, $t \geq 0$, where $\tilde{w}(t;\varphi)$ is the unique solution of (4.20) with $\tilde{w}_0 = \varphi \in \mathcal{Q}^+$. Using similar arguments to Lemma 3.8 in [122] through the Krein-Rutman theorem, it is shown that the stability of the zero solution for system (4.20) on $\mathcal{X}$ equals to that on $\mathcal{Q}^+$.

Lemma 4.3.7. *Two Poincaré maps* $W(1) : \mathcal{X} \to \mathcal{X}$ *and* $\tilde{W}(1) : \mathcal{Q}^+ \to \mathcal{Q}^+$ *have the same spectral radius, that is,* $r(W(1)) = r(\tilde{W}(1))$.

Based on the above lemmas and results, we obtain the following global dynamics for system (4.14).

Theorem 4.3.1. *The following statements are valid:*

1. *If* $\mathcal{R}_0 < 1$, *then the zero solution is globally asymptotically stable for system (4.14) in* $\mathcal{Q}^+$;
2. *If* $\mathcal{R}_0 > 1$, *then system (4.14) admits a unique positive* 1*-periodic solution* $A^*(t)$, *which is globally asymptotically stable in* $\mathcal{Q}^+ \setminus \{[0]\}$.

Proof. We fix an integer n_0 such that $n_0 > 4$. According to Lemma 4.3.7, $\tilde{\Phi}(t)$ can be regarded as an n_0-periodic semiflow on $\mathcal{Q}^+$. It follows from Lemma 4.3.3 and Lemma 4.3.5, the solution map $\tilde{\Phi}(n_0)$ is strongly monotone and strictly subhomogeneous on $\mathcal{Q}^+$. By Theorem 2.1.3, we obtain

(i) If $r(D\tilde{\Phi}(n_0)(0)) \leq 1$, then the zero solution is globally asymptotically stable for system 4.14 in $\mathcal{Q}^+$;

(ii) If $r(D\tilde{\Phi}(n_0)(0)) > 1$, then system (4.14) admits a unique positive n_0-periodic solution $A^*(t)$, which is globally asymptotically stable in $\mathcal{Q}^+ \setminus \{[0]\}$.

Note that $r(D\tilde{\Phi}(n_0)(0)) = r(\tilde{W}(n_0)) = (r(\tilde{W}(1)))^{n_0}$. Based on Lemmas 4.3.6 and 4.3.7, we have $sign(\mathcal{R}_0 - 1) = sign(r(D\tilde{\Phi}(n_0)(0)) - 1)$. It remains to prove that $A^*(t)$ is also 1-periodic with respect to case (ii). Let $\varphi^* = v_0^* \in \mathcal{Q}$ with $v^*(t) = A^*(t)$. Then $\tilde{\Phi}(n_0)(\varphi^*) = \varphi^*$. Note that

$$\tilde{\Phi}^{n_0}(1)(\tilde{\Phi}(1)(\varphi^*)) = \tilde{\Phi}(1)(\tilde{\Phi}^{n_0}(1)(\varphi^*)) = \tilde{\Phi}(1)(\tilde{\Phi}(n_0)(\varphi^*)) = \tilde{\Phi}(1)(\varphi^*).$$

By the uniqueness of the positive fixed point of $\tilde{\Phi}^{n_0}(1) = \tilde{\Phi}(n_0)$, we have $\tilde{\Phi}(1)(\varphi^*) = \varphi^*$, which implies that $A^*(t) = u(t; \varphi^*)$ is an 1-periodic solution of system (4.14). □

Next we will analyze the dynamics for the variables $L_1(t)$, $L_2(t)$ and $J(t)$ in system (4.12). Given the initial values

$$\begin{aligned}
L_1(0) &= \int_{-\theta_1(0)}^{0} p_1 B(\xi, A(\xi)) e^{-\int_{\xi}^{0} \mu_1(s)ds} d\xi, \\
L_2(0) &= \int_{-\theta_2(0)}^{0} (1-p_1) B(\xi, A(\xi)) e^{-\int_{\xi}^{\lfloor t \rfloor - 1 + T} \mu_2(s)ds - \int_{\lfloor t \rfloor - 1 + T}^{\lfloor t \rfloor} d_2(s)ds - \int_{\lfloor t \rfloor}^{0} \mu_2(s)ds} d\xi, \\
J(0) &= \int_{-\theta_J(0)}^{0} [p_1 B(\xi - \theta_1(\xi), A(\xi - \theta_1(\xi)))(1 - \theta_1'(\xi)) e^{-\int_{\xi-\theta_1(\xi)}^{\xi} \mu_1(\alpha)d\alpha} \\
&\quad + (1-p_1) B(\xi - \theta_2(\xi), A(\xi - \theta_2(\xi)))(1 - \theta_2'(\xi)) \\
&\quad \cdot e^{-\int_{\xi-\theta_2(\xi)}^{\lfloor t \rfloor - 2 + T} \mu_2(\alpha)d\alpha - \int_{\lfloor t \rfloor - 2 + T}^{\lfloor t \rfloor - 1} d_2(\alpha)d\alpha - \int_{\lfloor t \rfloor - 1}^{\xi} \mu_2(\alpha)d\alpha}] e^{-\int_{\xi}^{0} \mu_J(s)ds} d\xi,
\end{aligned}$$

we obtain

$$\begin{aligned}
L_1(t) &= \int_{t-\theta_1(t)}^{t} p_1 B(\xi, A(\xi)) e^{-\int_{\xi}^{t} \mu_1(s)ds} d\xi, \\
L_2(t) &= \int_{t-\theta_2(t)}^{t} (1-p_1) B(\xi, A(\xi)) e^{-\int_{\xi}^{\lfloor t \rfloor - 1 + T} \mu_2(s)ds - \int_{\lfloor t \rfloor - 1 + T}^{\lfloor t \rfloor} d_2(s)ds - \int_{\lfloor t \rfloor}^{t} \mu_2(s)ds} d\xi, \\
J(t) &= \int_{t-\theta_J(t)}^{t} [p_1 B(\xi - \theta_1(\xi), A(\xi - \theta_1(\xi)))(1 - \theta_1'(\xi)) e^{-\int_{\xi-\theta_1(\xi)}^{\xi} \mu_1(\alpha)d\alpha} \\
&\quad + (1-p_1) B(\xi - \theta_2(\xi), A(\xi - \theta_2(\xi)))(1 - \theta_2'(\xi)) \\
&\quad \cdot e^{-\int_{\xi-\theta_2(\xi)}^{\lfloor t \rfloor - 2 + T} \mu_2(\alpha)d\alpha - \int_{\lfloor t \rfloor - 2 + T}^{\lfloor t \rfloor - 1} d_2(\alpha)d\alpha - \int_{\lfloor t \rfloor - 1}^{\xi} \mu_2(\alpha)d\alpha}] e^{-\int_{\xi}^{t} \mu_J(s)ds} d\xi,
\end{aligned} \tag{4.21}$$

It follows that when $\mathcal{R}_0 < 1$, we have $\lim_{t \to \infty} (L_1(t), L_2(t), J(t)) = 0$. Therefore, we can obtain the global dynamics for system (4.12) as follows.

Theorem 4.3.2. *The following statements are valid for system (4.12):*

1. *If* $\mathcal{R}_0 < 1$*, then* $(0, 0, 0, 0)$ *is globally asymptotically stable;*
2. *If* $\mathcal{R}_0 > 1$*, then there exists a positive* 1*-periodic solution* $(L_1^*(t), L_2^*(t), J^*(t), A^*(t))$*, which is globally asymptotically stable for all nontrivial solutions.*

4.4 Numerical Simulations

This section presents numerical simulations to illustrate quantitative results on seasonal frog patterns.

4.4.1 Parameters

(i) Seasonal air temperature

Temperature is reported to affect the larval duration and has been proposed to play a role in determining the vital rates in the life cycle, as well as the overwintering phenomenon [188]. We may take the actual temperature from a specific study air; that would be better. If not, choose a periodic function as some studies in leading ecology journals. In this study, we take the temperature data (in degrees °C) as a function of time t (in a day) in the following form [139] for illustration purpose of the conceptual framework

$$T_a(t) = c_K + d_K \times \sin\left(\frac{2\pi}{365} \times (t - t_0)\right). \tag{4.22}$$

where $c_K = 10$°C is mean annual temperature and $d_K = 15$°C is the amplitude of temperature variation, suppose to be 15°C [139].

(ii) Water temperature

The water temperature, not the air temperature, is an important indicator for frog development, growth, and overwintering in an aquatic environment [188]. Many theoretical models have been proposed and calibrated to convert air temperature into water temperature, including neural network or wavelet transform-based approaches and empirical regression model [208]. Here we are going to use a lumped and physically-statistically based hybrid model, called *air2water* model, developed in [146, 147, 148] to describe the temporal evolution of water temperature in lakes, with the seasonal temperature in (4.22) as input force. The *air2water* model is credited as a widely used approach with its simplicity and accuracy [208]. The 6-parameter version of the model [147] takes the following form

$$\frac{dT_w(t)}{dt} = \frac{1}{\delta}\left[a_1 + a_2 T_a(t) - a_3 T_w(t) + a_5 \cos\left(2\pi\left(\frac{t}{365} - a_6\right)\right)\right]$$

with

$$\delta = \begin{cases} \exp\left(-\frac{T_w(t)-T_h}{a_4}\right), & \text{if } T_w(t) \geq T_h, \\ 1, & \text{if } T_w(t) < T_h. \end{cases}$$

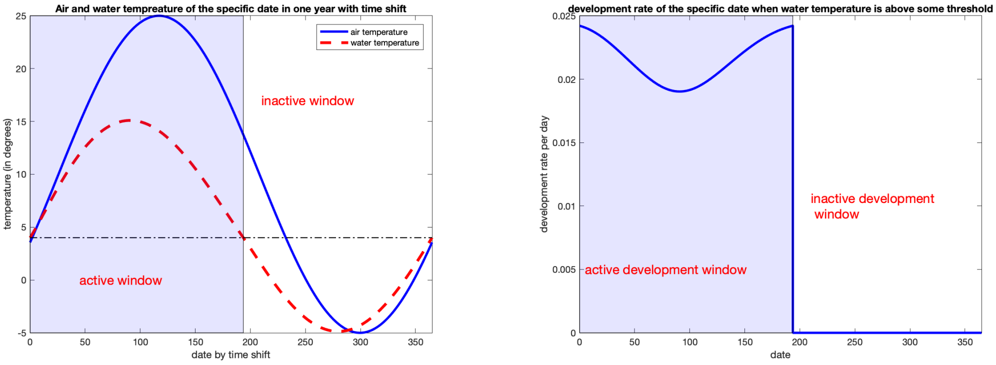

Figure 4.1: Left: The temperature profiles, as well as the active and hibernation seasons determined by the threshold temperature. Right: the development velocity for type 1 tadpoles.

In this *air2water* model, T_h is the reference value of deep water temperature, which can be set as 4°C for domestic lakes [208]. The parameter values for a_i with $i = 1, 2, \cdots,$

6 are taken from the fitted parameters in `https://github.com/marcotoffolon/air2water` as

$$
\begin{aligned}
&a_1 \in [-0.1726, 2], && a_2 \in [7.989 \times 10^{-4}, 5.071 \times 10^{-2}], && a_3 \in [1.357 \times 10^{-3}, 0.2] \\
&a_4 \in [1, 17.435], && a_5 \in [0, 2.954], && a_6 \in [0, 1].
\end{aligned}
$$

For easy reference, we are resetting the initial day by a time shift such that the active window starts from day 0 of the year. Therefore, the temperature profiles can be simulated as in Figure 4.1.

(iii) Thermal threshold and temperature-dependent parameters

The model in its form can easily accommodate the thermal thresholds for individual growth and development. For example, the development rate when the temperature is blow the lower temperature threshold (LTT) can be set to be zero. Describing the biological temperature responses with mathematical models is one of the most important questions in ecology [23].

Various functions have been employed to fit the experimental and field data to illustrate the relationship between the metabolic rates and environmental conditions, such as temperature. Some widely functions form include quadratic, Gaussian, Arrhenius, modified Gaussian, exponentially modified Gaussian, Weibull and beta functions [23, 142]. In our simulations, the beta functional response fitted in [142] will be used to describe the relationship between the water temperature T_w and the development rate

$$
r(T_w) = \frac{a\left(\frac{T_w - b + \frac{c(d-1)}{d+e-2}}{c}\right)^{d-1}\left(1 - \frac{T_w - b + \frac{c(d-1)}{d+e-2}}{c}\right)^{e-1}}{\left(\frac{d-1}{d+e-2}\right)^{d-1}\left(\frac{e-1}{d+e-2}\right)^{e-1}} \text{ when } T_w \geq TLL \tag{4.23}
$$

with $a = 0.024431$, $b = 29.63653$, $c = 21.64977$, $d = 2.194146$, $e = 1.30143$.

Different stages have variable tolerance responses to the temperatures [178], and we may assume a lower temperature threshold (LTT) for the aquatic environment to determine the range $[0, T]$ during which the birth rate is not vanishing and the individual develops. We use the temperature $4°$C to determine the time window and overwinter duration. Then the development velocity can be simulated by combining the functional response and temperature data. Here, as an illustration, we simulated the temperature-dependent (therefore, time-dependent) development velocity, which will be used to derive the time delays in the model system. The results are reported in Figure 4.1.

Table 4.1: Model parameters with means, ranges, description, and sources for each parameter estimate.

Parameter	Mean	Range	Description	Reference
p_1	0.75	0.65-0.85	Proportion of tadpoles spending 1 year	[53]
$b(t)$	1105 mated couple^{-1}	884-1326	Fecundity	[53]
μ_1	7.55 year^{-1}	6.19-9.71 year^{-1}	Natural death rate of tadpoles spending 1 year per capita	[138]
μ_2	7.55 year^{-1}	6.19-9.71 year^{-1}	Natural death rate of tadpoles spending 2 year per capita	[138]
μ_J	0.73 year^{-1}	0.3-4 year^{-1}	Natural death rate of juvenile per capita	[138]
μ_A	0.73 year^{-1}	0.3-2.25 year^{-1}	Natural death rate of adult per capita	[138]
K	14000	10000-40000	Maximum adult frog population size	[138]
T	$\frac{8\times30}{360}$ year^{-1}	—	Normal development period of frog population	[130]
τ_1	$\theta_J(t) + \theta_1(t - \theta_J(t))$	—	Time delay	—
τ_2	$\theta_J(t) + \theta_2(t - \theta_J(t))$	—	Time delay	—

4.4.2 Population persistence and seasonal pattern

Using the given parameters in Table 4.1, the net reproduction number can be computed by the algorithm proposed in [203]. The solutions in Table 4.2 indicate that the species persists when $\mathcal{R}_0 = 1.4761$, and illustrate the seasonality of the population in a periodic environment.

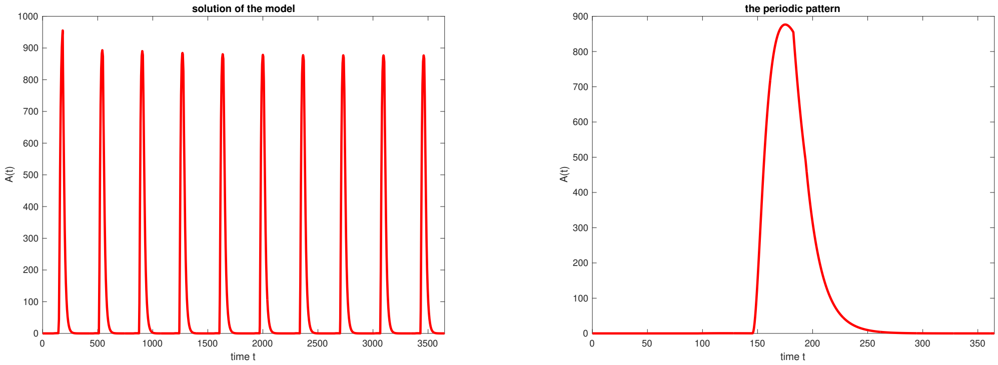

Figure 4.2: Left: The long-term dynamics when $R_0 = 1.4761$. Right: Seasonality of species when $R_0 = 1.4761$.

4.5 Discussion

In this paper, based on the actual growth of the frog population at a specific temperature, we formulate a seasonal succession model consisting of delay differential equations to reflect the effects of different seasons and temperatures on the frogs' growth. This model combines breeding and hibernation seasons, where frogs can grow normally during the breeding season; however, there is no development during their hibernation phases. The dynamics of the frogs' population are structured in four stages: two types of tadpoles L_1 and L_2 representing spend 1 and 2 years in the tadpole stage, one juvenile stage J, and one adult stage A. Decoupling the first three equations from others, we focus on dynamically analyzing the last equation for the adult stage. Then we sequentially explore the existence and uniqueness of the solution for the adult subsystem and the strong monotonicity by introducing the quotient space. According to the theory of monotone dynamical systems and the comparison method, we study the threshold dynamics for the system based on the derivation of the basic reproduction number $\mathcal{R}_0$. Biologically, the theoretical results imply that the frog population will go to extinction eventually when $\mathcal{R}_0 < 1$ and keep growing steadily to a stable cycle when $\mathcal{R}_0 > 1$. The final simulations numerically illustrate the temperature-dependent development velocity, thereby determining the time delays within the model system. These numerical results validate the global dynamics of the system and were employed to demonstrate the seasonality of the mature frog population.

Our model incorporates seasonal climate factors, growth, and developmental characteristics of frog populations. We divide the population into different growth stages and introduce temperature-dependent delays to describe the developmental duration of frogs. Due to the complexity of the ecological environment, this model that considers abiotic factors can more accurately analyze the growth and development of frog species in a specific ecological environment. Indeed, in addition to temperature, other abiotic factors such as rain relative humidity, hazardous chemicals, and habitat damage may also have a particular impact on population density, and some life stages may be more sensitive to the impact of one of these factors. These aspects can therefore be considered in future research. Besides, the division of the two types of tadpoles, including those that take one and two years to grow, is conducive to specifically characterizing the different characteristics in different life stages of frog species.

Mathematically, we introduce the concept of quotient space based on the natural phase space and study the strong monotonicity in addition to presenting some basic properties of the solutions, which is one of our research highlights. More importantly, due to the duration division of breeding and hibernation seasons, we need to analyze the existence and uniqueness of the solutions concerning the two different seasons in one period, respectively, thereby expanding to more periods. This theoretical proof differs slightly from other previous studies. In addition, the introduction of quotient space is essential to explore the global dynamical results by the strong monotonicity property of the solution semiflow, which is the basis for further applying the theory of asymptotically periodic semiflows to establish the global dynamics of population system. This theoretical method to study the globally asymptotic behavior of solutions can also be employed to analyze some delay differential equations with seasonal divisions in other population systems.

Based on the current model, we notice that all threshold dynamics of the frog population are analyzed in a particular ecological environment, and the diversity of habitats is not considered here. Frogs can also move freely between different habitats, and through this migration, the growth and reproduction of frog populations will be affected by the various living conditions of these habitats. Due to the ubiquity of such diverse ecological environments, it is necessary to integrate fragments into our systemic model to characterize better the development of frog populations, which will be a valuable entry point for future research. Furthermore, we can incorporate the specific impact of abiotic factors on the development of frog populations into future research to analyze the reasons for the current reduction or even extinction of amphibians and propose animal protection suggestions to relevant ecological management departments.

Chapter 5

Infection-induced host extinction for the frog population

5.1 Introduction

This chapter is devoted to evaluate the risk of frog extinction due to disease transmission. Numerous studies have been conducted to uncover the mechanisms of disease-induced extinction and assess the relative significance of these mechanisms in threatening natural populations [55, 98, 124, 166]. Key theoretical mechanisms proposed include: (i) the pronounced impact of small population sizes and stochastic events on extinction risk, exacerbated by disease outbreaks in endangered populations or the Allee effect, where low genetic variability facilitates pathogen invasion, diminishing population size and genetic diversity; (ii) the role of frequency-dependent transmission and non-uniform mixing in driving extinctions, with disease spread being influenced by the proportion of infected individuals rather than the total number of susceptible or infectious hosts [35]; (iii) the ability of generalist pathogens, including those with biotic and abiotic reservoirs, to overcome host density thresholds and cause extinction of a particular host species, with external reservoirs heightening extinction risk when external infection rates are high [156]; and (iv) the potential for indirect or trophic-mediated extinctions, where disease-induced declines or extinctions can trigger broader ecological consequences within the community [66]. However, simple deterministic models for specialist parasites with density-dependent transmission often fail to exhibit disease-induced extinction, as these models typically illustrate that parasites will go extinct before their hosts [55]. This study aims to propose a straightforward deterministic model with density-dependent transmission that predicts the disease-induced extinction, which offers additional mechanisms for this phenomenon.

Environmental factors, including floating pathogens, significantly influence the dissemination of the *Bd* fungus among frog populations [37, 65]. Transmission dynamics of infectious diseases with both host-to-host and environment-to-host transmission pathways have been extensively examined by mathematical models [10, 47, 49, 85, 115, 113, 114, 175, 192, 196]. Sun et al. [175] provided a thorough review on studies of multi-transmission routes, encompassing direct contact and environmental-mediated infection. Codeço [49] developed a model incorporating environmental factors, such as the concentration of *V. cholerae* in water, within an epidemiological framework. Ghosh et al. [85] explored a model that integrates vibrio concentration and environmental discharge density, which influences vibrio proliferation. Wang and Liao [192] proposed a deterministic model with nonlinear incidence rates and a generalized representation of pathogen levels in contaminated water, with the model's global dynamics subsequently analyzed using geometric and matrix-theoretic methods [47, 115], respectively. Despite these advances, the impact of the pathogen on host species extinction risk remains underexplored. Most existing models are disease-specific, focusing on the transmission dynamics of the pathogen, with little attention given to host persistence and extinction. This gap highlights the need for integrating disease transmission into models of host extinction risk.

To explore the mechanisms that determine the persistence or extinction of a host population within a host-pathogen interaction cycle, we will employ a compartmental modeling framework involving variables for numbers of susceptible and infected individuals, denoted by S and I respectively, as well as the concentration of the pathogen in the environment, denoted by B. Unlike traditional epidemiological models, which depict the transmission of infectious diseases as a process occurring when a susceptible host comes into direct contact with an infectious host, the compartment B allows us to incorporate an additional pathogen transmission route through an environment (reservoir) containing infectious agents deposited by infected hosts and accessed by recipient hosts [81]. Although the model formulation is primarily inspired by *chytridiomycosis* transmission in frogs, other diseases have also been described by the SIB compartmental models, such as bacterial (e.g., cholera [191] and brucellosis [175]), viral (e.g., avian influenza or hepatitis E in pigs), prion (e.g., chronic wasting disease), and parasitic (e.g., *cryptosporidium*) infections [81]. Various deterministic and stochastic models have been proposed to describe different mechanisms of disease transmission [15, 128, 129]. Unlike existing modeling studies that focus on the transmission dynamics, our aim is to examine the conditions that contribute to the potential decline and extinction of the host population. We will formulate and analyze two versions of the SIB epidemiological models. By examining the stability of various equilibria and uniform persistence of the deterministic model, we identify some important indices and the underlying mechanisms that lead to population extinction or persistence. The corresponding stochastic model is used to estimate the probabilities of disease extinction, major outbreaks, and host population extinction. Numerical simulations will be employed to verify the stability and persistence of the deterministic epidemic model, calculate the probability of disease extinction, simulate different sample paths of the continuous-time Markov chain (CTMC) model, and predict the time of extinction for the stochastic epidemic model. By integrating deterministic and stochastic approaches, we get a better understanding of potential factors that influence the persistence or extinction of host populations in the context of host-pathogen interactions with two types of transmission.

5.2 A deterministic model for environmentally transmitted pathogens

Let $S(t)$, $I(t)$ and $B(t)$ denote the population densities of susceptible hosts, infected hosts and the concentration of environmental pathogens, respectively. To keep the model simple while incorporating the direct transmission among hosts and indirect transmission between host and environment, we formulate the following model:

$$\begin{aligned}
\frac{\mathrm{d}S(t)}{\mathrm{d}t} &= f_1(S(t)+\eta I(t))(S(t)+\eta I(t)) - d_N S(t) - \kappa B(t)S(t) - \beta\frac{S(t)I(t)}{1+\alpha I(t)},\\
\frac{\mathrm{d}I(t)}{\mathrm{d}t} &= \kappa B(t)S(t) + \beta\frac{S(t)I(t)}{1+\alpha I(t)} - d_N I(t) - \mu I(t),\\
\frac{\mathrm{d}B(t)}{\mathrm{d}t} &= f_2(B(t))B(t) - d_B B(t) + \gamma I(t).
\end{aligned} \tag{5.1}$$

The birth functions $f_1(\cdot)$ and $f_2(\cdot)$ of the host and pathogen populations are assumed to take the Beverton-Holt form [123, 185], namely

$$f_1(x) = \frac{b_N}{1+\xi_N x} \quad \text{and} \quad f_2(x) = \frac{b_B}{1+\xi_B x}.$$

The parameter $\eta \in (0,1]$ represents the reduced reproductivity of infected individuals [157, 170]. A susceptible host can become infected through direct contact with an infected host or exposure to an environmental pathogen with infection rates β and κ, respectively. Taking into account the impact of behavioral changes, we incorporate the Holling type II function into host-to-host transmission [84, 176]. Here, $\frac{1}{1+\alpha I}$ measures the inhibition effects resulting from the behavioral adaptations of susceptible individuals as the number of infected individuals increases, where α is a nonnegative constant. Furthermore, *Bd* pathogens possess the capability to reproduce independently at function $f_2(B(t))$ or be shed into the environment by infected individuals at rate γ. The inclusion of this term distinguishes our model from most existing studies. A summary of the model parameters and their corresponding descriptions is provided in Table 5.1.

It should be noted that model (5.1) aligns with the framework presented in Lanzas et al. [110]. For the reproduction of the host and pathogen populations and the pathogen transmission term, various functional forms have been proposed and fitted in modeling references. For illustrative purposes, in this study, the Beverton-Holt function is used to describe the host and bacteria proliferation, while the Holling type II functional response is adopted for the force of infection in the direct transmission route. These functional forms have been employed widely in existing studies [82, 84, 176, 201]. Several discrete-time models commonly utilize the Beverton-Holt function as a recruitment mechanism [123, 186, 185, 202]. Further functional forms can be found in the paper [110] in a general model for environmentally transmitted pathogens.

Table 5.1: Parameter descriptions and baseline values in model (5.1).

Parameter	Description	Value	Reference
b_N	Background birth rate of hosts	0.55 day^{-1}	[151]
ξ_N	Crowding effect of host population	0.05 host^{-1}	Assumed
η	Reduced host reproduction due to infection	0.7	Assumed
d_N	Death rate of host population	0.05 day^{-1}	[96]
κ	Infection rate of a susceptible host by the environmental pathogen	0.0015 pathogen^{-1}day^{-1}	[65]
β	Infection rate of a susceptible host by an infected host	0.012 host^{-1}day^{-1}	[96]
α	Crowding effect of infected hosts	0.05 host^{-1}	Assumed
μ	Disease-induced death of an infected host	0.019 day^{-1}	[145]
b_B	Background birth rate of the pathogen	0.25 day^{-1}	[37]
ξ_B	Crowding effect of the pathogen	0.1 pathogen^{-1}	Assumed
d_B	Death rate of the pathogen	0.01 day^{-1}	[65]
γ	Release rate of the pathogen by an infected host	0.5 day^{-1}	[145]

5.2.1 Well-posedness of the model

The dynamic behavior of the deterministic model 5.1 is initiated in this section by studying the well-posedness of the model.

Proposition 5.2.1. *For each initial value* $(S(0), I(0), B(0)) \in \mathbb{R}^3_+$*, system* (5.1) *admits a unique solution* $(S(t), I(t), B(t)) \in \mathbb{R}^3_+$ *for all* $t \geq 0$.

Proof. Let $\boldsymbol{g} : \mathbb{R}^3_+ \to \mathbb{R}^3$ be the vector field given by the right hand side of system (5.1), which is obviously Lipschitz continuous on any bounded subset of $\mathbb{R}^3_+$. It follows that a unique solution $(S(t), I(t), B(t))$ through the initial values in $(S(0), I(0), B(0)) \in \mathbb{R}^3_+$ exists for $t \in [0, t_0)$. Furthermore, the following observations hold for $\boldsymbol{u} = (u_1, u_2, u_3) = (S, I, B) \in \mathbb{R}^3_+$: (i) if $u_1 = 0$, then $g_1(u) = \frac{b_N \cdot \eta u_2}{1+\xi_N \cdot \eta u_2} \geq 0$; (ii) if $u_2 = 0$, then $g_2(u) = \kappa u_3 u_1 \geq 0$; and (iii) if $u_3 = 0$, then $g_3(u) = \gamma u_2 \geq 0$. Based on [73] and [167], these observations imply that solutions starting in $\mathbb{R}^3_+$ are still in $\mathbb{R}^3_+$ once they exist. It remains to show that $t_0 = \infty$. To do that, we consider the sum of three variables

$$G(t) = S(t) + I(t) + B(t),$$

which satisfies

$$\begin{aligned}\frac{\mathrm{d}G(t)}{\mathrm{d}t} &\leq \frac{b_N(S(t)+I(t))}{1+\xi_N(S(t)+I(t))} + \frac{b_B B(t)}{1+\xi_B B(t)} + \gamma I(t)\\ &\leq b_N S(t) + b_B B(t) + (b_N+\gamma)I(t)\\ &\leq cG(t)\end{aligned}$$

with $c = \max\{b_B, b_N + \gamma\}$. Therefore,

$$G(t) = S(t) + I(t) + B(t) \leq G(0)e^{ct}$$

for all $t \geq 0$, which implies $t_0 = \infty$. □

Remark 4.2.1. Actually, it is easy to verify through [167, Remark 5.2.1] that the following set

$$\Omega = \left\{ (S, I, B) \in \mathbb{R}^3_+ : S + I \leq \frac{b_N}{\xi_N d_N} \text{ and } B \leq \frac{b_B}{\xi_B d_B} \right\}$$

is positively invariant.

5.2.2 Three reproduction numbers and summarized qualitative results

To simplify the presentation, we first introduce three biologically meaningful indices based on which some qualitative findings are established. Theoretical justifications for these results will be presented later.

We first check the host population growth model with no pathogen transmission ($I(t) = B(t) = 0$):

$$\frac{\mathrm{d}S(t)}{\mathrm{d}t} = \frac{b_N S(t)}{1 + \xi_N S(t)} - d_N S(t). \tag{5.2}$$

By using the idea in Fan et al. [73], we can introduce the net reproduction number for host population $\mathcal{R}_H := \frac{b_N}{d_N}$. For the scalar equation (5.2), it is easy to make the following conclusion.

Proposition 5.2.2. *The following statements are valid for system (5.2):*

(i) If $\mathcal{R}_H \leq 1$, the trivial steady state 0 is global asymptotically stable;

(ii) If $\mathcal{R}_H > 1$, then there exists a unique positive steady state $S_0 = \frac{1}{\xi_N}(\frac{b_N}{d_N} - 1) = \frac{1}{\xi_N}(\mathcal{R}_H - 1)$, which is globally asymptotically stable in $\mathbb{R}_+ \backslash \{0\}$.

Remark 4.2.2. The first two equations in (5.1) show that the total host population size $H(t) = S(t) + I(t)$ satisfies

$$\frac{dH(t)}{dt} \leq \frac{b_N H(t)}{1 + \xi_N H(t)} - d_N H(t).$$

A simple comparison argument, combined with Proposition 5.2.2 (i) shows that the host population will go extinct as $\mathcal{R}_H \leq 1$.

If we ignore the shedding of pathogen from infectious hosts, then the dynamics of pathogen population are governed by

$$\frac{\mathrm{d}B(t)}{\mathrm{d}t} = \frac{b_B B(t)}{1+\xi_B B(t)} - d_B B(t). \tag{5.3}$$

Define the pathogen reproduction number in the habitat as $\mathcal{R}_B := \frac{b_B}{d_B}$. Similar to Proposition 5.2.2, we have the following conclusion.

Proposition 5.2.3. *The following statements are valid for system (5.3):*

(i) If $\mathcal{R}_B \leq 1$, the trivial steady state 0 is globally asymptotically stable;

(ii) If $\mathcal{R}_B > 1$, then there exists a unique positive steady state $B_0 = \frac{1}{\xi_B}(\frac{b_B}{d_B} - 1) = \frac{1}{\xi_B}(\mathcal{R}_B - 1)$, which is globally asymptotically stable in $\mathbb{R}_+ \backslash \{0\}$.

When $\mathcal{R}_H > 1$ and $\mathcal{R}_B \leq 1$, we can introduce the basic reproduction number through the unique infection-free steady state $E_{10} = (S_0, 0, 0)$ of system (5.1) where $S_0 = \frac{1}{\xi_N}(\frac{b_N}{d_N} - 1)$. The new infection and transition matrices are given by:

$$F = \begin{pmatrix} \beta S_0 & \kappa S_0 \\ 0 & 0 \end{pmatrix} \text{ and } V = \begin{pmatrix} d_N + \mu & 0 \\ -\gamma & d_B - b_B \end{pmatrix}, \tag{5.4}$$

respectively. The next generation matrix of infection is

$$FV^{-1} = \begin{bmatrix} \frac{\beta S_0}{d_N+\mu} + \frac{\gamma\kappa S_0}{(d_N+\mu)(d_B-b_B)} & \frac{\kappa S_0}{d_B-b_B} \\ 0 & 0 \end{bmatrix},$$

and therefore, the basic reproduction number of model (5.1) can be defined as

$$\mathcal{R}_0 = \rho(FV^{-1}) = \frac{\beta S_0}{d_N + \mu} + \frac{\gamma \kappa S_0}{(d_N + \mu)(d_B - b_B)}.$$

The two terms in the above formula represent the secondary cases produced by direct contact and contaminated environment, respectively.

Based on these three reproduction numbers, $\mathcal{R}_H$, $\mathcal{R}_B$ and $\mathcal{R}_0$, we can establish the results as summarized in Table 5.2 and Figure 5.1 on the existence and local/global stability of all possible equilibria. It is interesting to observe from Table 5.2 and region E in Figure 5.1 that the host-free equilibrium $E_{01} = (0, 0, B_0)$ can retain locally stable even if $\mathcal{R}_H > 1$. This observation suggests the potential for host extinction in the event of disease spread. The proofs will be provided in the subsequent subsections.

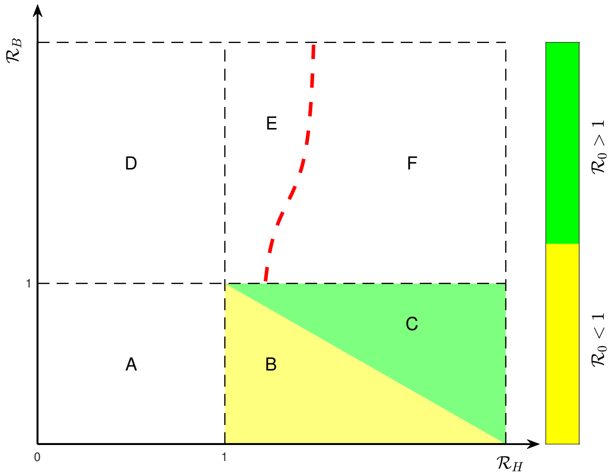

Figure 5.1: Partition area based on the stability conditions of the equilibria. Region A: $E_{00} = (0, 0, 0)$ is globally asymptotically stable; Region B: $E_{10} = (S_0, 0, 0)$ is globally asymptotically stable; Region C and F: the positive equilibrium $E^* = (S^*, I^*, B^*)$ exists; Region D and E: $E_{01} = (0, 0, B_0)$ is locally stable. The red dashed line represents $b_N = \frac{(d_N + \kappa B_0)(d_N + \mu)}{\eta \kappa B_0 + d_N + \mu}$.

Table 5.2: Existence and stability of equilibrium in system (5.1).

Equilibrium	Existence	Local stability	Global stability
$(0,0,0)$	Always exists	Locally stable if $\mathcal{R}_H < 1$ and $\mathcal{R}_B < 1$	Globally asymptotically stable
		Unstable if $\mathcal{R}_H > 1$ or $\mathcal{R}_B > 1$	
$(S_0,0,0)$	Exists if $\mathcal{R}_H > 1$	Locally stable if $\mathcal{R}_H > 1$, $\mathcal{R}_B < 1$ and $\mathcal{R}_0 < 1$	Globally asymptotically stable
		Unstable if $\mathcal{R}_H > 1$, but (i) $\mathcal{R}_B \geq 1$; or (ii) $\mathcal{R}_B < 1$ and $\mathcal{R}_0 > 1$	
	Does not exist if $\mathcal{R}_H \leq 1$		
$(0,0,B_0)$	Exists if $\mathcal{R}_B > 1$	Locally stable if (i) $\mathcal{R}_B > 1$, $\mathcal{R}_H \leq 1$; or (ii) $\mathcal{R}_B > 1$, $d_N < b_N < \frac{(d_N+\kappa B_0)(d_N+\mu)}{\eta\kappa B_0+d_N+\mu}$	
		Unstable if $\mathcal{R}_B > 1$, $b_N > \frac{(d_N+\kappa B_0)(d_N+\mu)}{\eta\kappa B_0+d_N+\mu}$	
	Does not exist if $\mathcal{R}_B \leq 1$		
(S^*,I^*,B^*)	Exists if (i) $\mathcal{R}_H > 1$, $\mathcal{R}_B < 1$ and $\mathcal{R}_0 > 1$; or (ii) $\mathcal{R}_H > 1$, $\mathcal{R}_B > 1$ and $b_N > \frac{(d_N+\kappa B_0)(d_N+\mu)}{\eta\kappa B_0+d_N+\mu}$		
	Does not exist if (i) $\mathcal{R}_H \leq 1$, or (ii) $\mathcal{R}_H > 1$, $\mathcal{R}_B < 1$ and $\mathcal{R}_0 < 1$; or (iii) $\mathcal{R}_H > 1$, $\mathcal{R}_B > 1$ and $d_N < b_N < \frac{(d_N+\kappa B_0)(d_N+\mu)}{\eta\kappa B_0+d_N+\mu}$		

5.2.3 Dynamical analysis of the deterministic model

This subsection is dedicated to the dynamical analysis of the model by providing theoretical arguments to those results reported in Table 5.2 and Figure 5.1.

(i) The equilibrium $E_{00} = (0,0,0)$

It is easy to see that system (5.1) always admits the trivial equilibrium $E_{00} = (0,0,0)$, where both hosts and pathogens are absent within the habitat. At this equilibrium, the Jacobian matrix takes the following form:

$$J\Big|_{E_{00}} = \begin{bmatrix} b_N - d_N & b_N\eta & 0 \\ 0 & -d_N - \mu & 0 \\ 0 & \gamma & b_B - d_B \end{bmatrix}.$$

Therefore, when $b_N - d_N > 0$ or $b_B - d_B > 0$ ($\mathcal{R}_H > 1$ or $\mathcal{R}_B > 1$), the equilibrium E_{00} is unstable.

Next, we investigate the case when $\mathcal{R}_H \leq 1$ and $\mathcal{R}_B \leq 1$. In this case, Remark 4.2.2 indicates that

$$\lim_{t\to\infty}(S(t), I(t)) = (0, 0).$$

Then the B-equation in system (5.1) is asymptotic to (5.3). Since $\mathcal{R}_B \leq 1$, we have $\lim\limits_{t\to\infty} B(t) = 0$ through the theory of asymptotically autonomous systems [167]. This shows that E_{00} is globally asymptotically stable when $\mathcal{R}_H < 1$ and $\mathcal{R}_B < 1$, implying that both hosts and pathogens will go extinct in this habitat under these conditions.

(ii) The equilibrium $E_{10} = (S_0, 0, 0)$

When $\mathcal{R}_H > 1$, the model (5.1) has a disease-free equilibrium $E_{10} = (S_0, 0, 0)$ with $S_0 = \frac{1}{\xi_N}(\frac{b_N}{d_N} - 1)$. This equilibrium represents the infection-free state. Its stability can be summarized as follows.

Proposition 5.2.4. *For model (5.1), if $\mathcal{R}_H > 1$, then the equilibrium $E_{10} = (S_0, 0, 0)$ exists. Furthermore,*

(i) it is globally asymptotically stable if $\mathcal{R}_B < 1$ and $\mathcal{R}_0 < 1$;

(ii) this equilibrium is unstable if $\mathcal{R}_B \geq 1$, or $\mathcal{R}_B < 1$ and $\mathcal{R}_0 > 1$.

Proof. Define an auxiliary matrix

$$M(\epsilon) = \begin{bmatrix} \beta(S_0+\epsilon) - d_N - \mu & \kappa(S_0+\epsilon) \\ \gamma & b_B - d_B \end{bmatrix},$$

by perturbating the matrix $M(0) = F - V$ with F and V in (5.4). It follows from Theorem 2 in [184] that $s(M(0)) < 0$, where $s(M)$ is the spectral bound of the matrix M. By the continuity of spectral bound, there exists small enough $\epsilon > 0$ such that $s(M(\epsilon)) < 0$. Since the total host population size satisfies

$$\frac{\mathrm{d}H(t)}{\mathrm{d}t} \leq \frac{b_N H(t)}{1+\xi_N H(t)} - d_N H(t).$$

we have $\limsup_{t\to\infty} S(t) \leq \limsup_{t\to\infty} H(t) \leq S_0 = \frac{1}{\xi_N}(\frac{b_N}{d_N}-1)$. Therefore, for $\epsilon > 0$, there exists $t_1 = t(\epsilon) > 0$ such that $S(t) \leq S_0 + \epsilon$ for any $t \geq t_1$. Thus for $t \geq t_1$, we have

$$\begin{aligned}
\frac{\mathrm{d}I(t)}{\mathrm{d}t} &\leq \beta(S_0+\epsilon)I(t) + \kappa(S_0+\epsilon)B(t) - d_N I(t) - \mu I(t),\\
\frac{\mathrm{d}B(t)}{\mathrm{d}t} &\leq b_B B(t) - d_B B(t) + \gamma I(t).
\end{aligned}$$

Considering the following auxiliary linear system

$$\frac{\mathrm{d}x(t)}{\mathrm{d}t} = M(\epsilon)x(t),$$

where the vector $x(t) = (x_1(t), x_2(t))^{\mathrm{T}}$. We have $\lim\limits_{t\to\infty} x_i(t) = 0$ for $i = 1, 2$ for all initial values since $s(M(\epsilon)) < 0$. Choosing $x(0) = (I(t_1), B(t_1))$, the comparison principle implies that

$$(0,0) \leq \lim_{t\to\infty}(I(t), B(t)) \leq \lim_{t\to\infty}(x_1(t-t_1), x_2(t-t_1)) = (0,0).$$

Then based on the theory of asymptotically autonomous systems in [207] (see also Section 2.1), we have $\lim\limits_{t\to\infty} S(t) = S_0$, which implies that E_{10} is globally asymptotically stable when $\mathcal{R}_H > 1$, $\mathcal{R}_B < 1$ and $\mathcal{R}_0 < 1$. Statement (i) holds.

The corresponding Jacobian matrix is

$$J\Big|_{E_{10}} = \begin{bmatrix} \frac{b_N}{(1+\xi_N S_0)^2} - d_N & \frac{b_N\eta}{(1+\xi_N S_0)^2} - \beta S_0 & -\kappa S_0 \\ 0 & \beta S_0 - d_N - \mu & \kappa S_0 \\ 0 & \gamma & b_B - d_B \end{bmatrix}.$$

All eigenvalues of the Jacobian matrix are

$$\lambda_{1,2} = \frac{(a_{11}+a_{22}) \pm \sqrt{(a_{11}-a_{22})^2 + 4a_{12}a_{21}}}{2}$$
$$\text{and} \quad \lambda_3 = \frac{b_N}{(1+\xi_N S_0)^2} - d_N = d_N(\frac{1}{\mathcal{R}_H} - 1) < 0,$$

where $a_{11} = \beta S_0 - d_N - \mu$, $a_{12} = \kappa S_0$, $a_{21} = \gamma$ and $a_{22} = b_B - d_B$.

It is easy to see that if $b_B \geq d_B$, then $a_{22} \geq 0$ and $\lambda_1 = \frac{(a_{11}+a_{22})+\sqrt{(a_{11}-a_{22})^2+4a_{12}a_{21}}}{2} > 0$. If $b_B < d_B$ and $\frac{\beta S_0}{d_N+\mu} + \frac{\gamma\kappa S_0}{(d_N+\mu)(d_B-b_B)} < 1$, then $a_{11} < 0$ and $a_{22} < 0$ and

$$a_{12}a_{21} = \gamma\kappa S_0 < (d_N + \mu - \beta S_0)(d_B - b_B) = a_{11}a_{22}.$$

In this case $\lambda_2 = \frac{(a_{11}+a_{22})-\sqrt{(a_{11}-a_{22})^2+4a_{12}a_{21}}}{2} < 0$ and

$$\lambda_1 \quad < \quad \frac{(a_{11}+a_{22})+\sqrt{(a_{11}-a_{22})^2+4a_{11}a_{22}}}{2} = \frac{(a_{11}+a_{22})+|a_{11}+a_{22}|}{2} = 0.$$

If $b_B < d_B$ and $\frac{\beta S_0}{d_N+\mu} + \frac{\gamma\kappa S_0}{(d_N+\mu)(d_B-b_B)} > 1$, then

$$a_{12}a_{21} = \gamma\kappa S_0 > (d_N + \mu - \beta S_0)(d_B - b_B) = a_{11}a_{22}.$$

In this case,

$$\lambda_1 \quad > \quad \frac{(a_{11}+a_{22})+\sqrt{(a_{11}-a_{22})^2+4a_{11}a_{22}}}{2} = \frac{(a_{11}+a_{22})+|a_{11}+a_{22}|}{2} = 0.$$

In summary, statement (ii) holds. □

(iii) The equilibrium $E_{01} = (0, 0, B_0)$

It is easy to see that system (5.1) admits the equilibrium $E_{01} = (0, 0, B_0)$ if and only if $\mathcal{R}_B > 1$. This equilibrium represents the state in the absence of the host population. Then we can conclude its stability:

Proposition 5.2.5. *For model (5.1), if $\mathcal{R}_B > 1$, then the equilibrium $E_{01} = (0, 0, B_0)$ exists. Furthermore,*

(i) it is locally asymptotically stable if $\mathcal{R}_H < 1$ or $d_N < b_N < \frac{(d_N+\kappa B_0)(d_N+\mu)}{\eta\kappa B_0+d_N+\mu}$;

(ii) this equilibrium is unstable if $b_N > \frac{(d_N+\kappa B_0)(d_N+\mu)}{\eta\kappa B_0+d_N+\mu}$.

Proof. The corresponding Jacobian matrix is

$$J\Big|_{E_{01}} = \begin{bmatrix} b_N - d_N - \kappa B_0 & b_N\eta & 0 \\ \kappa B_0 & -d_N - \mu & 0 \\ 0 & \gamma & \frac{b_B}{(1+\xi_B B_0)^2} - d_B \end{bmatrix}.$$

All eigenvalues of the Jacobian matrix are

$$\lambda_{1,2} = \frac{(a_{11}+a_{22}) \pm \sqrt{(a_{11}-a_{22})^2 + 4a_{12}a_{21}}}{2}$$
$$\text{and } \lambda_3 = \frac{b_B}{(1+\xi_B B_0)^2} - d_B = d_B(\frac{1}{\mathcal{R}_B} - 1) < 0,$$

where $a_{11} = b_N - d_N - \kappa B_0$, $a_{12} = b_N\eta$, $a_{21} = \kappa B_0$ and $a_{22} = -d_N - \mu < 0$. Then we have

(a) if $a_{11} = b_N - d_N - \kappa B_0 \geq 0$, then

$$\lambda_1 = \frac{(a_{11}+a_{22}) + \sqrt{(a_{11}-a_{22})^2 + 4a_{12}a_{21}}}{2} > \frac{a_{11}+a_{22}+|a_{11}-a_{22}|}{2} = a_{11} \geq 0.$$

The equilibrium is unstable;

(b) if $a_{11} = b_N - d_N - \kappa B_0 < 0$, then

$$\lambda_2 = \frac{(a_{11}+a_{22}) - \sqrt{(a_{11}-a_{22})^2 + 4a_{12}a_{21}}}{2} < 0.$$

Note that $\lambda_1 = \frac{(a_{11}+a_{22})+\sqrt{(a_{11}-a_{22})^2+4a_{12}a_{21}}}{2} < 0$ holds if and only if $(a_{11}+a_{22})^2 > (a_{11} -$

$a_{22})^2 + 4a_{12}a_{21}$, that is, $(d_N + \kappa B_0 - b_N)(d_N + \mu) > \eta b_N \cdot \kappa B_0$. Then we discuss the following scenarios:

(bi) if $d_N \geq b_N$, then $(d_N + \kappa B_0 - b_N)(d_N + \mu) \geq \kappa B_0(d_N + \mu) > \eta b_N \cdot \kappa B_0$ since $\eta \leq 1$. Therefore, $\lambda_1 < 0$;

(bii) if $d_N < b_N$ and $d_N + \kappa B_0 > b_N$, namely $d_N < b_N < d_N + \kappa B_0$, then $\lambda_1 < 0$ holds if and only if $b_N < \frac{(d_N+\kappa B_0)(d_N+\mu)}{\eta\kappa B_0+d_N+\mu}$.

Note that $\frac{(d_N+\kappa B_0)(d_N+\mu)}{\eta\kappa B_0+d_N+\mu} < d_N + \kappa B_0$. In summary, the statements hold. □

(iv) Existence and uniqueness of the positive equilibrium

This part is devoted to the study of the positive equilibrium, which contains two propositions.

Proposition 5.2.6. *For system (5.1), if (i)* $\mathcal{R}_H = \frac{b_H}{d_H} \leq 1$*; or (ii)* $\mathcal{R}_H > 1$, $\mathcal{R}_B < 1$ *and* $\mathcal{R}_0 < 1$*; or (iii)* $\mathcal{R}_B > 1$ *and* $d_N < b_N < \frac{(d_N+\kappa B_0)(d_N+\mu)}{\eta\kappa B_0+d_N+\mu}$*, then there is no positive equilibrium.*

Proof. The first two cases can immediately be obtained by applying Remark 4.2.2 and Proposition 5.2.4. Suppose $\mathcal{R}_B > 1$ and $d_N < b_N < \frac{(d_N+\kappa B_0)(d_N+\mu)}{\eta\kappa B_0+d_N+\mu}$, we can also show that the positive equilibrium does not exists as follows. Let $E^* = (S^*, I^*, B^*)$ be a positive equilibrium, we claim that $B^* > B_0$. Suppose not, then $B^* \leq B_0$, and

$$\frac{b_B B^*}{1+\xi_B B^*} - d_B B^* + \gamma I^* \geq \left(\frac{b_B}{1+\xi_B B_0} - d_B\right) B^* + \gamma I^* = \gamma I^* > 0,$$

contradicting to the fact that E^* is an equilibrium. Moreover, we have

$$\begin{aligned} &\frac{b_N}{1+\xi_N \cdot (S^* + \eta I^*)}(S^* + \eta I^*) - d_N S^* - d_N I^* - \mu I^* = 0, \\ &\kappa \cdot B^* \cdot S^* + \beta \cdot \frac{S^* \cdot I^*}{1+\alpha I^*} - d_N I^* - \mu I^* = 0. \end{aligned} \tag{5.5}$$

The second equation of (5.5) implies that $S^* < \frac{d_N+\mu}{\kappa \cdot B^*} I^*$. Therefore,

$$\frac{b_N}{1+\xi_N(S^*+\eta I^*)}(S^*+\eta I^*) - d_N S^* - d_N I^* - \mu I^* < 0$$

contradicts with the first equation of (5.5). That is,

$$\begin{aligned}
&\frac{b_N}{1+\xi_N(S^*+\eta I^*)}(S^*+\eta I^*) - d_N S^* - d_N I^* - \mu I^* \\
&< b_N(S^*+\eta I^*) - d_N S^* - d_N I^* - \mu I^* \\
&< (b_N - d_N)\frac{d_N+\mu}{\kappa B^*} I^* + b_N \eta I^* - d_N I^* - \mu I^* \\
&< (b_N - d_N)\frac{d_N+\mu}{\kappa B_0} I^* + b_N \eta I^* - d_N I^* - \mu I^* \\
&= [(b_N - d_N)(d_N+\mu) + (b_N\eta - d_N - \mu)(\kappa B_0)]\frac{I^*}{\kappa \cdot B_0} \\
&< \left[\left(\frac{(d_N+\kappa B_0)(d_N+\mu)}{\eta\kappa B_0 + d_N + \mu} - d_N\right)(d_N+\mu)\right. \\
&\quad \left. + \left(\frac{(d_N+\kappa B_0)(d_N+\mu)}{\eta\kappa B_0 + d_N + \mu}\eta - d_N - \mu\right)(\kappa B_0)\right]\frac{I^*}{\kappa \cdot B_0} \\
&= 0.
\end{aligned}$$

□

Proposition 5.2.7. *For system (5.1), if (i)* $\mathcal{R}_H > 1$*,* $\mathcal{R}_B < 1$ *and* $\mathcal{R}_0 > 1$*; or (ii)* $\mathcal{R}_B > 1$ *and* $b_N > \frac{(d_N+\kappa B_0)(d_N+\mu)}{\eta\kappa B_0+d_N+\mu}$*, then there is a positive equilibrium* $E^* = (S^*, I^*, B^*)$*. Moreover, the positive equilibrium is unique when it exists.*

Proof. The existence of a positive equilibrium, (S^*, I^*, B^*), for the system (5.1) is obtained as a result of the disease persistence (Theorem 5.2.1 and Theorem 5.2.2) [205]. We aim to establish the uniqueness of the positive equilibrium. It is easy to see that

$$I^* = \frac{d_B B^*}{\gamma} - \frac{b_B B^*}{\gamma(1+\xi_B B^*)} \quad \text{and} \quad S^* = \frac{(d_N+\mu)I^*}{\frac{\beta I^*}{1+\alpha I^*} + \kappa B^*}.$$

Assume that there are two positive equilibria (S_1^*, I_1^*, B_1^*) and (S_2^*, I_2^*, B_2^*). Without loss of generality, we assume that $I_1^* > I_2^*$. Then there must be $0 < m < 1$ such that $I_2^* = mI_1^*$. It follows from the last equation of system (5.1) that

$$(d_B - f_2(B)) \cdot B = \gamma \cdot I > 0,$$

which implies that $d_B > f_2(B)$. Since $\gamma I_2^* < \gamma I_1^*$, we have

$$d_B \cdot B_2^* - f_2(B_2^*) \cdot B_2^* < d_B \cdot B_1^* - f_2(B_1^*) \cdot B_1,$$

which implies that

$$\begin{aligned} d_B \cdot (B_1^* - B_2^*) > f_2(B_1^*) \cdot B_1^* - f_2(B_2^*) \cdot B_2^* \\ &= f_2(B_1^*) \cdot B_1^* - f_2(B_1^*) \cdot B_2^* + f_2(B_1^*) \cdot B_2^* - f_2(B_2^*) \cdot B_2^* \\ &= f_2(B_1^*)(B_1^* - B_2^*) + (f_2(B_1^*) - f_2(B_2^*))B_2^*. \end{aligned}$$

It follows that

$$(d_B - f_2(B_1^*)) \cdot (B_1^* - B_2^*) > (f_2(B_1^*) - f_2(B_2^*))B_2^*. \tag{5.6}$$

Note that $d_B - f_2(B_1^*) > 0$. If $B_1^* \leq B_2^*$, then the left hand side of the inequality (5.6) is non-positive, while the right hand side is non-negative since $f_2(B_1^*) \geq f_2(B_2^*)$. This contradicts the inequality (5.6). Thus we obtain $B_1^* > B_2^*$.

Moreover, since $d_B - f_2(B_2^*) > 0$, $f_2(B_2^*) > f_2(B_1^*)$ and $d_B - f_2(B_1^*) > 0$, we have

$$(d_B - f_2(B_1^*)) \cdot B_1^* = \rho I_1^* = \frac{1}{m}\rho I_2^* = \frac{1}{m}(d_B - f_2(B_2^*)B_2^*) < \frac{1}{m}((d_B - f_2(B_1^*))B_2^*),$$

which implies that $B_1^* < \frac{1}{m}B_2^*$. That is, $mB_1^* < B_2^* < B_1^*$.

According to the second equation of system (5.1), we have

$$\kappa \cdot B \cdot S + \beta \cdot \frac{S \cdot I}{1 + \alpha I} = (d_N + \mu)I,$$

that is

$$S = \frac{d_N + \mu}{\frac{\kappa B}{I} + \frac{\beta}{1+\alpha I}}.$$

Hence,

$$S_2^* = \frac{d_N + \mu}{\frac{\kappa B_2^*}{I_2^*} + \frac{\beta}{1+\alpha I_2^*}} < \frac{d_N + \mu}{\frac{\kappa B_1^*}{I_1^*} + \frac{\beta}{1+\alpha I_1^*}} = S_1^*.$$

Moreover,

$$\begin{aligned} S_2^* = \frac{d_N + \mu}{\frac{\kappa B_2^*}{I_2^*} + \frac{\beta}{1+\alpha I_2^*}} &= \frac{d_N + \mu}{\frac{\kappa B_2^*}{m I_1^*} + \frac{\beta}{1+\alpha m I_1^*}} \\ > \frac{d_N + \mu}{\frac{\kappa B_1^*}{m I_1^*} + \frac{\beta}{m(1+\alpha I_1^*)}} &= m\frac{d_N + \mu}{\frac{\kappa B_1^*}{I_1^*} + \frac{\beta}{1+\alpha I_1^*}} = m S_1^*. \end{aligned}$$

Hence, we conclude that $mS_1^* < S_2^* < S_1^*$, $mI_1^* = I_2^* < I_1^*$ and $mB_1^* < B_2^* < B_1^*$.

Next, we need to make sure that the equilibrium satisfies the first equation of system (5.1). Hence,

$$\begin{aligned} &m(f_1(S_1^* + \eta I_1^*)(S_1^* + \eta I_1^*) - d_N S_1^*) = (d_N + \mu) m I_1^* \\ &= (d_N + \mu) I_2^* = f_1(S_2^* + \eta I_2^*)(S_2^* + \eta I_2^*) - d_N S_2^*. \end{aligned} \tag{5.7}$$

Therefore, we have

$$m(f_1(S_1^* + \eta I_1^*)(S_1^* + \eta I_1^*) - d_N S_1^*) - d_N \eta I_2^* = f_1(S_2^* + \eta I_2^*)(S_2^* + \eta I_2^*) - d_N S_2^* - d_N \eta I_2^*$$

and thus,

$$m(f_1(S_1^* + \eta I_1^*)(S_1^* + \eta I_1^*) - d_N(S_1^* + \eta I_1^*)) = f_1(S_2^* + \eta I_2^*)(S_2^* + \eta I_2^*) - d_N(S_2^* + \eta I_2^*).$$

For any positive solution (S, I, B), we have

$$f_1(S + \eta I)(S + \eta I) - d_N S - d_N I - \mu I = 0,$$

which implies

$$f_1(S + \eta I)(S + \eta I) = d_N(S + I) + \mu I > d_N(S + I) > d_N(S + \eta I).$$

Therefore,

$$f_1(S+\eta I) > d_N.$$

However, we also have

$$\begin{aligned}
&m(f_1(S_1^*+\eta I_1^*)(S_1^*+\eta I_1^*) - d_N(S_1^*+\eta I_1^*)) \\
<&f_1(S_2^*+\eta I_2^*)(mS_1^*+m\eta I_1^*) - d_N(mS_1^*+m\eta I_1^*) \\
=&(f_1(S_2^*+\eta I_2^*) - d_N)(mS_1^*+m\eta I_1^*) \\
<&(f_1(S_2^*+\eta I_2^*) - d_N)(S_2^*+\eta I_2^*),
\end{aligned}$$

which contradicts equation (5.7). Therefore, the positive equilibrium must be unique. □

5.2.4 Persistence of the pathogens and the host population

This subsection analyzes the persistence for the pathogens in the habitat and the host population. We first explore the trivial case when $\mathcal{R}_B > 1$. In this case, we have

$$\frac{\mathrm{d}B(t)}{\mathrm{d}t} \geq \frac{b_B B(t)}{1+\xi_B B(t)} - d_B B(t).$$

Then Proposition 5.2.3 and a comparison principle imply that

$$\liminf_{t\to\infty} B(t) \geq B_0 = \frac{1}{\xi_B}\left(\frac{b_B}{d_B} - 1\right) = \frac{1}{\xi_B}(\mathcal{R}_B - 1).$$

The case where $\mathcal{R}_H > 1$, $\mathcal{R}_B < 1$ and $\mathcal{R}_0 < 1$ has been studied in Proposition 5.2.4, which shows that the pathogen goes extinction. The subsequent result illustrates the pathogen's persistence in the habitat under the remaining scenario: $\mathcal{R}_H > 1$, $\mathcal{R}_B < 1$ and $\mathcal{R}_0 > 1$.

Theorem 5.2.1. *For system (5.1), if $\mathcal{R}_H > 1$, $\mathcal{R}_B < 1$ and $\mathcal{R}_0 > 1$, then the pathogen and host population uniformly persist, namely there exists a constant $\epsilon > 0$ such that any solution $(S(t), I(t), B(t))$ in $\mathbb{R}_+^3$ with $S(0) \geq 0, I(0) \geq 0, B(0) \geq 0$ satisfies $\liminf_{t\to\infty}(I(t), B(t)) \geq (\epsilon, \epsilon)$.*

Proof. Let

$$X_0 := \{x = (x_1, x_2, x_3) \in \mathbb{R}^3_+ : x_2 > 0 \text{ and } x_3 > 0\}$$
$$\text{and } \partial X_0 := \mathbb{R}^3_+ \backslash X_0 = \{x \in \mathbb{R}^3_+ : x_2 = 0 \text{ or } x_3 = 0\}.$$

Clearly, X_0 is an open set relative to $\mathbb{R}^3_+$. For any solution of system (5.1) through the initial value x, define the solution map $\Phi_t(x) = (S(t;x), I(t;x), B(t;x))$ and period-1 solution map $P = \Phi_1$. It is easy to see that $\Phi_t(X_0) \subset X_0$, $\forall t \geq 0$. Since the total population size $H(t) = S(t) + I(t)$ satisfies

$$\frac{\mathrm{d}H(t)}{\mathrm{d}t} \leq \frac{b_N H(t)}{1 + \xi_N H(t)} - d_N H(t).$$

We have $\limsup\limits_{t\to\infty}(S(t) + I(t)) = S_0$. Hence for any $\epsilon > 0$, there exists $t_0 > 0$ such that $S(t) + I(t) \leq S_0 + \epsilon$ when $t > t_0$. Therefore, we have

$$\frac{\mathrm{d}B(t)}{\mathrm{d}t} = \frac{b_B B(t)}{1 + \xi_B B(t)} - d_B B(t) + \gamma I(t) \leq \frac{b_B B(t)}{1 + \xi_B B(t)} - d_B B(t) + \gamma(S_0 + \epsilon).$$

Since the equation

$$\frac{\mathrm{d}B(t)}{\mathrm{d}t} = \frac{b_B B(t)}{1 + \xi_B B(t)} - d_B B(t) + \gamma(S_0 + \epsilon)$$

admits a globally asymptotically stable equilibrium

$$\hat{B} = \frac{-(d_B - \gamma\xi_B(S_0 + \epsilon) - b_B) + \sqrt{(d_B - \gamma\xi_B(S_0 + \epsilon) - b_B)^2 + 4d_B\xi_B\gamma(S_0 + \epsilon)}}{2d_B\xi_B}.$$

We have $\limsup\limits_{t\to\infty} B(t) = \hat{B}$. Therefore, $P : \mathbb{R}^3_+ \to \mathbb{R}^3_+$ is point dissipative. It then follows from Theorem 2.9 in [126] that P admits a global attractor in $\mathbb{R}^3_+$. Next we prove that P is uniformly persistent with respect to $(X_0, \partial X_0)$.

Let $M_1 := \{(0, 0, 0)\}$ and $M_2 := \{(S_0, 0, 0)\}$. Since $\lim\limits_{x\to M_1}(\Phi_t(x) - M_1) = 0$ uniformly for

$t \in [0,1]$, for any ε_1, there exists δ_1 such that if $\| x - M_1 \| \le \delta_1$,

$$\| \Phi_t(x) - M_1 \| \le \varepsilon_1, \ \ \forall t \in [0,1]. \tag{5.8}$$

We first claim that $\limsup_{n\to\infty} \| \Phi_n(x) - M_1 \| \ge \delta_1$ for all $x \in X_0$. Suppose, by contradiction, that $\limsup_{n\to\infty} \| \Phi_n(z) - M_1 \| < \delta_1$ for some $z \in X_0$. Then there exists an integer $N_1 \ge 1$ such that $\| \Phi_n(z) - M_1 \| < \delta_1, \forall n \ge N_1$. This implies that for $n \ge N_1$, we have

$$\| (S(n), I(n), B(n)) \| < \delta_1.$$

By (5.8), we obtain $\| (S(t), I(t), B(t)) \| \le \varepsilon_1$ and then $|S(t)| \le \varepsilon_1$, $|I(t)| \le \varepsilon_1$, $|B(t)| \le \varepsilon_1$ as $t \ge N_1$. However, when $t > N_1$, solution $S(t)$ through initial value z satisfies

$$\begin{aligned}\frac{\mathrm{d}S(t)}{\mathrm{d}t} &= \frac{b_N(S(t)+\eta I(t))}{1+\xi_N(S(t)+\eta I(t))} - d_N S(t) - \kappa B(t) S(t) - \frac{\beta S(t) I(t)}{1+\alpha I(t)} \\ &> \frac{b_N S(t)}{1+\xi_N S(t)} - d_N S(t) - \kappa \varepsilon_1 S(t) - \beta \varepsilon_1 S(t).\end{aligned}$$

Since $R_H > 1$, there exists $\varepsilon_1 > 0$ such that $b_N - d_N - \kappa\varepsilon_1 - \beta\varepsilon_1 > 0$. By comparison principle, we obtain a contradiction to $|S(t)| \le \varepsilon_1$ for $t \ge N_1$.

Since $\lim_{x\to M_2} (\Phi_t(x) - M_2) = 0$ uniformly for $t \in [0,1]$, for any ε_2, there exists δ_2 such that if $\| x - M_2 \| \le \delta_2$, we have

$$\| \Phi_t(x) - M_2 \| \le \varepsilon_2, \ \ \forall t \in [0,1]. \tag{5.9}$$

Now we claim that $\limsup_{n\to\infty} \| \Phi_n(x) - M_2 \| \ge \delta_2$ for all $x \in X_0$. Assume, by contradiction, that $\limsup_{n\to\infty} \| \Phi_n(z) - M_2 \| < \delta_2$ for some $z \in X_0$. Then there exists an integer $N_2 \ge 1$ such that $\| \Phi_n(z) - M_2 \| < \delta_2, \ \forall n \ge N_2$, which implies that

$$\| (S(n) - S_0, I(n), B(n)) \| < \delta_2.$$

It follows from (5.9) that $\| (S(t) - S_0, I(t), B(t)) \| \le \varepsilon_2$ and therefore $|S(t) - S_0| \le \varepsilon_2$,

$|I(t)| \leq \varepsilon_2$, $|B(t)| \leq \varepsilon_2$ when $t \geq N_2$. Then for any $t \geq N_2$, we have

$$\begin{aligned} \frac{\mathrm{d}I(t)}{\mathrm{d}t} &\geq \kappa(S_0 - \varepsilon_2)B(t) + \frac{\beta(S_0 - \varepsilon_2)}{1 + \alpha\varepsilon_2} I(t) - d_N I(t) - \mu I(t), \\ \frac{\mathrm{d}B(t)}{\mathrm{d}t} &\geq \frac{b_B}{1 + \xi_B \varepsilon_2} B(t) + \gamma I(t) - d_B B(t). \end{aligned} \tag{5.10}$$

Consider the linear system

$$\frac{\mathrm{d}w(t)}{\mathrm{d}t} = M_{\varepsilon_2} w(t), \tag{5.11}$$

where

$$M_{\varepsilon_2} = \begin{bmatrix} \frac{\beta(S_0-\varepsilon_2)}{1+\alpha\varepsilon_2} - d_N - \mu & \kappa(S_0 - \varepsilon_2) \\ \gamma & \frac{b_B}{1+\xi_B\varepsilon_2} - d_B \end{bmatrix}.$$

Since $\mathcal{R}_0 > 1$, it then follows that $r_0 = s(M_0) > 0$ and $\frac{\mathrm{d}w(t)}{\mathrm{d}t} = M_0 w(t)$ is unstable. Then there exists $\varepsilon_2 > 0$ such that $r_{\varepsilon_2} = s(M_{\varepsilon_2})$, the principle eigenvalue of M_{ε_2}, is positive. Therefore, system (5.11) admits a solution $w(t) = e^{r_{\varepsilon_2} t} w(0)$ with appropriate positive initial value $w(0)$. On the other hand, for a specific $(I(N_2), B(N_2)) > 0$, there exists δ_3 such that $(I(N_2), B(N_2)) > \delta_3 w(0)$. Based on (5.10) and comparison principle, when $t \geq N_2$, we have

$$(I(t), B(t)) > \delta_3 e^{r_{\varepsilon_2}(t-N_2)} w(0),$$

which implies that $I(t)$ and $B(t)$ go to infinity, contradicting to the boundedness of solutions.

Define

$$\begin{aligned} M_\partial &:= \{x \in \partial X_0 : P^n(x) \in \partial X_0, n \geq 0\}, \\ D_1 &:= \{x \in \mathbb{R}^3_+ : x_2 = 0 \text{ and } x_3 = 0\}, \\ D_2 &:= \{x \in \mathbb{R}^3_+ : x_1 = 0 \text{ and } x_2 = 0\}. \end{aligned}$$

Then we claim that $M_\partial = D_1 \cup D_2$. We first prove that $D_1 \cup D_2 \subset M_\partial$. For any $x \in D_1$, the second and third equations of system (5.1) show that $I(t; x) = 0$ and $B(t; x) = 0$ for all $t \geq 0$. Hence $x \in M_\partial$ and $D_1 \subset M_\partial$. For any $x \in D_2$, then it follows from the first and second equations of system (5.1) that $S(t; x) = 0$ and $I(t; x) = 0$ for all $t \geq 0$. Hence

$x \in M_\partial$ and $D_2 \subset M_\partial$. Now it remains to show that $M_\partial \subset D_1 \cup D_2$. For any $x \in M_\partial$, $P^n(x) \in \partial X_0$, that is, $I(n;x) = 0$ or $B(n;x) = 0$ for all $n \geq 0$. Then there are two cases:

(i) If $I(n;x) = 0$ for all $n \geq 0$, it then follows from the second equation of system (5.1) that $B(n;x) = 0$ and $S(n;x) = 0$. Hence we must have $x_1 = 0$ and $x_3 = 0$. Moreover, $x_2 = 0$. Therefore $x \in D_1 \cup D_2$.

(ii) If $B(n;x) = 0$ for all $n \geq 0$, then based on the third equation of system (5.1), $I(n;x) = 0$ for all $n \geq 0$. Then we have $x_2 = 0$ and $x_3 = 0$.

It is easy to see that for any $x \in D_1 \cup D_2$, we have $\lim\limits_{t\to\infty}(S(t;x), I(t;x), B(t;x)) = (0,0,0)$ or $\lim\limits_{t\to\infty}(S(t;x), I(t;x), B(t;x)) = (S_0,0,0)$. Based on the above arguments, we conclude that condition (C_2) in Theorem 1.3.1 of [207] holds. It then follows that M_1 and M_2 are disjoint, compact and isolated invariant sets for P in M_∂, and no subset of $\{M_1, M_2\}$ forms a cycle in M_∂. This implies that M_1 and M_2 are isolated invariant sets for P in $\mathbb{R}^3_+$, and $W^s(M_i) \cap X_0 = \emptyset$, $\forall i = 1, 2$, where $W^s(M_i)$ is the stable set of M_i for P.

According to the acyclicity theorem on uniform persistence for maps [207] (see also Section 2.2), it follows that $P : \mathbb{R}^3_+ \to \mathbb{R}^3_+$ is uniformly persistent with respect to X_0. Thus the semiflow $\Phi_t : \mathbb{R}^3_+ \to \mathbb{R}^3_+$ is also uniformly persistent with respect to X_0. $\square$

The next result also indicates the pathogen persistence in the habitat, but under a different scenario. Note that in this case, $b_N > d_N$, i.e., $\mathcal{R}_H > 1$.

Theorem 5.2.2. *If $\mathcal{R}_B > 1$ and $b_N > \frac{(d_N+\kappa B_0)(d_N+\mu)}{\eta\kappa B_0 + d_N + \mu}$, then the pathogen and host population uniformly persist, namely there exists a constant $\epsilon > 0$ such that any solution $(S(t), I(t), B(t))$ of the system (5.1) in $\mathbb{R}^3_+$ with $S(0) > 0$, $I(0) > 0$, $B(0) > 0$ satisfies $\liminf\limits_{t\to\infty}(I(t), B(t)) \geq (\epsilon, \epsilon)$.*

Proof. The proof is similar to that of Theorem 5.2.1, with different disjoint, compact and isolated invariant sets for P in M_∂. In addition to M_1, M_2 in the proof of Theorem 5.2.1, there is an additional compact and isolated invariant set

$$M_3 = \{(0, 0, B_0)\}.$$

Adapting the similar arguments in Theorem 5.2.1, it suffices to show that $W^s(M_i) \cap X_0 = \emptyset$, $\forall i = 1, 2, 3$, where $W^s(M_i)$ is the stable set of M_i for P.

We will use the same notations as those in the proof of Theorem 5.2.1, and first claim that $\limsup_{n\to\infty} \parallel \Phi_n(x) - M_i \parallel \geq B_0$ for all $x \in X_0$, and $i = 1, 2$. In fact, based on the third equation of system (5.1), we have

$$\frac{\mathrm{d}B(t)}{\mathrm{d}t} \geq \frac{b_B B(t)}{1 + \xi_B B(t)} - d_B B(t).$$

The comparisonal principle and Proposition 5.2.3 imply that

$$\liminf_{t\to\infty} B(t) \geq B_0$$

and hence this claim holds.

Since $\mathcal{R}_B > 1$ and $b_N > \frac{(d_N+\kappa B_0)(d_N+\mu)}{\eta\kappa B_0+d_N+\mu}$, the arguments for the Jacobian matrix (5.12) shows that it is unstable. Then there exists $\varepsilon_3 > 0$ such that $r_{\varepsilon_3} = s(M_{\varepsilon_3})$, the principle eigenvalue of the perturbed matrix with parameter ε_3

$$M_{\varepsilon_3} = \begin{bmatrix} \frac{b_N}{1+(1+\eta)\xi_N\varepsilon_3} - d_N - \kappa(B_0 + \varepsilon_3) - \beta\varepsilon_3 & \frac{b_N}{1+(1+\eta)\xi_N\varepsilon_3}\eta \\ \kappa(B_0 - \varepsilon_3) & -d_N - \mu \end{bmatrix} \tag{5.12}$$

is positive. Since $\lim_{x\to M_3}(\Phi_t(x) - M_3) = 0$ uniformly for $t \in [0, 1]$, for any ε_3, there exists δ_3 such that if $\parallel x - M_3 \parallel \leq \delta_3$, we have

$$\parallel \Phi_t(x) - M_3 \parallel \leq \varepsilon_3, \quad \forall t \in [0, 1]. \tag{5.13}$$

Now we claim that $\limsup_{n\to\infty} \parallel \Phi_n(x) - M_3 \parallel \geq \delta_3$ for all $x \in X_0$. Assume, by contradiction, that $\limsup_{n\to\infty} \| \Phi_n(z) - M_3 \| < \delta_3$ for some $z \in X_0$. Then there exists an integer $N_3 \geq 1$ such that $\| \Phi_n(z) - M_3 \| < \delta_3$, $\forall n \geq N_3$, which implies that

$$\| (S(n), I(n), (B(n) - B_0)) \| < \delta_3.$$

It follows from (5.13) that $\| (S(t), I(t), B(t) - B_0) \| \leq \varepsilon_3$ and therefore $S(t) \leq \varepsilon_3$, $I(t) \leq \varepsilon_3$, $|B(t) - B_0| \leq \varepsilon_3$ when $t \geq N_2$. Then for any $t \geq N_3$, we have

$$\begin{aligned}
\frac{\mathrm{d}S(t)}{\mathrm{d}t} &\geq \frac{b_N(S(t) + \eta I(t))}{1 + \xi_N(1+\eta)\varepsilon_3} - d_N S(t) - \kappa(B_0 + \varepsilon_3)S(t) - \beta\varepsilon_3 S(t), \\
\frac{\mathrm{d}I(t)}{\mathrm{d}t} &\geq \kappa(B_0 - \varepsilon_3)S(t) - (d_N + \mu)I(t).
\end{aligned}$$

Similar to the arguments in the proof of Theorem 5.2.1, we can conclude that $S(t)$ and $I(t)$ go to infinity, contradicting to the boundedness of solutions. This completes the proof. ☐

5.2.5 Host extinction scenarios

This subsection focuses on examining the extinction and persistence of host population under specific scenarios.

(I) No self-reproduction of the pathogen

We assume that the pathogens cannot reproduce by themselves, namely $b_B = 0$. In this case, the possibility of host population extinction is precluded, as shown in the next result with its proof.

Proposition 5.2.8. *For system (5.1), if* $b_B = 0$ *and* $\mathcal{R}_H > 1$, *then* $\lim_{t\to\infty}(S(t) + I(t)) = 0$ *does not hold for any solution* $(S(t), I(t), B(t))$ *in* $\mathbb{R}^3_+$ *with* $S(0) > 0$, $I(0) \geq 0$, $B(0) \geq 0$.

Proof. We assume that the pathogens cannot reproduce by themselves, namely $b_B = 0$.

Then the third equation of system (5.1) can be reduced to

$$\frac{\mathrm{d}B(t)}{\mathrm{d}t} = -d_B B(t) + \gamma I(t).$$

Assume that there exists a specific solution $(S(t), I(t), B(t))$ such that $\lim_{t\to\infty}(S(t)+I(t)) = 0$. Then for any $\epsilon_1 > 0$, there exists $t_1 > 0$ such that $S(t) + I(t) < \epsilon_1$ for $t > t_1$. Since $\frac{\mathrm{d}B(t)}{\mathrm{d}t} = -d_B B(t) + \gamma I(t) \leq -d_B B(t) + \gamma\epsilon_1, \ \ \forall t > t_1$, then

$$B(t) \leq B(t_1)e^{-d_B(t-t_1)} + \frac{\gamma\epsilon_1}{d_B}(1 - e^{-d_B(t-t_1)}).$$

Hence, there exist some $t_2 > t_1$ such that

$$B(t) \leq \epsilon_1 + \frac{\gamma\epsilon_1}{d_B} = \left(1 + \frac{\gamma}{d_B}\right)\epsilon_1 \text{ when } t > t_2.$$

It follows that when $t > t_2$, we have

$$\begin{aligned}
\frac{\mathrm{d}S(t)}{\mathrm{d}t} &= f_1(S(t) + \eta I(t))(S(t) + \eta I(t)) - d_N S(t) - \kappa B(t)S(t) - \beta\frac{S(t)I(t)}{1 + \alpha I(t)} \\
&\geq f_1(S(t))S(t) - \left(d_N + \kappa\left(1 + \frac{\gamma}{d_B}\right)\epsilon_1 + \beta\epsilon_1\right)S(t) \\
&= \frac{b_N S(t)}{1 + \xi_N S(t)} - \left(d_N + \kappa\left(1 + \frac{\gamma}{d_B}\right)\epsilon_1 + \beta\epsilon_1\right)S(t).
\end{aligned}$$

Then we can choose $\epsilon_1 > 0$ small enough such that $b_N > d_N + \kappa(1 + \frac{\gamma}{d_B})\epsilon_1 + \beta\epsilon_1$. Assume that $\widetilde{S}(t)$ is the solution to the following equation

$$\frac{\mathrm{d}\widetilde{S}(t)}{\mathrm{d}t} = \frac{b_N\widetilde{S}(t)}{1 + \xi_N\widetilde{S}(t)} - \left(d_N + \kappa\left(1 + \frac{\gamma}{d_B}\right)\epsilon_1 + \beta\epsilon_1\right)\widetilde{S}(t)$$

with $\widetilde{S}(t_2) = S(t_2) > 0$. According to similar arguments in Proposition 5.2.2, we have

$$\lim_{t\to\infty}\widetilde{S}(t) = \frac{1}{\xi_N}\left(\frac{b_N}{d_N + \kappa(1 + \frac{\gamma}{d_B})\epsilon_1 + \beta\epsilon_1} - 1\right).$$

On the other hand, there is $S(t) \geq \widetilde{S}(t)$ when $t \geq t_2$. Therefore, this contradicts the assumption $\lim_{t\to\infty}(S(t) + I(t)) = 0$. □

(II) No impact of the pathogen on the hosts

We consider that the pathogen has no impact on the fecundity and survival of the hosts, namely $\eta = 1$ and $\mu = 0$. Then the total population $N(t) = S(t) + I(t)$ satisfies

$$\frac{\mathrm{d}N(t)}{\mathrm{d}t} = f_1(N(t))N(t) - d_N N(t),$$

which implies that

$$\lim_{t\to\infty} N(t) = \frac{1}{\xi_N}\left(\frac{b_N}{d_N} - 1\right) > 0$$

provided $\mathcal{R}_H = \frac{b_N}{d_N} > 1$. Consequently, the extinction of the host population driven solely by disease transmission is impossible.

The aforementioned observations demonstrate that the host population is persistent under certain conditions: (i) no pathogen self-replication, and (ii) pathogens do not affect host reproductivity or cause additional mortality. Conversely, pathogen-driven population extinction is possible upon two critical factors: (i) the pathogen's capacity to influence host fecundity or cause increased mortality, and (ii) the pathogen's ability to self-replicate within the environment. We will illustrate these observations through numerical simulations later.

5.3 A stochastic model for environmental pathogens

Stochastic models incorporate the discrete transitions of individuals between epidemiological compartments, rather than the average transition rates between compartments [31]. In a stochastic epidemic model, numbers in each group are integers instead of continuously varying quantities. It is possible that the last infected individual could die or recover before the disease becomes endemic, and the disease can only reoccur if an infectious individual

Table 5.3: State transitions and rates for the CTMC host-pathogen model.

Event	Transition	Rate
Birth of host	$(S, I, B) \to (S+1, I, B)$	$\frac{b_N(S+\eta I)}{1+\xi_N(S+\eta I)}$
Death of S	$(S, I, B) \to (S-1, I, B)$	$d_N S$
Infection of host	$(S, I, B) \to (S-1, I+1, B)$	$(\kappa B + \frac{\beta I}{1+\alpha I})S$
Death of I	$(S, I, B) \to (S, I-1, B)$	$(d_N + \mu)I$
Birth of pathogen	$(S, I, B) \to (S, I, B+1)$	$\frac{b_B B}{1+\xi_B B}$
Release of pathogen	$(S, I, B) \to (S, I, B+1)$	γI
Death of B	$(S, I, B) \to (S, I, B-1)$	$d_B B$

from outside the population is reintroduced [109, 128, 129]. In this section, we will propose a continuous-time Markov chain (CTMC) model, which is usually more realistic than our deterministic model [109].

We develop a CTMC model in line with the assumptions of the corresponding deterministic model (5.1) since the random variables related to the deterministic variables are discrete and time is continuous [127, 129]. For simplicity, we employ the same notations for the random variables and parameters as used in the deterministic model (5.1). Let time, $t \in [0, \infty)$, be continuous, and let $S(t)$, $I(t)$ and $B(t)$ denote the discrete-valued random variables for the numbers of susceptible hosts, infected hosts and environmental pathogens, respectively, with finite state space,

$$S(t), I(t) \in \{0, 1, 2, 3, \dots, G_H\} \text{ and } B(t) \in \{0, 1, 2, 3, \dots, G_B\},$$

where $G_H = \frac{b_N}{\xi_N d_N}$ and $G_B = \frac{b_B}{\xi_B d_B}$.

The transition from one state to another may take place at any time t. Let $X(t) = \{S(t), I(t), B(t)\}$ and $\Delta X(t) = X(t + \Delta t) - X(t)$ for $t \geq 0$ and $\Delta t > 0$. By the Markov assumption, the waiting time between event transitions is exponentially distributed. For instance, the probability of the birth of a host in time Δt is given by

$$\mathbb{P}\left(\Delta X(t) = (1,0,0)|X(t)\right) = \frac{b_N(S(t)+\eta I(t))}{1+\xi_N(S(t)+\eta I(t))} + o(\Delta t).$$

All state transitions and rates for the CTMC epidemic model are given in Table 5.3.

5.3.1 Stochastic disease extinction

The probabilities of disease extinction and invasion will be estimated by employing the theoretical framework of the Galton–Watson multitype branching process [14].

(I) Probability of disease extinction

In the CTMC model, the disease spreads via two pathways: 1) infected hosts transmit the disease to susceptible hosts; 2) environmental pathogens infect susceptible hosts. Approximation of the nonlinear dynamics of CTMC model near the disease-free equilibrium leads to a multitype branching process in disease variables $I(t)$ and $B(t)$.

Let $P_{(i,b),(i+j_i,b+j_b)}(s,s+t)$ denote the transition probability of the process $\{Y(t) = (I(t), B(t))\}$ from $Y(s) = (i,b)$ to $Y(s+t) = (i+j_i, b+j_b)$ given $Y(s) = (i,b)$ for $s,t \geq 0$. Then we derive the backward Kolmogorov differential equation of the branching process approximation regarding (I,B) in Table 5.4. If initially there exists one single infected host, $I(0) = 1$, and no pathogen, $B(0) = 0$, then we define the offspring probability generating function (pgf) for infected host I as

$$y_1(u_1,u_2) = \frac{(d_N+\mu)+\beta S_0 u_1^2 + \gamma u_1 u_2}{d_N+\mu+\gamma+\beta S^*}. \tag{5.14}$$

The terms in (5.14) can be interpreted as follows: $\frac{\beta S_0}{d_N+\mu+\gamma+\beta S_0}$ represents the probability of disease transmission from an infected host to a susceptible host, resulting in one new infection. $\frac{\gamma}{d_N+\mu+\gamma+\beta S_0}$ specifies the probability that pathogen is shed by the infectious host

Table 5.4: Transition probabilities of the branching process approximation for I and B.

Event	Transition	Rate
Infection of host	$I \to I+1$	$(\kappa B + \beta I)S_0$
Death of I	$I \to I-1$	$(d_N + \mu)I$
Birth of pathogen	$B \to B+1$	$b_B B$
Release of pathogen	$B \to B+1$	γI
Death of B	$B \to B-1$	$d_B B$

resulting in one infectious host and one free-living pathogen in the environment. Lastly, $\frac{d_N+\mu}{d_N+\mu+\gamma+\beta S_0}$ corresponds to the probability of an infected host's death.

Likewise, the offspring pgf for B given that $I(0) = 0$ and $B(0) = 1$ can be derived as

$$y_2(u_1, u_2) = \frac{b_B u_2^2 + d_B + \kappa S_0 u_1 u_2}{b_B + d_B + \kappa S_0}. \tag{5.15}$$

In (5.15), the term $\frac{b_B}{b_B+d_B+\kappa S_0}$ denotes the probability of the birth of one environmental pathogen. The term $\frac{\kappa S_0}{b_B+d_B+\kappa S_0}$ represents the probability that the environmental pathogen successfully infects a susceptible host, resulting in one newly infected host and keeping the original pathogen. The term $\frac{d_B}{b_B+d_B+\kappa S_0}$ gives the probability of the death of a single environmental pathogen.

Since the process $\{Y(t) : t \geq 0\}$ is time-homogeneous, we define $P_{(1,0),(0,0)}(s,t)$ and $P_{(0,1),(0,0)}(s,t)$ as $P_{(1,0)}(s)$ and $P_{(0,1)}(s)$ respectively. It follows from [17] that

$$\begin{aligned}
\frac{\mathrm{d}P_{(1,0)}(s)}{ds} &= (\beta S_0 + d_N + \mu + \gamma)\left(P_{(1,0)}(s) - y_1\left(P_{(1,0)}(s), P_{(0,1)}(s)\right)\right), \\
\frac{\mathrm{d}P_{(0,1)}(s)}{ds} &= (\kappa S_0 + b_B + d_B)\left(P_{(0,1)}(s) - y_2\left(P_{(1,0)}(s), P_{(0,1)}(s)\right)\right),
\end{aligned}$$

subject to the termination conditions $P_{(1,0)}|_{s=t} = P_{(0,1)}|_{s=t} = 0$, where $P_{(1,0)}$ and $P_{(0,1)}$ denote the functions of initial time s for any fixed termination time t.

Then the expectation matrix is

$$\mathbb{M} = \begin{bmatrix} \frac{\partial y_1(u_1,u_2)}{\partial u_1} & \frac{\partial y_2(u_1,u_2)}{\partial u_1} \\ \frac{\partial y_1(u_1,u_2)}{\partial u_2} & \frac{\partial y_2(u_1,u_2)}{\partial u_2} \end{bmatrix}_{u_1=1,u_2=1} = \begin{bmatrix} \frac{2\beta S_0+\gamma}{d_N+\mu+\gamma+\beta S_0} & \frac{\kappa S_0}{b_B+d_B+\kappa S_0} \\ \frac{\gamma}{d_N+\mu+\gamma+\beta S_0} & \frac{2b_B+\kappa S_0}{b_B+d_B+\kappa S_0} \end{bmatrix}.$$

By the Threshold Theorem in [16], $\rho(\mathbb{M}) < 1 \ (= 1, > 1)$ if and only if $\mathcal{R}_0 < 1 \ (= 1, > 1)$. Based on the theory of branching process [24, 64] and the Threshold Theorem, the probability of ultimate disease extinction is one if $\mathcal{R}_0 < 1$. When $\mathcal{R}_0 > 1$, the probability of ultimate disease extinction is determined by $\mathbb{P}_0 = q_1^{i_0} q_2^{b_0}$, where q_1 and q_2 are the fixed point of the probability generating functions on $(0,1)^2$ by setting $y_i(q_1,q_2) = q_i$, $i = 1,2$, and i_0 and b_0 are the initial numbers of infected hosts and environmental pathogens, respectively. That is,

$$\begin{aligned} y_1(q_1,q_2) &= \frac{(d_N+\mu) + \beta S_0 q_1^2 + \gamma q_1 q_2}{d_N+\mu+\gamma+\beta S_0} = q_1, \\ y_2(q_1,q_2) &= \frac{b_B q_2^2 + d_B + \kappa S_0 q_1 q_2}{b_B+d_B+\kappa S_0} = q_2. \end{aligned} \tag{5.16}$$

(II) Mean and variance of disease extinction time

The mean and variance of disease extinction time can be investigated by the approach presented in [17]. Let $Y(t) = (I(t), B(t))$. Define

$$T = T_{(i_0,b_0)} = \inf\{t > 0 : I(t) = B(t) = 0 \ \text{ given } \ Y(0) = (i_0,b_0)\},$$

as the first time until disease extinction given $Y(0) = (i_0,b_0)$. Then the cumulative distribution function of T satisfies

$$\begin{aligned} \mathrm{P}\left(T \le t | T < \infty\right) &= \mathrm{P}\left(I(t) = B(t) = 0 | T < \infty, Y(0) = (i_0,b_0)\right) \\ &= \frac{\mathrm{P}\left(I(t) = B(t) = 0 | Y(0) = (i_0,b_0)\right)}{\mathrm{P}\left(T < \infty | Y(0) = (i_0,b_0)\right)} \approx \frac{P_{(i_0,b_0)}(t)}{\mathbb{P}_0}, \end{aligned}$$

which implies that

$$\mathrm{P}\left(T \leq t | T < \infty\right) \approx \frac{(P_{(1,0)}(t))^{i_0}(P_{(0,1)}(t))^{b_0}}{q_1^{i_0} q_2^{b_0}}.$$

Let $\Phi(i_0, b_0, t) = \mathrm{P}\left(T > t | T < \infty\right)$. The probability density of T is $-\frac{\partial \Phi(i_0,b_0,t)}{\partial t}$. Suppose that $\mathrm{E}(T) < \infty$, then the associated mean extinction time is given by

$$\begin{aligned}\mathrm{E}\left(T | T < \infty\right) &= -\int_0^\infty t\frac{\partial \Phi(i_0,b_0,t)}{\partial t}dt = \int_0^\infty \Phi(i_0,b_0,t)dt \\ &\approx \int_0^\infty \left[1 - \frac{(P_{(1,0)}(t))^{i_0}(P_{(0,1)}(t))^{b_0}}{q_1^{i_0} q_2^{b_0}}\right] dt,\end{aligned}$$

where integration by parts is applied and $\lim_{t\to\infty} t\Phi(i_0, b_0, t) = 0$. Similarly, the variance of the extinction time is

$$\begin{aligned}\mathrm{Var}\left(T | T < \infty\right) =& \mathrm{E}\left(T^2 | T < \infty\right) - \left(\mathrm{E}\left(T | T < \infty\right)\right)^2 \\ =& \int_0^\infty 2t\Phi(i_0,b_0,t)dt - \left(\mathrm{E}\left(T | T < \infty\right)\right)^2 \\ \approx& \int_0^\infty 2t\left[1 - \frac{(P_{(1,0)}(t))^{i_0}(P_{(0,1)}(t))^{b_0}}{q_1^{i_0} q_2^{b_0}}\right] dt \\ &- \left\{\int_0^\infty \left[1 - \frac{(P_{(1,0)}(t))^{i_0}(P_{(0,1)}(t))^{b_0}}{q_1^{i_0} q_2^{b_0}}\right] dt\right\}^2\end{aligned}$$

provided that $\mathrm{E}(T^2) < \infty$.

5.3.2 Stochastic host population extinction

(I) Probability of population extinction

In the CTMC model, the presence of susceptible and infectious hosts in the system is accounted for by the reproduction of the host population and pathogen infection, respectively. Analogous to the stochastic disease model, we utilize the state transitions and rates in Table 5.3 to derive the offspring probability generating functions for the host population variables

S and I. Specifically, assume that $\mathcal{R}_B > 1$ and we will approximate the CTMC model near the host-free steady state $(0, 0, B_0)$.

Similar to the above stochastic disease model, we acquire the backward Kolmogorov differential equation in terms of (S, I) based on the branching process approximation. Assuming an initial condition of a single susceptible host, $S(0) = 1$, and no infected individuals, $I(0) = 0$, the offspring probability generating function for the susceptible host S can be expressed as follows:

$$g_1(u_1, u_2) = \frac{b_N u_1^2 + d_N + \kappa B_0 u_2}{b_N + d_N + \kappa B_0}. \tag{5.17}$$

In (5.17), $\frac{b_N}{b_N+d_N+\kappa B_0}$ denotes the probability of the birth of one susceptible host; $\frac{d_N}{b_N+d_N+\kappa B_0}$ presents the probability of the death of one susceptible host and $\frac{\kappa B_0}{b_N+d_N+\kappa B_0}$ gives the probability that one susceptible host is infected by the pathogen and becomes an infected host.

Similarly, the offspring pgf for I can be derived under the conditions $S(0) = 0$ and $I(0) = 1$, as follows:

$$g_2(u_1, u_2) = \frac{b_N \eta \cdot u_1 u_2 + d_N + \mu}{b_N \eta + d_N + \mu}. \tag{5.18}$$

In (5.18), $\frac{b_N \cdot \eta}{b_N \cdot \eta + d_N + \mu}$ gives the probability that one infected host gives birth to one susceptible host, which results in one infected host and one susceptible host in the population, and $\frac{d_N + \mu}{b_N \cdot \eta + d_N + \mu}$ represents the probability of the death of one infected host.

Similar to the expectation matrix $\mathbb{M}$ for disease extinction, we introduce the expectation matrix for host extinction

$$\mathbb{M}_p = \begin{bmatrix} \frac{\partial g_1(u_1,u_2)}{\partial u_1} & \frac{\partial g_2(u_1,u_2)}{\partial u_1} \\ \frac{\partial g_1(u_1,u_2)}{\partial u_2} & \frac{\partial g_2(u_1,u_2)}{\partial u_2} \end{bmatrix}_{u_1=1,u_2=1} = \begin{bmatrix} \frac{2b_N}{b_N+d_N+\kappa B_0} & \frac{b_N \cdot \eta}{b_N \cdot \eta + d_N + \mu} \\ \frac{\kappa B_0}{b_N+d_N+\kappa B_0} & \frac{b_N \cdot \eta}{b_N \cdot \eta + d_N + \mu} \end{bmatrix}.$$

According to the Threshold Theorem in [16], we conclude that the probability of population extinction in the CTMC model satisfies

$$\rho(\mathbb{M}_p) < 1 \ (= 1, > 1 \text{ respectively }) \text{ if and only if } \ \rho(J_B) < 1 \ (= 1, > 1 \text{ respectively}),$$

where

$$J_B = \begin{bmatrix} b_N - d_N - \kappa B_0 & b_N\eta \\ \kappa B_0 & -d_N - \mu \end{bmatrix}$$

corresponds to the Jacobian matrix of model (5.1) involving only variables S and I in the host-free steady state. Then we conclude that the probability of population extinction in the CTMC model satisfies

$$\rho(\mathbb{M}_p) < 1 \ (= 1, > 1 \text{ respectively }) \text{ if and only if } \ \rho(J_B) < 1 \ (= 1, > 1 \text{ respectively}).$$

It follows from the theory of branching process and the Threshold Theorem that the probability of ultimate host population extinction is 1 if $\rho(J_B) < 1$, which is consistent with the conclusion drawn from the deterministic model. For $\rho(\mathbb{M}_p) > 1$, there exists a fixed point of the offspring pgfs on $(0,1)^2$, which gives the probability of host population extinction. We set the fixed point as $g_i(p_1,p_2) = p_i$, $p_i \in (0,1)$, $\forall i = 1,2$, where the values p_1 and p_2 are the probabilities of ultimate population extinction of susceptible and infected hosts respectively, which satisfies

$$\begin{aligned} g_1(p_1,p_2) &= \frac{b_N p_1^2 + d_N + \kappa B_0 p_2}{b_N + d_N + \kappa B_0} = p_1, \\ g_2(p_1,p_2) &= \frac{b_N\eta \cdot p_1 p_2 + d_N + \mu}{b_N\eta + d_N + \mu} = p_2. \end{aligned}$$

Then the probability of ultimate host extinction is given by $\mathbb{P}_0^H = p_1^{s_0} p_2^{i_0}$, where $S(0) = s_0$ and $I(0) = i_0$.

(II) Mean and variance for time to host extinction

Let $H(t) = (S(t), I(t))$. Define

$$T^H = T^H_{(s_0,i_0)} = \inf\{t > 0 : S(t) = I(t) = 0 \ \text{ given } \ H(0) = (s_0,i_0)\},$$

as the first time instance of host extinction given $H(0) = (s_0, i_0)$. Then the cumulative distribution function of T^H satisfies

$$\begin{aligned}\mathrm{P}\left(T^H \le t | T^H < \infty\right) &= \mathrm{P}\left(S(t) = I(t) = 0 | T^H < \infty, H(0) = (s_0, i_0)\right)\\ &= \frac{\mathrm{P}\left(S(t) = I(t) = 0 | H(0) = (s_0, i_0)\right)}{\mathrm{P}\left(T^H < \infty | H(0) = (s_0, i_0)\right)} \approx \frac{P_{(s_0,i_0)}(t)}{\mathbb{P}_0^H}.\end{aligned}$$

It follows that

$$\mathrm{P}\left(T^H \le t | T^H < \infty\right) \approx \frac{(P_{(1,0)}(t))^{s_0}(P_{(0,1)}(t))^{i_0}}{p_1^{s_0} p_2^{i_0}}.$$

Let $\Psi(s_0, i_0, t) = \mathrm{P}\left(T^H > t | T^H < \infty\right)$. The probability density of T^H is $-\frac{\partial \Psi(s_0,i_0,t)}{\partial t}$. Suppose $\mathrm{E}(T^H) < \infty$. Then the associated mean extinction time is given by

$$\begin{aligned}\mathrm{E}\left(T^H | T^H < \infty\right) &= -\int_0^\infty t \frac{\partial \Psi(s_0, i_0, t)}{\partial t} dt = \int_0^\infty \Psi(s_0, i_0, t) dt\\ &\approx \int_0^\infty \left[1 - \frac{(P_{(1,0)}(t))^{s_0}(P_{(0,1)}(t))^{i_0}}{p_1^{s_0} p_2^{i_0}}\right] dt,\end{aligned}$$

where integration by parts is applied and $\lim_{t\to\infty} t\Psi(s_0, i_0, t) = 0$. By similar methods, the variance of host extinction time is given by

$$\begin{aligned}\mathrm{Var}\left(T^H | T^H < \infty\right) =& \mathrm{E}\left((T^H)^2 | T^H < \infty\right) - \left(\mathrm{E}\left(T^H | T^H < \infty\right)\right)^2\\ =& \int_0^\infty 2t\Psi(s_0, i_0, t) dt - \left(\mathrm{E}\left(T^H | T^H < \infty\right)\right)^2\\ \approx& \int_0^\infty 2t \left[1 - \frac{(P_{(1,0)}(t))^{s_0}(P_{(0,1)}(t))^{i_0}}{p_1^{s_0} p_2^{i_0}}\right] dt\\ &- \left\{\int_0^\infty \left[1 - \frac{(P_{(1,0)}(t))^{s_0}(P_{(0,1)}(t))^{i_0}}{p_1^{s_0} p_2^{i_0}}\right] dt\right\}^2\end{aligned}$$

provided that $\mathrm{E}((T^H)^2) < \infty$.

5.4 Numerical simulations

This section presents some numerical examples for the host-pathogen dynamics of the deterministic and stochastic models with parameter values in Table 5.1. The sample paths for the stochastic Markov chain model will be generated through the Gillespie algorithm [15].

Example 1 (Dynamical outcomes in the deterministic model). The existence and stability of each equilibrium, as outlined in Table 5.2, along with the corresponding partition areas depicted in Figure 5.1, are verified through a series of time-related simulations shown in Figure 5.2. Each subfigure illustrates the population sizes of the total hosts, infected hosts, and environmental pathogens as determined by the deterministic model under various scenarios and initial conditions. To simulate the existence and stability of the disease-free state, we set the parameters as follows: $b_B = 0.1$, $d_B = 0.75$, $\mu = 0.65$, and $b_N = 0.12$, with other parameter values specified in Table 5.1. Then $\mathcal{R}_H = 2.4 > 1$, $\mathcal{R}_B = 0.1333 < 1$, and $\mathcal{R}_0 = 0.4995 < 1$. Subfigure (a) demonstrates that all infections, including infected hosts and environmental pathogens, tend to become stably extinct, while the total host population persists stably. This outcome is consistent with Region B in Figure 5.1. To illustrate the host-free stability, we configure two sets of parameter values: (i) $b_N = 0.1$, $d_N = 0.15$, $d_B = 0.015$, $b_B = 0.06$ (then $\mathcal{R}_H = 0.667 < 1$ and $\mathcal{R}_B = 4 > 1$); and (ii) $b_N = 0.12$, $d_N = 0.1$, $d_B = 0.015$, $b_B = 0.15$ (therefore $\mathcal{R}_B = 10 > 1$ and $d_N < b_N < 0.131$). Additional parameter values are provided in Table 5.1. These configurations result in Subfigures (b) and (c), which show that both susceptible and infected host populations decrease to zero, while environmental pathogens stabilize at 30 and 90. This outcome occurs under conditions corresponding to Regions D and E in Figure 5.1, respectively. Subfigure (d) presents the existence of a positive equilibrium, denoted as $(S^*, I^*, B^*) = (15, 39, 104)$, with parameter values $b_B = 0.15$, $d_B = 0.2$, $b_N = 0.45$, and $d_N = 0.1$. This scenario aligns with Region C in Figure 5.1. These simulations elucidate four distinct scenarios concerning the existence and stability of equilibria, thereby validating the analytical results on the dynamics of each variable.

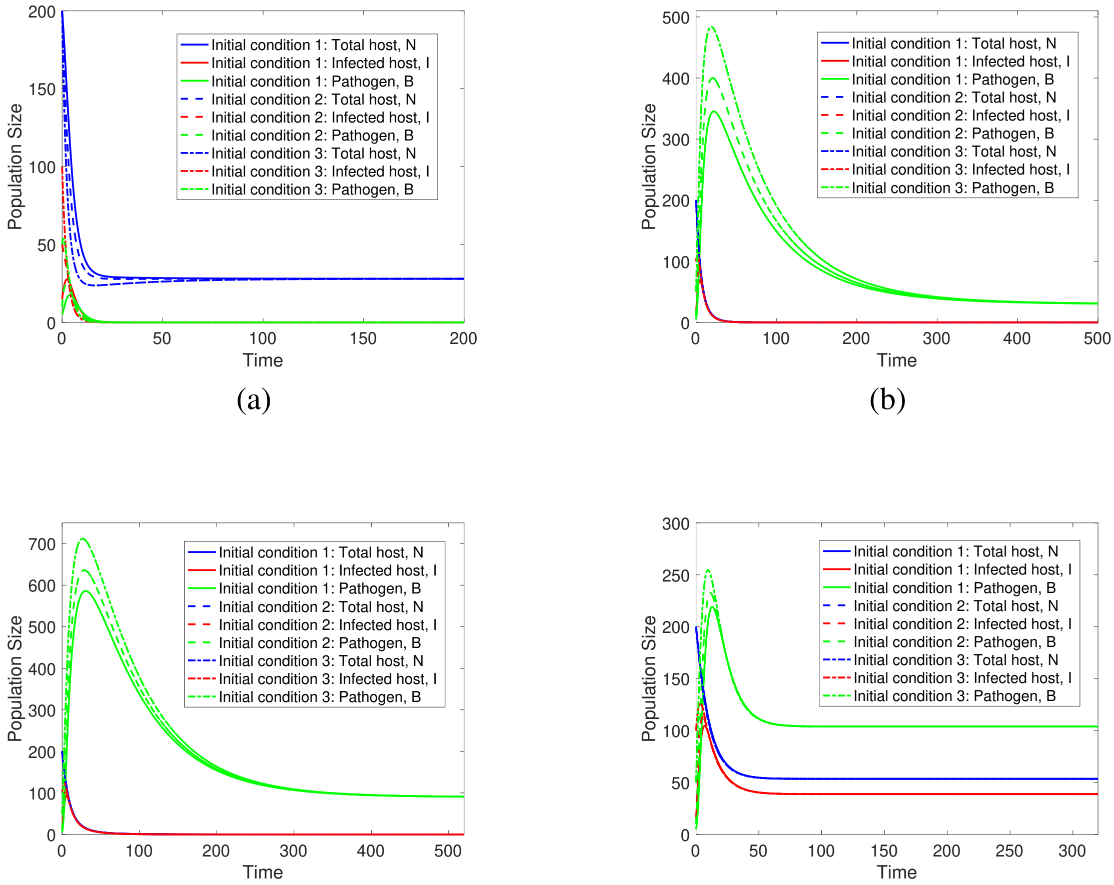

(a) (b)

(c) (d)

Figure 5.2: Population dynamics of the total host, infected host, and environmental pathogen in the deterministic model for various scenarios with diverse initial conditions. The initial conditions are specified as follows: (1.) $S(0) = 185, I(0) = 15, B(0) = 5$; (2.) $S(0) = 150, I(0) = 50, B(0) = 10$; (3.) $S(0) = 100, I(0) = 100, B(0) = 50$. Subfigure (a) illustrates the existence and stability of the disease-free equilibrium when $\mathcal{R}_H = 2.4 > 1$, $\mathcal{R}_B = 0.1333 < 1$, and $\mathcal{R}_0 = 0.4995 < 1$, corresponding to Region B in Figure 5.1. Subfigures (b) and (c) demonstrate the existence and stability of the host-free equilibrium under the conditions $\mathcal{R}_H = 0.667 < 1$ and $\mathcal{R}_B = 4 > 1$; and $\mathcal{R}_B = 10 > 1$ and $d_N < b_N < 0.131$, corresponding to Regions D and E in Figure 5.1, respectively. Subfigure (d) depicts the existence of the positive equilibrium with $\mathcal{R}_H = 4.5 > 1$, $\mathcal{R}_B = 0.75 < 1$, and $\mathcal{R}_0 = 15.882 > 1$, aligning with Region C in Figure 5.1.

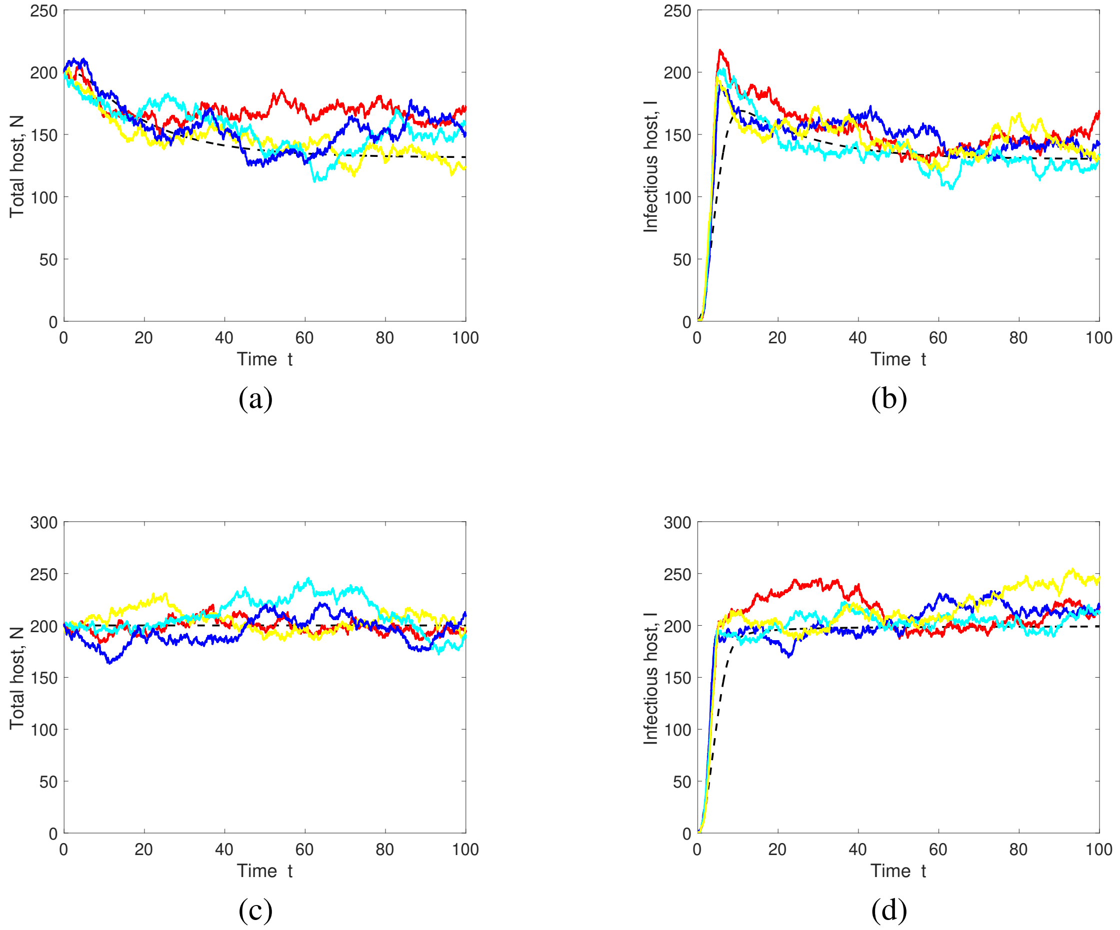

(a) (b)

(c) (d)

Figure 5.3: Four sample paths of the stochastic epidemic model for the total and infected hosts in both host and pathogen populations and the corresponding deterministic solution (dashed curve). The initial conditions are set as $S(0) = 199$, $I(0) = 1$ and $B(0) = 0$. The graphs (a) and (b) depict the scenario with no self-reproduction of pathogen population, namely $b_B = 0$, and other parameter values are shown in Table 5.1. Two graphs (c) and (d) present the scenario where the pathogen does not affect the reproduction and the disease-induced mortality of infected individuals, namely $\eta = 1$ and $\mu = 0$, and other parameter values are shown in Table 5.1.

Example 2 (Host persistence). To explore the effects of no self-reproduction of the pathogen and no impact of the pathogen on the hosts, we choose the initial values $S(0) = 199$, $I(0) = 1$ and $B(0) = 0$ and the parameter values are set in Table 5.3. Figure 5.3 presents four sample paths of a stochastic epidemic model. These paths illustrate the dynamics of the total and infected host populations over time under different scenarios, alongside their corresponding deterministic solutions (dashed curves). In the first row, panels (a) and (b) depict a scenario with no self-reproduction of the pathogen population ($b_B = 0$). Panel (a) shows the total host population (N) starting around 200 and generally trending downward with notable fluctuations, while panel (b) illustrates the infected host population (I) initially spiking to around 200 before gradually declining. The stochastic paths in these panels reveal significant variability compared to the smoother deterministic solutions. In the second row, panels (c) and (d) represent a scenario where the pathogen does not affect reproduction and disease-induced mortality of infected individuals is zero ($\eta = 1$ and $\mu = 0$). Panel (c) indicates a more stable total host population with slight upward trends and high variability, starting around 200, whereas panel (d) shows the infected host population rapidly increasing to approximately 200 and then fluctuating with a slight upward trend. The deterministic solutions in these panels also provide smoother trends but do not capture the full variability seen in the stochastic paths. This simulation highlights the impact of pathogen reproduction and mortality on host population dynamics, demonstrating how different parameters can influence the spread and persistence of infections in host populations. Understanding these dynamics is crucial for designing effective interventions and managing epidemic outbreaks.

Example 3 (Host extinction). The reduced reproductive capacity of infected hosts may lead to host extinction. Figure 5.4 illustrates four sample paths of a stochastic epidemic model for different scenarios with reduced reproductive capacity of infected hosts. These paths compare the dynamics of the total and infected host populations over time with their corresponding deterministic solutions (dashed curves). Panels (a) and (b) in the first row depict the model using baseline parameters as specified in Table 5.1. Panel (a) shows the

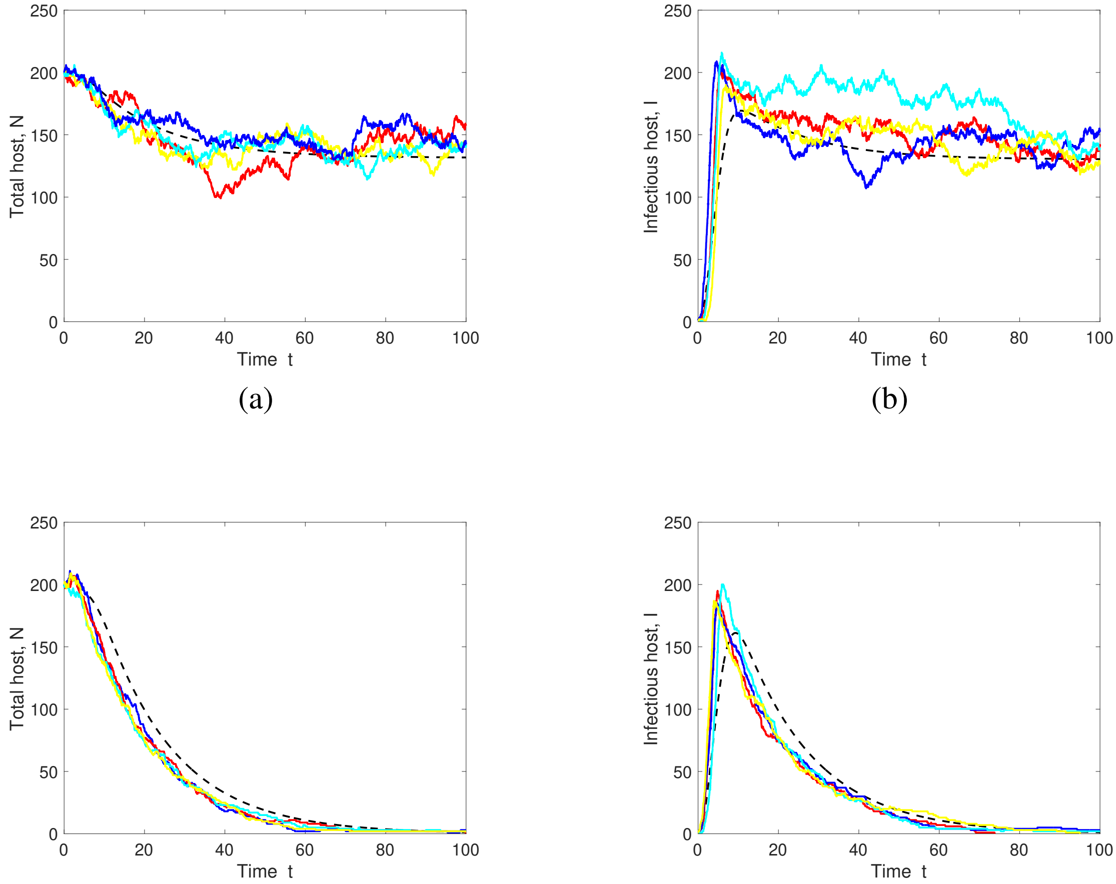

(a) (b) (c) (d)

Figure 5.4: Four sample paths of the stochastic epidemic model for the total and infected hosts in both host and pathogen populations and the corresponding deterministic solution (dashed curve). The initial conditions are set as $S(0) = 199$, $I(0) = 1$ and $B(0) = 0$. The graphs (a) and (b) illustrate the model with parameter values from Table 5.1. The graphs (c) and (d) depict a scenario where there is limited reproduction among infected hosts due to the impact of the infection, namely $\eta = 0.02$, and other parameter values are shown in Table 5.1.

total host population (N), which starts around 200 and trends downward with notable variability among the stochastic paths, while the deterministic solution provides a smoother decreasing trend. Panel (b) displays the infected host population (I), which initially spikes to around 200 before declining with significant fluctuations, contrasted by a smoother decline in the deterministic solution. Panels (c) and (d) in the second row present a scenario with reduced reproduction among infected hosts due to the infection's impact ($\eta = 0.02$). Panel (c) indicates a more rapid decline in the total host population starting from around 200, shown by the pronounced downward trend in both stochastic and deterministic paths. Panel (d) highlights the infected host population, which spikes to approximately 200 before a sharp decrease, as reflected in both the variable stochastic paths and the smoother deterministic solution. This analysis emphasizes the role of pathogen reproduction rates in shaping the persistence and extinction of host populations.

Example 4 (Extinction probability). The initial values of infected hosts and environmental pathogens impact disease extinction probability in the population. In Figure 5.5, we present the probability of disease extinction $\mathbb{P}_0$ as derived from the branching process model, considering varying initial sizes of infected hosts (i_0) and pathogens (b_0). These can be achieved by computing $q_1^{i_0} q_2^{b_0}$ with q_1 and q_2 determined by (5.16). Subfigure (a) indicates that the probability of disease extinction increases with smaller initial sizes of both infected hosts and pathogens. This is evidenced by the peak of the surface, which approaches $\mathbb{P}_0 = 1$ for low values of i_0 and b_0. The contour lines in subfigure (b) denote levels of constant extinction probability. It is observed that higher values of i_0 and b_0 correlate with higher extinction probabilities, reinforcing the conclusion that increasing initial numbers of infected hosts and environmental pathogens contribute positively to disease persistence. The probability of disease extinction is notably low when the disease is introduced by a few infected hosts, and it continues to decrease as the number of infected hosts increases. Conversely, if the disease originates from environmental pathogens with only a small initial count present at the onset of the epidemic, the probability of disease extinction is significantly high. Moreover, as the initial count of pathogens increases, the likelihood of a disease outbreak also rises. Therefore, the initial number of infected hosts poses a greater influence on the disease dynamics in this system during the early stages of the epidemic compared to the initial number of environmental pathogens. This behavior can be attributed to the scenario where a single infected host can release a larger quantity of environmental pathogens, which can subsequently infect more susceptible hosts, thereby diminishing the probability of disease extinction and amplifying the likelihood of a substantial disease outbreak.

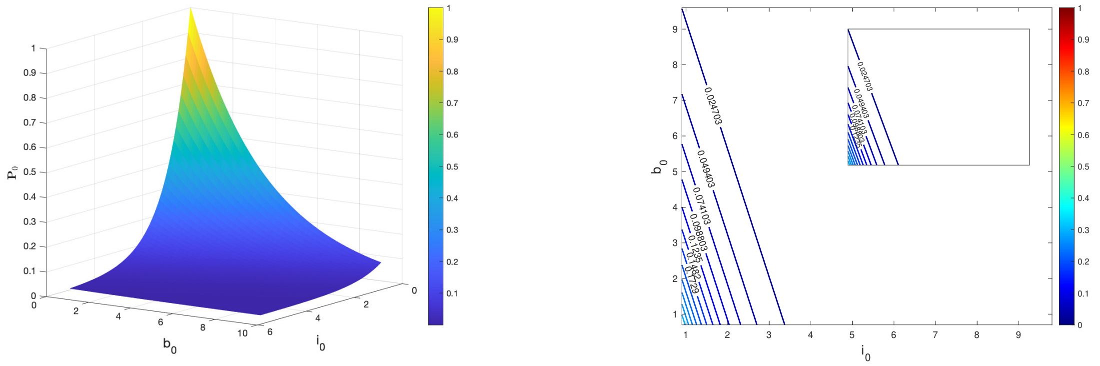

(a) (b)

Figure 5.5: Probability of disease extinction $\mathbb{P}_0$, solved from the branching process, for varying initial sizes of infected hosts and pathogens on (a) the 3D surface and (b) the contour plot with an inset. We set $b_N = 0.055$ day^{-1}, $\xi_N = 0.005$, $\beta = 1.2 \times 10^{-5}$ day^{-1} and $d_B = 0.245$ day^{-1}. Other parameter values are shown in Table 5.1.

Example 5 (Extinction time distribution of infection). To analyze the probability distribution of extinction times of infection under different initial conditions, we present the approximate probability distribution of extinction times for the number of infected individuals under varying initial conditions in Figure 5.6. In panel (a), where $S(0) = 50$, $I(0) = 1$ and $B(0) = 0$, the extinction time exhibits a pronounced peak around $0 - 1$ days with approximately 20% probability. This indicates that with only one initial infected individual and no environmental pathogens, the infection is likely to die out quickly, although there is a long tail extending up to 20 days suggesting occasional longer survival. Panel (b) with initial conditions $S(0) = 50$, $I(0) = 1$ and $B(0) = 1$ shows a similar peak but with a slightly lower probability. This suggests that the presence of one environmental pathogen marginally increases the infection persistence but does not significantly alter the extinction dynamics compared to panel (a). In panel (c), where $S(0) = 50$, $I(0) = 2$ and $B(0) = 0$, the extinction time distribution becomes more uniform with a peak around $1 - 3$ days and a tail extending to 25 days. This broader distribution indicates that with two initial infected individuals, the likelihood of infection persistence increases, thereby spreading the extinction times over a wider range. Finally, panel (d), which considers $S(0) = 50$, $I(0) = 10$ and $B(0) = 10$, displays a peak extinction time around $5 - 10$ days with a long tail reaching up to 40 days. The substantial increase in initial infected individuals and pathogens results in a significantly prolonged infection period. Overall, these simulations demonstrate that the initial number of infected individuals and environmental pathogens significantly impacts the extinction time distribution. Higher initial counts lead to longer infection durations due to increased transmission opportunities. All distributions exhibit a right-skewed pattern, indicating that while most infections extinguish quickly, a small number persist for extended periods.

5.5 Discussion

Addressing the incidence of *Bd* pathogens in frog-inhabited regions poses substantial challenges in fighting against *chytridiomycosis* and in protecting frog populations. To contribute to these efforts, we incorporate the reproductive mechanisms of frog and *Bd* pathogen populations, as well as their transmission pathways, into our model formulation. Both a deterministic model and its stochastic counterpart are constructed to illustrate the interplay among susceptible hosts, infectious hosts, and environmental pathogens. The model includes two transmission routes: direct transmission between susceptible and infected hosts, and indirect transmission of susceptible hosts by environmental pathogens. Environmental pathogens can reproduce independently and can also be released by infectious hosts. Furthermore, these pathogens may induce additional disease-induced mortality in infected hosts or reduce the fertility of these hosts. Additionally, we explore host-associated

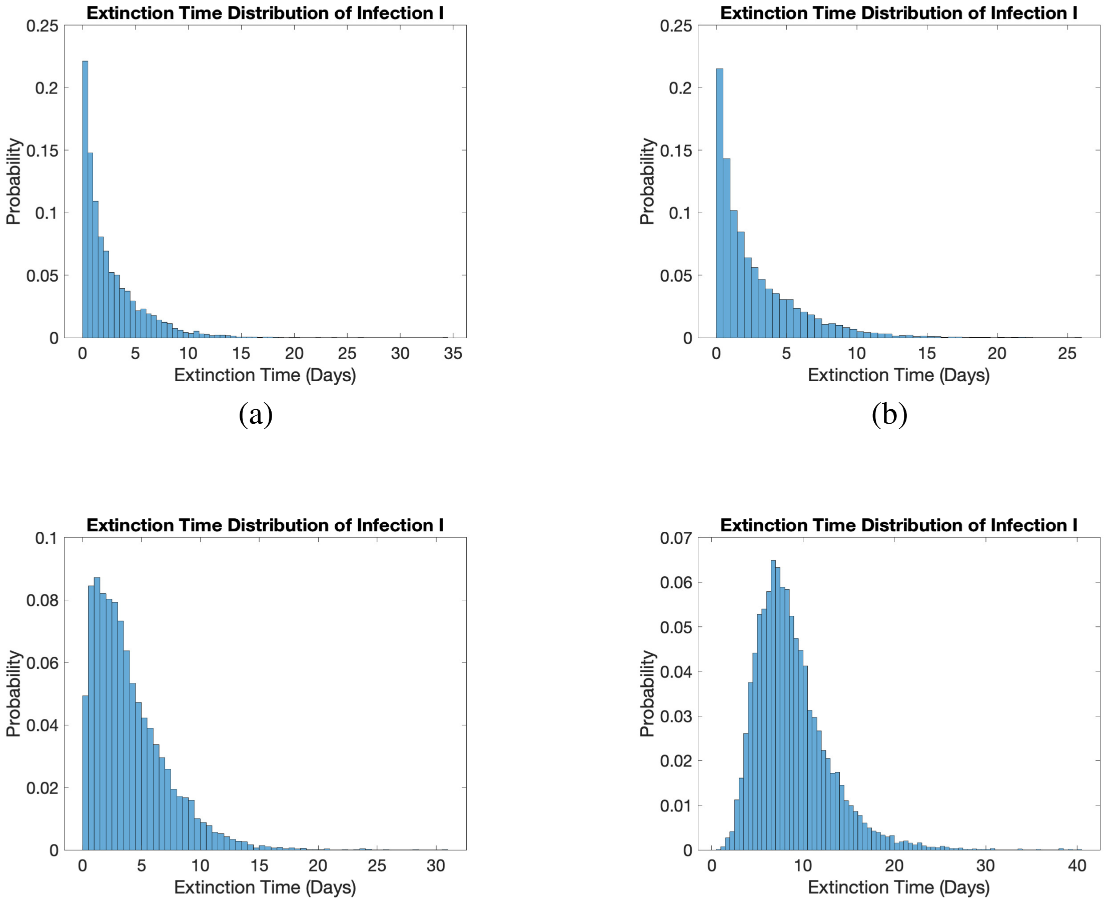

(a) (b) (c) (d)

Figure 5.6: Approximate probability distribution of extinction time for the number of infected individuals with varying initial conditions: (a) $S(0) = 50$, $I(0) = 1$ and $B(0) = 0$; (b) $S(0) = 50$, $I(0) = 1$ and $B(0) = 1$; (c) $S(0) = 50$, $I(0) = 2$ and $B(0) = 0$; (d) $S(0) = 50$, $I(0) = 10$ and $B(0) = 10$. The parameter d_N is set to 0.55, and other parameter values are provided in Table 5.1.

mechanisms for persistence and tolerance.

Theoretically, we confirm the well-posedness of the deterministic model by showing the existence, uniqueness, positivity, and boundedness of the solutions. Subsequently, we investigate the dynamics of the model system by three associated threshold parameters: the net reproduction number of the host population $\mathcal{R}_H$, the pathogen reproduction number $\mathcal{R}_B$, and the basic reproduction number of the infection $\mathcal{R}_0$. We determine the global stability of the disease-free and host-free equilibria, in addition to the uniform persistence under two sets of biologically interpretable conditions. Furthermore, we identify two scenarios under which the host population persists: one where the pathogens do not reproduce, and the other where the pathogen has no impact on the host population. In practical applications, we can calibrate the parameters of the deterministic model using data from specific habitats to calculate the corresponding threshold reproduction numbers. Based on the dynamical conditions derived from theoretical analysis, we can then assess the existence and stability of the host and pathogen equilibria. This information allows us to implement targeted intervention and management strategies to maintain the ecological balance of amphibians.

Although the extinction threshold in the deterministic model provides valuable insights into the potential extinction of the disease and host, the likelihood of these events would also be interesting. For that purpose, a stochastic continuous-time Markov chain model is constructed on the foundation of a deterministic model. This is accomplished by utilizing the theory of the multitype branching process, which is particularly relevant when there are only a few infected individuals at the beginning of an epidemic, a scenario that cannot be effectively addressed by a deterministic model. In the stochastic model, we apply the multitype branching process theory for both (I, B) and (S, I) to estimate the probabilities of disease and host population extinction, respectively. Analytical and numerical results demonstrate that the probabilities of disease and host population extinction, denoted as $\mathbb{P}_0$ and $\mathbb{P}_0^H$, obtained from the multitype branching process theory, align remarkably well with the numerically approximated probabilities derived from a proportion of sample paths that lead to zero before an outbreak occurs. In practice, empirical data on initially infected individuals can be utilized to approximate the probability of disease extinction and the probability distribution of extinction time, which are crucial for informing interventions and management strategies aimed at maintaining ecological balance.

Numerical simulations verify the existence and stability of equilibria as shown in Figure 5.2. Additionally, they illustrate four sample paths of the stochastic epidemic model for the total and infected hosts under different scenarios: no self-reproduction of the pathogen, no impact of the pathogen on the hosts, and reduced reproduction of infected hosts. The results indicate that the host population is persistent under conditions of no self-reproduction of the pathogen or no impact of the pathogen on the hosts, while the host population goes extinct under reduced fertility potential of infected hosts. Furthermore, Figure 5.6 illustrates the approximate probability distribution of extinction times for the number of infected individuals under varying initial conditions. It is observed that the extinction time distribution is influenced by the initial values of infected hosts and environmental pathogens: larger initial values generally lead to longer extinction times. Most infections extinguish quickly, but a small number persist for extended periods. Finally, we explore the probability of disease extinction for varying initial sizes of infected hosts and environmental pathogens using a 3D surface and contour plot in Figure 5.5. This demonstrates the relationship between the two initial sizes and the probability of disease extinction.

The present study integrates several critical aspects into the formulation of deterministic and stochastic models, including the self-reproduction of the pathogen in the environment, multiple transmission routes, and the pathogen's potential effects on infected host vital rates such as fertility potential and excess mortality. However, the model formulation is still highly simplified. Additional factors should be considered to improve the comprehensiveness of the model. For instance, the seasonal drivers of frog population growth, reproduction, and disease outbreaks, which depend on numerous spatial and temporal factors, are worth exploring. Several seasonal drivers have been proposed, including temperature, rainfall, and habitat conditions [135]. The environmental conditions contributing to outbreaks can differ between habitats. Therefore, it is essential to incorporate these seasonal factors, which are related to population persistence and disease outbreaks, into the model formulation and prediction. Future investigation will focus on deterministic and stochastic models of the frog-pathogen system in a periodic environment.

Chapter 6

Mating behaviors in frog population growth

6.1 Introduction

While anuran amphibians predominantly display monogamous mating patterns, certain frog species exhibit polygynous breeding strategies, whereby a single male copulates with multiple females over the course of a breeding season [107]. In these cases, the male plays a guardianship role, actively defending and safeguarding the egg clutches deposited by his multiple mating partners. The mating systems of *Hylidae* and *D. auratus* exhibit a polygynous breeding system, allowing both males and females to have multiple partners. Monogamy is infrequently observed among ectothermic vertebrates [174]. However, *R. imitator* and *R. vanzolinii* present unique examples of biparental care and monogamy within the amphibian taxa. Summers [173] illustrated that females may experience a potential cost, manifested as decreased offspring growth and survivorship, when their mates engage in polygynous mating and assume parental care responsibilities for offspring from other females. Pröhl [150] conducted a comprehensive examination on the relationship between the abundance of reproductive resources, population density, adult sex ratio, mating system, male reproductive success, and sexual selection in the strawberry dart-poison frog, *Dendrobates pumilio*. This study revealed that there was no significant difference in the level of polyandry observed across different habitats. Jennions, Bakwell, and Passmore [102] elucidated the reproductive behavior of *Chiromantis xerampelina*, an African frog species, and revealed the occurrence of multiple spawning and polyandry. These mating patterns and reproductive strategies represent crucial factors that must be accounted for when constructing models to study frog populations.

The population growth rate is affected by the mating function as it influences the level of partner availability, thus affecting the likelihood of successful breeding. Bessa-Gomes, Legendre, and Clobert [33] examined the outcomes of three commonly utilized alternative mating functions in discrete population models: minimum, harmonic mean, and modified harmonic mean. The study also explored the effects of these functions on three aspects: the likelihood of female breeding, the presence and intensity of the Allee effect, and the risk of extinction. In particular, the breeding probability of females is determined by the ratio of mated females (c) to the total number of potentially reproductive females (f), as females can only breed if they successfully mate,

$$r = \frac{c}{f}.$$

Several studies have fitted various commonly utilized mating functions, which can be summarized as follows:

(i) The minimum mating function: the number of pairs is determined by the less abundant sex [111]. In the context of monogamy, the frequency-dependent mating function can be expressed as a function of the sex ratio among reproductive individuals, denoted as σ, that is,

$$\sigma = \frac{f}{n},$$

$$c = \min(\sigma n, (1 - \sigma)n) = \min(\sigma, 1 - \sigma)n,$$

where $n = f + m$ is the size of the breeding population and m is the number of reproductive males.

If there is a deviation from one-to-one mating between males and females, the relative abundance of each sex within the mating population will favor the sex that can form multiple pair bonds. Suppose the maximum number of pair bonds that males can establish is denoted as h and is greater than one. In such a scenario,

$$c = \min(f, hm).$$

(ii) The harmonic mean mating function: it is possible to establish a mating function in which males and females mate on a one-to-one basis [117, 152]. This can be expressed as follows:

$$c = \frac{2fm}{f + m}.$$

Similar to the minimum function, the harmonic mean can also be modified to represent a polygynous mating system [117, 152], that is,

$$c = \frac{2f \cdot hm}{f + hm}.$$

(iii) The modified harmonic mean mating function: it is assumed that breeding occurs seasonally in most discrete time models, and that at most one breeding event can take place within each time interval [111], that is,

$$c = \min(f, \frac{2 \cdot f \cdot hm}{f + hm}) = \min(1, \frac{2hm}{f + hm})f.$$

In addition to the aforementioned mating functions that characterize mating conditions under general circumstances, the difficulty faced by females in locating mates under conditions of low male densities is commonly known as the mate-finding Allee effect [52, 77]. Allee effects are density-dependent phenomena where the per capita population growth rate or a component of individual fitness increases with an increase in population size or density.

The mate-finding Allee effect can be represented by the following hyperbolic function:

$$c = \frac{mf}{m+\theta}$$

with a positive parameter θ, which is an alternative class of mating functions commonly employed in sex-structured population models [52, 165].

In sexually reproducing organisms, the sex ratio and the success of pairing are important factors in finding reproductive partners. Engen et al. [70] demonstrated that fluctuations in sex ratios, both in monogamous and polygamous systems, contribute significantly to demographic variances. Schmickl and Karsai [163] examined the interplay between sex ratio, male success, and gender-specific density-independent mortality. They developed a time-continuous model to study the population dynamics of a sexually reproducing, iteroparous species. Araujo and Moura [19] proposed a novel model of mating dynamics and parental care, emphasizing the importance of clarity, mathematical and probabilistic reasoning, the significance of consistency conditions, and the fundamental role of spatial densities and the law of mass action. Considering the aforementioned points, we aim to propose a comprehensive framework to model sex ratio dynamics, pair bond formation, and mating behavior in population dynamics models.

In this chapter, we integrate two-sex division, polygynous mating behavior, and population competition into a stage-structured model for frog populations. Since climate-related factors impact the dynamics of frogs through various aspects such as reproduction, development, and hibernation, we also incorporate seasonality and time-varying delays. The remainder of this chapter is organized as follows: In Section 6.2, we develop a time-periodic, stage-structured model that accounts for pair formation, hibernation periods, and time-varying delays. Section 6.3 explores the qualitative dynamics of our model system, including basic properties in the natural phase space and quotient space. In Section 6.4, we introduce the net reproduction number $\mathcal{R}_0$ for the frog population model and analyze the threshold dynamics in terms of $\mathcal{R}_0$. Section 6.5 presents numerical simulations illustrating the effects of various factors on the population system. Finally, we conclude with a brief discussion.

6.2 Population model for frog mating behaviors

In the frog population, there are factors such as maturation, fecundity, and survival that affect individuals. Additionally, there are different patterns of individuals that undergo metamorphosis and reproduce. Therefore, we propose a two-sex succession model to describe the breeding, development, and hibernation of frogs. Taking into account the fact that juvenile amphibians do not display gender distinctions [83], we categorize individuals into three groups: juveniles, adult females, and adult males. The model assumptions are listed as follows:

(i) There are two seasons: normal growing season (from the beginning of year 0 to the time T) and hibernation season (from timing T to the end of the year). Adult frogs do not reproduce and generate the next generation at the end of normal developmental season, which occurs just before entering hibernation. In other words, all juvenile frogs complete their growth and development during the normal growing season within a one-year cycle.

(ii) It is assumed that juvenile individuals inhabit an environment characterized by sufficient resources, leading to no competition among them for the available living spaces. In contrast, adult individuals may require more resources to survive and develop, and males and females may also compete for mate selection. The competition assumption is taken into account when transitioning juveniles to adulthood by incorporating a decreasing function of the current density of adults. The density-dependent functions regulate the recruitment rates of the female and male adult stages, expressed as $\left(1-\frac{A_f(t)}{K_f}\right) r_J(t)j(1,t)$ and $\left(1-\frac{A_m(t)}{K_m}\right) r_J(t)j(1,t)$, respectively, where K_f and K_m represent the carrying capacity of female and male population, which determines the strength of population regulation.

(iii) Taking into consideration the prevalent polygynous behavior observed in the adult

> frog population, we incorporate a modified harmonic mean mating function into the birth function. Specifically, we define the birth function as $B(A_f(t), A_m(t)) = R \cdot \frac{2A_f(t) \cdot hA_m(t)}{A_f(t)+hA_m(t)}$, where R represents the intrinsic growth rate. This modified harmonic mean mating function accounts for the interaction between adult females (A_f) and adult males (A_m), with the parameter h influencing the maximum number of pair bonds that males can form as a result of engaging with multiple partners.

We introduce the notation $\lfloor t \rfloor$ to represent the floor function, which returns the nearest integer less than or equal to t. Consequently, $t - \lfloor t \rfloor \in [0, T]$ and $t - \lfloor t \rfloor \in (T, 1)$ indicate the normal growing and hibernation periods, respectively. The modeling approach employed in this study shares similarities with those used by Lou and Zhao [122], Wang and Zhao [195], and Lou and Sun [121]. To characterize the development of different stages, we introduce a measurement parameter, denoted as q, which reflects the proportion of development to the next stage. The total number of juveniles at time t is given by $J(t) = \int_0^1 j(q,t)dq$. During the normal growing season ($t - \lfloor t \rfloor \in [0, T]$), the population dynamics are described as follows:

$$\begin{cases} \dfrac{\partial j(q,t)}{\partial t} + \dfrac{\partial}{\partial q}[r_J(t) j(q,t)] = -\mu_J(t) j(q,t), & t - \lfloor t \rfloor \in [0, T], \\ \dfrac{\mathrm{d}A_f(t)}{\mathrm{d}t} = M_f(t) - \mu_A(t) A_f(t), & t - \lfloor t \rfloor \in [0, T], \\ \dfrac{\mathrm{d}A_m(t)}{\mathrm{d}t} = M_m(t) - \mu_A(t) A_m(t), & t - \lfloor t \rfloor \in [0, T], \end{cases} \tag{6.1}$$

with the boundary conditions for variable $j(q,t)$ given by

$$\begin{cases} r_J(t) j(0,t) = B(A_f(t), A_m(t)), \\ M_f(t) = \alpha r_J(t) j(1,t) \left(1 - \dfrac{A_f(t)}{K_f}\right), \\ M_m(t) = (1-\alpha) r_J(t) j(1,t) \left(1 - \dfrac{A_m(t)}{K_m}\right). \end{cases} \tag{6.2}$$

In the given population dynamics, the birth function $B(A_f(t), A_m(t))$ can be represented by the modified harmonic mean mating function $B(A_f(t), A_m(t)) = R \cdot \frac{2A_f \cdot hA_m}{A_f + hA_m}$. It is assumed that surplus adult frogs will migrate out of the population and join other breeding sites. The parameter α represents the sex ratio of female frogs at birth within the entire population. The parameters $\mu_J(t)$ and $\mu_A(t)$ denote the mortality rates of juvenile and adult frogs, respectively, during the normal growing season.

During the hibernation season, when $t - \lfloor t \rfloor \in (T, 1)$, there is no development, maturation, or fecundity. Consequently, the parameters $r_J(t)$, $M_f(t)$, and $M_m(t)$ are all equal to zero during this period. Note that, based on assumption (i), only hibernating adult frogs with a mortality rate of $d_A(t)$ exist. Thus, the dynamics of the population during the hibernation season can be described as follows:

$$\begin{cases} \dfrac{\mathrm{d}A_f(t)}{\mathrm{d}t} = -d_A(t)A_f(t), & t - \lfloor t \rfloor \in (T, 1), \\ \dfrac{\mathrm{d}A_m(t)}{\mathrm{d}t} = -d_A(t)A_m(t), & t - \lfloor t \rfloor \in (T, 1). \end{cases} \tag{6.3}$$

Now we are going to formulate the equations when $t - \lfloor t \rfloor \in [0, T]$. Suppose $q = 0$ at the start of juvenile stage J, $q = 1$ at the developmental transition from J to A_f or A_m. The equation

$$\frac{\partial j(q,t)}{\partial t} = -\frac{\partial}{\partial q}[r_J(t)j(q,t)] - \mu_J(t)j(q,t) \tag{6.4}$$

has the boundary condition

$$j(0,t) = \frac{B(A_f(t), A_m(t))}{r_J(t)}.$$

To solve system (6.4) with this boundary condition, we introduce a new variable

$$\xi = h(t) := \int_0^t r_J(s)ds.$$

Since $r_J(t) > 0$ when $t - \lfloor t \rfloor \in [0, T]$, $\xi = h(t)$ is strictly increasing on this interval. Let $h^{-1}(\xi)$ be the inverse function of $h(t)$, and define

$$\hat{j}(q,\xi) = j(q, h^{-1}(\xi)), \;\; \hat{\mu}_J(\xi) = \mu_J(h^{-1}(\xi)), \;\; \hat{r}_J(\xi) = r_J(h^{-1}(\xi)).$$

In view of (6.4), we have

$$\begin{aligned}\frac{\partial \hat{j}(q,\xi)}{\partial \xi} &= \frac{\partial j(q,h^{-1}(\xi))}{\partial t}\cdot\frac{\mathrm{d}t}{\mathrm{d}\xi}\\ &= \frac{\partial j(q,t)}{\partial t}\cdot\frac{1}{r_J(h^{-1}(\xi))}\\ &= \frac{1}{r_J(t)}\left[-\frac{\partial}{\partial q}[r_J(t)j(q,t)] - \mu_J(t)j(q,t)\right]\\ &= -\frac{\partial \hat{j}(q,\xi)}{\partial q} - \frac{\hat{\mu}_J(\xi)}{\hat{r}_J(\xi)}\hat{j}(q,\xi).\end{aligned}$$

The equation

$$\frac{\partial \hat{j}(q,\xi)}{\partial \xi} = -\frac{\partial \hat{j}(q,\xi)}{\partial q} - \frac{\hat{\mu}_J(\xi)}{\hat{r}_J(\xi)}\hat{j}(q,\xi) \tag{6.5}$$

exhibits a similar form to the standard von Foerster equation [143]. Let $V(s) = \hat{j}(s+q-\xi, s)$. It follows from (6.5) that

$$\frac{\mathrm{d}V(s)}{\mathrm{d}s} = -\frac{\hat{\mu}_J(s)}{\hat{r}_J(s)}V(s).$$

Since $\xi - q \le \xi$, we have

$$V(\xi) = V(\xi - q)e^{-\int_{\xi-q}^{\xi} -\frac{\hat{\mu}_J(s)}{\hat{r}_J(s)}ds},$$

and hence,

$$\hat{j}(q,\xi) = \hat{j}(q_J, \xi - q)e^{-\int_{\xi-q}^{\xi} -\frac{\hat{\mu}_J(s)}{\hat{r}_J(s)}ds}.$$

Define $\tau(q,t)$ to be the time taken to grow from development level 0 to level q by an individual who arrives at development level q at time t. Since $\frac{\mathrm{d}q}{\mathrm{d}t} = r_J(t)$, it follows that

$$q = \int_{t-\tau(q,t)}^{t} r_J(s)ds, \tag{6.6}$$

and then,

$$h(t-\tau(q,t)) = h(t) - \int_{t-\tau(q,t)}^{t} r(s)ds = h(t) - q.$$

By change of variable $s = h(\alpha)$, we have

$$\int_{\xi-q}^{\xi} \frac{\hat{\mu}_J(s)}{\hat{r}_J(s)} ds = \int_{t-\tau(q,t)}^{t} \mu_J(\alpha) d\alpha.$$

It follows that

$$\begin{aligned} j(q,t) &= \hat{j}(q, h(t)) \\ &= j(0, t-\tau(q,t)) e^{-\int_{t-\tau(q,t)}^{t} \mu_J(\alpha) d\alpha} \\ &= \frac{B(A_f(t-\tau(q,t)), A_m(t-\tau(q,t)))}{r_J(t-\tau(q,t))} e^{-\int_{t-\tau(q,t)}^{t} \mu_J(\alpha) d\alpha}. \end{aligned}$$

Denoting $\tau(t) = \tau(1,t)$, we obtain

$$r_J(t) j(1,t) = B(A_f(t-\tau(t)), A_m(t-\tau(t))) \frac{r_J(t)}{r_J(t-\tau(t))} e^{-\int_{t-\tau(t)}^{t} \mu_J(\alpha) d\alpha}.$$

Letting $q = 1$ in (6.6), we have

$$1 = \int_{t-\tau(t)}^{t} r_J(s) ds. \tag{6.7}$$

Taking the derivative with respect to t on both sides of (6.7), we have

$$1 - \tau'(t) = \frac{r_J(t)}{r_J(t-\tau(t))}.$$

Thus, there holds $1 - \tau'(t) > 0$. In virtue of (6.7), it is shown that if $r_J(t)$ is a periodic function, then so is $\tau(t)$ with the same period.

Therefore, when $t-\lfloor t\rfloor \in [0,T]$, we have the following model:

$$
\begin{aligned}
\frac{\mathrm{d}J(t)}{\mathrm{d}t} =& B(A_f(t),A_m(t)) - \mu_J(t)J(t) \\
& - (1-\tau^{'}(t))B(A_f(t-\tau(t)),A_m(t-\tau(t)))e^{-\int_{t-\tau(t)}^{t}\mu_J(\alpha)d\alpha}, \\
\frac{\mathrm{d}A_f(t)}{\mathrm{d}t} =& \alpha(1-\tau^{'}(t))\left(1-\frac{A_f(t)}{K_f}\right)B(A_f(t-\tau(t)),A_m(t-\tau(t)))e^{-\int_{t-\tau(t)}^{t}\mu_J(\alpha)d\alpha} \\
& - \mu_A(t)A_f(t), \\
\frac{\mathrm{d}A_m(t)}{\mathrm{d}t} =& (1-\alpha)(1-\tau^{'}(t))\left(1-\frac{A_m(t)}{K_m}\right)B(A_f(t-\tau(t)),A_m(t-\tau(t)))e^{-\int_{t-\tau(t)}^{t}\mu_J(\alpha)d\alpha} \\
& - \mu_A(t)A_m(t),
\end{aligned}
\tag{6.8}
$$

where $B(A_f(t),A_m(t)) = \frac{2R\cdot A_f(t)\cdot hA_m(t)}{A_f(t)+hA_m(t)}$.

Since the equations of $A_f(t)$ and $A_m(t)$ in system (6.8) and system (6.3) are decoupled from the juvenile equation, respectively, we focus on the following delay differential equation

$$
\begin{aligned}
\frac{\mathrm{d}A_f(t)}{\mathrm{d}t} =& \alpha\widetilde{B}(t)\frac{A_f(t-\tau(t))\cdot hA_m(t-\tau(t))}{A_f(t-\tau(t))+hA_m(t-\tau(t))}\left(1-\frac{A_f(t)}{K_f}\right) - \mu_A(t)A_f(t), \\
& \qquad t-\lfloor t\rfloor \in [0,T], \\
\frac{\mathrm{d}A_m(t)}{\mathrm{d}t} =& (1-\alpha)\widetilde{B}(t)\frac{A_f(t-\tau(t))\cdot hA_m(t-\tau(t))}{A_f(t-\tau(t))+hA_m(t-\tau(t))}\left(1-\frac{A_m(t)}{K_m}\right) - \mu_A(t)A_m(t), \\
& \qquad t-\lfloor t\rfloor \in [0,T], \\
\frac{\mathrm{d}A_f(t)}{\mathrm{d}t} =& -d_A(t)A_f(t), \quad t-\lfloor t\rfloor \in (T,1), \\
\frac{\mathrm{d}A_m(t)}{\mathrm{d}t} =& -d_A(t)A_m(t), \quad t-\lfloor t\rfloor \in (T,1),
\end{aligned}
\tag{6.9}
$$

where $\widetilde{B}(t) = 2R(1-\tau^{'}(t))e^{-\int_{t-\tau(t)}^{t}\mu_J(\alpha)d\alpha}$. Note that $\frac{A_f\cdot hA_m}{A_f+hA_m}$ is defined to be 0 if $(A_f,A_m)=(0,0)$.

6.3 Qualitative dynamics

It is easy to check that the system is cooperative when the following conditions hold: $0 \leq \tau^{'}(t) < 1$, $0 \leq A_f(t) \leq K_f$, $0 \leq A_m(t) \leq K_m$ and all other parameters are non-negative.

6.3.1 Natural phase space and basic properties

Based on the frog ecology, we assume that $0 < \tau(t) < 1$. Let $\hat{\tau} = \max\limits_{t\in[0,T]} \tau(t)$, $\mathcal{X} = C([-\hat{\tau}, 0], \mathbb{R}^2)$. Choose the natural phase space $\mathcal{X}$, it is a Banach space equipped with the supremum norm

$$||\varphi||_{\mathcal{X}} = \max_{\theta\in[-\hat{\tau},0]} ||\varphi(\theta)||.$$

For any φ, $\psi \in \mathcal{X}$ and $\alpha \in \mathbb{R}$, we have

1. $||\varphi||_{\mathcal{X}} = \max_{\theta\in[-\hat{\tau},0]} ||\varphi(\theta)|| \geq 0$ and $||\varphi||_{\mathcal{X}} = 0$ if and only if $\varphi = 0$.
2. $||\alpha\varphi||_{\mathcal{X}} = \max_{\theta\in[-\hat{\tau},0]} ||\alpha\varphi|| = |\alpha| \max_{\theta\in[-\hat{\tau},0]} ||\varphi|| = |\alpha|||\varphi||_{\mathcal{X}}$.
3. $||\varphi + \psi||_{\mathcal{X}} = \max_{\theta\in[-\hat{\tau},0]} ||\varphi(\theta) + \psi(\theta)|| \leq \max_{\theta\in[-\hat{\tau},0]}(||\varphi(\theta)|| + ||\psi||)$
   $\leq \max_{\theta\in[-\hat{\tau},0]} ||\varphi(\theta)|| + \max_{\theta\in[-\hat{\tau},0]} ||\psi(\theta)|| = ||\varphi(\theta)||_{\mathcal{X}} + ||\psi||_{\mathcal{X}}$.
4. for any Cauchy sequence $\{\varphi_n\}$ in $\mathcal{X}$, according to the properties of the maximum norm, for each fixed $\theta \in [-\hat{\tau}, 0]$, the sequence of vectors $\{\varphi_n\}$ in $\mathbb{R}^2$ is a Cauchy sequence in $\mathbb{R}^2$. Since $\mathbb{R}^2$ is complete, $\{\varphi_n(\theta)\}$ converges to a vector, denoted as φ. It can be proved that $\varphi \in C([-\hat{\tau}, 0], \mathbb{R}^2)$, and $\{\varphi_n\}$ converges to φ under the maximum norm.

A closed convex subset $\mathcal{X}^+ \in \mathcal{X}$ can be introduced as $\mathcal{X}^+ = \{\varphi \in \mathcal{X} : \varphi(\theta) \geq 0 \text{ for all } \theta \in [-\hat{\tau}, 0]\}$, which induces a partial ordering on the Banach space ($\mathcal{X}$, $|| \cdot ||_{\mathcal{X}}$). Furthermore, $\mathcal{X}^+$ is non-empty since $0 \in \mathcal{X}^+$ and **int**$(\mathcal{X}^+) = \{\varphi \in \mathcal{X} : \varphi(\theta) > 0 \text{ for all } \theta \in [-\hat{\tau}, 0]\}$. For any φ, $\psi \in \mathcal{X}^+$, for all $\theta \in [-\hat{\tau}, 0]$, $\varphi(\theta) \in \mathbb{R}^2_+$ and $\psi(\theta) \in \mathbb{R}^2_+$. Then $(\varphi + \psi)(\theta) = \varphi(\theta) + \psi(\theta) \in \mathbb{R}^2_+$, thus $\varphi + \psi \in \mathcal{X}^+$. For any $\varphi \in \mathcal{X}^+$ and $\alpha \geq 0$, for all $\theta \in [-\hat{\tau}, 0]$, $(\alpha\varphi)(\theta) = \alpha\varphi(\theta) \in \mathbb{R}^2_+$, thus $\alpha\varphi \in \mathcal{X}^+$. Suppose $\varphi \in \mathcal{X}^+ \cap (-\mathcal{X}^+)$, for all $\theta \in [-\hat{\tau}, 0]$, $\varphi(\theta) \in \mathbb{R}^2_+$ and $\varphi(-\theta) \in \mathbb{R}^2_+$. This implies that $\varphi(\theta) = 0$, thus $\varphi = 0$.

Suppose $0 \leq \varphi \leq \psi$ such that $\psi - \varphi \in \mathcal{X}^+$. By the definition of $\mathcal{X}^+$, for all $\theta \in [-\hat{\tau}, 0]$, $0 \leq \varphi(\theta) \leq \psi(\theta)$. Therefore, $||\varphi(\theta)|| \leq ||\psi(\theta)||$, and then $\max_{\theta\in[-\hat{\tau},0]} ||\varphi(\theta)|| \leq \max_{\theta\in[-\hat{\tau},0]} ||\psi(\theta)||$, namely $||\varphi||_{\mathcal{X}} \leq ||\psi||_{\mathcal{X}}$. It follows that $(\mathcal{X}, \mathcal{X}^+)$ is an ordered Banach space equipped with the maximum norm and the partial order induced by the positive cone $\mathcal{X}^+$. For any given continuous function $u = (u_1, u_2) : [-\hat{\tau}, \sigma) \to \mathbb{R}^2$ with $\sigma > 0$, we define $u_t \in \mathcal{X}$ by

$$u_t(\theta) = u(t+\theta), \ \ \forall \theta \in [-\hat{\tau}, 0]$$

for all $t \in [0, \sigma)$. Then let $\bar{\tau} = \min\{\min_{t\in[0,T]} \tau(t), T\}$.

Lemma 6.3.1. *For any $\varphi \in \mathcal{X}^+$, system (6.9) admits a unique non-negative solution $u(t;\varphi)$ on $[0,\infty)$ with $u_0 = \varphi$. Moreover, there exist $0 \leq \varphi_1(\theta) \leq K_f$ and $0 \leq \varphi_2(\theta) \leq K_m$ for all $\theta \in [-\hat{\tau}, 0]$, then $0 \leq u_1(t;\varphi) \leq K_f$ and $0 \leq u_2(t;\varphi) \leq K_m$.*

Proof. Since $1 - \tau^{'}(t) > 0$, $t - \tau(t)$ is strictly increasing in t. For any $t \in [0, \bar{\tau}]$, we have

$$-\tau(0) = 0 - \tau(0) \leq t - \tau(t) \leq \tau - \tau(\bar{\tau}) \leq \bar{\tau} - \bar{\tau} = 0,$$

and hence, $u_1(t-\tau(t)) = \varphi_1(t-\tau(t))$ and $u_2(t-\tau(t)) = \varphi_2(t-\tau(t))$. Then for $t \in [0, \bar{\tau}]$, we have the following equations:

$$\begin{aligned} \frac{\mathrm{d}u_1(t)}{\mathrm{d}t} &= \alpha\widetilde{B}(t)\frac{\varphi_1(t-\tau(t))\cdot h\varphi_2(t-\tau(t))}{\varphi_1(t-\tau(t)) + h\varphi_2(t-\tau(t))}\left(1 - \frac{u_1(t)}{K_f}\right) - \mu_A(t)u_1(t), \\ \frac{\mathrm{d}u_2(t)}{\mathrm{d}t} &= (1-\alpha)\widetilde{B}(t)\frac{\varphi_1(t-\tau(t))\cdot h\varphi_2(t-\tau(t))}{\varphi_1(t-\tau(t)) + h\varphi_2(t-\tau(t))}\left(1 - \frac{u_2(t)}{K_m}\right) - \mu_A(t)u_2(t). \end{aligned} \tag{6.10}$$

According to the existence and uniqueness of solutions of ordinary differential equations, the solutions to (6.10) can be written as

$$u_1(t) = \varphi_1(0)e^{-\int_0^t\left(\frac{\alpha q(s)}{K_f}+\mu_A(s)\right)ds} + e^{-\int_0^t\left(\frac{\alpha q(s)}{K_f}+\mu_A(s)\right)ds} \cdot \int_0^t \alpha q(s)e^{\int_0^s\left(\frac{\alpha q(\xi)}{K_f}+\mu_A(\xi)\right)d\xi}ds$$

and

$$\begin{aligned}
u_2(t) =&\varphi_2(0)e^{-\int_0^t\left(\frac{(1-\alpha)q(s)}{K_m}+\mu_A(s)\right)ds}\\
&+e^{-\int_0^t\left(\frac{(1-\alpha)q(s)}{K_m}+\mu_A(s)\right)ds}\cdot\int_0^t(1-\alpha)q(s)e^{\int_0^s\left(\frac{(1-\alpha)q(\xi)}{K_m}+\mu_A(\xi)\right)d\xi}ds
\end{aligned}$$

where $q(s)=\widetilde{B}(s)\frac{\varphi_1(s-\tau(s))\cdot h\varphi_2(s-\tau(s))}{\varphi_1(s-\tau(s))+h\varphi_2(s-\tau(s))}\geq 0$. Therefore, $u_1(t)\geq 0$ and $u_2(t)\geq 0$. The non-negative solution $(u_1(t),u_2(t))$ of system (6.10) exists for $t\in[0,\bar{\tau}]$.

For any $\varphi\in\mathcal{X}^+$, there exist $0\leq\varphi_1(\theta)\leq K_f$ and $0\leq\varphi_2(\theta)\leq K_m$ with $\theta\in[-\hat{\tau},0]$. Then we have

$$\begin{aligned}
u_1(t)=&\varphi_1(0)e^{-\int_0^t\left(\frac{\alpha q(s)}{K_f}+\mu_A(s)\right)ds}+K_f\cdot\int_0^t\frac{\alpha q(s)}{K_f}e^{-\int_s^t\left(\frac{\alpha q(\xi)}{K_f}+\mu_A(\xi)\right)d\xi}ds\\
=&\varphi_1(0)e^{-\int_0^t\left(\frac{\alpha q(s)}{K_f}+\mu_A(s)\right)ds}+K_f\cdot\int_0^t\left(\frac{\alpha q(s)}{K_f}+\mu_A(s)\right)e^{-\int_s^t\left(\frac{\alpha q(\xi)}{K_f}+\mu_A(\xi)\right)d\xi}ds\\
&-K_f\cdot\int_0^t\mu_A(s)e^{-\int_s^t\left(\frac{\alpha q(\xi)}{K_f}+\mu_A(\xi)\right)d\xi}ds\\
=&\varphi_1(0)e^{-\int_0^t\left(\frac{\alpha q(s)}{K_f}+\mu_A(s)\right)ds}+K_f\cdot\left[1-e^{-\int_0^t\left(\frac{\alpha q(\xi)}{K_f}+\mu_A(\xi)\right)d\xi}\right]\\
&-K_f\cdot\int_0^t\mu_A(s)e^{-\int_s^t\left(\frac{\alpha q(\xi)}{K_f}+\mu_A(\xi)\right)d\xi}ds\\
\leq&K_f-K_f\cdot\int_0^t\mu_A(s)e^{-\int_s^t\left(\frac{\alpha q(\xi)}{K_f}+\mu_A(\xi)\right)d\xi}ds\\
\leq&K_f.
\end{aligned}$$

Hence $0\leq u_1(t)\leq K_f$. Similarly, $0\leq u_2(t)\leq K_m$ for $t\in[0,\bar{\tau}]$.

For any $t\in[\bar{\tau},2\bar{\tau}]$ with $2\bar{\tau}\leq T$, we have

$$-\tau(0)\leq\bar{\tau}-\tau(\bar{\tau})\leq t-\tau(t)\leq 2\bar{\tau}-\tau(2\bar{\tau})\leq 2\bar{\tau}-\bar{\tau}=\bar{\tau},$$

and hence, $u_1(t-\tau(t))=\psi_1(t-\tau(t))$. Solving the following equations for $t\in[\bar{\tau},2\bar{\tau}]$

with $u_1(\bar{\tau}) = \psi_1(\bar{\tau})$ and $u_2(\bar{\tau}) = \psi_2(\bar{\tau})$:

$$\begin{aligned}
\frac{\mathrm{d}u_1(t)}{\mathrm{d}t} &= \alpha\widetilde{B}(t)\frac{\psi_1(t-\tau(t))\cdot h\psi_2(t-\tau(t))}{\psi_1(t-\tau(t))+h\psi_2(t-\tau(t))}\left(1-\frac{u_1(t)}{K_f}\right)-\mu_A(t)u_1(t),\\
\frac{\mathrm{d}u_2(t)}{\mathrm{d}t} &= (1-\alpha)\widetilde{B}(t)\frac{\psi_1(t-\tau(t))\cdot h\psi_2(t-\tau(t))}{\psi_1(t-\tau(t))+h\psi_2(t-\tau(t))}\left(1-\frac{u_2(t)}{K_m}\right)-\mu_A(t)u_2(t).
\end{aligned}$$

Then we get the solution $(u_1(t), u_2(t))$ on $[\bar{\tau}, 2\bar{\tau}]$. We also have $0 \le u_1(t) \le K_f$ and $0 \le u_2(t) \le K_m$ for all $t \in [\bar{\tau}, 2\bar{\tau}]$. Similar arguments remain valid for $t \in [2\bar{\tau}, 3\bar{\tau}], \dots, [\lfloor n \rfloor \bar{\tau}, n\bar{\tau}]$ with $n = \frac{T}{\bar{\tau}}$. Therefore, the solution $(u_1(t), u_2(t))$ exists on $[0, T]$ and $0 \le u_1(t) \le K_f$, $0 \le u_2(t) \le K_m$.

For $t \in (T, 1)$, we have

$$\begin{aligned}
\frac{\mathrm{d}A_f(t)}{\mathrm{d}t} &= -d_A(t)A_f(t), \quad t-\lfloor t\rfloor \in (T,1),\\
\frac{\mathrm{d}A_m(t)}{\mathrm{d}t} &= -d_A(t)A_m(t), \quad t-\lfloor t\rfloor \in (T,1).
\end{aligned}$$

It follows that

$$u_1(t) = u_1(T)e^{-\int_T^t d_A(s)ds} \text{ and } u_2(t) = u_2(T)e^{-\int_T^t d_A(s)ds}$$

where $u_1(T)$ and $u_2(T)$ are known from the previous procedures. Thus the unique solution $(u_1(t), u_2(t))$ exists and $0 \le u_1(t) \le K_f$, $0 \le u_2(t) \le K_m$ for $t \in (T, 1)$. Repeating the similar arguments for $t \in [1, 2], [2, 3], \dots$, the statement still holds. $\square$

Based on the expressions of $u_1(t)$ and $u_2(t)$ in the proof, we can further obtain that $\limsup_{t\to\infty} u_1(t) \le K_f$ and $\limsup_{t\to\infty} u_2(t) \le K_m$ for any $\varphi \in \mathcal{X}^+$. Therefore, it is sufficient to study the long-term behaviors of solutions through initial values φ with

$$\varphi \in \mathcal{X}_K := \{\varphi : 0 \le \varphi_1(\theta) \le K_f \text{ and } 0 \le \varphi_2(\theta) \le K_m \text{ for all } \theta \in [-\hat{\tau}, 0]\}.$$

Suppose $\Phi(t)$ be the solution maps of system (6.9) on $\mathcal{X}$, that is, $\Phi(t)\varphi = u_t(\varphi)$, $t \ge 0$, where $u(t;\varphi)$ is the unique solution of system (6.9) with $u_0 = \varphi \in \mathcal{X}$. Without loss of generality, we assume initial value φ satisfies $0 \le \varphi_1(0) \le K_f$ and $0 \le \varphi_2(0) \le K_m$. Based on lemma 3.5 in [122], we have the following statements.

Lemma 6.3.2. $\Phi(t) : \mathcal{X} \to \mathcal{X}$ *is an* 1*-periodic semiflow in the sense that (i)* $\Phi(0) = I$*; (ii)* $\Phi(t+1) = \Phi(t) \circ \Phi(1)$, $\forall t \ge 0$*; (iii)* $\Phi(t)\varphi$ *is continuous in* $(t, \varphi) \in [0, \infty) \times \mathcal{X}$.

The next lemmas present that the periodic semiflow $\Phi(t)$ is monotone and strictly subhomogeneous.

Lemma 6.3.3. *For any* φ *and* ψ *in* $\mathcal{X}_K$ *with* $\varphi \ge \psi$*, the solutions* $u(t;\varphi)$ *and* $u(t;\psi)$ *of system (6.9) with* $u_0(\cdot;\varphi) = \varphi$ *and* $u_0(\cdot;\psi) = \psi$*, respectively, satisfy* $u(t;\varphi) \ge u(t;\psi)$ *for all* $t \ge 0$.

Proof. Denote $v(t) = u(t;\varphi)$ and $w(t) = u(t;\psi)$, then we have $v_t(\cdot) \in \mathcal{X}_K$ with $v_0(\cdot) = \varphi$ and $w_t(\cdot) \in \mathcal{X}_K$ with $w_0(\cdot) = \psi$, respectively. For $t \in [0, \bar{\tau}]$, we have

$$\begin{aligned}
v_1'(t) &= \alpha q(t)\left(1 - \frac{v_1(t)}{K_f}\right) - \mu_A(t)v_1(t), \;\; v_1(0) = \varphi_1(0);\\
v_2'(t) &= (1-\alpha)q(t)\left(1 - \frac{v_2(t)}{K_m}\right) - \mu_A(t)v_2(t), \;\; v_2(0) = \varphi_2(0);\\
w_1'(t) &= \alpha p(t)\left(1 - \frac{w_1(t)}{K_f}\right) - \mu_A(t)w_1(t), \;\; w_1(0) = \psi_1(0);\\
w_2'(t) &= (1-\alpha)p(t)\left(1 - \frac{w_2(t)}{K_m}\right) - \mu_A(t)w_2(t), \;\; w_2(0) = \psi_2(0),
\end{aligned} \tag{6.11}$$

where $q(t) = \widetilde{B}(t)\frac{\varphi_1(t-\tau(t))\cdot h\varphi_2(t-\tau(t))}{\varphi_1(t-\tau(t))+h\varphi_2(t-\tau(t))}$ and $p(t) = \widetilde{B}(t)\frac{\psi_1(t-\tau(t))\cdot h\psi_2(t-\tau(t))}{\psi_1(t-\tau(t))+h\psi_2(t-\tau(t))}$. Assume that two functions $z_1(t)$ and $z_2(t)$ satisfy the following equations:

$$\begin{aligned}
z_1'(t) &= \alpha q(t)\left(1 - \frac{z_1(t)}{K_f}\right) - \mu_A(t)z_1(t), \;\; z_1(0) = \psi_1(0),\\
z_2'(t) &= (1-\alpha)q(t)\left(1 - \frac{z_2(t)}{K_m}\right) - \mu_A(t)z_2(t), \;\; z_2(0) = \psi_2(0).
\end{aligned}$$

It follows that

$$z_1(t) = e^{-\int_0^t\left(\frac{\alpha q(s)}{K_f}+\mu_A(s)\right)ds}\left(\psi_1(0) + \int_0^t \alpha q(s)\cdot e^{\int_0^s\left(\frac{\alpha q(\xi)}{K_f}+\mu_A(\xi)\right)d\xi}ds\right)$$

and

$$z_2(t) = e^{-\int_0^t\left(\frac{(1-\alpha)q(s)}{K_m}+\mu_A(s)\right)ds}\left(\psi_2(0)+\int_0^t (1-\alpha)q(s)\cdot e^{\int_0^s\left(\frac{(1-\alpha)q(\xi)}{K_m}+\mu_A(\xi)\right)d\xi}ds\right).$$

Then we have

$$\begin{aligned}
z_1(t) =&\psi_1(0)e^{-\int_0^t\left(\frac{\alpha q(s)}{K_f}+\mu_A(s)\right)ds}+K_f\cdot\int_0^t\frac{\alpha q(s)}{K_f}e^{-\int_s^t\left(\frac{\alpha q(\xi)}{K_f}+\mu_A(\xi)\right)d\xi}ds\\
=&\psi_1(0)e^{-\int_0^t\left(\frac{\alpha q(s)}{K_f}+\mu_A(s)\right)ds}+K_f\cdot\int_0^t\left(\frac{\alpha q(s)}{K_f}+\mu_A(s)\right)e^{-\int_s^t\left(\frac{\alpha q(\xi)}{K_f}+\mu_A(\xi)\right)d\xi}ds\\
&-K_f\cdot\int_0^t\mu_A(s)e^{-\int_s^t\left(\frac{\alpha q(\xi)}{K_f}+\mu_A(\xi)\right)d\xi}ds\\
=&\psi_1(0)e^{-\int_0^t\left(\frac{\alpha q(s)}{K_f}+\mu_A(s)\right)ds}+K_f\cdot\left[1-e^{-\int_0^t\left(\frac{\alpha q(\xi)}{K_f}+\mu_A(\xi)\right)d\xi}\right]\\
&-K_f\cdot\int_0^t\mu_A(s)e^{-\int_s^t\left(\frac{\alpha q(\xi)}{K_f}+\mu_A(\xi)\right)d\xi}ds\\
\leq&K_f-K_f\cdot\int_0^t\mu_A(s)e^{-\int_s^t\left(\frac{\alpha q(\xi)}{K_f}+\mu_A(\xi)\right)d\xi}ds\\
\leq&K_f,
\end{aligned}$$

which implies that $0\leq z_1(t)\leq K_f$. Similarly, we have $0\leq z_2(t)\leq K_m$. Then there exist

$$(v_1(t)-z_1(t))' = v_1'(t)-z_1'(t) = -\left(\frac{\alpha q(t)}{K_f}+\mu_A(t)\right)(v_1(t)-z_1(t))$$

and $v_1(0)-z_1(0)=\varphi_1(0)-\psi_1(0)$, which implies that

$$v_1(t)-z_1(t) = (\varphi_1(0)-\psi_1(0))e^{-\int_0^t\left(\frac{\alpha q(s)}{K_f}+\mu_A(s)\right)ds}.$$

Similarly, we have

$$\begin{aligned}
(z_1(t)-w_1(t))' &= z_1'(t)-w_1'(t)\\
&= -\left(\frac{\alpha p(t)}{K_f}+\mu_A(t)\right)(z_1(t)-w_1(t))+\alpha\left(1-\frac{z_1(t)}{K_f}\right)(q(t)-p(t))
\end{aligned}$$

with $z_1(0) - w_1(0) = 0$. It follows that

$$z_1(t)-w_1(t) = e^{-\int_0^t \left(\frac{\alpha p(\xi)}{K_f}+\mu_A(\xi)\right)d\xi} \cdot \int_0^t \alpha(q(s)-p(s)) \left(1-\frac{z_1(s)}{K_f}\right) \cdot e^{\int_0^s \left(\frac{\alpha p(\xi)}{K_f}+\mu_A(\xi)\right)d\xi} ds.$$

Therefore, we have

$$\begin{aligned} v_1(t) - w_1(t) =&(v_1(t) - z_1(t)) + (z_1(t) - w_1(t)) \\ =&(\varphi_1(0) - \psi_1(0))e^{-\int_0^t \left(\frac{\alpha q(s)}{K_f}+\mu_A(s)\right)ds} + e^{-\int_0^t \left(\frac{\alpha p(\xi)}{K_f}+\mu_A(\xi)\right)d\xi} \\ &\cdot \int_0^t \alpha(q(s)-p(s)) \left(1-\frac{z_1(s)}{K_f}\right) \cdot e^{\int_0^s \left(\frac{\alpha p(\xi)}{K_f}+\mu_A(\xi)\right)d\xi} ds \\ \geq& 0. \end{aligned}$$

Repeating the procedures for $t \in [\bar{\tau}, 2\bar{\tau}], [2\bar{\tau}, 3\bar{\tau}], \ldots, [\lfloor n \rfloor \bar{\tau}, n\bar{\tau}]$ with $n = \frac{T}{\bar{\tau}}$, we have $v_1(t) \geq w_1(t)$ for all $t \in [0, T]$. Similar arguments remain valid, that is $v_2(t) \geq w_2(t)$ for all $t \in [0, T]$.

For $t \in (T, 1)$, we have $v_1(t) = \varphi_1(T)e^{-\int_T^t d_A(s)ds}$ and $w_1(t) = \psi_1(T)e^{-\int_T^t d_A(s)ds}$. Since $\varphi_1(T) \geq \psi_1(T)$, it follows that $v_1(t)-w_1(t) = (\varphi_1(T)-\psi_1(T))e^{-\int_T^t d_A(s)ds} \geq 0$. Similarly, we have $v_2(t) - w_2(t) \geq 0$ since $\varphi_2(T) \geq \psi_2(T)$ for $t \in (T, 1)$.

Therefore, $\Phi(t) : \mathcal{X} \to \mathcal{X}$ is monotone for $t \in [0, 1]$. Repeating the procedures to the next intervals $[1, 2], [2, 3], \ldots$, we have $\Phi(t) : \mathcal{X} \to \mathcal{X}$ is monotone for all $t \geq 0$. ☐

Lemma 6.3.4. *For any* $\varphi \gg 0$ *in* $\mathcal{X}_K$ *and any* $\gamma \in (0, 1)$, *we have* $u_i(t; \gamma\varphi) > \gamma u_i(t; \varphi)$ *for all* $t > 0$, $i = 1, 2$.

Proof. Denote $z(t) = u(t; \gamma\varphi)$ with $z_0(\cdot) = \gamma\varphi$ and $v(t) = u(t; \varphi)$ with $v_0(\cdot) = \varphi \gg 0$ in $\mathcal{X}_K$. It follows from Lemma 6.3.3 that $z(t) > 0$ and $v(t) > 0$ for all $t > 0$. For all $\theta \in [-\hat{\tau}, 0]$, we have

$$z_1(\theta) = \gamma\varphi_1(\theta) = \gamma v_1(\theta) \text{ and } z_2(\theta) = \gamma\varphi_2(\theta) = \gamma v_2(\theta).$$

For any $t \in [0, \overline{\tau}]$, we have

$$\begin{aligned} z_1(t) &= e^{-\int_0^t \left(\frac{\alpha\gamma q(s)}{K_f} + \mu_A(s) \right) ds} \left(\gamma\varphi_1(0) + \int_0^t \alpha\gamma q(s) \cdot e^{\int_0^s \left(\frac{\alpha\gamma q(\xi)}{K_f} + \mu_A(\xi) \right) d\xi} ds \right) \\ &> \gamma e^{-\int_0^t \left(\frac{\alpha q(s)}{K_f} + \mu_A(s) \right) ds} \left(\varphi_1(0) + \int_0^t \alpha q(s) \cdot e^{\int_0^s \left(\frac{\alpha q(\xi)}{K_f} + \mu_A(\xi) \right) d\xi} ds \right) \\ &= \gamma v_1(t) \end{aligned}$$

and

$$\begin{aligned} z_2(t) &= e^{-\int_0^t \left(\frac{(1-\alpha)\gamma q(s)}{K_m} + \mu_A(s) \right) ds} \left(\gamma\varphi_2(0) + \int_0^t (1-\alpha)\gamma q(s) \cdot e^{\int_0^s \left(\frac{(1-\alpha)\gamma q(\xi)}{K_m} + \mu_A(\xi) \right) d\xi} ds \right) \\ &> \gamma e^{-\int_0^t \left(\frac{(1-\alpha) q(s)}{K_m} + \mu_A(s) \right) ds} \left(\varphi_1(0) + \int_0^t (1-\alpha) q(s) \cdot e^{\int_0^s \left(\frac{(1-\alpha) q(\xi)}{K_m} + \mu_A(\xi) \right) d\xi} ds \right) \\ &= \gamma v_2(t) \end{aligned}$$

where $q(s) = \widetilde{B}(s) \frac{\varphi_1(s-\tau(s)) \cdot h\varphi_2(s-\tau(s))}{\varphi_1(s-\tau(s)) + h\varphi_2(s-\tau(s))}$. Similar arguments deduce that $z_1(t) > \gamma v_1(t)$ and $z_2(t) > \gamma v_2(t)$ for all $t \in [\overline{\tau}, T]$. Hence, we easily obtain $z_1(T) > \gamma v_1(T)$ and $z_2(T) > \gamma v_1(T)$.

For any $t \in (T, 1)$, we have

$$z_1(t) = z_1(T) e^{-\int_T^t d_A(s) ds} > \gamma v_1(T) e^{-\int_T^t d_A(s) ds} = \gamma v_1(t)$$

and

$$z_2(t) = z_2(T) e^{-\int_T^t d_A(s) ds} > \gamma v_2(T) e^{-\int_T^t d_A(s) ds} = \gamma v_2(t).$$

This concludes that $z_1(t) > \gamma v_1(t)$ and $z_2(t) > \gamma v_2(t)$ for $t \in [0, 1]$. Repeating the procedure for $t \in [1, 2], [2, 3], \ldots$, we have $z_1(t) > \gamma v_1(t)$ and $z_2(t) > \gamma v_2(t)$ for all $t > 0$. □

6.3.2 Quotient space and strong monotonicity

Regarding the equations as an ordinary differential equations, we have the following observations: When $t \in [0, T]$, we need the values of $u(0)$ and $u(t-\tau(t))$. It is easy to see that $t-\tau(t) \in I := \{-\tau(0), \min\{T-\tau(T), 0\}\}$ is satisfied by the monotonicity of the function $f(t) = t - \tau(t)$. Since $t-\tau(t)$ is strictly increasing, then we have a more reasonable choice of $t-\tau(t) \in I$. That is, the information of initial value is on the set $\{0\} \cup I$.
By checking the structure of the model, we define a closed set $A \subset \mathcal{X}$ as

$$A = \{\varphi \in \mathcal{X} : \varphi(\theta) = 0 \ \text{ for all } \ \theta \in \{0\} \cup I\}.$$

Based on the set A, we have the following interesting observations:

Lemma 6.3.5. *For any two initial data φ, $\psi \in \mathcal{X}$ and the respective solutions through them $u(t;\varphi)$ and $u(t;\psi)$ satisfy:*

(i) if $\varphi - \psi \in A$, then $u(t;\varphi) - u(t;\psi) \equiv 0$ for all $t \geq 0$;

(ii) if furthermore, $\varphi \in A$, then $u(t;\varphi) \equiv 0$ for all $t \geq 0$.

Proof. Denote $v(t) = u(t;\varphi)$ and $w(t) = u(t;\psi)$, then we have $v_t(\cdot) \in \mathcal{X}$ with $v_0(\cdot) = \varphi$ and $w_t(\cdot) \in \mathcal{X}$ with $w_0(\cdot) = \psi$, respectively. When $\varphi - \psi \in A$, then $\varphi_1(\theta) - \psi_1(\theta) = 0$ and $\varphi_2(\theta) - \psi_2(\theta) = 0$ for all $\theta \in \{0\} \cup I$. Two solutions $v(t) = u(t;\varphi)$ and $w(t) = u(t;\psi)$ satisfy that $u(0;\varphi_1) - u(0;\psi_1) = \varphi_1(0) - \psi_1(0) = 0$ and $u(0;\varphi_2) - u(0;\psi_2) = \varphi_2(0) - \psi_2(0) = 0$.
For $t \in [0, \overline{\tau}]$, we have equations (6.11) involving $v_1^{'}(t)$, $v_2^{'}(t)$, $w_1^{'}(t)$ and $w_2^{'}(t)$. Since $t - \tau(t) \in [-\tau(0), \overline{\tau} - \tau(\overline{\tau})] \subset I$, then $\varphi_1(t-\tau(t)) = \psi_1(t-\tau(t))$ and $\varphi_2(t-\tau(t)) = \psi_2(t-\tau(t))$. Thus $q(t) = p(t)$ and then

$$\begin{aligned} v_1^{'}(t) - w_1^{'}(t) &= \alpha q(t)\left[\left(1 - \frac{v_1(t)}{K_f}\right) - \left(1 - \frac{w_1(t)}{K_f}\right)\right] - \mu_A(t)[v_1(t) - w_1(t)] \\ &= \left[-\frac{\alpha q(t)}{K_f} - \mu_A(t)\right][v_1(t) - w_1(t)] \end{aligned} \tag{6.12}$$

and

$$\begin{aligned} v_2^{'}(t) - w_2^{'}(t) &= (1-\alpha)q(t)\left[\left(1-\frac{v_2(t)}{K_m}\right) - \left(1-\frac{w_2(t)}{K_m}\right)\right] - \mu_A(t)[v_2(t) - w_2(t)] \\ &= \left[-\frac{(1-\alpha)q(t)}{K_m} - \mu_A(t)\right][v_2(t) - w_2(t)]. \end{aligned} \tag{6.13}$$

Since equations (6.12) and (6.13) are linear and the initial values $v_1(0) - w_1(0) = 0$ and $v_2(0) - w_2(0) = 0$, then $v_1(t) - w_1(t) \equiv 0$ and $v_2(t) - w_2(t) \equiv 0$ for all $t \in [0, \overline{\tau}]$ if $\varphi - \psi \in A$. Similar arguments hold for $t \in [\overline{\tau}, 2\overline{\tau}]$, $[2\overline{\tau}, 3\overline{\tau}]$,..., $[\lfloor n \rfloor \overline{\tau}, n\overline{\tau}]$, with $n = \frac{T}{\overline{\tau}}$, thus we have $v_1(t) - w_1(t) \equiv 0$ and $v_2(t) - w_2(t) \equiv 0$, namely $u(t;\varphi) - u(t;\psi) \equiv 0$ for all $t \in [0, T]$.

For $t \in (T, 1)$, we have

$$\begin{aligned} v_1^{'}(t) - w_1^{'}(t) &= -d_A(t)(v_1(t) - w_1(t)), \\ v_2^{'}(t) - w_2^{'}(t) &= -d_A(t)(v_2(t) - w_2(t)). \end{aligned}$$

Therefore, $v_1(t) - w_1(t) \equiv 0$ and $v_2(t) - w_2(t) \equiv 0$, namely $u(t;\varphi) - u(t;\psi) \equiv 0$ for all $t \in (T, 1)$ if $\varphi - \psi \in A$. Repeating these procedures to all time intervals $[1, 2]$, $[2, 3]$, $\ldots$, we have $u(t;\varphi) - u(t;\psi) \equiv 0$ for all $t \geq 0$. Therefore, statement (i) holds.

If $\varphi \in A$, choose $\psi = 0$ as the zero function in $\mathcal{X}$, then $\varphi - \psi \in A$ and the solution through ψ is identically zero for all $t \geq 0$. Hence

$$u(t;\varphi) \equiv u(t;\psi) \equiv 0,$$

which implies that statement (ii) holds. □

It follows that, if we choose two initial data $\varphi > \psi$ in the ordering $\mathcal{X}^+$, but $\varphi - \psi \in A$, then $u(t;\varphi) - u(t;\psi) \equiv 0$. Hence, the periodic semiflow $\Phi(t)$ is not strongly monotone. The above observation on the identical solutions through two initial values φ and ψ with $\varphi - \psi \in A$ motivates us to classify these initial data into the same class and partition the phase space $\mathcal{X}$ into different classes. This can be done by using the quotient space

$\mathcal{Q} = \mathcal{X}/A$, consisting of equivalence classes

$$[\varphi] = \{\varphi + a : a \in A\}.$$

As solutions from two initial values φ and ψ taken from an equivalence class have the property that $\varphi - \psi \in A$, Lemma 6.3.5 illustrates that the solutions $u(t;\varphi) - u(t;\psi) \equiv 0$ for all $t \geq 0$. Then we may study the solution through a given equivalence class from the quotient space $\mathcal{Q}$. For $[\varphi] \in \mathcal{Q}$, the solution through this equivalence is exactly the solution $u(t;\varphi)$, based on which, the solution map $\widetilde{\Phi}(t) : \mathcal{Q} \to \mathcal{Q}$ can be defined as

$$\widetilde{\Phi}(t)([\varphi]) = [\Phi(t)(\varphi)] = [u_t(\cdot;\varphi)]$$

with $u_t(\theta;\varphi) = u(t+\theta;\varphi)$ for all $\theta \in [-\hat{\tau}, 0]$. Then the positive cone $\mathcal{Q}^+ \subset \mathcal{Q}$ can be introduced, consisting of equivalence classes $[\varphi]$ with

$$\mathcal{Q}^+ := \{[\varphi] \in \mathcal{Q} : \varphi(\theta) \geq 0 \ \text{ for all } \ \theta \in \{0\} \cup I\}.$$

For the coned space $(\mathcal{Q}, \mathcal{Q}^+)$, we can show that the solution map $\widetilde{\Phi}(t)$ is strongly monotone when $t \geq 2$.

Lemma 6.3.6. *For any two initial data equivalence classes $[\varphi]$ and $[\psi]$, if $[\varphi] > [\psi]$ under the cone $\mathcal{Q}^+$, then $\widetilde{\Phi}(t)([\varphi]) \gg \widetilde{\Phi}(t)([\psi])$ when $t \geq 2$.*

Proof. Suppose two typical elements φ and ψ are from two different equivalence classes, and $[\varphi] > [\psi]$ with partial ordering defined by $\mathcal{Q}^+$, then $\varphi(\theta) \geq \psi(\theta)$ for all $\theta \in \{0\} \cup I$, and there is $\theta_0 \in \{0\} \cup I$ such that $\varphi(\theta_0) > \psi(\theta_0)$.

Denote $v(t) = u(t;\varphi)$ and $w(t) = u(t;\psi)$, then we have $v_t(\cdot) \in \mathcal{Q}^+$ with $v_0(\cdot) = \varphi$ and $w_t(\cdot) \in \mathcal{Q}^+$ with $w_0(\cdot) = \psi$. It follows that

$$\begin{aligned} v_1(t) - w_1(t) =& (\varphi_1(0) - \psi_1(0)) e^{-\int_0^t \left(\frac{\alpha q(s)}{K_f} + \mu_A(s)\right) ds} + e^{-\int_0^t \left(\frac{\alpha p(\xi)}{K_f} + \mu_A(\xi)\right) d\xi} \\ & \cdot \int_0^t \alpha(q(s) - p(s)) \left(1 - \frac{z_1(s)}{K_f}\right) \cdot e^{\int_0^s \left(\frac{\alpha p(\xi)}{K_f} + \mu_A(\xi)\right) d\xi} ds \end{aligned} \tag{6.14}$$

and

$$\begin{aligned} v_2(t) - w_2(t) =& (\varphi_2(0) - \psi_2(0)) e^{-\int_0^t \left(\frac{(1-\alpha)q(s)}{K_f} + \mu_A(s) \right) ds} + e^{-\int_0^t \left(\frac{(1-\alpha)p(\xi)}{K_f} + \mu_A(\xi) \right) d\xi} \\ & \cdot \int_0^t (1-\alpha)(q(s) - p(s)) \left(1 - \frac{z_1(s)}{K_f} \right) \cdot e^{\int_0^s \left(\frac{(1-\alpha)p(\xi)}{K_f} + \mu_A(\xi) \right) d\xi} ds \end{aligned} \tag{6.15}$$

where $q(s) = \widetilde{B}(s) \frac{\varphi_1(s-\tau(s)) \cdot h\varphi_2(s-\tau(s))}{\varphi_1(s-\tau(s)) + h\varphi_2(s-\tau(s))}$ and $p(s) = \widetilde{B}(s) \frac{\psi_1(s-\tau(s)) \cdot h\psi_2(s-\tau(s))}{\psi_1(s-\tau(s)) + h\psi_2(s-\tau(s))}$.

If $\theta_0 \in \{0\}$, we have $\varphi_1(0) > \psi_1(0)$ and $\varphi_2(0) > \psi_2(0)$. Then $v_1(t) > w_1(t)$ and $v_2(t) > w_2(t)$ for all $t > 0$.

If $\theta_0 \in I$, we can choose a unique $t_0 \in [0, T]$ such that $t_0 - \tau(t_0) = \theta_0$. These uniqueness and existence of t_0 is guaranteed by the fact that the inverse function of the bijection function $f(t) = t - \tau(t)$ with the domain $[0, 1]$ and range I exists. Next we will present $v_1(t_0) > w_1(t_0)$ and $v_2(t_0) > w_2(t_0)$. If $t_0 \in [0, \overline{\tau}]$ and suppose, by contradiction, that $v_1(t_0) = w_1(t_0)$ and $v_2(t_0) = w_2(t_0)$. Then it follows from equation (6.14) and (6.15) that $\varphi_1(0) = \psi_1(0)$, $\varphi_2(0) = \psi_2(0)$ and $q_{(}s) = p(s)$ for all $s \in [0, t_0]$. That is,

$$\widetilde{B}(s) \frac{\varphi_1(s-\tau(s)) \cdot h\varphi_2(s-\tau(s))}{\varphi_1(s-\tau(s)) + h\varphi_2(s-\tau(s))} = \widetilde{B}(s) \frac{\psi_1(s-\tau(s)) \cdot h\psi_2(s-\tau(s))}{\psi_1(s-\tau(s)) + h\psi_2(s-\tau(s))}.$$

When $s = t_0$, we have $\varphi_1(\theta_0) = \varphi_1(t_0 - \tau(t_0)) = \psi_1(t_0 - \tau(t_0)) = \psi_1(\theta_0)$ and $\varphi_2(\theta_0) = \varphi_2(t_0 - \tau(t_0)) = \psi_2(t_0 - \tau(t_0)) = \psi_2(\theta_0)$, which contradicts with $\varphi_1(\theta_0) > \psi_1(\theta_0)$ and $\varphi_2(\theta_0) > \psi_2(\theta_0)$. If $t_0 \in [\overline{\tau}, T]$, similar arguments remain valid.

Hence, we can always find an $t_0 \in [0, 1]$ such that $v_1(t_0) > w_1(t_0)$ and $v_2(t_0) > w_2(t_0)$. Then we may choose $\hat{\varphi} = u_{t_0}(\cdot; \varphi) \in \mathcal{Q}^+$ and $\hat{\psi} = u_{t_0}(\cdot; \psi) \in \mathcal{Q}^+$. It follows that $\hat{\varphi} \geq \hat{\psi}$ and $\hat{\varphi}(0) = u(t_0; \varphi) > u(t_0; \psi) = \hat{\psi}(0)$. For any $t_0 \leq t \leq T$, we have

$$\begin{aligned} v_1(t) - w_1(t) =& (\hat{\varphi}_1(0) - \hat{\psi}_1(0)) e^{-\int_{t_0}^t \left(\frac{\alpha q(s)}{K_f} + \mu_A(s) \right) ds} + e^{-\int_{t_0}^t \left(\frac{\alpha p(\xi)}{K_f} + \mu_A(\xi) \right) d\xi} \\ & \cdot \int_{t_0}^t \alpha(q(s) - p(s)) \left(1 - \frac{z_1(s)}{K_f} \right) \cdot e^{\int_{t_0}^s \left(\frac{\alpha p(\xi)}{K_f} + \mu_A(\xi) \right) d\xi} ds > 0 \end{aligned}$$

and

$$\begin{aligned} v_2(t) - w_2(t) =& (\hat{\varphi}_2(0) - \hat{\psi}_2(0)) e^{-\int_{t_0}^{t}\left(\frac{(1-\alpha)q(s)}{K_f}+\mu_A(s)\right)ds} + e^{-\int_{t_0}^{t}\left(\frac{(1-\alpha)p(\xi)}{K_f}+\mu_A(\xi)\right)d\xi} \\ & \cdot \int_{t_0}^{t} (1-\alpha)(q(s)-p(s)) \left(1 - \frac{z_1(s)}{K_f}\right) \cdot e^{\int_{t_0}^{s}\left(\frac{(1-\alpha)p(\xi)}{K_f}+\mu_A(\xi)\right)d\xi} ds > 0. \end{aligned}$$

If $T \leq t_0 \leq 1$, for $t_0 \leq t \leq 1$, we have

$$v_1(t) - w_1(t) = (v_1(t_0) - w_1(t_0)) e^{-\int_{t_0}^{t} d_A(s)ds} > 0$$

and

$$v_2(t) - w_2(t) = (v_2(t_0) - w_2(t_0)) e^{-\int_{t_0}^{t} d_A(s)ds} > 0.$$

Similar arguments hold if t_0 is in other intervals $[1, 2], [2, 3], \ldots$. The arguments show that if for $t_0 \geq 0$, we have $v_1(t_0) > w_1(t_0)$ and $v_2(t_0) > w_2(t_0)$, then $v_1(t) > w_1(t)$ and $v_2(t) > w_2(t)$ for all $t \geq 1 > t_0$. Hence, the solution map $\widetilde{\Phi}(t)$ is strongly monotone whenever $t \geq 2$. □

6.4 Net reproduction number and stability

The net reproduction ratio $\mathcal{R}_0$ is a key threshold parameter analyzing the dynamics of population models in a periodic environment, referring to Bacaër and Ait Dads [26], Thieme [179], Wang and Zhao [193], Wu et al. [200], Lou and Zhao [122] and the references therein. Based on the theories in Zhao [206], we introduce the net reproduction number $\mathcal{R}_0$ to explore the dynamics of our model with a periodic time delay.

First investigate a nonlinear eigenvalue problem, and then introduce the net reproduction number $\mathcal{R}_0$ by using the cone spectral radius of a monotone and homogeneous operator. Furthermore, we explore the global stability of the host population model. Then we start with the following auxiliary system:

$$\begin{aligned}
\frac{\mathrm{d}A_f(t)}{\mathrm{d}t} &= \alpha\widetilde{B}(t)\frac{A_f(t-\tau(t))\cdot hA_m(t-\tau(t))}{A_f(t-\tau(t))+hA_m(t-\tau(t))} - \mu_A(t)A_f(t), && t-\lfloor t\rfloor \in [0,T],\\
\frac{\mathrm{d}A_m(t)}{\mathrm{d}t} &= (1-\alpha)\widetilde{B}(t)\frac{A_f(t-\tau(t))\cdot hA_m(t-\tau(t))}{A_f(t-\tau(t))+hA_m(t-\tau(t))} - \mu_A(t)A_m(t), && t-\lfloor t\rfloor \in [0,T],\\
\frac{\mathrm{d}A_f(t)}{\mathrm{d}t} &= -d_A(t)A_f(t), && t-\lfloor t\rfloor \in (T,1),\\
\frac{\mathrm{d}A_m(t)}{\mathrm{d}t} &= -d_A(t)A_m(t), && t-\lfloor t\rfloor \in (T,1).
\end{aligned} \tag{6.16}$$

where $\widetilde{B}(t) = 2R(1-\tau^{'}(t))e^{-\int_{t-\tau(t)}^{t}\mu_J(\alpha)d\alpha}$.

Let $\Psi(t)$ be the 1-periodic semiflow of system (6.16) on $\mathcal{X}$. Note that for any $\varphi \in \mathcal{X}^+$, if $\hat{u}(t;\varphi) = (\hat{u}_1(t;\varphi), \hat{u}_2(t;\varphi))$ is a solution of (6.16) with $\hat{u}(0;\varphi) = \varphi$, then so is $\lambda\hat{u}(t;\varphi)$ for any $t > 0$ and $0 < \lambda < 1$. Similar to te proof of Lemma 6.3.4, we have

$$\hat{u}(t;\lambda\varphi) = \lambda\hat{u}(t;\varphi), \ \ \forall t \geq 0, \ 0 < \lambda < 1.$$

This presents that for each $t > 0$, $\Psi(t)$ is strictly homogeneous on $\mathcal{X}^+$ in the sense that $\Psi(t)(\lambda\varphi) = \lambda\Psi(t)\varphi$, $\forall 0 < \lambda < 1$. In addition, it follows from the similar proving process of Lemma 6.3.3 that for each $t \geq 0$, Ψ is monotone on $\mathcal{X}^+$ and strongly monotone on $\mathcal{Q}^+$. By Theorem 4.9 in [131], it then follows that $\Psi := \Psi(1)$ has a simple principal eigenvalue $r := r(\Psi) > 0$, where $r(\Psi)$ is the cone spectral radius of Ψ, that is, $\Psi(t)\varphi^* = r\varphi^*$ for some $\varphi^* \gg 0$ in $\mathcal{X}^+$ and such an eigenvalue is unique.

Lemma 6.4.1. *Let $\Lambda^* = \ln r$. Then there exists a positive 1-periodic function $u^*(t)$ such that $e^{\Lambda^* t}u^*(t)$ is a solution of system (6.16).*

Proof. Similar to the proof of Lemma 5 in [28], let $\hat{u}(t;\varphi^*) = (\hat{u}_1(t;\varphi^*), \hat{u}_2(t;\varphi^*))$ be the solution of system (6.16) with $\hat{u}_0(\cdot;\varphi^*) = \varphi^*$, where φ^* is from an equivalence class $[\varphi^*]$ with partial ordering defined by $\mathcal{Q}^+$. Since $\varphi^* > 0$, it is easy to see that $\hat{u}_t(\varphi^*) \gg 0$ for all $t \geq 2$.

Define

$$u_1^*(t) = e^{-\Lambda^* t}\hat{u}_1(t;\varphi^*) \ \text{ and } \ u_2^*(t) = e^{-\Lambda^* t}\hat{u}_2(t;\varphi^*).$$

Then $u^*(t) = (u_1^*(t), u_2^*(t)) \gg 0$ for all $t \geq 2$, and u^* satisfies the following periodic system with parameter Λ^*:

$$\begin{aligned}
\frac{\mathrm{d}u_1^*(t)}{\mathrm{d}t} &= \alpha\widetilde{B}(t)\frac{e^{-\Lambda^*\tau(t)}u_1^*(t-\tau(t))\cdot hu_2^*(t-\tau(t))}{u_1^*(t-\tau(t))+hu_2^*(t-\tau(t))} - \mu_A(t)u_1^*(t), && t-\lfloor t\rfloor \in [0,T],\\
\frac{\mathrm{d}u_2^*(t)}{\mathrm{d}t} &= (1-\alpha)\widetilde{B}(t)\frac{e^{-\Lambda^*\tau(t)}u_1^*(t-\tau(t))\cdot hu_2^*(t-\tau(t))}{u_1^*(t-\tau(t))+hu_2^*(t-\tau(t))} - \mu_A(t)u_2^*(t), && t-\lfloor t\rfloor \in [0,T],\\
\frac{\mathrm{d}u_1^*(t)}{\mathrm{d}t} &= -d_A(t)u_1^*(t), && t-\lfloor t\rfloor \in (T,1),\\
\frac{\mathrm{d}u_2^*(t)}{\mathrm{d}t} &= -d_A(t)u_2^*(t), && t-\lfloor t\rfloor \in (T,1).
\end{aligned} \tag{6.17}$$

Thus, $u^*(t) = (u_1^*(t), u_2^*(t))$ is a solution of the 1-periodic system (6.17) and $u_0^*(\theta) = (u_1^*(\theta), u_2^*(\theta)) = (e^{-\Lambda^*\theta}\varphi_1^*(\theta), e^{-\Lambda^*\theta}\varphi_2^*(\theta))$ for all $\theta \in [-\hat{\tau}, 0]$, where $u_t^*(\cdot) = (u_{1t}^*(\cdot), u_{2t}^*(\cdot))$ for all $t \geq 0$ with

$$\begin{aligned}
u_{1t}^*(\theta) &= u_1^*(t+\theta) = e^{-\Lambda^*(t+\theta)}\hat{u}_1(t+\theta;\varphi^*), \quad \forall \theta \in [-\hat{\tau}, 0],\\
u_{2t}^*(\theta) &= u_2^*(t+\theta) = e^{-\Lambda^*(t+\theta)}\hat{u}_2(t+\theta;\varphi^*), \quad \forall \theta \in [-\hat{\tau}, 0].
\end{aligned}$$

For any $\theta \in [-\hat{\tau}, 0]$, we have

$$\begin{aligned}
u_1^*(1+\theta) &= e^{-\Lambda^*(1+\theta)}(\Psi(\cdot)\varphi^*(\theta))_1 = e^{-\Lambda^*(1+\theta)}\cdot r\varphi_1^*(\theta) = e^{-\Lambda^*\theta}\varphi_1^*(\theta) = u_1^*(\theta),\\
u_2^*(1+\theta) &= e^{-\Lambda^*(1+\theta)}(\Psi(\cdot)\varphi^*(\theta))_2 = e^{-\Lambda^*(1+\theta)}\cdot r\varphi_2^*(\theta) = e^{-\Lambda^*\theta}\varphi_2^*(\theta) = u_2^*(\theta).
\end{aligned}$$

Therefore, $u_0^*(\theta;\cdot) = u_1^*(\theta;\cdot)$ for all $\theta \in [-\hat{\tau}, 0]$, and hence, the existence and uniqueness of solutions of system (6.17) imply that

$$u_1^*(t) = u_1^*(t+1) \text{ and } u_2^*(t) = u_2^*(t+1), \quad \forall t \geq 0.$$

It then follows that $u^*(t)$ is an 1-periodic solution of system (6.17) and $e^{\Lambda^* t}u^*(t)$ is a solution of system (6.16). □

Define $F(t) : \mathcal{X} \to \mathbb{R}^2$ and $V(t) : \mathbb{R}^2 \to \mathbb{R}^2$ by

$$F(t)\begin{pmatrix}\varphi_1\\ \varphi_2\end{pmatrix} = \begin{cases}\begin{pmatrix}\alpha\widetilde{B}(t)\frac{\varphi_1(-\tau(t))\cdot h\varphi_2(-\tau(t))}{\varphi_1(-\tau(t))+h\varphi_2(-\tau(t))}\\ (1-\alpha)\widetilde{B}(t)\frac{\varphi_1(-\tau(t))\cdot h\varphi_2(-\tau(t))}{\varphi_1(-\tau(t))+h\varphi_2(-\tau(t))}\end{pmatrix}, & t-\lfloor t\rfloor \in [0,T],\\ \begin{pmatrix}0\\ 0\end{pmatrix}, & t-\lfloor t\rfloor \in (T,1),\end{cases}$$

and

$$-V(t)\begin{pmatrix}\varphi_1\\ \varphi_2\end{pmatrix} = \begin{cases}\begin{pmatrix}-\mu_A(t)\varphi_1\\ -\mu_A(t)\varphi_2\end{pmatrix}, & t-\lfloor t\rfloor \in [0,T],\\ \begin{pmatrix}-d_A(t)\varphi_1\\ -d_A(t)\varphi_2\end{pmatrix}, & t-\lfloor t\rfloor \in (T,1).\end{cases}$$

One easily sees that for each $t \geq 0$, $F(t)$ is a positive operator from $\mathcal{X}$ to $\mathbb{R}^2$. Let $Y(t,s)$, $t \geq s$, be the evolution operator on $\mathbb{R}^2$ associated with the following system:

$$\frac{\mathrm{d}v(t)}{\mathrm{d}t} = -V(t)v(t),$$

that is, $Y(t,s)$, $t \geq s$, is the evolution family on $\mathbb{R}^2$ determined by

$$\begin{cases}\frac{\mathrm{d}A_f(t)}{\mathrm{d}t} = -\mu_A(t)A_f(t), & t-\lfloor t\rfloor \in [0,T],\\ \frac{\mathrm{d}A_m(t)}{\mathrm{d}t} = -\mu_A(t)A_m(t), & t-\lfloor t\rfloor \in [0,T],\\ \frac{\mathrm{d}A_f(t)}{\mathrm{d}t} = -d_A(t)A_f(t), & t-\lfloor t\rfloor \in (T,1),\\ \frac{\mathrm{d}A_m(t)}{\mathrm{d}t} = -d_A(t)A_m(t), & t-\lfloor t\rfloor \in (T,1).\end{cases}$$

Let C_1 be the ordered Banach space of all continuous and 1-periodic functions from $\mathbb{R}$ to $\mathbb{R}^2$, equipped with the maximum norm and the positive cone $C_1^+ := \{v \in C_1 : v(t) \geq 0, \forall t \in \mathbb{R}\}$. Suppose $v \in C_1$ is the initial distribution of adult females and males in the periodic environment, then $F(t-s)v_{t-s}$ is the distribution of newly born adult individuals at time $t-s$ with $t \geq s \geq 0$, and $Y(t,t-s)F(t-s)v_{t-s}$ represents the distribution of those adult individuals who were newly reproduced at time $t-s$ and still survive in the environment at time t for $t \geq s$. Hence,

$$\int_0^\infty Y(t,t-s)F(t-s)v_{t-s}ds = \int_0^\infty Y(t,t-s)F(t-s)v(t-s+\cdot)ds$$

gives the distribution of accumulative new adult females and males at time t produced by those female and male individuals introduced at all previous time.
We define the next generation operator L on C_1 given by

$$\begin{aligned}[Lv](t) &= \int_0^\infty Y(t,t-s)F(t-s)v(t-s+\cdot)ds \\ &= \int_{-\infty}^t Y(t,\xi)F(\xi)v(\xi+\cdot)d\xi \\ &= \int_{-\infty}^t Y(t,s)F(s)v(s+\cdot)ds, \ \ \forall t \in \mathbb{R}, \ v \in C_1.\end{aligned}$$

Next, we show that the operator L maps a continues function $v \in C_1$ to a periodic and continues function $Lv \in C_1$, that is $L : C_1 \to C_1$. For any given $v \in C_1$, we have $F(s)v(s+\cdot)$ is bounded. Then there exists an upper bounded F^* such that $\|F(s)\|\|v(s+\cdot)\| \leq F^*$. It follows from Theorem 2.6 in [189] that for any t, there exist $K > 0$ and $\sigma = \min\{\mu_A(t), d_A(t)\}$, such that

$$\|Y(t,s)\| \leq K \cdot e^{-\sigma(t-s)}, \ \ \forall t \geq s, s \in \mathbb{R}.$$

Thus, we have

$$\|Y(t,s)F(s)\| \leq K \cdot \|F(s)\| \cdot e^{-\sigma(t-s)}$$

and

$$\begin{aligned}
&\left\|\int_{\infty}^{t} Y(t,s)F(s)v(s+\cdot)ds\right\| \\
\leq\, & K\int_{-\infty}^{t} \|F(s)\|\|v(s+\cdot)\| \cdot e^{-\sigma(t-s)}ds \\
\leq\, & KF^{*}\int_{-\infty}^{t} e^{-\sigma(t-s)}ds \\
\leq\, & \frac{KF^{*}}{\sigma}.
\end{aligned}$$

For any $t \geq s$, we have $\|Y(t,s)\| \leq 1$. For any $\epsilon > 0$, choose $\delta = \min\{\frac{\epsilon}{2F^{*}}, -\frac{\ln(1-\frac{\epsilon\sigma}{2KF^{*}})}{\hat{\sigma}}\}$ with $\hat{\sigma} = \max_{t\in[0,1]}\{\mu_A(t), d_A(t)\}$. For any $t_1 \geq t_2 \geq s$, we have $Y(t_1,s) = Y(t_1,t_2)Y(t_2,s)$ and $\|Y(t_1,t_2)\| \geq e^{-\hat{\sigma}(t_1-t_2)}$. When $|t_1 - t_2| < \delta$, we have

$$\begin{aligned}
&\|[Lv](t_1) - [Lv](t_2)\| \\
=&\left\|\int_{-\infty}^{t_1} Y(t_1,s)F(s)v(s+\cdot)ds - \int_{-\infty}^{t_2} Y(t_2,s)F(s)v(s+\cdot)ds\right\| \\
=&\left\|\int_{-\infty}^{t_1} Y(t_1,s)F(s)v(s+\cdot)ds - \int_{-\infty}^{t_2} Y(t_1,s)F(s)v(s+\cdot)ds\right. \\
&\left.+\int_{-\infty}^{t_2} Y(t_1,s)F(s)v(s+\cdot)ds - \int_{-\infty}^{t_2} Y(t_2,s)F(s)v(s+\cdot)ds\right\| \\
\leq&\left\|\int_{t_2}^{t_1} Y(t_1,s)F(s)v(s+\cdot)ds\right\| + \left\|\int_{-\infty}^{t_2} \left[Y(t_1,s) - Y(t_2,s)\right] F(s)v(s+\cdot)ds\right\| \\
\leq&F^{*}(t_1-t_2) + \|1 - Y(t_1,t_2)\| \left\|\int_{-\infty}^{t_2} Y(t_2,s)F(s)v(s+\cdot)ds\right\| \\
\leq&F^{*}(t_1-t_2) + \left(1 - e^{-\hat{\sigma}(t_1-t_2)}\right) \cdot \frac{KF^{*}}{\sigma} \\
\leq&\epsilon.
\end{aligned}$$

This implies that $Lv \in C_1$.

Suppose $v(t+1) = v(t), \forall t \in \mathbb{R}$. Since

$$\begin{aligned}[Lv](t+1) &= \int_0^\infty Y(t+1, t+1-s)F(t+1-s)v(t+1-s+\cdot)ds \\ &= \int_0^\infty Y(t, t-s)F(t-s)v(t-s+\cdot)ds \\ &= [Lv](t),\end{aligned}$$

it follows that $[Lv](t)$ is also periodic with respect to t. Therefore, we have $L : C_1 \to C_1$. According to the concept and properties of next generation operator in [27, 206] (or Section 2.3), we define the cone spectral radius of L on $\mathbb{R}_+^2$ as the net reproduction number $\mathcal{R}_0 := r(L)$. Based on Theorem 2.3.1 (or Theorem 3.4 in [190]), we have

Lemma 6.4.2. *$\mathcal{R}_0 - 1$ has the same sign as $r(\Psi) - 1$.*

In addition, for any given $t \geq 0$, let $\widetilde{\Psi}(t)$ be the solution map of system (6.16) on $\mathcal{Q}^+$, such that $\widetilde{\Psi}(t)\varphi = \widetilde{u}_t(\varphi), t \geq 0$, where $\widetilde{u}(t;\varphi)$ is the unique solution of system (6.16) with $\widetilde{u}_0 = \varphi \in \mathcal{Q}^+$. Using similar arguments to lemma 3.8 in [122] through the Krein-Rutman theorem, it is shown that the stability of the zero solution for system (6.16) on $\mathcal{X}$ equals to that on $\mathcal{Q}^+$.

Lemma 6.4.3. *Two Poincaré maps $\Psi(1) : \mathcal{X} \to \mathcal{X}$ and $\widetilde{\Psi}(1) : \mathcal{Q}^+ \to \mathcal{Q}^+$ have the same spectral radius, that is, $r(\Psi) = r(\widetilde{\Psi})$.*

Based on the above lemmas and results, we obtain the following global dynamics for system (6.9).

Theorem 6.4.1. *The following statements are valid:*

(i) If $\mathcal{R}_0 < 1$, then the zero solution is globally asymptotically stable for system (6.9) in $\mathcal{Q}^+$;

(ii) If $\mathcal{R}_0 > 1$, then system (6.9) admits a unique positive 1-periodic solution $(A_f^*(t), A_m^*(t))$, which is globally asymptotically stable in $\mathcal{Q}^+$.

Proof. In the case where $\mathcal{R}_0 < 1$, Lemmas 6.4.2 and 6.4.3 imply $r < 1$. For any given φ from an equivalence class $[\varphi] \in \mathcal{Q}^+$, let $u(t;\varphi)$ be the solution of system (6.16) with the initial value $u(0;\varphi) = \varphi$. Note that system (6.16) dominates system (6.9) since $1 - \frac{A_f(t)}{K_f} \leq 1$ and $1 - \frac{A_m(t)}{K_m} \leq 1$ for all $t \geq 0$. Choose a sufficiently large $\alpha > 0$ such that $\varphi(\theta) \leq \alpha \cdot u^*(0)$, where u^* is defined in Lemma 6.4.1. Thus, the comparison principle implies that $u(t;\varphi) \leq \alpha e^{\Lambda^* t} u^*(t), \forall t \geq 0$. Owing to $\Lambda^* = \ln r < 0$, we have $\lim_{t\to\infty} u(t;\varphi) = 0$. Then the desired result immediately follows from Lemma 2.2.1 in [207].

In the case where $\mathcal{R}_0 > 1$, we suppose $\tilde{\Phi}(t)$ be the 1-periodic semiflow associated with system (6.9), and define $\tilde{\Phi} := \tilde{\Phi}(1)$. Clearly, $\tilde{\Phi}^{n_0}(1) = \tilde{\Phi}(n_0 \cdot 1), \forall n_0 \geq 2$. It then follows that for each $t > 0$, $\widetilde{\Phi}(t)$ is strongly monotone and strictly subhomogeneous on $\mathcal{Q}^+$. Let r_σ be the cone spectral radius of the Poincaré map of the following periodic system with σ_f and σ_m:

$$
\begin{aligned}
\frac{\mathrm{d}A_f(t)}{\mathrm{d}t} =& \alpha \widetilde{B}(t) \frac{A_f(t-\tau(t)) \cdot hA_m(t-\tau(t))}{A_f(t-\tau(t)) + hA_m(t-\tau(t))} \left(1 - \frac{\sigma_f}{K_f}\right) - \mu_A(t)A_f(t), \\
& \qquad\qquad\qquad\qquad\qquad\qquad\qquad\qquad\qquad t - \lfloor t \rfloor \in [0,T], \\
\frac{\mathrm{d}A_m(t)}{\mathrm{d}t} =& (1-\alpha) \widetilde{B}(t) \frac{A_f(t-\tau(t)) \cdot hA_m(t-\tau(t))}{A_f(t-\tau(t)) + hA_m(t-\tau(t))} \left(1 - \frac{\sigma_m}{K_m}\right) - \mu_A(t)A_m(t), \\
& \qquad\qquad\qquad\qquad\qquad\qquad\qquad\qquad\qquad t - \lfloor t \rfloor \in [0,T], \\
\frac{\mathrm{d}A_f(t)}{\mathrm{d}t} =& - d_A(t)A_f(t), \quad t - \lfloor t \rfloor \in (T,1), \\
\frac{\mathrm{d}A_m(t)}{\mathrm{d}t} =& - d_A(t)A_m(t), \quad t - \lfloor t \rfloor \in (T,1),
\end{aligned}
\tag{6.18}
$$

where $\widetilde{B}(t) = 2R(1-\tau'(t))e^{-\int_{t-\tau(t)}^{t} \mu_J(\alpha) d\alpha}$. Under the condition $\mathcal{R}_0 > 1$, it follows from Lemma 6.4.2 and 6.4.3 that $r > 1$. Since $\lim\limits_{\sigma_f \to 0; \sigma_m \to 0} r_\sigma = r > 1$, we can fix two sufficiently small number σ_f and σ_m such that $\sigma_f \in (0, K_f)$, $\sigma_m \in (0, K_m)$ and $r_\sigma > 1$. Since $\lim\limits_{\varphi \to 0} \|\widetilde{\Phi}(t)\varphi\|_{\mathcal{Q}^+} = 0$ uniformly for $t \in [0,1]$, there exists $\sigma^* > 0$ such that

$$
\|\widetilde{\Phi}(t)\varphi\|_{\mathcal{Q}^+} < \sigma, \ \ \forall t \in [0,1], \ \ \|\varphi\|_{\mathcal{Q}^+} \leq \sigma^*,
$$

where σ satisfies $\sigma = \min\{\sigma_f, \sigma_m\}$. We need to claim that

$$\limsup_{n_0\to\infty} \|\widetilde{\Phi}^{n_0}(1)\varphi\|_{\mathcal{Q}^+} \geq \sigma^*, \ \ \forall \varphi \in \mathcal{Q}^+ \backslash \{([0],[0])\}.$$

Suppose by contradiction, $\limsup\limits_{n_0\to\infty} \|\widetilde{\Phi}^{n_0}(1)\tilde{\varphi}\|_{\mathcal{Q}^+} < \sigma^*$ for some $\tilde{\varphi} \in \mathcal{Q}^+\backslash\{([0],[0])\}$. Then there exists $n_1 \geq 2$ such that $\|\widetilde{\Phi}^{n_0}(1)\tilde{\varphi}\|_{\mathcal{Q}^+} < \sigma^*$ for all $n_0 \geq n_1$. For any $t \geq n_1$, letting $t = n_0 + t_\Delta$ with $n_0 = \lfloor t \rfloor$ and $t_\Delta \in [0,1)$, it holds that

$$\|\widetilde{\Phi}(t)\tilde{\varphi}\|_{\mathcal{Q}^+} = \left\|\widetilde{\Phi}(t_\Delta)\left(\widetilde{\Phi}(n_0)\tilde{\varphi}\right)\right\|_{\mathcal{Q}^+} = \left\|\widetilde{\Phi}(t_\Delta)\left(\widetilde{\Phi}^{n_0}(1)\tilde{\varphi}\right)\right\|_{\mathcal{Q}^+} < \sigma.$$

Then we have

$$\begin{aligned}
\frac{\mathrm{d}A_f(t)}{\mathrm{d}t} \geq& \alpha\widetilde{B}(t)\frac{A_f(t-\tau(t))\cdot hA_m(t-\tau(t))}{A_f(t-\tau(t))+hA_m(t-\tau(t))}\left(1-\frac{\sigma_f}{K_f}\right) - \mu_A(t)A_f(t),\\
&\qquad\qquad\qquad\qquad\qquad t-\lfloor t\rfloor \in [0,T],\\
\frac{\mathrm{d}A_m(t)}{\mathrm{d}t} \geq& (1-\alpha)\widetilde{B}(t)\frac{A_f(t-\tau(t))\cdot hA_m(t-\tau(t))}{A_f(t-\tau(t))+hA_m(t-\tau(t))}\left(1-\frac{\sigma_m}{K_m}\right) - \mu_A(t)A_m(t),\\
&\qquad\qquad\qquad\qquad\qquad t-\lfloor t\rfloor \in [0,T],\\
\frac{\mathrm{d}A_f(t)}{\mathrm{d}t} =& -d_A(t)A_f(t), \quad t-\lfloor t\rfloor \in (T,1),\\
\frac{\mathrm{d}A_m(t)}{\mathrm{d}t} =& -d_A(t)A_m(t), \quad t-\lfloor t\rfloor \in (T,1).
\end{aligned} \tag{6.19}$$

By Lemma 6.4.1, there exists a positive 1-periodic solution $u^*_\sigma(t)$ such that $e^{\Lambda^*_\sigma t}u^*_\sigma(t)$ is a solution of system (6.18), where $\Lambda^*_\sigma = \ln r_\sigma > 0$. It is easy to verify that $u(t;\tilde{\varphi}) \gg 0$ for all $t > 0$. Then choose a $\kappa > 0$ such that

$$u(n_1;\tilde{\varphi}) \geq \kappa e^{\Lambda^*_\sigma n_1}u^*_\sigma(n_1).$$

Based on the comparison principle, we have

$$u(t;\tilde{\varphi}) \geq \kappa e^{\Lambda^*_\sigma t}u^*_\sigma(t), \ \ \forall t \geq n_1.$$

Letting $t \to \infty$, we obtain that $u(t; \tilde{\varphi})$ is unbounded, a contradiction.

Let $\omega(\varphi)$ be the omega limit set of the discrete-time orbit $\{\widetilde{\Phi}^{n_0}(\varphi)\}_{n_0 \geq 2}$. By the acyclicity theorem on uniform persistence, it easy follows that $\widetilde{\Phi}^{n_0} : \mathcal{Q}^+ \to \mathcal{Q}^+$, $n_0 \geq 2$, is uniformly persistent on $\mathrm{Int}(\mathcal{Q}^+)$, and hence, $\omega(\varphi) \subset \mathrm{Int}(\mathcal{Q}^+)$, $\forall \varphi \in \mathrm{Int}(\mathcal{Q}^+)$. For any $\varphi \in \mathcal{Q}^+$, since $\widetilde{\Phi}(\varphi) \in \mathrm{Int}(\mathcal{Q}^+)$, we have $\omega(\varphi) \subset \mathrm{Int}(\mathcal{Q}^+)$.

It follows that $\widetilde{\Phi}^{n_0}$ is strongly monotone and strictly subhomogeneous on $\mathcal{Q}^+$. By virtue of Theorem 2.3.2 in [207] (or Section 2.2), if follows that $\widetilde{\Phi}^{n_0}$ has a unique fixed point ψ^* such that $\omega(\varphi) = \psi^*$, $\forall \varphi \in \mathcal{Q}^+$. Thus, $(A_f^*(t), A_m^*(t)) := \left(\widetilde{\Phi}^{n_0}(t)\psi^*\right)$ is an n_0-periodic solution of system (6.9), and it is globally attractive in $\mathcal{Q}^+$. In view of Lemma 2.2.1, ψ^* is a Liapunov stable fixed point of $\widetilde{\Phi}^{n_0}$. Note that

$$\widetilde{\Phi}^{n_0}(t)(\widetilde{\Phi}(t)\psi^*) = \widetilde{\Phi}(t)(\widetilde{\Phi}^{n_0}(t)\psi^*) = \widetilde{\Phi}(t)\psi^*,$$

which implies that $\widetilde{\Phi}(t)\psi^* = \psi^*$. Consequently, $(A_f^*(t), A_m^*(t))$ is also a 1-periodic solution and is globally asymptotically stable for system (6.9) in $\mathcal{Q}^+$. □

6.5 Numerical simulations

In this section, we conduct numerical simulations to illustrate the patterns of the frog population in response to environment-related parameters. Subsequently, a sensitivity analysis is performed to demonstrate the impact of these parameters on population dynamics. From an in-depth examination of the combined effects of growth delay and natural death rates, several implications for maintaining the ecological stability of frog populations are derived.

6.5.1 Time-dependent parameters

Environmental temperature has profound consequences for amphibian development and has been proposed to play a role in determining vital rates throughout the life cycle, as well as the overwintering phenomenon [22]. We take the temperature data (in degrees °C) as a function of time t (in a day) in the following form [139] for illustration purpose of the conceptual framework

$$T(t) = c_K + d_K \times \sin\left(\frac{2\pi}{365} \times (t - t_0)\right).$$

where $c_K = 16.5$°C is mean annual temperature, $d_K = 15.5$°C is the amplitude of temperature variation and $t_0 = 121$ is day to the year when temperature increases to its annual mean [22, 164].

To determine the maturation time $\tau(t)$ for the cohort maturing at time t, as shown in equation (6.7), we need to obtain the development proportion $r_J(s)$ over the interval $s \in [t-\tau(t), t]$. This proportion can be evaluated as the reciprocal of the development duration $\widetilde{\tau}(T(s))$ required under the temperature $T(s)$ on day s, that is:

$$r_J(s) = \frac{1}{\widetilde{\tau}(T(s))}.$$

The development duration $\widetilde{\tau}(T)$ can be estimated by the following Sharpe-Schoolfield formula [139]:

$$\begin{aligned}&\widetilde{\tau}(T)\\ =&\tau_0 \times \exp\left(-\frac{E_\tau}{k_B}\left(\frac{1}{T} - \frac{1}{T_0}\right)\right) \times \left(1 + \exp\left(\frac{E_\tau^L}{k_B}\left(\frac{1}{T} - \frac{1}{T_\tau^L}\right)\right) + \frac{E_\tau^H}{k_B}\left(-\frac{1}{T} + \frac{1}{T_\tau^H}\right)\right).\end{aligned}$$

It follows that the accumulative development proportions over the previous $\tau(t)$ days, specifically days $t-1, t-2, \ldots, t-\tau(t)$, should sum to unity. That is,

$$\int_{t-\tau(t)}^{t} \frac{1}{\widetilde{\tau}(T(s))} ds = 1, \tag{6.20}$$

with $T(s)$ being the mean temperature at day s. The maturation time $\tau(t)$ can be estimated from the above relation (6.20).

The immature death rate under the temperature $T = T(t)$ can be described by the following

Sharpe-Schoolfield models [139]:

$$\begin{aligned}&\mu_J(T)\\=&\mu_0 \times \exp\left(-\frac{E_\mu}{k_B}\left(\frac{1}{T}-\frac{1}{T_0}\right)\right) \times \left(1+\exp\left(\frac{E_\mu^L}{k_B}\left(\frac{1}{T}-\frac{1}{T_\mu^L}\right)\right)+\frac{E_\mu^H}{k_B}\left(-\frac{1}{T}+\frac{1}{T_\mu^H}\right)\right).\end{aligned}$$

For simplicity, we assume $\mu_A(t)$ and $d_A(t)$ are taken as 0.015 per day and 0.01 per day in the model system, respectively. To numerical computation, other related parameters with their biological explanations are summarized in Table 6.1.

Table 6.1: Parameter descriptions with baseline values in model (6.9).

Parameter	Description	Baseline value	Reference
c_K	Mean annual temperature	16.5°C	[22],[139],[164]
d_K	The amplitude of temperature variation	15.5°C	[22],[139],[164]
t_0	Day of the year when temperature increases to its annual mean	121	[22],[139],[164]
T_0	The reference temperature	25°C	[40],[139]
τ_0	The scaling factor for development time at temperature T_0	27.6 days	[40],[139]
μ_0	The scaling factor for mortality rate at temperature T_0	0.056 per day	[86],[139]
T_τ^L	Lower temperature threshold for development	10°C	[86],[139]
T_τ^H	Upper temperature threshold for development	32.5°C	[86],[139]
T_μ^L	Lower temperature threshold where abruptly mortality increases	-5°C	[86],[139]

Continued on next page

Table 6.1 – *Continued from previous page*

Parameter	Description	Baseline value	Reference
T_μ^H	Upper temperature threshold where abruptly mortality increases	35°C	[86],[139]
E_μ, E_τ	Average activation energy	0.65 eV	[139],[177]
E_τ^L	Inactivation energy for lower temperature threshold	$5 \times E_\tau$	[139],[177]
E_τ^H	Inactivation energy for upper temperature threshold	$5 \times E_\tau$	[139],[177]
E_μ^L	An index analogous to the inactivation energy	$5 \times E_\mu$	[139],[177]
E_μ^H	An index analogous to the inactivation energy	$5 \times E_\mu$	[139],[177]
k_B	Boltzmann's constant	8.62×10^{-5}	[139]
K_f	Carrying capacity of female population	5000 frogs	[163]
K_m	Carrying capacity of male population	2000 frogs	[163]
α	Birth sex ratio	0.3	[163]
R	Intrinsic growth rate	2	[163]
h	A male's maximum number of establishable pair bonds	3	[33]
μ_A	Mortality rate of adults during normal period	0.015 per day	[111]
d_A	Mortality rate of adults during hibernation	0.01 per day	[111]

6.5.2 Parametric curves and analysis

Using the baseline parameters, the annual temperature variation exhibits a cyclical pattern, as depicted in Figure 6.1(a). Subsequently, applying the metabolic theory of ecology proposed by [139], we obtain the temperature-dependent developmental duration $\widetilde{\tau}(t)$, immature mortality rate $\mu_J(t)$, and survival probability $\exp\left(-\int_{t-\tau(t)}^{t}\mu_J(s)ds\right)$, which are illustrated in Figures 6.1(b), (c), and (d), respectively.

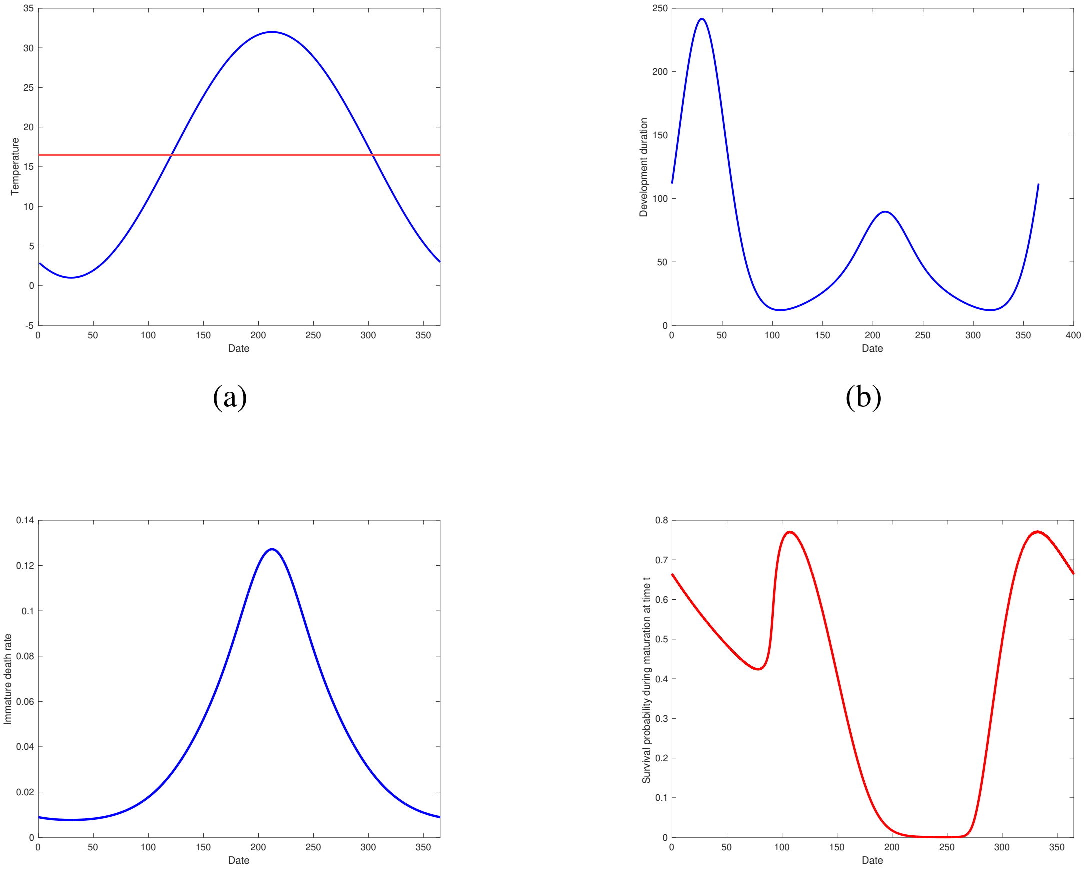

(a) (b)

(c) (d)

Figure 6.1: Temperature data and seasonal parameters: development duration $\widetilde{\tau}(t)$ at temperature on day t, immature death rate $\mu_J(t)$, and survival probability $\exp\left(-\int_{t-\tau(t)}^{t}\mu_J(s)ds\right)$.

A comparison between Figures 6.1(a) and (b) reveals a highly nonlinear relationship between the developmental duration $\widetilde{\tau}(t)$ and the temperature on a given day, exhibiting neither positive nor negative correlation. The annual temperature profile exhibits a single peak (around day 220), whereas the developmental duration $\widetilde{\tau}(t)$ displays approximately two minima (around days 100 and 320) under moderate temperatures, neither excessively high nor low. These results align with previous studies by [139] and [122], which demonstrated that excessively high or low temperatures prolong developmental duration. Analogous patterns are observed for the immature mortality rate in Figure 6.1(c) and the survival probability from the immature to adult stage in Figure 6.1(d). All three temperature-dependent parameters exhibit distinct patterns from the temperature variation itself, underscoring the necessity for precise characterization of the metabolic relationships between biological parameters and temperature conditions.

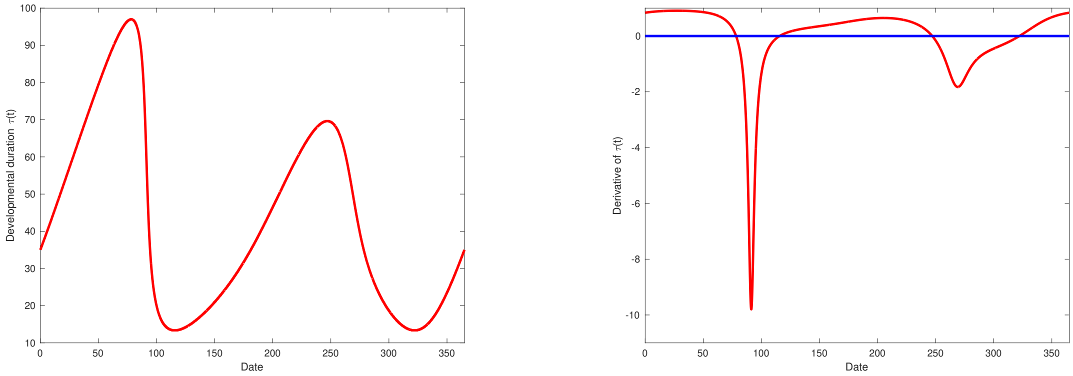

(a) (b)

Figure 6.2: The time-dependent developmental delay $\tau(t)$ and its derivative.

As illustrated in Figure 6.2(a), the developmental delay $\tau(t)$ exhibits two minima and two local maxima, which can also be inferred from the four points where its derivative vanishes in Figure 6.2(b). Moderate temperatures preceding the dates of these minima tend to yield smaller developmental delays $\tau(t)$. Furthermore, a discernible phase shift is observed between the extrema of Figures 6.1(b) and 6.2(a), as the latter evaluates the cumulative environmental conditions (as per equation (6.20)) relevant for estimating the developmental delay of adults maturing on day t. Figure 6.2(b) depicts the derivative of $\tau(t)$ with respect to time t (with a maximum value of 0.92), numerically validating the inequality $1-\tau^{'}(t) > 0$, as discussed in the preceding section. Additionally, it can be observed that frogs maturing between days 210 and 265 encounter adverse conditions, as evidenced by the extremely low survival likelihood exhibited in Figure 6.1(d). This can be attributed to the combined effect of a relatively prolonged developmental delay (Figure 6.2(a)) and an elevated mortality rate during this period (Figure 6.1(c)). An examination of Figure 6.1(b) suggests that the maximum developmental duration $\widetilde{\tau}(t)$ under the temperature of a specific date occurs around day 240, attributable to the extreme (excessively low) temperature conditions on approximately the 30th day. However, the actual developmental delay $\tau(t)$ depicted in Figure 6.2(a) exhibits a maximum value below 100 days, owing to the cumulative effect of moderate ambient temperatures preceding the date of the most adverse conditions. Furthermore, an obvious temporal difference is evident between the peak occurrences in Figures 6.1(b) and 6.2(a).

6.5.3 Model simulations

Using the parameters from the previous subsections, we can conduct simulations for the solutions illustrated in Figure 6.3. These simulations consider two different scenarios for adult mortality rates: $\mu_A = 0.015$ per day, $d_A = 0.01$ per day; and $\mu_A = 0.1$ per day, $d_A = 0.05$ per day. The initial populations for females and males are set at 100 and 200 individuals, respectively. The results indicate that the population dynamics of female and male frogs eventually stabilize into seasonal patterns, oscillating periodically between maximum and minimum values. During the normal growth period, the frog population experiences a dramatic increase, quickly reaching a peak and maintaining a relatively stable state of development, followed by a sharp decline as the hibernation period begins. When examining the annual population patterns in Figures 6.3(b) and 6.3(d), subtle differences between the two mortality rate scenarios become apparent. Higher mortality rates result in fewer individuals entering the hibernation period after the normal growth period, leading to a relatively sharper decline during hibernation. Post-hibernation, the surviving individuals resume development, mate, and reproduce.

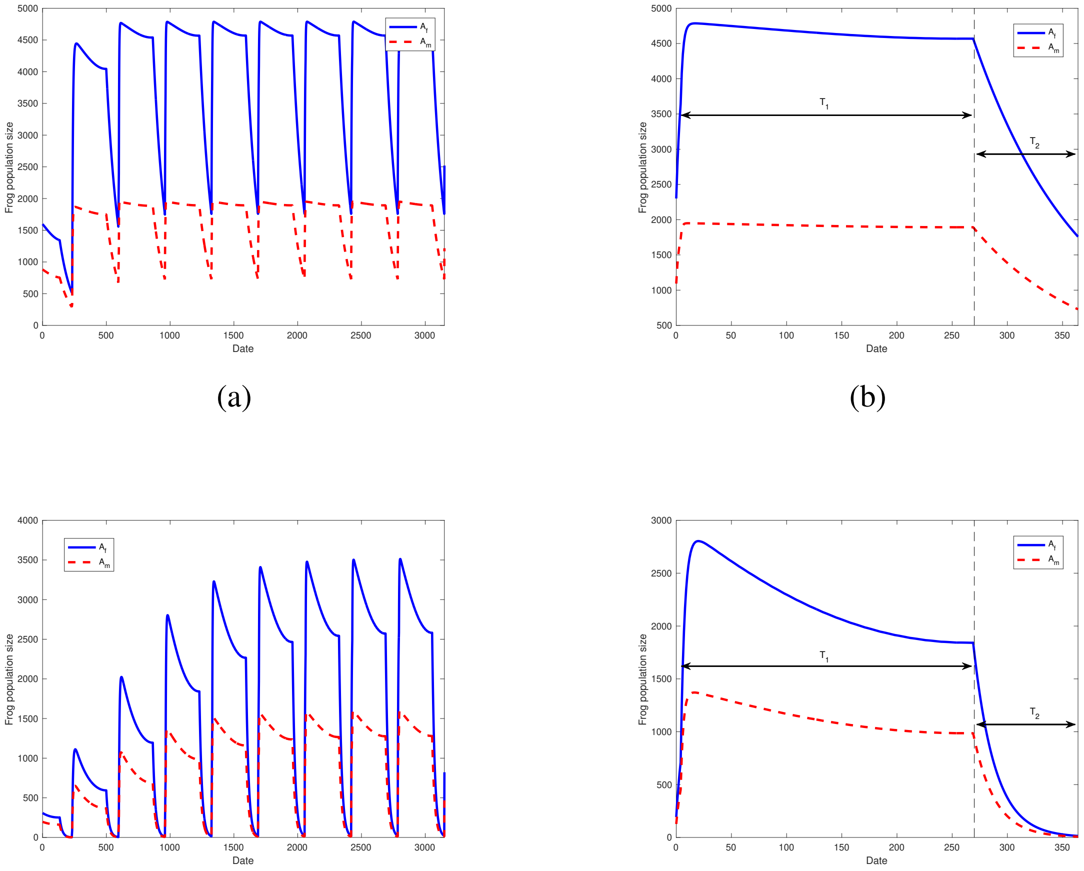

(a) (b)

(c) (d)

Figure 6.3: Solution simulations for multiple periods and one single period under two distinct mature mortality rate scenarios: (a) and (b) with $\mu_A = 0.015$ per day, $d_A = 0.01$ per day; (c) and (d) with $\mu_A = 0.1$ per day, $d_A = 0.05$ per day.

The ability of frogs to survive under adverse environmental conditions is considered a crucial factor in preserving population size and ensuring subsequent normal development [22]. The sensitivity analysis primarily examines the effects of mortality rates during the normal development and diapause periods, which are closely related to the total population size. The maximum population abundance, a key metric characterizing frog population dynamics, is primarily employed to evaluate the effects of mortality rates on population growth. Figures 6.4(a) and 6.4(b) illustrate the consequences of varying the mortality rates

μ_A and d_A during the normal development and hibernation periods, respectively. The surface and contour plots in Figure 6.4 clearly demonstrate that enhancing the survivability of adult frogs may foster subsequent population growth during the normal phase, manifested as larger total population abundances at lower mortality rates. For both female and male individuals, the total population exhibits an apparent decreasing trend as the normal development and hibernation mortality rates increase, respectively. Consequently, these findings underscore that reducing mortality rates during the normal developmental and hibernation periods constitutes an effective strategy to mitigate the decline of frog populations.

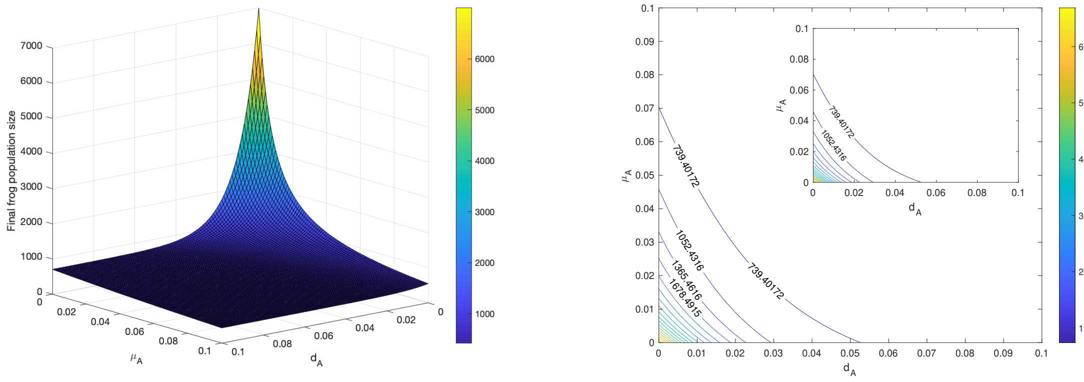

(a) (b)

Figure 6.4: The surfaces and contour plots depicting the variations of total frog population size with varying mature mortality rates.

The mating modes of frog populations are among the most critical aspects in the growth and development of male and female frogs. Consequently, we simulate the population dynamics under varying mating parameters $h = 1, 3, 5$, which implies that a male's maximum number of establishable pair bonds are 1, 3, and 5, respectively, over multiple periods (Figure 6.5(a)) and a single period (Figure 6.5(b)). Over multiple periods, the simulations demonstrate that the female and male frog populations exhibit regular seasonal periodicity, characterized by sharp declines followed by gradual recoveries. Higher mating parameters ($h = 3, 5$) result in more pronounced oscillations, suggesting increased population variability compared to $h = 1$, which indicates that mating parameters influence the stability of frog populations to a certain degree, particularly during normal growth periods. This effect is more clearly observed in the single cycle simulation, where higher mating parameters lead to a higher stabilized population size during the normal period before the decline associated with hibernation. Consequently, while higher mating parameters contribute to greater population fluctuations and higher initial stabilization during the normal development period, the populations ultimately experience significant declines as they approach hibernation. Nonetheless, the overall trends in frog population sizes remain consistent.

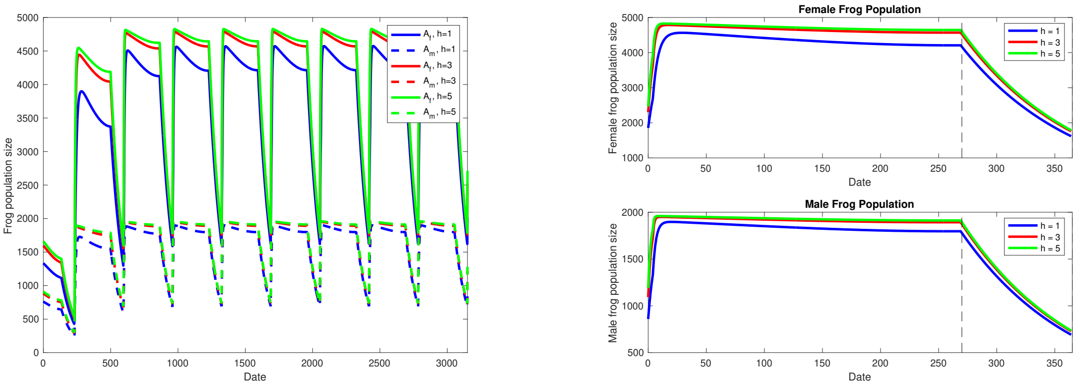

(a) (b)

Figure 6.5: Solution simulations for multiple periods and one single period under different mating parameters: $h = 1, 3, 5$.

6.6 Discussion

Various mating behaviors, seasonal patterns, and mortality rates are all believed to play significant roles in preserving frog population size and maintaining population growth. The effects of these survival mechanisms on the persistence of frog species require further study. In this paper, we aimed to explore these factors by constructing comprehensive mathematical models, in which the hibernation period is treated as an independent dynamic process. During hibernation, the population growth, mating behaviors, and mortality rates differ significantly from those in the normal developmental periods. Accordingly, the annual growth period is divided into two distinct intervals, each governed by its own set of equations. To explicitly describe population growth across different developmental stages, we constructed two sets of equations to model the female and male populations during the normal developmental period and the hibernation period, respectively. The comprehensive model incorporates sex division, polygynous behavior, and seasonal patterns. The qualitative dynamics of the frog population were investigated using the decoupled adult system. We examined the existence and uniqueness of solutions, the monotonicity, and strictly subhomogeneous nature of the periodic semiflow on the natural phase space. To further analyze strong monotonicity, we introduced a quotient space to derive properties of the population system. Additionally, we explored the threshold dynamics and global stability by applying the theory of monotone dynamical systems. However, it is worth noting that it would be interesting to use a biologically meaningful index in a nonlinearizable population system with periodic delays, namely the net reproduction number $\mathcal{R}_0$ as the threshold index. This approach could be theoretically introduced using the ideas presented in Bai et al. [28], Wang et al. [190], and Zhao [206]. Further sensitivity analysis on $\mathcal{R}_0$ could provide valuable insights into the development and survival of the frog population. This direction remains a subject for further study.

Chapter 7

Summary and future work

In this chapter, we first briefly summarize the main results in this thesis, and then present some possible future research works.

7.1 Research summary

While various continuous age-structured models with time-delay have been proposed to investigate the population dynamics of single species, few models consider other factors regulating population growth, such as seasonal succession, time-varying periodic delays, environmental pathogens, and mating behaviors in frog population dynamics. Specifically, time-varying developmental durations or chronological age thresholds are rarely incorporated into models analyzing age-structured frog population growth, as the induced time-dependent delays and other biological and abiotic factors pose significant challenges to model derivation and theoretical analysis. In this thesis, we analyzed stage-structured frog population growth subject to the aforementioned factors through four distinct projects.

To elucidate the stage-structured modeling approach for single population growth, Chapter 3 reviewed continuous stage-structured models that involve stage duration distributions and intraspecific competition. We presented two fundamental modeling approaches utilizing integral equations and partial differential equations, which can be reduced to ordinary and delay differential equations based on gamma and Dirac distributions. The integral equations offer the advantage of explicitly deriving the net reproduction number and initial growth rate, and better conveying the biological implications of stage progression. However, integrating density-dependent regulations on stage distribution and survival probabilities within an integral equation framework proves challenging, a difficulty that structured partial differential equation models can potentially overcome. We then demonstrated population models based on Dirac distributions for immature stage duration and intraspecific competition under various assumptions.

Chapter 4 integrated temperature-dependent developmental durations, breeding, and hibernation seasons into an age-structured model with delay differential equations. By decoupling the adult equation from the total system, we derive the basic properties of solutions within the natural phase space, including uniqueness, boundedness, monotonicity, and strict subhomogeneity of the periodic semiflow. To investigate the strong monotonicity of the solution semiflow, we introduce the quotient space and obtain relevant results. Subsequently, we introduce the basic reproduction number $\mathcal{R}_0$ as a threshold quantity and demonstrate the continuity and periodicity of the operator L. Using theories of monotone dynamical systems, periodic semiflows, and related results, we established the global dynamics: the zero solution is globally asymptotically stable in the adult population system if $\mathcal{R}_0 < 1$, whereas a unique positive 1-periodic solution $A^*(t)$ exists which is globally asymptotically stable.

Given that numerous amphibian populations have experienced catastrophic declines due to the emergence of pathogens, particularly *Bd* pathogens, Chapter 5 constructed a deterministic frog-pathogen model and its stochastic counterpart. This model includes direct transmission between susceptible and infected hosts as well as indirect transmission through environmental pathogens, which can reproduce independently or be released by infectious frogs, potentially leading to additional disease-induced mortality or reduced fertility in infected hosts. For the deterministic model, we presented the well-posedness and dynamics using three threshold parameters: $\mathcal{R}_H$, $\mathcal{R}_B$ and $\mathcal{R}_0$. We demonstrated that the disease-free equilibrium is globally asymptotically stable under $\mathcal{R}_B < 1$ and $\mathcal{R}_0 < 1$; the host-free equilibrium is locally asymptotically stable if $\mathcal{R}_H < 1$ or $d_N < b_N < \frac{(d_N+\kappa B_0)(d_N+\mu)}{\eta\kappa B_0+d_N+\mu}$. Additionally, for the entire host-pathogen system, a unique positive equilibrium exists under two conditions: (i) $\mathcal{R}_H > 1, \mathcal{R}_B < 1$ and $\mathcal{R}_0 > 1$; or (ii) $\mathcal{R}_B > 1$ and $b_N > \frac{(d_N+\kappa B_0)(d_N+\mu)}{\eta\kappa B_0+d_N+\mu}$. Furthermore, under these conditions, the pathogen and host population uniformly persist. Importantly, we identified two scenarios where the host population cannot go extinct: one where pathogens cannot reproduce, and the other where pathogens have no impact on the host population. To explore the probabilities of disease and host population extinction, we formulated a stochastic continuous-time Markov chain model, demonstrating the probabilities $\mathbb{P}_0$ and $\mathbb{P}_0^H$ through multiple branching process theory. We also derived the mean and variance of disease extinction time and host extinction time, respectively. The final numerical simulations illustrated host persistence, host extinction, extinction probability, and extinction time distribution of infection, demonstrating that higher initial counts of infected individuals and environmental pathogens significantly extend infection durations due to increased transmission opportunities.

Building on the succession model discussed in Chapter 4, we incorporated mating behaviors of female and male frogs to propose a two-sex succession model. This model describes breeding, mating, competition, and hibernation, effectively decoupling the equations for female and male adults to focus on analyzing the two populations during normal growth and hibernation periods. Similar to the previous chapter, we conducted a qualitative analysis to determine the uniqueness and boundedness of solutions, as well as the monotonicity and strict subhomogeneity of the periodic semiflow in the natural phase space. We then introduced the quotient space to examine the strong monotonicity of the solution semiflow. Subsequently, the net reproduction number $\mathcal{R}_0$ was derived using the cone spectral radius of a monotone and homogeneous operator. The global dynamics were established by introducing an auxiliary system, determining the continuity and periodicity of the evolution operator, and applying the theory of monotone dynamical systems and the comparison principle. It was shown that a unique positive periodic solution exists for the female-male population system, which is globally asymptotically stable if $\mathcal{R}_0 > 1$. Numerically, we presented temperature data and time-dependent parameters to illustrate the trend of developmental delays. Based on these parameters, we analyzed the frog population size over multiple periods and a single period under two different mature mortality rates. The results indicated that higher mortality rates result in fewer individuals entering the hibernation period after normal growth, leading to a steeper decline during hibernation. Additionally, the total population exhibited a noticeable decreasing trend as the normal development and hibernation mortality rates increased, respectively. Regarding mating behaviors, we found that higher mating parameters lead to more pronounced oscillations, suggesting increased population variability. This indicates that mating parameters significantly influence the stability of frog populations, particularly during normal growth periods, although the populations ultimately experience substantial declines as they approach hibernation.

In summary, we have developed a framework to study the population dynamics of frog species that incorporates seasonal factors and disease transmission. This framework extensively utilizes the modeling approach of continuous stage-structured models and demonstrates global stability through various theories related to monotone periodic systems. The theoretical and numerical results can serve as a reference for dynamic analyses of other species populations.

7.2 Future work

Inevitably, and perhaps encouragingly, several issues remain worthy of further study, both in terms of model analysis and construction. In this section, we delineate some of these possible directions.

7.2.1 Spatial diffusion of succession model

Spatial heterogeneity is central to many leading ecological concepts including habitat fragmentation, foraging, biodiversity, and the development of ecological niches [48]. Spatial heterogeneity arises universally due to variations in temperature, humidity, and resource availability across different regions; for instance, the sex ratio and age composition of certain species are influenced by spatial factors [32, 137]. Moreover, Buonomo et al. [42] and Kang et al. [106] found that the random drift of populations and external toxicants, as well as the effect of random drift within living populations on internal toxicants, led to some degree of spatial diffusion of both populations and toxicants. Furthermore, patches within the reaction-diffusion model are characterized by individuals' average movement rates and the local intrinsic growth rate of the population, which are assumed to correlate with environmental conditions, resource availability, and organism behavior within the patch [48]. Therefore, heterogeneous parameters and a reaction-diffusion mechanism should be considered in the seasonal succession model discussed in Chapter 4, to explore the effects of spatial movement on frog populations across different ecological environments. Additionally, pathogen transmission should be considered to study the influence of spatial heterogeneity on disease transmission and population extinction within frog populations.

7.2.2 Modeling analysis of other species

As previously mentioned, the framework can also be applied to analyze the population dynamics of other species, such as ticks, ladybirds, and others. Take the tick population as an example: ticks play a critical role as vectors in the transmission and spread of Lyme disease, an emerging infectious disease that can cause severe illness in humans and animals. Diapause occurs after ticks are exposed to an induction stimulus, typically at a specific time of year. We could formulate a continuous stage-structured model to describe condition-dependent developmental diapause and normal growth and explore the global dynamics. This approach may enhance control management strategies for tick populations in targeted areas and reduce the associated disease transmission risks.

References

[1] Azmy S Ackleh, Jacoby Carter, Vinodh K Chellamuthu, and Baoling Ma. A model for the interaction of frog population dynamics with batrachochytrium dendrobatidis, janthinobacterium lividum and temperature and its implication for chytridiomycosis management. *Ecological Modelling*, 320:158–169, 2016.

[2] Azmy S Ackleh, Jacoby Carter, Keng Deng, Qihua Huang, Nabendu Pal, and Xing Yang. Fitting a structured juvenile–adult model for green tree frogs to population estimates from capture–mark–recapture field data. *Bulletin of Mathematical Biology*, 74:641–665, 2012.

[3] Azmy S Ackleh and Keng Deng. A nonautonomous juvenile-adult model: well-posedness and long-time behavior via a comparison principle. *SIAM Journal on Applied Mathematics*, 69(6):1644–1661, 2009.

[4] Azmy S Ackleh, Keng Deng, and Qihua Huang. Existence-uniqueness results and difference approximations for an amphibian juvenile-adult model. *Contemporary Mathematics*, 513:1–23, 2010.

[5] Azmy S Ackleh, Keng Deng, and Qihua Huang. Difference approximation for an amphibian juvenile-adult dispersal mode. In *Conference Publications*, volume 2011, pages 1–12. Conference Publications, 2011.

[6] Azmy S Ackleh, Keng Deng, and Qihua Huang. Stochastic juvenile–adult models with application to a green tree frog population. *Journal of Biological Dynamics*, 5(1):64–83, 2011.

[7] Azmy S Ackleh, Keng Deng, and Xing Yang. Sensitivity analysis for a structured juvenile–adult model. *Computers & Mathematics with Applications*, 64(3):190–200, 2012.

[8] Azmy S Ackleh, Youssef M Dib, and Sophia R-J Jang. A three-stage discrete-time population model: continuous versus seasonal reproduction. *Journal of Biological Dynamics*, 1(4):291–304, 2007.

[9] Azmy S Ackleh and Sophia R-J Jang. A discrete two-stage population model: continuous versus seasonal reproduction. *Journal of Difference Equations and Applications*, 13(4):261–274, 2007.

[10] Bedr'Eddine Aïnseba, Chahrazed Benosman, and Pierre Magal. A model for ovine brucellosis incorporating direct and indirect transmission. *Journal of Biological Dynamics*, 4(1):2–11, 2010.

[11] Nofe Al-Asuoad, Roumen Anguelov, Keith Berven, and Meir Shillor. Model and simulations of a wood frog population. *Biomath*, 1(1):ID–1209032, 2012.

[12] Jafar Fawzi Al-Omari and Stephen A Gourley. Monotone travelling fronts in an age-structured reaction-diffusion model of a single species. *Journal of Mathematical Biology*, 45(4):294–312, 2002.

[13] Jafar Fawzi Al-Omari and Stephen A Gourley. A nonlocal reaction-diffusion model for a single species with stage structure and distributed maturation delay. *European Journal of Applied Mathematics*, 16(1):37–51, 2005.

[14] Linda JS Allen. *An Introduction to Stochastic Processes with Applications to Biology*. CRC press, 2010.

[15] Linda JS Allen. Stochastic population and epidemic models. *Mathematical Biosciences Lecture Series, Stochastics in Biological Systems*, 1:120–128, 2015.

[16] Linda JS Allen and Pauline van den Driessche. Relations between deterministic and stochastic thresholds for disease extinction in continuous-and discrete-time infectious disease models. *Mathematical Biosciences*, 243(1):99–108, 2013.

[17] Linda JS Allen and Xueying Wang. Stochastic models of infectious diseases in a periodic environment with application to cholera epidemics. *Journal of Mathematical Biology*, 82(6):48, 2021.

[18] Roy M Anderson and Robert M May. *Infectious Diseases of Humans: Dynamics and Control*. Oxford university press, 1991.

[19] Gui Araujo and Rafael Rios Moura. Beyond classical theories: An integrative mathematical model of mating dynamics and parental care. *Journal of Evolutionary Biology*, 36(10):1411–1427, 2023.

[20] Roger Arditi, Claude Lobry, and Tewfik Sari. Asymmetric dispersal in the multipatch logistic equation. *Theoretical Population Biology*, 120:11–15, 2018.

[21] Julien Arino, Lin Wang, and Gail SK Wolkowicz. An alternative formulation for a delayed logistic equation. *Journal of Theoretical Biology*, 241(1):109–119, 2006.

[22] Juliana M Arrighi, Ezra S Lencer, Advait Jukar, Daesik Park, Patrick C Phillips, and Robert H Kaplan. Daily temperature fluctuations unpredictably influence developmental rate and morphology at a critical early larval stage in a frog. *BMC Ecology*, 13:1–11, 2013.

[23] José Ignacio Arroyo, Beatriz Díez, Christopher P Kempes, Geoffrey B West, and Pablo A Marquet. A general theory for temperature dependence in biology. *Proceedings of the National Academy of Sciences*, 119(30):e2119872119, 2022.

[24] Krishna B Athreya, Peter E Ney, and PE Ney. *Branching Processes*. Courier Corporation, 2004.

[25] Nicolas Bacaër and El Hadi Ait Dads. Genealogy with seasonality, the basic reproduction number, and the influenza pandemic. *Journal of Mathematical Biology*, 62:741–762, 2011.

[26] Nicolas Bacaër and El Hadi Ait Dads. On the biological interpretation of a definition for the parameter r 0 in periodic population models. *Journal of Mathematical Biology*, 65:601–621, 2012.

[27] Nicolas Bacaër and Souad Guernaoui. The epidemic threshold of vector-borne diseases with seasonality: the case of cutaneous leishmaniasis in chichaoua, morocco. *Journal of Mathematical Biology*, 53(3):421–436, 2006.

[28] Zhenguo Bai, Rui Peng, and Xiao-Qiang Zhao. A reaction–diffusion malaria model with seasonality and incubation period. *Journal of Mathematical Biology*, 77:201–228, 2018.

[29] Gabriel M Barrile, Anna D Chalfoun, and Annika W Walters. Livestock grazing, climatic variation, and breeding phenology jointly shape disease dynamics and survival in a wild amphibian. *Biological Conservation*, 261:109247, 2021.

[30] Paul E Bartelt, Peter E Thornton, and Robert W Klaver. Modelling physiological costs to assess impacts of climate change on amphibians in yellowstone national park, usa. *Ecological Indicators*, 135:108575, 2022.

[31] Maurice S Bartlett. Monte carlo studies in ecology and epidemiology. In *Proceedings of the Fourth Berkeley Symposium on Mathematical Statistics and Probability*, volume 4, pages 39–55. University of California Press London, UK, 1961.

[32] Ian P Bell, Justin Meager, Jason P van de Merwe, and Christine A Madden Hof. Green turtle (chelonia mydas) population demographics at three chemically distinct

foraging areas in the northern great barrier reef. *Science of the Total Environment*, 652:1040–1050, 2019.

[33] Carmen Bessa-Gomes, Stéphane Legendre, and Jean Clobert. Discrete two-sex models of population dynamics: on modelling the mating function. *Acta Oecologica*, 36(5):439–445, 2010.

[34] Katharine Best and Alan S Perelson. Mathematical modeling of within-host zika virus dynamics. *Immunological Reviews*, 285(1):81–96, 2018.

[35] Michael Boots and Akira Sasaki. Parasite evolution and extinctions. *Ecology Letters*, 6(3):176–182, 2003.

[36] Fred Brauer, Carlos Castillo-Chavez, Zhilan Feng, et al. *Mathematical Models in Epidemiology*, volume 32. Springer, 2019.

[37] Cheryl J Briggs, Roland A Knapp, and Vance T Vredenburg. Enzootic and epizootic dynamics of the chytrid fungal pathogen of amphibians. *Proceedings of the National Academy of Sciences*, 107(21):9695–9700, 2010.

[38] Cheryl J Briggs, Vance T Vredenburg, Roland A Knapp, and Lara J Rachowicz. Investigating the population-level effects of chytridiomycosis: an emerging infectious disease of amphibians. *Ecology*, 86(12):3149–3159, 2005.

[39] Kenneth J Brown and Yanping Zhang. On a system of reaction–diffusion equations describing a population with two age groups. *Journal of Mathematical Analysis and Applications*, 282(2):444–452, 2003.

[40] Robert Kenneth Browne and DL Edwards. The effect of temperature on the growth and development of the endangered green and golden bell frog (litoria aurea). *Journal of Thermal Biology*, 28(4):295–299, 2003.

[41] Hermann Brunner, Stephen A Gourley, Rongsong Liu, and Yanyu Xiao. Pauses of larval development and their consequences for stage-structured populations. *SIAM Journal on Applied Mathematics*, 77(3):977–994, 2017.

[42] Bruno Buonomo, Andrea Di Liddo, and Ivonne Sgura. A diffusive-convective model for the dynamics of population-toxicant interactions: some analytical and numerical results. *Mathematical Biosciences*, 157(1-2):37–64, 1999.

[43] Robert Stephen Cantrell, Chris Cosner, and Salomé Martínez. Persistence for a two-stage reaction-diffusion system. *Mathematics*, 8(3):396, 2020.

[44] Karoline Ceron, Diego J Santana, Elaine M Lucas, Jairo José Zocche, and Diogo B Provete. Climatic variables influence the temporal dynamics of an anuran metacommunity in a nonstationary way. *Ecology and Evolution*, 10(11):4630–4639, 2020.

[45] David Champredon, Jonathan Dushoff, and David JD Earn. Equivalence of the erlang-distributed seir epidemic model and the renewal equation. *SIAM Journal on Applied Mathematics*, 78(6):3258–3278, 2018.

[46] Dennis L Chao, Miles P Davenport, Stephanie Forrest, and Alan S Perelson. Stochastic stage-structured modeling of the adaptive immune system. In *Computational Systems Bioinformatics. CSB2003. Proceedings of the 2003 IEEE Bioinformatics Conference. CSB2003*, pages 124–131. IEEE, 2003.

[47] Yuanji Cheng, Jin Wang, and Xiuxiang Yang. On the global stability of a generalized cholera epidemiological model. *Journal of Biological Dynamics*, 6(2):1088–1104, 2012.

[48] Ryan St Clair, Andrew Nevai, and Richard Schugart. A reaction-diffusion model for population dynamics in patchy landscapes. *Journal of Differential Equations*, 405:247–286, 2024.

[49] Cláudia Torres Codeço. Endemic and epidemic dynamics of cholera: the role of the aquatic reservoir. *BMC Infectious Diseases*, 1:1–14, 2001.

[50] James P Collins. Amphibian decline and extinction: what we know and what we need to learn. *Diseases of Aquatic Organisms*, 92(2-3):93–99, 2010.

[51] Kenneth L Cooke. Functional-differential equations: some models and perturbation problems, 1967.

[52] Franck Courchamp, Ludek Berec, and Joanna Gascoigne. *Allee Effects in Ecology and Conservation*. OUP Oxford, 2008.

[53] Brian A Crawford, John C Maerz, Vanessa CK Terrell, and Clinton T Moore. Population viability analysis for a pond-breeding amphibian under future drought scenarios in the southeastern united states. *Global Ecology and Conservation*, 36:e02119, 2022.

[54] Jim Michael Cushing. *An Introduction to Structured Population Dynamics*. SIAM, 1998.

[55] Francisco De Castro and Benjamin Bolker. Mechanisms of disease-induced extinction. *Ecology Letters*, 8(1):117–126, 2005.

[56] Fábio P de Sá, Rafael C Consolmagno, Pavitra Muralidhar, Cinthia A Brasileiro, Kelly R Zamudio, and Célio FB Haddad. Unexpected reproductive fidelity in a polygynous frog. *Science Advances*, 6(33):eaay1539, 2020.

[57] Perry de Valpine, Katherine Scranton, Jonas Knape, Karthik Ram, and Nicholas J Mills. The importance of individual developmental variation in stage-structured population models. *Ecology Letters*, 17(8):1026–1038, 2014.

[58] Donald L DeAngelis, Wei-Ming Ni, and Bo Zhang. Effects of diffusion on total biomass in heterogeneous continuous and discrete-patch systems. *Theoretical Ecology*, 9:443–453, 2016.

[59] Odo Diekmann, Mats Gyllenberg, Haiyang Huang, Markus Kirkilionis, JAJ Metz, and Horst R Thieme. On the formulation and analysis of general deterministic struc-

tured population models ii. nonlinear theory: Ii. nonlinear theory. *Journal of Mathematical Biology*, 43:157–189, 2001.

[60] Odo Diekmann, Mats Gyllenberg, and Johan AJ Metz. On models of physiologically structured populations and their reduction to ordinary differential equations. *Journal of Mathematical Biology*, 80:189–204, 2020.

[61] Odo Diekmann and Johan Andre Peter Heesterbeek. *Mathematical Epidemiology of Infectious Diseases: Model Building, Analysis and Interpretation*, volume 5. John Wiley & Sons, 2000.

[62] Odo Diekmann, Johan Andre Peter Heesterbeek, and Johan Anton Jacob Metz. On the definition and the computation of the basic reproduction ratio $\mathcal{R}_0$ in models for infectious diseases in heterogeneous populations. *Journal of Mathematical Biology*, 28:365–382, 1990.

[63] Benjamin J Doddington, Jaime Bosch, Joan A Oliver, Nicholas C Grassly, Gerardo Garcia, Benedikt R Schmidt, Trenton WJ Garner, and Matthew C Fisher. Context-dependent amphibian host population response to an invading pathogen. *Ecology*, 94(8):1795–1804, 2013.

[64] Karin S Dorman, Janet S Sinsheimer, and Kenneth Lange. In the garden of branching processes. *SIAM Review*, 46(2):202–229, 2004.

[65] Brian Drawert, Marc Griesemer, Linda R Petzold, and Cheryl J Briggs. Using stochastic epidemiological models to evaluate conservation strategies for endangered amphibians. *Journal of the Royal Society Interface*, 14(133):20170480, 2017.

[66] Jennifer A Dunne, Richard J Williams, and Neo D Martinez. Network structure and biodiversity loss in food webs: robustness increases with connectance. *Ecology Letters*, 5(4):558–567, 2002.

[67] Sharon B Emerson and Sunny K Boyd. Mating vocalizations of female frogs: control and evolutionary mechanisms. *Brain Behavior and Evolution*, 53(4):187–197, 1999.

[68] Keith E Emmert and Linda JS Allen. Population persistence and extinction in a discrete-time, stage-structured epidemic model. *Journal of Difference Equations and Applications*, 10(13-15):1177–1199, 2004.

[69] Keith E Emmert and Linda JS Allen. Population extinction in deterministicand stochastic discrete-time epidemic models with periodic coefficients with applications to amphibian populations. *Natural Resource Modeling*, 19(2):117–164, 2006.

[70] Steinar Engen, Russell Lande, and Bernt-Erik Sæther. Demographic stochasticity and allee effects in populations with two sexes. *Ecology*, 84(9):2378–2386, 2003.

[71] David Andrew Ewing, Christina A Cobbold, BV Purse, MA Nunn, and Steven M White. Modelling the effect of temperature on the seasonal population dynamics of temperate mosquitoes. *Journal of Theoretical Biology*, 400:65–79, 2016.

[72] Guihong Fan, Junli Liu, P Van den Driessche, Jianhong Wu, and Huaiping Zhu. The impact of maturation delay of mosquitoes on the transmission of West Nile virus. *Mathematical Biosciences*, 228(2):119–126, 2010.

[73] Guihong Fan, Yijun Lou, Horst R Thieme, and Jianhong Wu. Stability and persistence in ode modelsfor populations with many stages. *Mathematical Biosciences & Engineering*, 12(4):661–686, 2015.

[74] Jian Fang, Stephen A Gourley, and Yijun Lou. Stage-structured models of intra- and inter-specific competition within age classes. *Journal of Differential Equations*, 260(2):1918–1953, 2016.

[75] Jian Fang, Yijun Lou, and Jianhong Wu. Can pathogen spread keep pace with its host invasion? *SIAM Journal on Applied Mathematics*, 76(4):1633–1657, 2016.

[76] Alex P Farrell, James P Collins, Amy L Greer, and Horst R Thieme. Times from infection to disease-induced death and their influence on final population sizes after epidemic outbreaks. *Bulletin of Mathematical Biology*, 80:1937–1961, 2018.

[77] Xavier Fauvergue. A review of mate-finding a llee effects in insects: from individual behavior to population management. *Entomologia Experimentalis et Applicata*, 146(1):79–92, 2013.

[78] Anyin Feng, Uri Obolski, Lewi Stone, and Daihai He. Modelling covid-19 vaccine breakthrough infections in highly vaccinated israel—the effects of waning immunity and third vaccination dose. *PLoS Global Public Health*, 2(11):e0001211, 2022.

[79] Zhilan Feng. *Applications of Epidemiological Models to Public Health Policymaking: The Role of Heterogeneity in Model Predictions*. World Scientific, 2014.

[80] Zhilan Feng and Horst R Thieme. Endemic models with arbitrarily distributed periods of infection I: fundamental properties of the model. *SIAM Journal on Applied Mathematics*, 61(3):803–833, 2000.

[81] Anna M Gamża, Thomas J Hagenaars, Miriam GJ Koene, and Mart CM De Jong. Combining a parsimonious mathematical model with infection data from tailor-made experiments to understand environmental transmission. *Scientific Reports*, 13(1):12986, 2023.

[82] Shujing Gao, Lansun Chen, and Lihua Sun. Dynamic complexities in a seasonal prevention epidemic model with birth pulses. *Chaos, Solitons & Fractals*, 26(4):1171–1181, 2005.

[83] Braulio Ayala García, Alma L Fuentes Farías, and Gabriel Gutiérrez Ospina. Phenotypic variation in american bullfrogs (lithobates catesbeianus) bred under intensive systems in mexico: A preliminary report. *Veterinaria México*, 7(1):1–15, 2020.

[84] Yunfeng Geng and Frithjof Lutscher. Competitive coexistence of seasonal breeders. *Journal of Mathematical Biology*, 83:1–35, 2021.

[85] Mini Ghosh, Peeyush Chandra, Prawal Sinha, and JB Shukla. Modelling the spread of carrier-dependent infectious diseases with environmental effect. *Applied Mathematics and Computation*, 152(2):385–402, 2004.

[86] Jeffrey A Goldstein, Karin von Seckendorr Hoff, and Stanley D Hillyard. The effect of temperature on development and behaviour of relict leopard frog tadpoles. *Conservation Physiology*, 5(1):cow075, 2017.

[87] Stephen A Gourley and Rongsong Liu. Delay equation models for populations that experience competition at immature life stages. *Journal of Differential Equations*, 259(5):1757–1777, 2015.

[88] Stephen A Gourley, Rongsong Liu, and Yijun Lou. Intra-specific competition and insect larval development: a model with time-dependent delay. *Proceedings of the Royal Society of Edinburgh Section A: Mathematics*, 147(2):353–369, 2017.

[89] Stephen A Gourley, Rongsong Liu, and Jianhong Wu. Spatiotemporal distributions of migratory birds: Patchy models with delay. *SIAM Journal on Applied Dynamical Systems*, 9(2):589–610, 2010.

[90] Stephen A Gourley and Jianhong Wu. Delayed non-local diffusive systems in biological invasion and disease spread. *Nonlinear Dynamics and Evolution Equations*, 48:137–200, 2006.

[91] Adam W Green, Mevin B Hooten, Evan H Campbell Grant, and Larissa L Bailey. Evaluating breeding and metamorph occupancy and vernal pool management effects for wood frogs using a hierarchical model. *Journal of Applied Ecology*, 50(5):1116–1123, 2013.

[92] Laura F Grogan, Lee F Skerratt, Lee Berger, Scott D Cashins, Robert D Trengove, and Joel PA Gummer. Chytridiomycosis causes catastrophic organism-wide metabolic dysregulation including profound failure of cellular energy pathways. *Scientific Reports*, 8(1):8188, 2018.

[93] Mats Gyllenberg. Mathematical aspects of physiologically structured populations: the contributions of J.A.J. Metz. *Journal of Biological Dynamics*, 1(1):3–44, 2007.

[94] Peter Hess and Edward Norma Dancer. Stability of fixed points for order-preserving discrete-time dynamical systems. *Journal für die reine und angewandte Mathematik*, 419:125–140, 1991.

[95] Morris W Hirsch and Hal Smith. Monotone dynamical systems. *Handbook of Differential Equations: Ordinary Differential Equations*, 2:239–357, 2006.

[96] Matthijs Hollanders, Laura F Grogan, Catherine J Nock, Hamish I McCallum, and David A Newell. Recovered frog populations coexist with endemic batrachochytrium dendrobatidis despite load-dependent mortality. *Ecological Applications*, 33(1):e2724, 2023.

[97] Frank Hoppensteadt and Paul Waltman. A problem in the theory of epidemics. *Mathematical Biosciences*, 9:71–91, 1970.

[98] Peter J Hudson, Annapaola Rizzoli, Bryan T Grenfell, Hans Heesterbeek, and Andy P Dobson. *The Ecology of Wildlife Diseases*, volume 501. Oxford University Press Oxford, 2002.

[99] Qazi A Hussain, Ashok K Pandit, et al. Global amphibian declines: a review. *International Journal of Biodiversity and Conservation*, 4(10):348–357, 2012.

[100] Mimmo Iannelli, Fabio Milner, et al. The basic approach to age-structured population dynamics. *Lecture Notes on Mathematical Modelling in the Life Sciences. Springer, Dordrecht*, 2017.

[101] Hisashi Inaba. *Age-Structured Population Dynamics in Demography and Epidemiology*, volume 1. Springer, 2017.

[102] Michael D Jennions, Patricia RY Bakwell, and Neville I Passmore. Breeding behaviour of the african frog, chiromantis xerampelina: multiple spawning and polyandry. *Animal Behaviour*, 44(6):1091–1100, 1992.

[103] Wang Jin, Scott W McCue, and Matthew J Simpson. Extended logistic growth model for heterogeneous populations. *Journal of Theoretical Biology*, 445:51–61, 2018.

[104] Wen Jin, Hal L Smith, and Horst R Thieme. Persistence versus extinction for a class of discrete-time structured population models. *Journal of Mathematical Biology*, 72:821–850, 2016.

[105] Marjorie T Jones, William R Milligan, Lee B Kats, Thomas L Vandergon, Rodney L Honeycutt, Robert N Fisher, Courtney L Davis, and Timothy A Lucas. A discrete stage-structured model of california newt population dynamics during a period of drought. *Journal of Theoretical Biology*, 414:245–253, 2017.

[106] Ting Kang, Yanyan Du, Ming Ye, and Qimin Zhang. Approximation of invariant measure for a stochastic population model with markov chain and diffusion in a polluted environment. *Mathematical Biosciences and Engineering*, 17(6):6702–6719, 2020.

[107] Caitlin Karniski. Polygyny with mate fidelity in the saxicolous frog. *Communications Biology*, 3(1):530, 2020.

[108] Yang Kuang and Stephen A Gourley. Wavefronts and global stability in a time-delayed population model with stage structure. *Proceedings of the Royal Society of London. Series A: Mathematical, Physical and Engineering Sciences*, 459(2034):1563–1579, 2003.

[109] Glenn E Lahodny and Linda JS Allen. Probability of a disease outbreak in stochastic multipatch epidemic models. *Bulletin of Mathematical Biology*, 75:1157–1180, 2013.

[110] Cristina Lanzas, Kale Davies, Samantha Erwin, and Daniel Dawson. On modelling environmentally transmitted pathogens. *Interface Focus*, 10(1):20190056, 2020.

[111] Stéphane Legendre. Age structure, mating system and population viability. *Evolutionary Conservation Biology*, pages 41–58, 2004.

[112] Jia Li and Fred Brauer. Continuous-time age-structured models in population dynamics and epidemiology. In *Mathematical Epidemiology*, pages 205–227. Springer, 2008.

[113] Ming-Tao Li, Zhen Jin, Gui-Quan Sun, and Juan Zhang. Modeling direct and indirect disease transmission using multi-group model. *Journal of Mathematical Analysis and Applications*, 446(2):1292–1309, 2017.

[114] Ming-tao Li, Xin Pei, Juan Zhang, and Li Li. Asymptotic analysis of endemic equilibrium to a brucellosis model. *Mathematical Biosciences and Engineering*, 16(5):5836–5850, 2019.

[115] Shu Liao and Jin Wang. Global stability analysis of epidemiological models based on volterra–lyapunov stable matrices. *Chaos, Solitons & Fractals*, 45(7):966–977, 2012.

[116] Chiu-Ju Lin, Lin Wang, and Gail SK Wolkowicz. An alternative formulation for a distributed delayed logistic equation. *Bulletin of Mathematical Biology*, 80:1713–1735, 2018.

[117] Jan Lindström and Hanna Kokko. Sexual reproduction and population dynamics: the role of polygyny and demographic sex differences. *Proceedings of the Royal Society of London. Series B: Biological Sciences*, 265(1395):483–488, 1998.

[118] Rongsong Liu, Gergely Roest, and Stephen A Gourley. Age-dependent intra-specific competition in pre-adult life stages and its effects on adult population dynamics. *European Journal of Applied Mathematics*, 27(1):131–156, 2016.

[119] Alfred J Lotka. Relation between birth rates and death rates. *Science*, 26(653):21–22, 1907.

[120] Yijun Lou, Kaihui Liu, Daihai He, Daozhou Gao, and Shigui Ruan. Modelling diapause in mosquito population growth. *Journal of Mathematical Biology*, 78(7):2259–2288, 2019.

[121] Yijun Lou and Bei Sun. Stage duration distributions and intraspecific competition: a review of continuous stage-structured models. *Mathematical Biosciences and Engineering*, 19(8):7543–7569, 2022.

[122] Yijun Lou and Xiao-Qiang Zhao. A theoretical approach to understanding population dynamics with seasonal developmental durations. *Journal of nonlinear science*, 27:573–603, 2017.

[123] Xinling Ma and Wendi Wang. A discrete model of avian influenza with seasonal reproduction and transmission. *Journal of Biological Dynamics*, 4(3):296–314, 2010.

[124] Calum MacNeil, Jaimie TA Dick, Melanie J Hatcher, Rebecca S Terry, Judith E Smith, and Alison M Dunn. Parasite-mediated predation between native and invasive amphipods. *Proceedings of the Royal Society of London. Series B: Biological Sciences*, 270(1521):1309–1314, 2003.

[125] Pierre Magal and Shigui Ruan. *Theory and Applications of Abstract Semilinear Cauchy Problems*. Springer, 2018.

[126] Pierre Magal and Xiao-Qiang Zhao. Global attractors and steady states for uniformly persistent dynamical systems. *SIAM Journal on Mathematical Analysis*, 37(1):251–275, 2005.

[127] Sunil Maity and Partha Sarathi Mandal. A comparison of deterministic and stochastic plant-vector-virus models based on probability of disease extinction and outbreak. *Bulletin of Mathematical Biology*, 84(3):41, 2022.

[128] Milliward Maliyoni. Probability of disease extinction or outbreak in a stochastic epidemic model for west nile virus dynamics in birds. *Acta Biotheoretica*, 69(2):91–116, 2021.

[129] Milliward Maliyoni, Faraimunashe Chirove, Holly D Gaff, and Keshlan S Govinder. A stochastic tick-borne disease model: exploring the probability of pathogen persistence. *Bulletin of Mathematical Biology*, 79:1999–2021, 2017.

[130] DK Mallawaarachchi, Linda JS Allen, and Cynthia Carey. Stability and permanence in gender-and stage-structured models for the boreal toad. *Journal of Biological Dynamics*, 5(1):1–26, 2011.

[131] John Mallet-Paret and Roger D Nussbaum. Generalizing the krein–rutman theorem, measures of noncompactness and the fixed point index. *Journal of Fixed Point Theory and Applications*, 7(1):103–143, 2010.

[132] Lorenzo Mari, Renato Casagrandi, Enrico Bertuzzo, Andrea Rinaldo, and Marino Gatto. Metapopulation persistence and species spread in river networks. *Ecology Letters*, 17(4):426–434, 2014.

[133] Rebecca M McCaffery, Lisa A Eby, Bryce A Maxell, and Paul Stephen Corn. Breeding site heterogeneity reduces variability in frog recruitment and population dynamics. *Biological Conservation*, 170:169–176, 2014.

[134] Rebecca M McCaffery and Bryce A Maxell. Decreased winter severity increases viability of a montane frog population. *Proceedings of the National Academy of Sciences*, 107(19):8644–8649, 2010.

[135] Rebecca M McCaffery, Antti Solonen, and Elizabeth Crone. Frog population viability under present and future climate conditions: a bayesian state-space approach. *Journal of Animal Ecology*, 81(5):978–985, 2012.

[136] Anderson Gray McKendrick. Applications of mathematics to medical problems. *Proceedings of the Edinburgh Mathematical Society*, 44:98–130, 1925.

[137] Joseph R Mendelson III, Karen R Lips, Ronald W Gagliardo, George B Rabb, James P Collins, James E Diffendorfer, Peter Daszak, Roberto Ibáñez D, Kevin C Zippel, Dwight P Lawson, et al. Confronting amphibian declines and extinctions. *Science*, 313(5783):48–48, 2006.

[138] Kate M Mitchell, Thomas S Churcher, Trenton WJ Garner, and Matthew C Fisher. Persistence of the emerging pathogen batrachochytrium dendrobatidis outside the

amphibian host greatly increases the probability of host extinction. *Proceedings of the Royal Society B: Biological Sciences*, 275(1632):329–334, 2008.

[139] Péter K Molnár, Susan J Kutz, Bryanne M Hoar, and Andrew P Dobson. Metabolic approaches to understanding climate change impacts on seasonal host-macroparasite dynamics. *Ecology Letters*, 16(1):9–21, 2013.

[140] E Muths, Blake R Hossack, EH Campbell Grant, DS Pilliod, and Brittany A Mosher. Effects of snowpack, temperature, and disease on demography in a wild population of amphibians. *Herpetologica*, 76(2):132–143, 2020.

[141] Kentaro Nagahara and Eiji Yanagida. Maximization of the total population in a reaction–diffusion model with logistic growth. *Calculus of Variations and Partial Differential Equations*, 57:1–14, 2018.

[142] Amanda C Niehaus, Michael J Angilletta Jr, Michael W Sears, Craig E Franklin, and Robbie S Wilson. Predicting the physiological performance of ectotherms in fluctuating thermal environments. *Journal of Experimental Biology*, 215(4):694–701, 2012.

[143] Roger M Nisbet and William Gurney. *Modelling fluctuating populations: reprint of first Edition (1982)*. Blackburn Press, 2003.

[144] Toshinori Okuyama. Stage duration distributions in matrix population models. *Ecology and Evolution*, 8(16):7936–7945, 2018.

[145] Angela Peace, Suzanne M O'Regan, Jennifer A Spatz, Patrick N Reilly, Rachel D Hill, E Davis Carter, Rebecca P Wilkes, Thomas B Waltzek, Debra L Miller, and Matthew J Gray. A highly invasive chimeric ranavirus can decimate tadpole populations rapidly through multiple transmission pathways. *Ecological Modelling*, 410:108777, 2019.

[146] Sebastiano Piccolroaz. Prediction of lake surface temperature using the air2water model: guidelines, challenges, and future perspectives. *Advances in Oceanography and Limnology*, 7(1), 2016.

[147] Sebastiano Piccolroaz, Nathan C Healey, John D Lenters, S Geoffrey Schladow, Simon J Hook, Goloka Behari Sahoo, and Marco Toffolon. On the predictability of lake surface temperature using air temperature in a changing climate: A case study for lake tahoe (usa). *Limnology and Oceanography*, 63(1):243–261, 2018.

[148] Sebastiano Piccolroaz, Marco Toffolon, and Bruno Majone. A simple lumped model to convert air temperature into surface water temperature in lakes. *Hydrology and Earth System Sciences*, 17(8):3323–3338, 2013.

[149] Alan J Pounds, Martín R Bustamante, Luis A Coloma, Jamie A Consuegra, Michael PL Fogden, Pru N Foster, Enrique La Marca, Karen L Masters, Andrés Merino-Viteri, Robert Puschendorf, et al. Widespread amphibian extinctions from epidemic disease driven by global warming. *Nature*, 439(7073):161–167, 2006.

[150] Heike Pröhl. Population differences in female resource abundance, adult sex ratio, and male mating success in dendrobates pumilio. *Behavioral Ecology*, 13(2):175–181, 2002.

[151] Lara J Rachowicz and Cheryl J Briggs. Quantifying the disease transmission function: effects of density on batrachochytrium dendrobatidis transmission in the mountain yellow-legged frog rana muscosa. *Journal of Animal Ecology*, pages 711–721, 2007.

[152] Esa Ranta, Veijo Kaitala, and Jan Lindström. Sex in space: population dynamic consequences. *Proceedings of the Royal Society of London. Series B: Biological Sciences*, 266(1424):1155–1160, 1999.

[153] Jane M Reid, Justin MJ Travis, Francis Daunt, Sarah J Burthe, Sarah Wanless, and Calvin Dytham. Population and evolutionary dynamics in spatially structured seasonally varying environments. *Biological Reviews*, 93(3):1578–1603, 2018.

[154] Francis J Richards. A flexible growth function for empirical use. *Journal of experimental Botany*, 10(2):290–301, 1959.

[155] Suzanne L Robertson and Kevin A Caillouët. A host stage-structured model of enzootic west nile virus transmission to explore the effect of avian stage-dependent exposure to vectors. *Journal of Theoretical Biology*, 399:33–42, 2016.

[156] Roberto Rosà, Andrea Pugliese, Alessandro Villani, and Annapaola Rizzoli. Individual-based vs. deterministic models for macroparasites: host cycles and extinction. *Theoretical Population Biology*, 63(4):295–307, 2003.

[157] Elizabeth A Roznik, Sarah J Sapsford, David A Pike, Lin Schwarzkopf, and Ross A Alford. Condition-dependent reproductive effort in frogs infected by a widespread pathogen. *Proceedings of the Royal Society B: Biological Sciences*, 282(1810):20150694, 2015.

[158] Shigui Ruan. Delay differential equations in single species dynamics. In *Delay Differential Equations and Applications*, pages 477–517. Springer, 2006.

[159] Paul Leonard Salceanu and Hal L Smith. Persistence in a discrete-time stage-structured fungal disease model. *Journal of Biological Dynamics*, 3(2-3):271–285, 2009.

[160] Paul Leonard Salceanu and Hal L Smith. Persistence in a discrete-time, stage-structured epidemic model. *Journal of Difference Equations and Applications*, 16(1):73–103, 2010.

[161] Ben C Scheele, Frank Pasmans, Lee F Skerratt, Lee Berger, AN Martel, Wouter Beukema, Aldemar A Acevedo, Patricia A Burrowes, Tamilie Carvalho, Alessandro

Catenazzi, et al. Amphibian fungal panzootic causes catastrophic and ongoing loss of biodiversity. *Science*, 363(6434):1459–1463, 2019.

[162] Rick D Scherer, Erin Muths, Barry R Noon, and Paul Stephen Corn. An evaluation of weather and disease as causes of decline in two populations of boreal toads. *Ecological Applications*, 15(6):2150–2160, 2005.

[163] Thomas Schmickl and Istvan Karsai. The interplay of sex ratio, male success and density-independent mortality affects population dynamics. *Ecological Modelling*, 221(8):1089–1097, 2010.

[164] Frank Seebacher and Veronica S Grigaltchik. Embryonic developmental temperatures modulate thermal acclimation of performance curves in tadpoles of the frog limnodynastes peronii. *PLoS One*, 9(9):e106492, 2014.

[165] Allison K Shaw, Hanna Kokko, and Michael G Neubert. Sex difference and allee effects shape the dynamics of sex-structured invasions. *Journal of Animal Ecology*, 87(1):36–46, 2018.

[166] Katriona Shea and Peter Chesson. Community ecology theory as a framework for biological invasions. *Trends in Ecology & Evolution*, 17(4):170–176, 2002.

[167] Hal L Smith. *Monotone Dynamical Systems: An Introduction to The Theory of Competitive and Cooperative Systems*. Number 41. American Mathematical Society, 1995.

[168] Hal L Smith. Distributed delay equations and the linear chain trick. *An Introduction to Delay Differential Equations with Applications to the Life Sciences*, pages 119–130, 2011.

[169] Hal L Smith and Xiao-Qiang Zhao. Robust persistence for semidynamical systems. *Nonlinear Analysis, Theory, Methods and Applications*, 47(9):6169–6179, 2001.

[170] Matthew J Smith, Andrew White, Jonathan A Sherratt, Sandra Telfer, Michael Begon, and Xavier Lambin. Disease effects on reproduction can cause population cycles in seasonal environments. *Journal of Animal Ecology*, 77(2):378–389, 2008.

[171] Navjot S Sodhi, David Bickford, Arvin C Diesmos, Tien Ming Lee, Lian Pin Koh, Barry W Brook, Cagan H Sekercioglu, and Corey JA Bradshaw. Measuring the meltdown: drivers of global amphibian extinction and decline. *PloS One*, 3(2):e1636, 2008.

[172] Simon N Stuart, Janice S Chanson, Neil A Cox, Bruce E Young, Ana SL Rodrigues, Debra L Fischman, and Robert W Waller. Status and trends of amphibian declines and extinctions worldwide. *Science*, 306(5702):1783–1786, 2004.

[173] Kyle Summers. Paternal care and the cost of polygyny in the green dart-poison frog. *Behavioral Ecology and Sociobiology*, 27:307–313, 1990.

[174] Kyle Summers and James Tumulty. Parental care, sexual selection, and mating systems in neotropical poison frogs. In *Sexual selection*, pages 289–320. Elsevier, 2014.

[175] Gui-Quan Sun, Ming-Tao Li, Juan Zhang, Wei Zhang, Xin Pei, and Zhen Jin. Transmission dynamics of brucellosis: Mathematical modelling and applications in china. *Computational and Structural Biotechnology Journal*, 18:3843–3860, 2020.

[176] Sanyi Tang and Robert A Cheke. Models for integrated pest control and their biological implications. *Mathematical Biosciences*, 215(1):115–125, 2008.

[177] GJ Tattersall and RG Boutilier. Balancing hypoxia and hypothermia in cold-submerged frogs. *Journal of Experimental Biology*, 200(6):1031–1038, 1997.

[178] Glenn J Tattersall and Gordon R Ultsch. Physiological ecology of aquatic overwintering in ranid frogs. *Biological Reviews*, 83(2):119–140, 2008.

[179] Horst R Thieme. Spectral bound and reproduction number for infinite-dimensional population structure and time heterogeneity. *SIAM Journal on Applied Mathematics*, 70(1):188–211, 2009.

[180] Horst R Thieme. *Mathematics in Population Biology*, volume 12. Princeton University Press, 2018.

[181] Horst R Thieme, Thanate Dhirasakdanon, Zhun Han, and Roy Trevino. Species decline and extinction: synergy of infectious disease and allee effect? *Journal of Biological Dynamics*, 3(2-3):305–323, 2009.

[182] Ursina Tobler, Adrian Borgula, and Benedikt R Schmidt. Populations of a susceptible amphibian species can grow despite the presence of a pathogenic chytrid fungus. *PLoS One*, 7(4):e34667, 2012.

[183] Anastasios Tsoularis and James Wallace. Analysis of logistic growth models. *Mathematical Biosciences*, 179(1):21–55, 2002.

[184] Pauline van den Driessche and James Watmough. Reproduction numbers and subthreshold endemic equilibria for compartmental models of disease transmission. *Mathematical Biosciences*, 180(1-2):29–48, 2002.

[185] Pauline van den Driessche and Abdul-Aziz Yakubu. Disease extinction versus persistence in discrete-time epidemic models. *Bulletin of Mathematical Biology*, 81(11):4412–4446, 2019.

[186] Pauline van Den Driessche and Abdul-Aziz Yakubu. Age structured discrete-time disease models with demographic population cycles. *Journal of Biological Dynamics*, 14(1):308–331, 2020.

[187] James R Vonesh and Omar De la Cruz. Complex life cycles and density dependence: assessing the contribution of egg mortality to amphibian declines. *Oecologia*, 133:325–333, 2002.

[188] Patrick Walsh, J Roger Downie, and Pat Monaghan. Factors affecting the overwintering of tadpoles in a temperate amphibian. *Journal of Zoology*, 298(3):183–190, 2016.

[189] Bin-Guo Wang and Xiao-Qiang Zhao. Basic reproduction ratios for almost periodic compartmental epidemic models. *Journal of Dynamics and Differential Equations*, 25:535–562, 2013.

[190] Feng-Bin Wang, Lei Zhang, and Xiao-Qiang Zhao. Basic reproduction ratios for time-periodic homogeneous evolution systems. *SIAM Journal on Applied Mathematics*, 83(5):1806–1831, 2023.

[191] Jin Wang. Mathematical models for cholera dynamics—a review. *Microorganisms*, 10(12):2358, 2022.

[192] Jin Wang and Shu Liao. A generalized cholera model and epidemic–endemic analysis. *Journal of Biological Dynamics*, 6(2):568–589, 2012.

[193] Wendi Wang and Xiao-Qiang Zhao. Threshold dynamics for compartmental epidemic models in periodic environments. *Journal of Dynamics and Differential Equations*, 20:699–717, 2008.

[194] Xiang-Sheng Wang, Jianhong Wu, and Yong Yang. Richards model revisited: Validation by and application to infection dynamics. *Journal of Theoretical Biology*, 313:12–19, 2012.

[195] Xiunan Wang and Xiao-Qiang Zhao. A malaria transmission model with temperature-dependent incubation period. *Bulletin of Mathematical Biology*, 79(5):1155–1182, 2017.

[196] Xueying Wang, Xiao-Qiang Zhao, and Jin Wang. A cholera epidemic model in a spatiotemporally heterogeneous environment. *Journal of Mathematical Analysis and Applications*, 468(2):893–912, 2018.

[197] Helen J Wearing, Pejman Rohani, Tom C Cameron, and Steven M Sait. The dynamical consequences of developmental variability and demographic stochasticity for host-parasitoid interactions. *The American Naturalist*, 164(4):543–558, 2004.

[198] Kentwood D Wells. *The Ecology and Behavior of Amphibians*. University of Chicago press, 2019.

[199] Mark Q Wilber, Roland A Knapp, Mary Toothman, and Cheryl J Briggs. Resistance, tolerance and environmental transmission dynamics determine host extinction risk in a load-dependent amphibian disease. *Ecology Letters*, 20(9):1169–1181, 2017.

[200] Xiaotian Wu, Felicia Maria G Magpantay, Jianhong Wu, and Xingfu Zou. Stage-structured population systems with temporally periodic delay. *Mathematical Methods in the Applied Sciences*, 38(16):3464–3481, 2015.

[201] Yanni Xiao, Roger G Bowers, and Sanyi Tang. The effect of delayed host self-regulation on host–pathogen population cycles in forest insects. *Journal of Theoretical Biology*, 258(2):240–249, 2009.

[202] Abdul-Aziz Yakubu. Introduction to discrete-time epidemic models. In *Modeling Paradigms and Analysis of Disease Trasmission Models*, pages 83–107, 2010.

[203] Tianhui Yang and Lei Zhang. Remarks on basic reproduction ratios for periodic abstract functional differential equations. *Discrete & Continuous Dynamical Systems-Series B*, 25(12):p6771, 2019.

[204] Bo Zhang, Xin Liu, Donald L DeAngelis, Wei-Ming Ni, and G Geoff Wang. Effects of dispersal on total biomass in a patchy, heterogeneous system: Analysis and experiment. *Mathematical Biosciences*, 264:54–62, 2015.

[205] Xiao-Qiang Zhao. Permanence implies the existence of interior periodic solutions for fdes. *Qualitative theory of Differential Equations and Applications*, 2:125–137, 2008.

[206] Xiao-Qiang Zhao. Basic reproduction ratios for periodic compartmental models with time delay. *Journal of Dynamics and Differential Equations*, 29(1):67–82, 2017.

[207] Xiao-Qiang Zhao. *Dynamical Systems in Population Biology*. Springer, 2017.

[208] Senlin Zhu, Mariusz Ptak, Zaher Mundher Yaseen, Jiangyu Dai, and Bellie Sivakumar. Forecasting surface water temperature in lakes: A comparison of approaches. *Journal of Hydrology*, 585:124809, 2020.

[209] Richard George Zweifel. *Ecology, Distribution and Systematics of Frogs of the Rana Boylei Group*. University of California Press, 1955.